

CLINICOPATHOLOGICAL CORRELATES IN TAUOPATHY AND AGING

by

Selena Peggy-Lynn Maxwell

Submitted in partial fulfillment of the requirements
for the degree of Doctor of Philosophy

at

Dalhousie University

Halifax, Nova Scotia

August 2022

To my father. I wish you were here to read this.

TABLE OF CONTENTS

LIST OF TABLES vi

LIST OF FIGURES vii

ABSTRACT viii

LIST OF ABBREVIATIONS USED ix

ACKNOWLEDGEMENTS xiii

CHAPTER 1 INTRODUCTION 1

 1.1. PREFACE 1

 1.2. OVERVIEW 2

 1.3. TAU (TUBULIN-ASSOCIATED UNIT)..... 2

 1.3.1. TAU GENE STRUCTURE..... 2

 1.3.2. TAU POST-TRANSCRIPTIONAL PROCESSING 1

 1.3.3. TAU PROTEIN STRUCTURE..... 2

 1.3.4. TAU POST-TRANSLATIONAL MODIFICATION 5

 1.3.4.1. Tau phosphorylation..... 5

 1.4. TAUOPATHY 6

 1.4.1. ALZHEIMER’S DISEASE (AD)..... 9

 1.4.1.1. Clinical Presentation 9

 1.4.1.2. Preclinical diagnostic techniques 14

 1.4.1.3. Treatment 15

 1.4.1.4. Neuropathological evaluation 17

 1.5. THE CHOLINERGIC SYSTEM..... 22

 1.5.1. COGNITION AND THE CHOLINERGIC SYSTEM..... 25

 1.5.2. CHOLINESTERASES 26

 1.5.3. NORMAL CHOLINESTERASE DISTRIBUTION 28

 1.5.4. CHOLINESTERASES IN AD..... 28

 1.6. THESIS OBJECTIVE AND HYPOTHESIS 29

 1.7. CHAPTER OVERVIEWS..... 33

 1.8. AUTHORSHIP 34

**CHAPTER 2 CLINICOPATHOLOGICAL CORRELATES IN AGING:
NEUROPATHOLOGY AND CHOLINESTERASE EXPRESSION IN
OCTOGENARIANS AND OLDER..... 35**

 2.1. PUBLICATION STATUS 35

 2.2. OVERVIEW 35

 2.3. ABSTRACT..... 35

 2.4. INTRODUCTION..... 36

 2.5. MATERIALS AND METHODS 39

 2.5.1. BRAIN TISSUES 39

 2.5.2. IMMUNOHISTOCHEMICAL STAINING..... 41

2.5.4.	DATA ANALYSIS	45
2.6.	RESULTS.....	47
2.6.2.	PARCELLATION OF THE HIPPOCAMPAL FORMATION	50
2.6.3.	ROSTRAL PREFRONTAL CORTEX PATHOLOGY	52
2.6.4.	DENTATE GYRUS PATHOLOGY	59
2.6.5.	HIPPOCAMPAL PATHOLOGY.....	65
2.6.6.	SUBICULAR COMPLEX PATHOLOGY.....	67
2.6.7.	ENTORHINAL CORTEX PATHOLOGY.....	72
2.7.	DISCUSSION.....	74
2.8.	ACKNOWLEDGEMENTS	84

**CHAPTER 3 CLINICOPATHOLOGICAL CORRELATES IN SPORADIC
TAUOPATHY: NEUROPATHOLOGY AND CHOLINESTERASE
EXPRESSION IN PROGRESSIVE SUPRANUCLEAR PALSY..... 86**

3.1.	PUBLICATION STATUS	86
3.2.	OVERVIEW	86
3.3.	ABSTRACT.....	86
3.4.	INTRODUCTION.....	87
3.5.	MATERIALS AND METHODS	89
3.5.1.	BRAIN TISSUES	89
3.5.2.	IMMUNOHISTOCHEMISTRY.....	92
3.5.3.	HISTOCHEMICAL STAINING	93
3.5.4.	DATA ANALYSIS	94
3.6.	RESULTS.....	95
3.7.	DISCUSSION.....	101
3.8.	ACKNOWLEDGEMENTS.....	103

**CHAPTER 4 CLINICOPATHOLOGICAL CORRELATES IN HERITABLE
TAUOPATHY: A FAMILY WITH THE RARE IVS10+14 *MAPT* MUTATION. 105**

4.1.	PUBLICATION STATUS	105
4.2.	OVERVIEW	105
4.3.	ABSTRACT.....	105
4.4.	INTRODUCTION.....	106
4.5.	METHODS.....	110
4.6.	RESULTS.....	112
4.6.1.	CLINICAL DESCRIPTIONS.....	112
4.6.2.	PATHOLOGY	115
4.6.2.1.	Gross Findings.....	115
4.6.2.2.	Microscopic findings.....	116
4.7.	DISCUSSION.....	121
4.7.1.	PREVIOUSLY REPORTED FAMILIES	121
4.7.2.	CLINICOPATHOLOGICAL CORRELATES	125
4.8.	CONCLUSION.....	134

4.9. ACKNOWLEDGEMENTS	135
CHAPTER 5 CONCLUSIONS.....	136
5.1. OVERVIEW	136
5.2. GENERAL CONCLUSIONS	136
5.3. FUTURE WORK AND SIGNIFICANCE.....	140
REFERENCES.....	143
APPENDIX A	192
APPENDIX B	196

LIST OF TABLES

Table 1.1	Neuropathological and clinical characteristics of tauopathies	8
Table 1.2	ABC Score for level of neuropathologic change	18
Table 2.1	Demographics of CNOO and AD cases.....	40
Table 2.2	Antibodies used in immunohistochemical staining.....	42
Table 2.3	Mean scores of aggregate abundance in CNOO compared to AD rPFC and hippocampal formation	53
Table 3.1	Demographics of PSP, AD, and CN cases.....	90
Table 4.1	IVS10 + 14 cohort case demographics and availability of clinical and neuropathological testing.....	111
Table 4.2	Summary of clinical features of the IVS10 + 14 cohort	126
Table A.1	Mean scores of aggregate abundance in CNOO male compared to female rPFC and hippocampal formation	192
Table A.2	Mean scores of aggregate abundance in AD male compared to female rPFC and hippocampal formation.....	193
Table A.3	Mean scores of aggregate abundance in male CNOO compared to AD rPFC and hippocampal formation.....	194
Table A.4	Mean scores of aggregate abundance in female CNOO compared to AD rPFC and hippocampal formation.....	195

LIST OF FIGURES

Figure 1.1 Tau functions and isoforms	3
Figure 1.2 Example of CERAD scoring	18
Figure 1.3 Life cycle of acetylcholine and cholinergic pathways.....	23
Figure 1.4 A β and BChE burden in cognitively normal with A β , and AD brains.....	30
Figure 1.5 BChE staining in several non-AD neuropathologies.....	31
Figure 2.1 Parcellation of the rPFC	46
Figure 2.2 Parcellation of the hippocampal formation	48
Figure 2.3 A β , tau, AChE and BChE staining in AD and CNOO PFC	55
Figure 2.4 Tau, AChE and BChE staining in ARTAG	57
Figure 2.5 A β , tau, AChE and BChE staining in AD and CNOO DG and hippocampus	60
Figure 2.6 pTDP-43 staining in the AD and CNOO hippocampal formation	63
Figure 2.7 A β , tau, AChE and BChE staining in AD and CNOO subicular complex and EC.....	68
Figure 3.1 Graphs of mean neuropathological scores in PSP, AD, and CN rPFC	96
Figure 3.2 Tau, AChE and BChE staining of PSP tau neuropathology.....	98
Figure 3.3 A β , AChE and BChE plaque staining in PSP, AD, and CN rPFC	100
Figure 4.1 <i>MAPT</i> structure, tau isoforms and location of pathogenic mutations.....	108
Figure 4.2 Neuropathology in one member of the IVS10 + 14 <i>MAPT</i> mutation Canadian cohort	119

ABSTRACT

Cognitive decline can result from both neurodegenerative or normal aging processes. Definitive diagnosis of many neurodegenerative diseases, such as Alzheimer's disease (AD) and progressive supranuclear palsy (PSP), requires post-mortem neuropathological examination and focuses on the identification of structural changes and protein aggregation in the brain, in addition to a clinical presentation consistent with the disease during life.

Herein, we examined clinicopathological correlates of cognitive decline in sporadic and familial tauopathy, and normal aging. We hypothesized that structural neuropathological changes would be insufficient to explain symptomology in these cases, and that alternate mechanisms, such as cholinesterase expression, may bridge the gap between observed neuropathological changes and clinical symptoms in regions that are important to cognition, including the rostral prefrontal cortex (rPFC) and hippocampal formation.

In cognitively normal (CN) octogenarians and older, there is an accumulation of β -amyloid plaque, tau neurofibrillary tangle, and phosphorylated TAR DNA-binding protein pathology comparable to AD. Butyrylcholinesterase (BChE), however, remains specific to AD pathology and lower acetylcholinesterase and BChE deposition in these pathological structures may contribute to their preserved cognition. In PSP, there are low levels of AD-associated neuropathological aggregation and cholinesterase-positive neuropathology in the rPFC, comparable to CN individuals. This suggests that disruption of rPFC function in this condition may occur through alternate means. Finally, in familial tauopathy caused by the IVS10 + 14 *MAPT* mutation, there was a high degree of intra- and inter-familial phenotypic heterogeneity, with one case presenting severe cognitive symptoms which did not correspond to the mild neuropathology observed in regions associated with cognition.

Our findings support the need to explore alternate diagnostic and therapeutic targets for neurodegeneration as the protein aggregates do not always accurately reflect clinical phenotype in tauopathy and aging.

LIST OF ABBREVIATIONS USED

Å	angstrom
°C	degree Celsius
µL	microlitre
µm	micrometre
0N	0 N-terminal cassettes
1N	1 N-terminal cassettes
2N	2 N-terminal cassettes
3R	3 C-terminal microtubule binding domain repeats
4R	4 C-terminal microtubule binding domain repeats
Aβ	β-amyloid
ACh	acetylcholine
AChE	acetylcholinesterase
AD	Alzheimer's disease
al	alveus
ALS	amyotrophic lateral sclerosis
AMPA	α-amino-3-hydroxy-5-methyl-4-isoxazolepropionic acid
ANOVA	Analysis of Variance
ARTAG	aging-related tau astrogliopathy
BChE	butyrylcholinesterase
BW 284 C 51	1,5-bis (4-allyl dimethylammonium phenyl) pentan-3-one dibromide
CA	cornu ammonis
CA3h	cornu ammonis 3 hilar extent
CB	oligodendrocytic coiled body
cc	corpus callosum
CERAD	consortium to establish a registry for Alzheimer's disease
CG	cingulate gyrus
ChAT	choline acetyltransferase
ChI	cholinesterase inhibitor
ChT	choline transporter

CN	cognitively normal
CNS	central nervous system
CNOO	cognitively normal octogenarians and older
CSF	cerebral spinal fluid
CT	computed tomography
DAB	3,3'-diaminobenzidine
<i>DCTN1</i>	dynactin-1 encoding gene
DDPAC	disinhibition-dementia-parkinsonism-amyotrophy complex
DG	dentate gyrus
dH ₂ O	distilled water
DN	dystrophic neurite
DNA	deoxyribonucleic acid
EC	entorhinal cortex
EEG	electroencephalogram
eNFT	extra-neurofibrillary tangle
fi	fimbria
FTD	frontotemporal dementia
g	gram
GSK3	glycogen synthase kinase-3
H ₂ O ₂	hydrogen peroxide
HI	hippocampus
hr	hour
IFPG	inferior frontopolar gyrus
IVS10 + 14	intronic 10 + 14 splice site mutation
kb	kilobase
kDa	kilodalton
LV	lateral ventricle
M	molar
mAChT	muscarinic acetylcholine receptor
MAPT	microtubule-associated protein tau
<i>MAPT</i>	tau encoding gene

MB	Maleate buffer, pH 7.4
MCI	mild cognitive impairment
mdDG	margo denticulatus of the dentate gyrus
MFGP	medial frontopolar gyrus
mL	millilitre
mM	millimolar
mm	millimetre
MMSE	mini-mental state examination
MOrG	medial orbital gyrus
MRI	magnetic resonance imaging
mRNA	messenger ribonucleic acid
MS	medial septal nucleus
nAChR	nicotinic acetylcholine receptor
nbM	nucleus basalis of Meynert
NCI	neuronal cytoplasmic inclusion
NFT	neurofibrillary tangle
NIA-AA	National Institute of Aging and Alzheimer's Association
nM	nanometre
NT	neuropil thread
NwA β	cognitively normal with β -amyloid plaques
PaS	parasubiculum
PB	phosphate buffer, pH 7.4
PCR	polymerase chain reaction
PET	positron emission tomography
pH	potential hydrogen
PHG	parahippocampal gyrus
PL	polymorphic layer
PrS	presubiculum
PSP	progressive supranuclear palsy
pTDP-43	phosphorylated Tar DNA-binding protein 43
RLS	restless leg syndrome

RNA	ribonucleic acid
RoG	rostral gyrus
rPFC	rostral prefrontal cortex
S	subiculum
scc	splenium of the corpus callosum
SFPG	superior frontopolar gyrus
SG	straight gyrus
SG	stratum granulosum
SL-M	stratum lacunosum-moleculare
SLu	stratum lucidum
SM	stratum moleculare
snRNP	small nuclear ribonucleoproteins
SO	stratum oriens
SP	stratum pyramidale
SPECT	single photon emission computed tomography
SR	stratum radiatum
TA	tufted astrocyte
un	uncus
VACHT	vesicular acetylcholine transporter
WM	white matter
y	years

ACKNOWLEDGEMENTS

Firstly, I would like to extend my most sincere gratitude to my supervisor, Dr. Sultan Darvesh. You took a chance on me as an undergraduate student with no research experience years ago, and again by letting me stay on as a graduate student. Your support and mentorship have allowed me to find a field I am passionate about and have shaped me into a scientist.

Thank you to the Darvesh group, past and present, namely Meghan Cash, Andrew Reid, Dr. Drew DeBay, Dr. Ian MacDonald, and Hillary Malliet. It has been a pleasure to collaborate with and work alongside you all.

I am grateful for the guidance provided by my thesis supervisory committee including Dr. Kazue Semba, Dr. Alon Friedman, and Dr. James Fawcett as well as my external examiner, Dr. Satyabrata Kar. Your feedback has shaped this thesis to be as rigorous as possible.

Finally, a heartfelt thank you to my friends and family. To my fellow graduate student friends, especially Chad, for your empathy. To my mother and father, who encouraged my love of science since birth and put up with the, often questionable, experiments scattered about the house. To my fiancé, Donald, for his unwavering encouragement these past few years.

CHAPTER 1 Introduction

1.1. Preface

Auguste Deter of Kassel, Germany started exhibiting abnormal behavioural and cognitive changes at the age of 51, including delusions regarding her husband's fidelity and progressive memory impairment that interfered with her daily life (Hippius and Neundörfer, 2003). She was admitted into a Frankfurt mental hospital under the care of Dr. Alois Alzheimer who diagnosed her with 'presenile dementia' (Hippius and Neundörfer, 2003). Post-mortem analysis of Auguste's brain revealed atrophy of the cerebral cortex, senile plaques, tangles and atherosclerosis (Alzheimer, 2006). Alzheimer published his clinical and neuropathological account of Auguste Deter's disease and brain in his seminal paper, which roughly translates to "Concerning a unique disease of the cerebral cortex" (Alzheimer, 2006). Later, Alzheimer's mentor Emil Kraepelin named the disease Alzheimer's disease (AD) in acknowledgement of Alzheimer's contribution to characterizing the disease process (Hippius and Neundörfer, 2003). While senile plaques had been described previously (Walker, 2020), Alzheimer was the first to describe intraneuronal filaments that remained as a "tangled bundle of fibrils" after cell death (Alzheimer, 2006). We now know these inclusions as neurofibrillary tangles (NFTs), a pathological hallmark of AD composed of the microtubule-associated protein tau. Since Alzheimer's description of NFTs in 1907, tau has been implicated in a wide range of neurodegenerative disorders. This thesis sought to characterize the neuropathological and cholinergic changes the brain undergoes as a result of tau deposition in neurodegenerative diseases like AD, progressive supranuclear palsy (PSP), and familial tauopathy, as well as aging.

1.2. Overview

In this chapter we review the present understanding of tau-associated dysfunction in neurodegeneration and aging.

1.3. Tau (Tubulin-associated unit)

The protein tau was accidentally identified as a contaminant during purification of microtubules by Weingarten *et al.* (1975). They determined that when microtubule-associated proteins were removed from tubulin, the protein was incapable of self-assembly, and therefore, tau is a regulator of cytoskeletal integrity through tubulin stabilization and polymerization. Functions of tau include axonal transport (Baird and Bennett, 2013; Scholz and Mandelkow, 2014), synaptic plasticity and function (Biundo *et al.*, 2018; Boehm, 2013; Spires-Jones and Hyman, 2014) and nucleic acid protection (Sultan *et al.*, 2011; Violet *et al.*, 2015, 2014) among others (Fig. 1.1A). Human tau is predominantly expressed in the central nervous system (CNS) in neurons, although low levels are also expressed in astrocytes and oligodendrocytes (Binder *et al.*, 1985; Müller *et al.*, 1997; Papasozomenos and Binder, 1987). Its presence is increased during pathogenic conditions (Binder *et al.*, 1985; Kahlson and Colodner, 2016). Additionally, tau is expressed at relatively lower levels in the peripheral nervous system than compared to the CNS under both normal and pathological conditions (François *et al.*, 2014; Miklossy *et al.*, 2010; Shi *et al.*, 2011; Souter and Lee, 2009).

1.3.1. Tau gene structure

The tau encoding gene, *MAPT*, is located on the long arm of chromosome 17 at band position 17q21 and is comprised of 16 exons (Andreadis *et al.*, 1995; Neve *et al.*, 1986). In the CNS, alternate splicing of tau pre-mRNA results in six developmentally

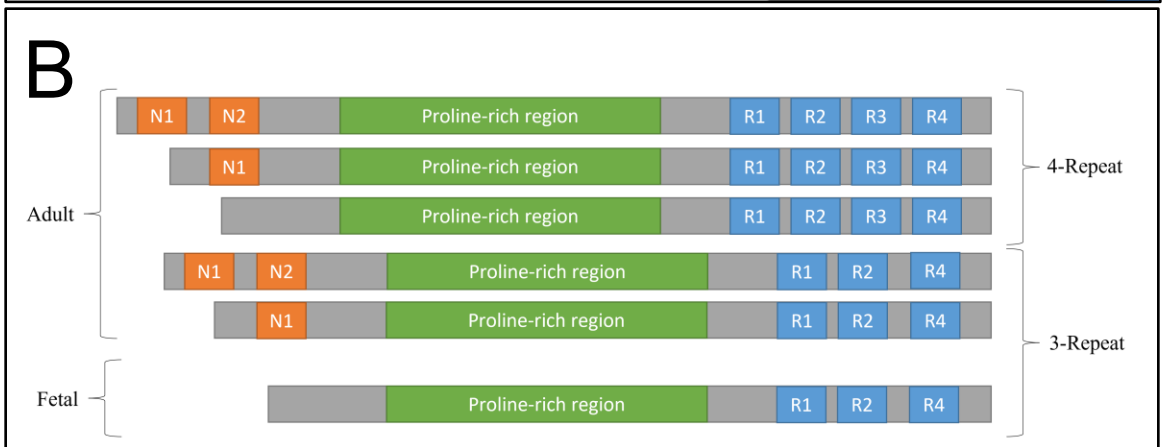
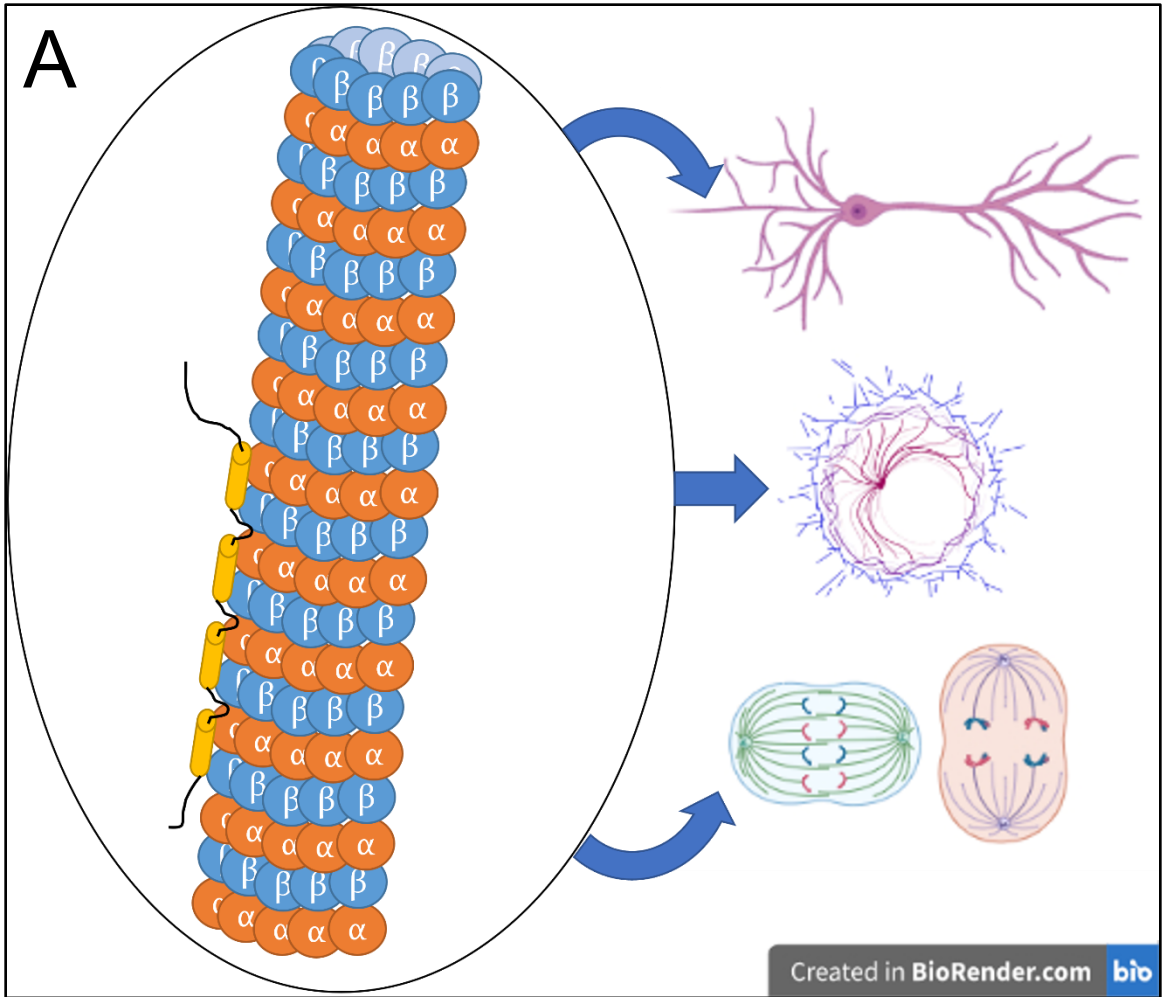


Figure 1.1 A simplified representation of a 4-repeat tau isoform associating with a microtubule, composed of α - and β -tubulin subunits (A) and human tau isoforms (B). Tau binds to the microtubule via repeated amino acid three, or in this isoform, four 31-32 amino acid imperfect repeats (yellow cylinder) promoting microtubule polymerization and stability (Adapted from Krestova et al., 2012) (A). Microtubules are important for dendritic arborization and axonal outgrowth, cytoskeletal stability and spindle formation during meiosis and mitosis as seen in representative images on the right. There are six tau isoforms present in the human brain comprised of a proline-rich region flanked by variable N-terminal and C-terminal region (B). Isoforms differ by both the number of N-terminal cassettes present (N1 and N2) and either three or four C-terminal microtubule binding repeat sequences (R1, R2, R3, and R4; Adapted from Andreadis et al., 1995; Neve et al., 1986). Alternate splicing of the third repeat (R3) results in an even ratio of 4-repeat and 3-repeat isoforms in a normal brain. The smallest tau isoform is only present in the fetal brain while the remaining five isoforms are expressed in the adult brain.

regulated tau isoforms. The six isoforms differ in their expression of zero (0N), one (1N), or two (2N) N-terminal cassettes, and three (3R) or four (4R) C-terminal repeats (Fig. 1.1B; Andreadis et al., 1992; Andreadis, 2005; Goedert et al., 1989a). Exon 1 contains part of the untranslated promoter sequence (Andreadis et al., 1996). The N-terminal cassettes are located in tau's projection domain, encoded by exon 2 as well as exon 3, which is not present independently of exon 2 (Andreadis et al., 1995). Exon 4, 5 and 7 are constitutively expressed while 4A, 6 and 8 are expressed almost exclusively in the periphery (Andreadis, 2005; Couchie et al., 1992; Nunez and Fischer, 1997). The microtubule-binding domain located at the C-terminus is encoded by exons 9 through 12 which all contain 33 amino acid repeat sequences (Himmler et al., 1989; Lee et al., 1989). Exon 13 is constitutively expressed (Andreadis, 2005; Couchie et al., 1992; Nunez and Fischer, 1997), and finally, exon 14 encodes the 3' untranslated region (Goedert et al., 1989b, 1989a). Alternate splicing of exon 10 determines 3R-tau and 4R-tau isoforms (Andreadis et al., 1996).

1.3.2. Tau post-transcriptional processing

Post-transcriptional processing of the tau primary transcript results in three separate mRNA species (2, 6, and 8/9 kb), which is dependent on the stage of neuronal maturation and neuronal subtype (Andreadis et al., 1996; Couchie et al., 1992; Goedert et al., 1989b, 1989a; Nunez and Fischer, 1997). The least abundant 2 kb transcript encodes nuclear tau (Wang et al., 1993). The 6 kb mRNA is primarily expressed in neurons of the CNS encoding tau-associated with soma and axons (Andreadis, 2005; Liu and Götz, 2013). The 8/9 kb transcript is expressed in the retina and peripheral nervous system (Georgieff et al., 1993; Nunez and Fischer, 1997). Inclusion of exon 4A during

pre-mRNA processing results in the 8/9 kb transcript (Andreadis, 2005; Georgieff et al., 1993; Goedert et al., 1989b), while the 2 and 6 kb mRNA transcripts are produced from the same pre-mRNA with different polyadenylation sites (Sadot et al., 1994).

Alternate splicing of exon 10 during tau pre-mRNA processing results in either three or four tandem repeats in the protein's microtubule binding region, conferring different microtubule binding affinities (Andreadis et al., 1992; Butner and Kirschner, 1991; Goedert et al., 1989b; Gustke et al., 1994). Splicing in humans is catalyzed by the spliceosome complex composed of five small nuclear RNA (U1, U2, U4, U5, and U6) bound to over 300 different proteins to form small nuclear ribonucleoproteins (snRNPs; Jurica and Moore, 2003; Lerner et al., 1980; Will and Lührmann, 2011). snRNPs mediate the binding of the spliceosome complex to pre-mRNA, catalyze the removal of introns, and ligate the remaining exons together. Alternate splicing of tau's exon 10, like all other sequences, is regulated by trans-acting proteins binding to cis elements in the pre-mRNA. Trans-acting factors include serine- and arginine-rich proteins, heterogenous nuclear ribonucleoproteins (Kornblihtt et al., 2013). One vital tau cis-element is the stem-loop structure at the exon 10/intron 10 interface that forms due to a high degree of complementarity (Goedert et al., 1989b). Disruption of the stem-loop results in an exon 10 inclusion and the production of more 4R tau isoforms often resulting in neuropathological aggregation (Grover et al., 1999; Hutton et al., 1998; Varani et al., 1999).

Alternate splicing of pre-mRNA increases the complexity of gene expression and allows for additional mechanisms of cellular and developmental regulation of proteins (Baralle and Giudice, 2017; Roy et al., 2013). Differential expression of exon 10 during

development indicates that tau isoforms likely have specific physiological roles to meet developmental and cellular requirements. For example, the smallest tau isoform, 0N3R, has the lowest rate of microtubule assembly and it is only expressed during fetal stages. The remaining five isoforms are expressed throughout adulthood (Goedert and Jakes, 1990; Kosik et al., 1989). In the developing CNS, tau drives the development of neuronal cell polarity, axonal elongation and transport, and growth cone translocation which requires dynamic microtubules (Caceres and Kosik, 1990; Dixit et al., 2008; Drechsel et al., 1992; Drubin et al., 1985; Esmaeli-Azad et al., 1994; Panda et al., 2003). In the mature brain, there is a shift to axonal and cytoskeletal maintenance through increased microtubule stability (Black et al., 1984; Panda et al., 2003). Fine tuning of microtubule dynamics is in part due to localized expression patterns of 3R and 4R isoforms (McMillan et al., 2008; Panda et al., 2003). While levels of 3R and 4R tau are approximately equal in the normal adult brain, isoform imbalance is observed in several tauopathies resulting in abnormal protein aggregates with distinct isoform compositions (Hong et al., 1998; Niblock and Gallo, 2012). For example, all six tau isoforms have been identified in neurofibrillary tangles in AD (Goedert et al., 1992), whereas in PSP, there are predominantly 4R tau isoforms in neuropathological aggregates (Rösler et al., 2019).

1.3.3. Tau protein structure

Tau belongs to the family of microtubule-associated proteins that act as stabilizers and organizers of the microtubule cytoskeleton (Bodakuntla et al., 2019). Like other microtubule-associated proteins, tau is resistant to thermal- and acid-induced loss of function due to its natively unfolded structure (Cleveland et al., 1977; Gamblin, 2005; Jeganathan et al., 2008). The absence of a tau secondary structure is primarily due to a

lack of hydrophobicity (Jeganathan et al., 2008; Uversky, 2002). Tau's primary structure, however, can be split into two major functional domains: the projection domain composed of an N-terminal acidic and proline-rich region, and the microtubule-binding repeat domain composed of short, tandem repeat sequences and the C-terminal region (Gustke et al., 1994; Mandelkow et al., 1995).

The projection domain, so named as it projects from the microtubule surface where it can interact with elements of the cytoskeleton, plasma membrane, and mitochondria, is composed of highly acidic amino acids followed by a proline-rich region (Brandt et al., 1995; Hirokawa et al., 1988; Jung et al., 1993). The projection domain varies between isoforms depending on the inclusion or exclusion of two 29 amino acid sequences encoded by exons 2 and 3 (Goedert et al., 1989a). In neurons, the projection domain determines the spacing between axonal microtubules which affects axon width (Chen et al., 1992). The addition of the sequence encoded by exon 4A at the N-terminus in neurons of the peripheral nervous system results in the "big tau" isoform which produces wide, long axons that demonstrate the effect of the N-terminal region of tau on axonal width and stabilization (Couchie et al., 1992; Georgieff et al., 1993; Goedert et al., 1992).

The proline-rich region within the projection domain of tau is involved in signal transduction and cytoskeletal stabilization (Buee et al., 2000). Regarding cytoskeletal interactions, the proline-rich region mediates binding to cytoskeletal elements such as spectrin and actin filaments, which allows for the connection of microtubules to neurofilaments and the regulation of cytoskeletal flexibility (Farias et al., 2002; He et al., 2009; Yu and Rasenick, 2006). The proline-rich domain has also been demonstrated to

interact with the SH3 domains of Src-family non-receptor tyrosine kinases at the plasma membrane that may allow tau to modify cell morphology (Lee et al., 1998). Tau likely plays a modulatory role in the phospholipase C- γ transduction pathway through interaction with the SH3 domain (Hwang et al., 1996; Jenkins and Johnson, 1998), further implicating tau in the regulation of several physiological functions such as chemotaxis, cell proliferation and survival, and opioid sensitivity (Lyon and Tesmer, 2013).

Tau's affinity for microtubules is determined by its C-terminal tandem repeat region. The repeats are encoded by exons 9-12 with alternative splicing of exon 10 during pre-mRNA processing resulting in either three or four copies of a highly conserved 18-amino acid repeat sequence resulting in 3R and 4R isoforms (Goedert et al., 1989b; Himmler et al., 1989; Lee et al., 1989). A less conserved 13- or 14-amino acid inter-repeat domain separates each repeat. The repeat sequences bind to microtubules through a series of relatively weak site-specific interactions (Butner and Kirschner, 1991; Lee et al., 1989). It has been demonstrated that 4R tau isoforms have a greater binding affinity for microtubules compared to 3R isoforms (Butner and Kirschner, 1991; Goedert and Jakes, 1990; Gustke et al., 1994). In part, isoform-specific microtubule binding affinity is due to the additional repeat sequence, but the region between repeats 1 and 2 that is present only in 4R tau isoforms solely accounts for the 40-fold difference (Goode and Feinstein, 1994; Panda et al., 1995). Additional roles of the microtubule-binding domain include embryonic development (Lee et al., 1996), metabolism (Stieler et al., 2011), and phosphorylation (Sontag et al., 1999; Takashima et al., 1998). The microtubule-binding domain may contribute to the degree of tau phosphorylation through its interactions with

phosphatase 2A and glycogen synthase kinase 3 β by way of presenilin 1 (Sontag et al., 1999; Takashima et al., 1998). Tau has also been demonstrated to have the capacity to bind mRNA, although, a functional significance has not been identified (Kampers et al., 1996).

1.3.4. Tau post-translational modification

Tau frequently undergoes various forms of post-translational modification, including truncation, nitration, glycation, glycosylation, SUMOylation, ubiquitination and polyamination, and phosphorylation, that can affect tau microtubule binding affinity, clearance, and aggregation (Alquezar et al., 2021). While post-translational modification of tau likely has a role in the context of both physiology and disease, it is difficult to identify whether each modification confers a causal, contributory or bystander effect (Alquezar et al., 2021).

1.3.4.1. Tau phosphorylation

Phosphorylation is the most common and arguably the most relevant post-translational modification of tau to neurodegeneration (Martin et al., 2011). Tau contains 85 potential serine, threonine, and tyrosine phosphorylation sites, the majority of which are located in the proline-rich region and the C-terminus flanking the microtubule-binding region (Buee et al., 2000). Under normal conditions, tau phosphorylation is highly regulated. During embryonic development, relative phosphorylation of tau is increased and promotes dynamic microtubules. However, in the adult brain, tau phosphorylation is relatively low (Bramblett et al., 1993; Brion et al., 1993; Kenessey and Yen, 1993; Morishima-Kawashima et al., 1995; Yu et al., 2009). Fetal tau is phosphorylated at many of the same sites as tau in AD brains, however, it retains its

function and does not abnormally aggregate unlike in AD (Alonso et al., 2001, 2006, 1994; Iqbal et al., 1986; Yoshida and Ihara, 1993). Tau hyperphosphorylation results in the dissociation of tau from microtubules due to a loss of affinity and in the formation of self-associated aggregates related to neurodegeneration (Bramblett et al., 1993; Lee et al., 2001).

A wide range of kinases are capable of phosphorylating tau including proline directed kinases (e.g. glycogen synthase kinase-3 (GSK3), cyclin dependent kinase, and adenosine monophosphate-activated protein kinase), non-proline directed kinases (e.g. casein kinase 1 and microtubule affinity-regulating kinases), and tyrosine kinases (e.g. Fyn, Abl, and Syk; Noble et al., 2013). Additionally, tau can be dephosphorylated by several phosphatases (e.g. protein phosphatases 1, 2A, 2B, and 5; Liu et al., 2005). Dysregulation of tau kinase and phosphatase activity results in the hyperphosphorylated tau observed in AD (Martin et al., 2013). The kinase GSK3 has been a particular focus in AD research as it is capable of phosphorylating tau at several of the epitopes identified in AD paired helical filaments (Ishiguro et al., 1993), and is found to accumulate in the cytoplasm of pretangle neurons (Pei et al., 1999). It is hypothesized that GSK3 is a link between A β and tau neuropathology, as A β increases GSK3 activation through the wnt (Magdesian et al., 2008) and insulin (Townsend et al., 2007) signaling pathways.

1.4. Tauopathy

Tauopathies are a family of clinically heterogenous neuropathological disorders characterized pathologically by abnormal deposition of microtubule-associated protein tau aggregates in the brain. Presently, recognized sporadic tauopathies include AD, aging-related tau astrogliopathy (ARTAG), argyrophilic grain disease, chronic traumatic

encephalopathy, corticobasal degeneration, globular glial tauopathy, a subset of Pick's disease, primary age-related tauopathy, and PSP (Josephs, 2017). While most tauopathies have a clinical phenotype, some, such as ARTAG, do not have a defined clinical presentation (Kovacs et al., 2016a).

Abnormally phosphorylated tau aggregation is a pathological hallmark of tauopathies (Lee et al., 2001; Table 1.1). Tau aggregates are composed of abnormal, hyperphosphorylated, fibrillar tau structures. The most common of which is the paired helical filament of AD-type NFTs. Loss of function and aggregation of tau is thought to be a direct result of dysregulation of tau phosphorylation (Alonso et al., 2008; Gong et al., 2006). Tau aggregation in neurodegenerative diseases can occur in the cell bodies and processes of neurons (e.g., argyrophilic grains and threads, NFTs, neuropil threads, and Pick bodies), astrocytes (e.g., astrocytic plaques, fuzzy astrocytes, globular glial inclusions, Pick bodies, thorn-shaped astrocytes, and tufted astrocytes), and oligodendrocytes (e.g., argyrophilic threads and coiled bodies). In different disorders, tau vary in tau isoform composition and phosphorylation, as well as the filament polymerization, conformation and size (Lee et al., 2001). While tau accumulation in the brain has long been correlated with clinical and neuropathological markers of neurodegeneration, such as cognitive decline and neuronal and synaptic loss, the definitive mechanism(s) of tau toxicity remains unknown (Falke et al., 2003; Guillozet et al., 2003; Ingelsson et al., 2004; Santacruz et al., 2005). The prevailing theory of tau-induced neurotoxicity suggests the effect occurs through synaptic dysfunction (Jadhav et al., 2015).

Table 1.1 Summary of the neuropathological and clinical features of primary, sporadic tauopathies

Tauopathy	Tau Isoform	Tau Aggregate			Primary Clinical Feature(s)
		Neuron	Astrocyte	Oligodendrocyte	
Aging-related tau astrogliopathy (Kovacs et al., 2016a)	4R	N/A	Thorn-shaped astrocyte	N/A	Unknown
Alzheimer's disease (Hyman and Trojanowski, 1997; McKhann et al., 2011)	3R and 4R	Neurofibrillary tangles, and pre-neurofibrillary tangles	N/A	N/A	Progressive cognitive decline, particularly memory
Argyrophilic grain disease (Grinberg and Heinsen, 2009)	4R	Argyrophilic grains, ballooned neurons, and pre-neurofibrillary tangles	Thorn-shaped astrocytes	Coiled bodies	Variable cognitive decline, and behavioural abnormalities
Chronic traumatic encephalopathy (Bieniek et al., 2021; Katz et al., 2021)	3R and 4R	Neurofibrillary tangles pre-neurofibrillary tangles, and dotlike neurites	Deep layer perivascular astrocytes	N/A	Cognitive, motor and psychiatric features with a history of head trauma
Corticobasal degeneration (Armstrong et al., 2013; Dickson et al., 2002)	4R	Corticobasal bodies, neuronal lesions, and thread-like structures	Astrocytic plaques	Coiled bodies	Parkinsonism motor features and cognitive impairment
Globular glial tauopathy (Ahmed et al., 2013)	4R	N/A	Globular astrocytic inclusions	Globular oligodendroglial inclusions, and coiled bodies	Behavioural and cognitive dysfunction, and/or parkinsonism and motor neuron disease
Pick's disease (Cairns et al., 2007; Zhukareva et al., 2002)	3R (limbic structures) and 4R (cerebral cortex and white matter)	Pick bodies and ballooned neurons	Ramified astrocytes	Pick body-like inclusions	Behavioural and cognitive deficits, extrapyramidal signs, and apraxia
Primary age-related tauopathy (Crary et al., 2014)	3R and 4R	Neurofibrillary tangles	N/A	N/A	Cognitive decline
Progressive supranuclear palsy (Collins et al., 1995; Hauw et al., 1994)	4R	Neurofibrillary tangles	Tufted astrocytes	Coiled bodies	Disordered movement including ocular dysfunction, postural instability, and parkinsonism

Tau hyperphosphorylation is a consistent feature of tauopathy (Feany et al., 1995; Grundke-Iqbal et al., 1986b), although each tauopathy has a distinct phosphorylation profile (Samimi et al., 2021). Once tau is hyperphosphorylated, it gains the ability to sequester normal tau and other microtubule-associated proteins resulting in microtubule disassembly, and self-assemble into neuropathological aggregates (Alonso et al., 2001, 1994).

1.4.1. Alzheimer's disease (AD)

AD is the most common tauopathy and cause of dementia in older adults contributing to 60-70% of cases (Alzheimer's Association, 2021). The prevalence of AD is expected to increase as the global population ages presenting a significant socioeconomical burden (Alzheimer's Association, 2021). Overlapping clinical presentation and neuropathology with other neurodegenerative disorders, as well as unknown pathogenesis have impeded the development of definitive diagnostic methods for AD prior to death (Swerdlow, 2007).

1.4.1.1. Clinical Presentation

The present consensus on the clinical criteria for AD was established by the National Institute of Aging and Alzheimer's Association (NIA-AA) in 2011 (McKhann et al., 2011). A diagnosis of AD relies on an initial diagnosis of dementia. Dementia is described as a decrease in cognitive function that interferes with activities of daily life and that is unexplained by delirium or psychiatric disorders. A documented history of cognitive decline is established through self-reporting or interview with knowledgeable informants such as family members, and an objective cognitive assessment is administered by a physician, such as the mini-mental state examination (Folstein et al.,

1975), Montreal cognitive assessment (Nasreddine et al., 2005), the Toronto cognitive assessment (Freedman et al., 2018), and the Behavioural Neurology Assessment (Darvesh et al., 2005). These interviews and tests must support impairment in a minimum of two cognitive domains, including learning, reasoning, visuospatial ability, language, and behaviour.

Impaired cognition, detected by formal cognitive assessment, can be attributed to numerous underlying causes including neurodegeneration, vascular disease, traumatic brain injury, medication side effects or other underlying health conditions such as depression (Knopman and Petersen, 2014). The differentiation of dementia from a diagnosis of mild cognitive impairment (MCI) relies on the demonstration of cognitive impairment on objective testing, but does not interfere with daily living unlike AD (Albert et al., 2011; McKhann et al., 2011; Petersen, 2004). Making the distinction between a clinical diagnosis of MCI or AD is important for clinical treatment and outlook. While MCI presents a higher risk of progression to dementia (Luck et al., 2012; Manly et al., 2008; Petersen, 2004, 2003; Ravaglia et al., 2008) and may encompass the symptomatic prodementia phase of AD, many individuals with MCI do not progress to dementia due to underlying co-morbidities (Ganguli et al., 2019). Other subsets of MCI may not progress significantly, and a lesser proportion of individuals with MCI may revert to normal cognition (Ganguli et al., 2019).

According to NIA-AA criteria (McKhann et al., 2011), dementia is attributable to probable AD if there is an insidious onset and a history indicating progressive cognitive decline. There should be no evidence of alternate explanatory conditions that cause dementia, including significant cerebrovascular events, dementia with Lewy bodies,

frontotemporal dementia, variants of primary progressive aphasia, or a side effect of a medication. The initial or prominent features of the disease course must fall into one of two categories: amnestic presentation, or non-amnestic presentation. Amnestic AD is the most common presentation, and it is characterized by impairment in learning and recall of new information, whereas non-amnestic presenting AD is characterized by predominant visuospatial, language, or executive function impairment.

The Consortium to Establish a Registry for AD (CERAD) developed a standard for the clinical and neuropsychological assessment of AD through consolidating pre-existing clinical batteries, neuropathological staging techniques, and rating scales (Mirra et al., 1991; Morris et al., 1989).

CERAD defines a typical clinical presentation of AD as a gradual onset of memory loss that progressively decline over at least 12 months (Mirra et al., 1991). The clinical battery developed and tested by CERAD was adopted and modified from the National Institute of Neurological and Communicative Disorders and Stroke/Alzheimer's Disease and Related Disorders Associations Work Groups criteria which defined diagnostic confidence in three levels: probable AD, possible AD, and definite AD (McKhann et al., 1984; Morris et al., 1989). Probable AD includes a typical presentation of AD without confounding symptoms that may indicate the involvement of other disorders. Possible AD includes a typical clinical presentation of AD, but with additional atypical symptoms (e.g., aphasia) or potentially contributing co-morbidities (e.g., stroke). Finally, a diagnosis of definitive AD requires clinical dementia with post-mortem neuropathological findings of β -amyloid (A β) plaques and tau NFTs.

Annual cognitive testing which assesses a patient's ability to complete simple tasks related to memory, language, calculation, and visuospatial orientation is used to confirm that there is an initial deficit and monitor the rate of disease progression using available cognitive (Darvesh et al., 2005; Folstein et al., 1975). Additionally, interviews are administered with someone close to the patient to evaluate the patients ability to complete activities of daily living (Erkinjuntti et al., 1988; Morris et al., 1989).

Consensus AD diagnostic criteria has been more recently revised to better reflect clinical heterogeneity, and advances in AD biomarkers (McKhann et al., 2011). Clinical heterogeneity presents a barrier for AD diagnosis. The original criteria centred on a typical amnesic presentation of AD, precluding patients with an atypical presentation from receiving a diagnosis of 'probable AD' (Morris et al., 1989). The revised criteria recognizes predominant language, visuospatial, and executive dysfunction as valid symptoms to meet the confidence threshold for a 'probable AD' clinical diagnosis (McKhann et al., 2011). While amnesic AD is the most common form, atypical variants of AD, such as frontal or behavioural variant AD, posterior cortical atrophy, and progressive aphasia also exist, and are associated with the same pathophysiology (Alladi et al., 2007; Galton et al., 2000). Atypical AD variants are often referred to as focal AD as there is often a clear clinicopathological correlation with atrophy predominantly isolated to specific brain regions (Alladi et al., 2007; Galton et al., 2000). For example, in posterior cortical atrophy, cognitive domains such as memory remain intact until late in the disease course while earlier symptoms predominantly affect visuospatial function. These symptoms correlate with marked atrophy in the parieto-occipital cortex (Benson et al., 1988). In addition to an atypical clinical presentation, a patient could receive a

diagnosis of probable AD if there is clinical evidence of a causative mutation, like family history or early disease onset (McKhann et al., 1984).

The category of possible AD was revised to focus more on unusual features of the disease course, like sudden onset, as well as insufficient or unreliable evidence of cognitive decline (McKhann et al., 2011; Morris et al., 1989). This updated prognosis also described potential co-morbidities such as cardiovascular disease, evidence of other neurodegenerative disorders like early Parkinsonism, and medications that could affect cognition and that disqualify a patient from a probable AD diagnosis (McKhann et al., 2011).

While not mentioned in AD diagnostic criteria, nuclear medical techniques can be used to differentiate AD from other conditions when there is an atypical disease course (Health Quality Ontario, 2014). Computed tomography (CT) scans provide structural images of the brain based on a tissues susceptibility to x-ray penetration (Pasi et al., 2011). Magnetic resonance imaging (MRI) uses a magnetic field and radio waves, causing protons in the water and other molecules in tissue to align with the magnetic field. Sensors detect the energy emitted by the protons as they realign once the field is turned off (Berger, 2002). While structural imaging modalities cannot be used to diagnose AD alone, they can be used to confirm structural changes in the brain that could be associated with the deposition of AD neuropathology. These modalities can also be used to rule out other causes of cognitive impairment, such as stroke (Mendez et al., 1992; Pasi et al., 2011). MRI is used for identical reasons as CT, but can provide higher resolution images that allow for the detection of more subtle structural and vascular changes (Frisoni et al., 2010; Pasi et al., 2011). Supporting evidence for an AD diagnosis

using either CT or MRI includes focal volume loss in the entorhinal cortex (EC) and hippocampus, generalized cortical volume loss, and ventricular enlargement (Frisoni et al., 2010; Pasi et al., 2011).

1.4.1.2. Preclinical diagnostic techniques

Since the introduction of the original CERAD criteria, the field has made significant progress in the development of neuroimaging techniques and cerebral spinal fluid (CSF) and blood-based assays for AD biomarkers (Blennow and Zetterberg, 2018; Hampel et al., 2018). However, the use of AD biomarkers remains a feature of research to increase confidence that clinical symptoms can be attributable to AD pathophysiology (McKhann et al., 2011), although consensus recommendations have recently been made to begin integrating AD biomarkers into clinical use (Dubois et al., 2021; Pemberton et al., 2022).

Positron emission tomography (PET) and single photon emission computed tomography (SPECT) both use radiotracers to visualize neuropathological aggregates, and brain function *in vivo* (Valotassiou et al., 2011). Both imaging modalities work similarly, the difference being that PET scans measure the emission of positrons while SPECT imaging measures gamma rays. Both modalities have different strengths. PET has greater sensitivity and resolution, whereas SPECT has the potential for dual tracer use (Rahmim and Zaidi, 2008). PET radioligands that target A β with [¹¹C]Pittsburgh compound B or [¹⁸F]florbetapir (Clark et al., 2011; Landau et al., 2013), and more recently, tau with [¹⁸F]flortaucipir (Leuzy et al., 2019) are most commonly used to visualize neuropathological burden of A β plaques and tau NFTs respectively. Changes to regional glucose metabolism can also be examined with 2-deoxy-2-[¹⁸F]fluoro-D-glucose

PET or [^{99m}Tc]-hexamethyl propylene amine oxime SPECT in AD patients, who typically exhibit reduced temporoparietal uptake (Coleman, 2005; Valotassiou et al., 2015). Additional PET and SPECT tracers are being developed to target other AD biomarkers such as butyrylcholinesterase (BChE; Darvesh, 2016; DeBay et al., 2017; Macdonald et al., 2010).

The development of CSF and blood-based biomarkers have also focused primarily in detecting changes in A β , tau, and neurofilament light, a marker of neuronal injury, *in vivo* as a lower cost alternative to radioimaging (Blennow and Zetterberg, 2018; Hampel et al., 2018). The abundance of AD biomarkers in patient CSF and blood plasma can be quantified with immune-PCR, immunoassays, or mass spectrometry (Blennow and Zetterberg, 2018; Schröder et al., 2017), although this is not standard of care in Canada (Ismail et al., 2020). While both techniques used identical detection strategies, blood sample collection is less invasive than the lumbar puncture required to extract CSF and most health care professionals are already trained to perform blood draws (Hampel et al., 2018). Increased total tau, phosphorylated tau and neurofilament levels, along with a lower 42-amino acid A β /40-amino acid A β ratio, are associated with clinical AD in CSF (Andreasen et al., 1999; Blennow et al., 1995; Delaby et al., 2022; Dhiman et al., 2020; Grundke-Iqbal et al., 1986a) and blood plasma (Brickman et al., 2021; Jiao et al., 2021; West et al., 2021).

1.4.1.3. Treatment

Treatment of AD is complicated by both limitations in clinical diagnostics and our lack of understanding of AD pathophysiology, thus, preventing the development of more effective pharmacologic therapies. The presence of A β and tau has resulted in a focus on

aggregate clearance through immunization, fueled by positive results in rodent models (Castillo-Carranza et al., 2015; Wilcock et al., 2003). However, all of these trials have failed to produce clinically meaningful results in humans (Giacobini and Gold, 2013; Sandusky-Beltran and Sigurdsson, 2020). Aducanumab, a monoclonal antibody targeting A β (Sevigny et al., 2016), was the first of these immunotherapies approved by the United States Food and Drug Administration in an accelerated process despite a near unanimous vote to reject the drug by their Peripheral and CNS Drugs Advisory Committee. It was stated that the drug's manufacturer, Biogen, failed to present sufficient evidence to correlate biomarker changes with cognitive benefits at the proposed dose, indicating a need for further research to prove it has a positive effect on cognition (Knopman et al., 2021).

The current standard for AD treatment are cholinesterase inhibitors (ChIs), namely rivastigmine, galantamine, and donepezil, which offer modest improvement in cognitive and behavioural symptoms and slows the rate of cognitive decline (Birks, 2006). Memantine, an N-methyl-D-aspartate antagonist, is sometimes used in conjunction with ChIs, enhancing their effects (Matsuzono et al., 2015), and it has been recommended over ChI monotherapy (Schmidt et al., 2015). While ChIs are usually only prescribed for a short period of 3-6 months, evidence suggests that these drugs have long term efficacy from 1-5 years, and offer a stabilizing effect in some patients, allowing them to live at home with a better quality of life for longer (Giacobini et al., 2022). However, many AD patients are not offered ChIs or are prescribed a suboptimal dose (Deardorff and Grossberg, 2016; Giacobini et al., 2022). In addition to exploring novel therapies for AD,

re-evaluation of these approved drugs, and how we use them may improve standard of care for AD patients and reduce healthcare burden (Giacobini et al., 2022).

1.4.1.4. Neuropathological evaluation

In addition to clinical consensus criteria for AD, CERAD also proposed the first major consensus criteria for the neuropathological diagnosis of AD (Mirra et al., 1991).

Gross neuropathological changes of the brain, spinal cord, meninges and vessels should be examined, and any abnormalities noted (Mirra et al., 1991). Such changes should include evidence of cortical atrophy and ventricular enlargement, along with evidence of possible comorbid conditions (e.g., pallor of the substantia nigra and locus coeruleus, the presence of infarcts, hemorrhages, and atherosclerosis).

Microscopic changes are then examined in five brain regions containing the middle frontal gyrus, superior and middle temporal gyrus, inferior parietal lobule, hippocampus and EC, and midbrain including the substantia nigra (Mirra et al., 1991). Histochemical techniques, such as Thioflavin-S or Bielschowsky silver staining, are used for visualization of neuritic plaques and NFTs, and immunohistochemical techniques may alternatively be used to visualize tau. Fibrillar appearing A β plaque and tau NFT abundance is semi-quantitatively scored as sparse, moderate, or frequent in a medium power field (Fig. 1.2). Age-related plaque score is determined to roughly account for the deposition of A β plaque pathology associate with aging, based predominantly on pathology in the frontal, temporal, and parietal cortices. Finally, the clinical history of the patient is integrated with the neuropathological findings. A history of dementia in combination with sufficient neuropathological deposition of A β relative to the patients age at death is required for a neuropathological AD diagnosis. Findings of additional

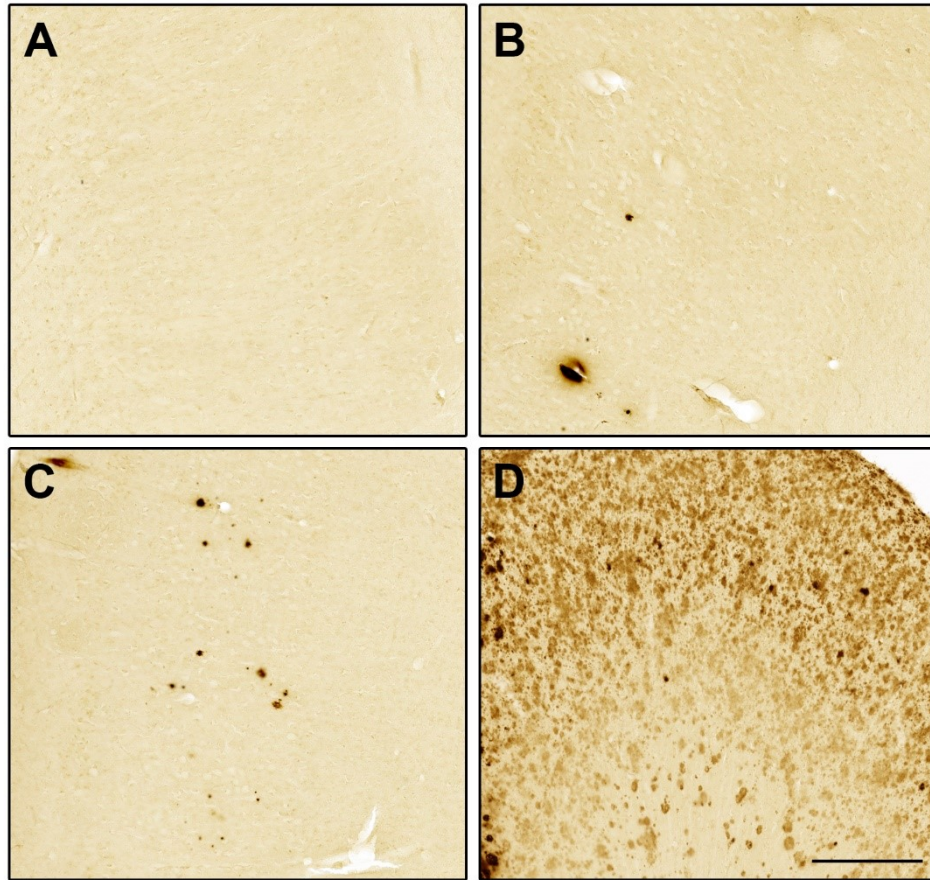


Figure 1.2 Photomicrographs depicted representative fields of view of tissue stained for β -amyloid based on a Consortium to Establish a Registry for Alzheimer's disease plaque score of 0 (A), sparse (B), moderate (C), and frequent (D) (Mirra et al., 1991).

comorbid conditions, such as infarcts associated with vascular dementia, or pallor of the substantia nigra associated with Parkinson's disease, reduce the level of diagnostic confidence that dementia can solely be attributed to AD neuropathology. A neuropathologist must rank concurrent conditions by their suspected contribution to the dementia phenotype.

The NIA-AA proposed a revision to AD neuropathological diagnostic criteria that incorporates the predominant neuropathological staging schemes for A β plaques, tau NFTs, and neuritic plaques throughout the disease course, often referred to as ABC score, and also screens for other common neuropathological aggregates such as α -synuclein (Montine et al., 2012).

The 'A' aspect is based on the Thal phase for A β plaque deposition (Montine et al., 2012; Thal et al., 2002). Localization of A β plaque pathology according to Thal phase is as follows (Thal et al., 2002): no deposition indicates phase 0, deposition in frontal, parietal, temporal, and occipital cortices indicates phase 1, deposition in entorhinal regions, CA1 of the hippocampus and insular cortex indicates phase 2, deposition in specific regions of basal forebrain indicates phase 3, deposition in specific midbrain and medulla structures indicates phase 4, and deposition in specific regions of the pons, and often cerebellum, indicates phase 5. Each sequential phase includes the identification of A β plaque pathology in the regions described in the previous phase.

ABC scoring simplifies Thal phase into four 'A' scores (Montine et al., 2012). A Thal phase of 0 corresponds to an 'A' score of 0, a Thal phase of 1 or 2 would receive an 'A' score of 1, a Thal phase of 3 would receive an 'A' score of 2, and a Thal phase of 4 or 5 would receive an 'A' score of 3 (Montine et al., 2012; Thal et al., 2002).

The 'B' aspect of the ABC score is Braak and Braak staging of tau NFT deposition (Braak et al., 2006; Braak and Braak, 1995; Montine et al., 2012). NFTs are identified in the following structures in each Braak stage: 0 denotes no NFTs identified, I denotes deposition in the transentorhinal region, II indicates deposition in the entorhinal region, III denotes deposition in the fusiform gyrus, IV denotes deposition in the medial temporal gyrus, V denotes deposition in the peristriate region of the occipital lobe, and VI denotes deposition in the parastriate and striate areas of the occipital cortex (Braak et al., 2006; Braak and Braak, 1995). Each stage includes the findings of the previous stages. ABC scoring simplifies Braak stage into four 'B' scores: a Braak stage of 0 corresponds to a 'B' score of 0, a Braak stage of I or II corresponds to a 'B' score of 2, and a Braak stage of V or VI corresponds to a 'B' score of 3 (Montine et al., 2012).

The 'C' aspect of the score incorporates CERAD scoring for neuritic plaques (Mirra et al., 1991; Montine et al., 2012), using either Thioflavin-S or Bielschowsky silver staining. Neuritic plaque deposition is examined in the middle frontopolar gyrus, superior and middle temporal gyrus, and inferior parietal lobule, and assigned a semi-quantitative score of absent, sparse, moderate, or frequent (Fig. 1.2), corresponding to 'C' scores of 0 through 3 respectively.

ABC score is then translated into not, low, intermediate, or high degree of AD neuropathologic change assuming neuropathology characteristic of other neurodegenerative disease (Table 1.2; Montine et al., 2012). Evidence of Lewy body disease, cerebrovascular disease, hippocampal sclerosis, and TAR DNA-binding protein 43 inclusions should also be reported and may indicate a non-AD or mixed diagnosis.

Table 1.2 ABC score for level of Alzheimer’s disease (AD) neuropathological changes

AD neuropathologic change		B		
A	C	0 or 1	2	3
0	0	Not	Not	Not
1	0 or 1	Low	Low	Low
	2 or 3	Low	Intermediate	Intermediate
2	Any C	Low	Intermediate	Intermediate ^e
3	0 or 1	Low	Intermediate	Intermediate ^e
	2 or 3	Low	Intermediate	High

Adapted from Montine *et al.* (2012).

1.5. The Cholinergic System

The cholinergic system refers to the molecular and neuronal networks that utilize the neurotransmitter acetylcholine (ACh; Fig. 1.3A; English and Jones, 2012). ACh is synthesised in neurons expressing the enzyme choline acetyltransferase, which catalyzes the transfer of an acetyl group from acetyl coenzyme A to choline (Taylor and Brown, 1999). Newly synthesized ACh is transported in vesicles bound to vesicular ACh transport and released at the synapse (Taylor and Brown, 1999). ACh can bind to one of two receptor subtypes, ligand-gated nicotinic ACh receptors and G-protein coupled muscarinic ACh receptors (Dani and Bertrand, 2007; van Koppen and Kaiser, 2003). Nicotinic ACh receptors (nAChR) are found in the CNS and peripheral nervous system, and mediate fast, excitatory neurotransmission for processes such as cognitive function as well as synaptic transmission from nerves to muscles (Ho et al., 2020). Muscarinic ACh receptors (mAChR), however, are found in the CNS and parasympathetic nervous system where they modulate neuronal excitability and initiate parasympathetic responses such as smooth muscle contraction or hormone secretion (Ishii and Kurachi, 2006). Cholinergic neurotransmission is co-regulated by the enzymes acetylcholinesterase (AChE) and BChE, which catalyze ACh hydrolysis (Darvesh et al., 2010).

Cholinergic dysfunction is characteristic of AD pathophysiology at different stages in ACh neurotransmission (Ferreira-Vieira et al., 2016). Selective loss of choline acetyltransferase expressing neurons reduces acetylcholine availability (Whitehouse et al., 1981). There is also a selective loss of nAChRs-positive synapses in the hippocampus and cerebral cortex in AD (Oddo and LaFerla, 2006). mAChRs specifically have been implicated with severe dementia associated with impaired mAChR G-protein coupling

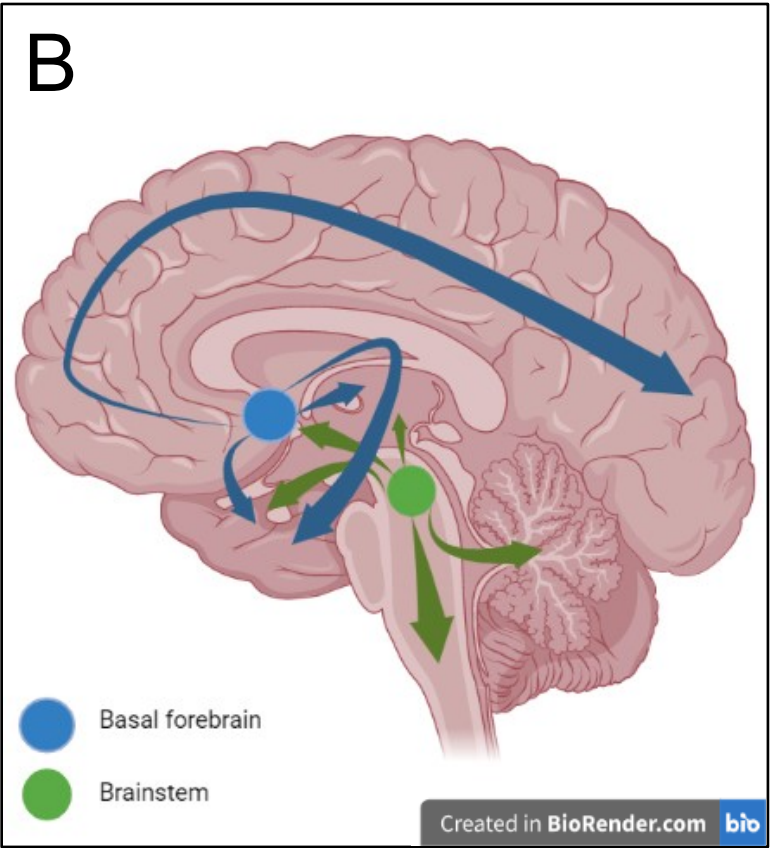
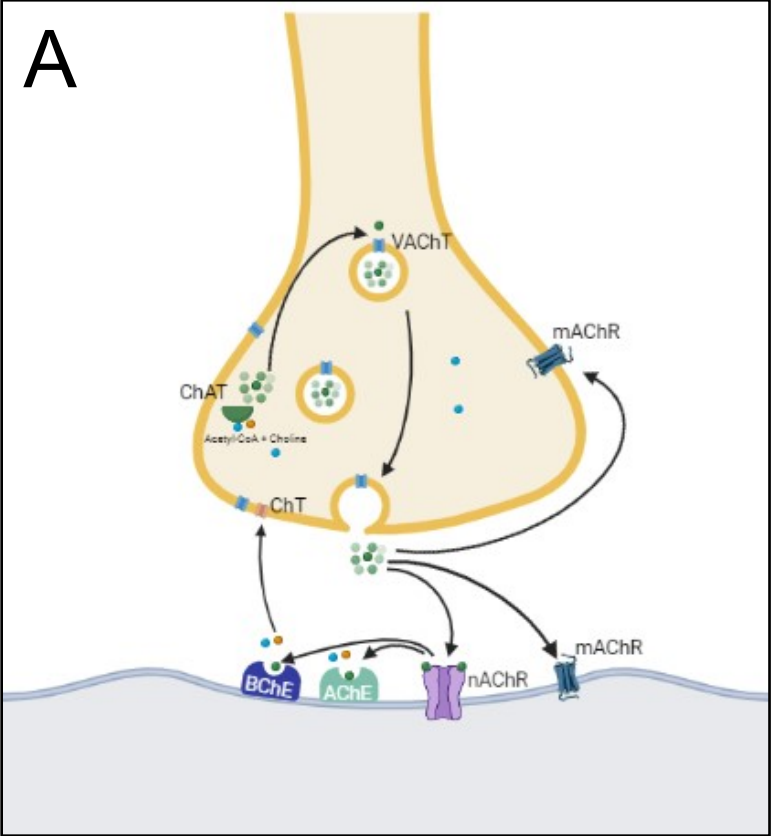


Figure 1.3 The life cycle of acetylcholine (ACh; Adapted from English and Jones, 2012) (A) and cholinergic pathways in the central nervous system (Adapted from Bertrand and Wallace, 2020; Hedreen et al., 1984) (B). ACh is synthesized from acetyl-CoA and choline by the enzyme choline acetyltransferase (ChAT) (A). Acetylcholine is then packaged into vesicles by vesicular ACh transporter (VAChT) and released at the synapse where it can bind to one of two receptor types: the ligand-gated ion channel, nicotinic ACh receptor (nAChR) and the G-protein coupled muscarinic ACh receptors (mAChR). nAChR are post-synaptic and are responsible for rapid depolarization of the cholinergic neuron while mAChR are most notably responsible for presynaptic modulation as well as post synaptic recovery response. Acetylcholinesterase (AChE) and butyrylcholinesterase (BChE) are co-regulators of cholinergic neurotransmission, through the hydrolysis of ACh. The choline molecules this produces can be taken up into the presynaptic terminal by choline transporters, to produce more ACh. The basal forebrain and brainstem are the two main cholinergic centres of the central nervous system (B). Basal forebrain cholinergic neurons project to the cerebral cortex, hippocampal formation, amygdala olfactory bulb, and thalamus whereas brainstem cholinergic neurons project to the basal ganglia, thalamus, hypothalamus, amygdala, basal forebrain, cerebellum, and the periphery.

(Tsang et al., 2006). mAChRs agonists been shown to reduce A β production (Buxbaum et al., 1992) and tau phosphorylation (Forlenza et al., 2000) providing an alternative target for AD therapeutics. Finally, and most pertinent to this thesis, ACh degradation, particularly in the cerebral cortex, is dysregulated (Darvesh et al., 2010; Geula and Mesulam, 1989a; Macdonald et al., 2017).

1.5.1. Cognition and the Cholinergic System

Cholinergic neurotransmission is responsible for cognition in the CNS, as well as chemical transmission at the neuromuscular junction, autonomic nervous system, and the peripheral nervous system (English and Jones, 2012). The CNS has two main cholinergic pathways (Fig. 1.3B). The magnocellular basal forebrain is comprised of cholinergic neurons in the nucleus basalis of Meynert (nbM), medial septal nucleus (MS) and diagonal band of Broca (Hedreen et al., 1984). Cholinergic neurons in the nbM project to the neocortex, while those in both the MS and the diagonal band of Broca project to the hippocampus and the olfactory system (Bertrand and Wallace, 2020). Additionally, the MS has neurons which project to the EC, and amygdala (Bertrand and Wallace, 2020; Liu et al., 2018). The brainstem cholinergic pathway has cholinergic neurons in the pedunculopontine nucleus and pontine tegmental nucleus which project to the thalamus and basal forebrain (Bertrand and Wallace, 2020).

Pharmacological, lesion, and functional MRI studies have implicated cholinergic neurotransmission in executive function, learning and memory (Blokland, 1995; Newman et al., 2012). The nbM and the MS are involved in cognition due to their projection to frontal cortices and the hippocampus (Blokland, 1995; Newman et al., 2012). The contribution of cholinergic neurons of the nbM to cognition has been further

demonstrated by their role in AD. There is a significant loss of neurons in the nbM in AD (Whitehouse et al., 1981), and reduced expression of choline acetyltransferase in frontal and temporal cortices (Bartus et al., 1982; Wilcock et al., 1982). These findings resulted in the formation of the cholinergic hypothesis of AD, that observed cognitive decline is associated with cholinergic dysfunction (Bartus et al., 1982).

1.5.2. Cholinesterases

AChE and BChE are serine hydrolases which coregulate cholinergic neurotransmission through the degradation of ACh (Darvesh et al., 2003a; Leuzinger, 1969). Historically, early work demonstrated that only AChE had a critical role in neural development (Bigbee et al., 1999), and nerve impulse transmission (Hawkins and Gunter, 1946; Mendel et al., 1943) caused research exploring the physiological function of BChE to stagnate for decades until its use as protection against organophosphate poisoning was demonstrated (Broomfield et al., 1991). AChE knock-out mice express several developmental delays, behavioural deficits, motor dysfunction and experience early death in adulthood from seizures or loss of gastrointestinal function, but are still viable (Duysen et al., 2002). AChE mutations that result in a loss of function have not been identified in humans, implying fetal lethality (Lockridge et al., 2016). However, BChE knock-out mice (Li et al., 2008), and humans who express one of the 34 identified BChE mutations which result in a loss of the enzyme function (Lockridge et al., 2016; Manoharan et al., 2007) are healthy. Interest in BChE grew as it's physiological redundancy meant its use does not interfere with other systems for clinical applications (Lockridge et al., 2016). Additionally, BChE was demonstrated to regulate cholinergic neurotransmission in the brain (Mesulam et al., 2002).

The enzymatic activity of both AChE and BChE is due to a 20-Å deep active site gorge containing a catalytic triad of serine, histidine, and glutamate residues (Nicolet et al., 2003; Sussman et al., 1991). The different substrate affinities of AChE and BChE is attributable to the aromatic residues present in the gorge, with AChE expressing 10 while BChE expresses 4 (Harel et al., 1992; Radić et al., 1993). This accounts for the different kinetic response to ACh concentrations, namely AChE is very efficient approaching diffusion controlled rates at low concentrations of ACh but is inhibited at high concentrations (Silver, 1974; Szegletes et al., 1999). BChE, however, is more efficient at low concentrations of ACh (Silver, 1974).

In addition to terminating cholinergic neurotransmission, several ‘non-classical’ roles can be attributed to AChE and BChE in humans (Silman, 2021). AChE acts as an adhesion molecule in certain contexts, such as at the neuromuscular junction (Rotundo et al., 2008) and during embryonic development (Genever et al., 1999; Paraoanu et al., 2006). AChE, and potentially BChE, may have a direct trophic effect on neurite outgrowth and synapse development (Silman, 2021; Sternfeld et al., 1998) and AMPA receptor potentiation (Olivera et al., 2003). Both cholinesterases are capable of hydrolyzing a wide range of esters (Silman, 2021), with BChE notably able to hydrolyze heroin (Williams et al., 2019) and cocaine (Stewart et al., 1977) demonstrating a potential for use as a clinical detoxicant (Larrimore et al., 2020). BChE may also have a specific role in regulating the hunger hormone ghrelin in plasma (Chen et al., 2015). Interactions via the peripheral anionic site of cholinesterases may promote A β fibril formation in AD (De Ferrari et al., 2001). The rapid rate at which AChE hydrolyzes ACh results in the accumulation of protons creating a more acidic microenvironment, which may have

localized effects such as increased ion channel generation (Silman, 2021). Finally, AChE is necessary during apoptosis for formation of the apoptosome (Park et al., 2004) and its function as a DNase (Du et al., 2015).

1.5.3. Normal Cholinesterase Distribution

AChE and BChE have distinct patterns of distribution in the normal brain (Darvesh et al., 1998; Darvesh and Hopkins, 2003; Green and Mesulam, 1988; Mesulam and Geula, 1991). AChE-positive neurons are observed throughout the cerebral cortex, hippocampus and other subcortical structures (Mesulam et al., 1983; Mesulam and Geula, 1991; Selden et al., 1998). AChE is consistently associated with cholinergic and cholinceptive neurons, and cholinergic positive fibres are visible at the terminal ends of medial and lateral cholinergic pathways (Mesulam et al., 1983; Mesulam and Geula, 1991; Selden et al., 1998). Neuronal expression of BChE is less widespread, and is found in distinct neuronal populations in the amygdala, hippocampal formation and thalamus (Darvesh et al., 1998; Darvesh and Hopkins, 2003). BChE is also expressed in cortical white matter and glial cells (Darvesh et al., 1998; Darvesh et al., 2010; Darvesh and Hopkins, 2003; Mesulam et al., 2002).

1.5.4. Cholinesterases in AD

Cholinesterase expression in the brain is altered in AD. Decreased AChE activity and increased BChE activity in the cerebral cortex, as well as the association of cholinesterase activity with A β plaques throughout the brain, are features of AD (Darvesh et al., 2010; Geula and Mesulam, 1989a; Macdonald et al., 2017). Due to low expression of BChE in the normal cerebral cortex compared to AChE, increased BChE activity in the cerebral cortex has been proposed as an ideal diagnostic biomarker for AD (Darvesh,

2016; DeBay et al., 2017; Macdonald et al., 2017). BChE associates with a subset of predominantly fibrillar A β plaques associated with AD rather than non-fibrillar A β plaques often observed in cognitively normal older adults (Fig. 1.4; Macdonald et al., 2017). It has been proposed that BChE may be involved in the maturation of benign, non-fibrillar plaques to neurotoxic, fibrillar plaques observed in AD (Darvesh et al., 2012; Mesulam and Geula, 1994; Reid and Darvesh, 2015). Cholinesterase have also been observed to associate with tau NFTs in AD (Cash et al., 2021; Gomez-Ramos et al., 1992; Hamodat et al., 2017; Mesulam and Asuncion Morán, 1987). In turn, BChE has not been shown to associate with tau pathology in corticobasal degeneration or frontotemporal dementia, α -synuclein pathology in dementia with Lewy bodies or infarcts in vascular dementia (Fig. 1.5; Macdonald et al., 2017). The importance of cholinesterase expression to AD pathophysiology is also demonstrated by the use of cholinesterase inhibitors for the treatment of AD to increase ACh availability (Birks, 2006; Giacobini et al., 2022).

1.6. Thesis Objective and Hypothesis

It has been an aim of the Darvesh Research Group to identify more sensitive and specific biomarkers for AD. Imaging techniques, the only window into the brain during an AD patient's lifetime, have predominantly focused on structural changes and the aggregates associated with AD pathophysiology, namely A β plaques and tau NFTs. However, none of these features are specific to AD. The development of diagnostics targeting a sensitive and specific biomarker for AD are a necessary step for optimal clinical management of the disease and to determine applicability of therapies as they are discovered.

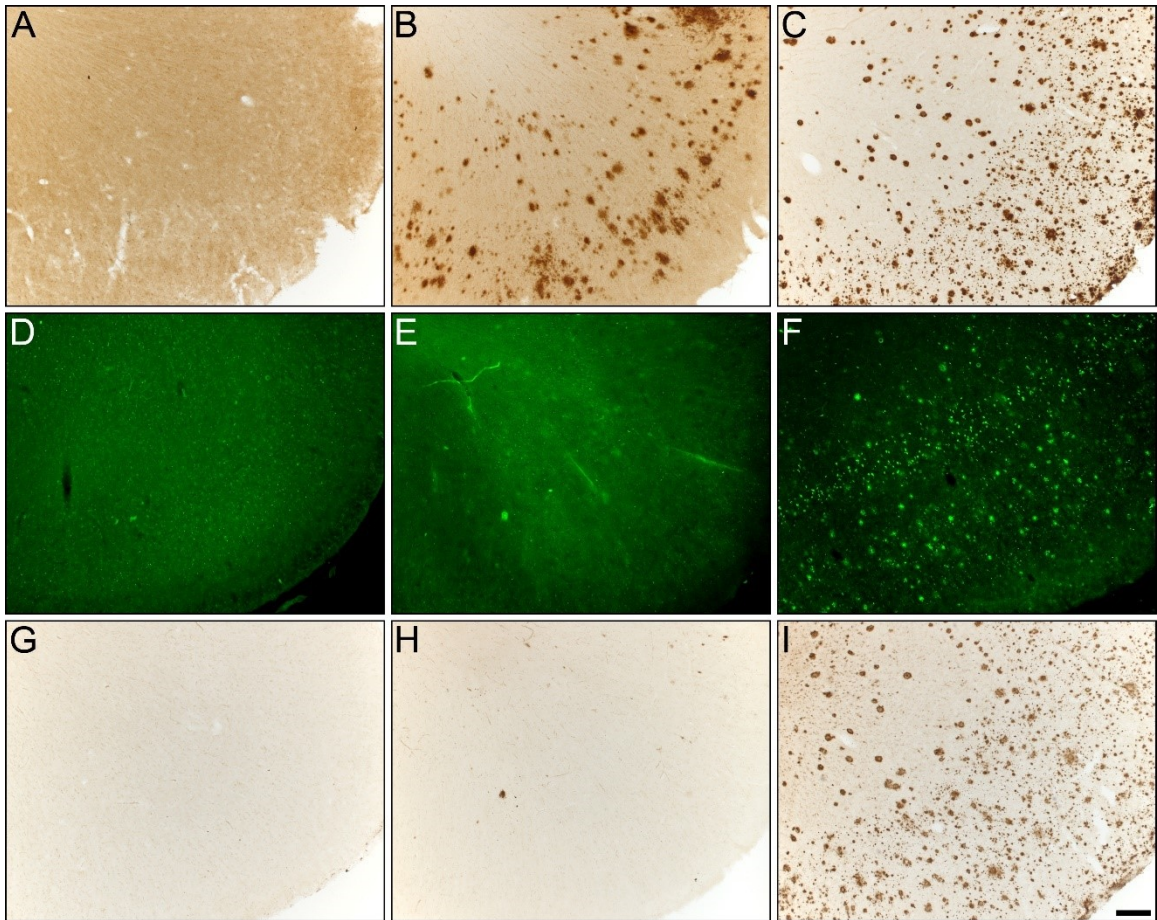


Figure 1.4 Photomicrographs of post-mortem human orbitofrontal cortex from normal (A,D,G), cognitively normal with A β plaques (NwA β ; B,E,H), and AD (C,F,I) brains stained for amyloid- β (A,B,C), thioflavin-S (D,E,F), and butyrylcholinesterase (BChE, G,H,I). Note, no BChE staining in normal orbitofrontal cortex (G), paucity of BChE activity associated with NwA β brain pathology (H), and significant BChE activity in AD (I). Scale bar for all frames (A-I) = 250 μ m (Macdonald et al., 2017).

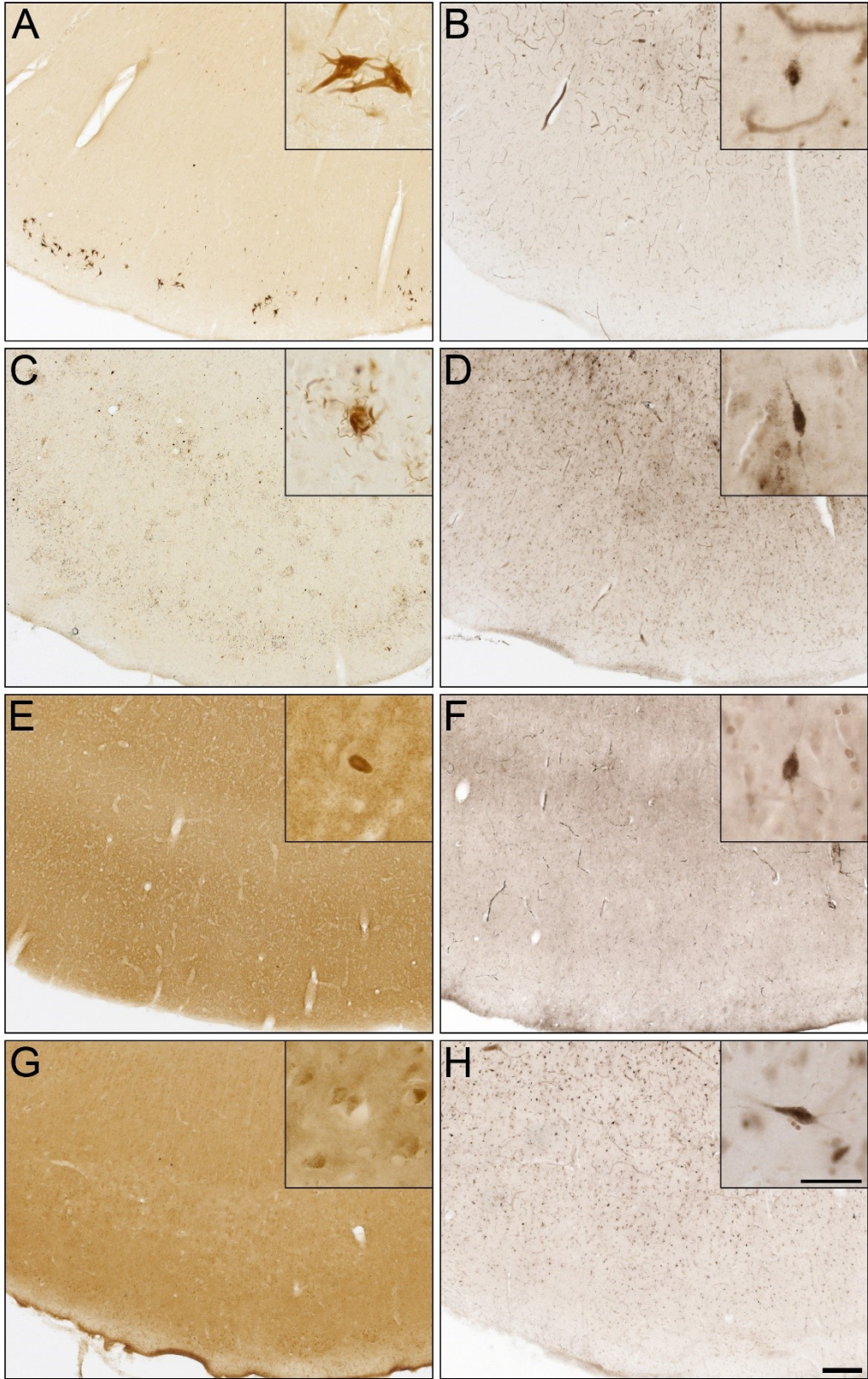


Figure 1.5 Photomicrographs of post-mortem human entorhinal cortex from corticobasal degeneration (A,B), frontotemporal dementia with tau (C,D), dementia with Lewy bodies (E,F), and vascular dementia (G,H) stained for tau 3R (A), tau 4R (C), α -synuclein (E), A β (G), and butyrylcholinesterase (BChE) activity (B,D,F,H). Note, insets are higher magnification photomicrographs demonstrating examples of the pathology observed in each of the neurodegenerative diseases including neurofibrillary tangles (A), neuropil threads and degenerating neurites (C), Lewy bodies (E), and intraneuronal inclusions (G). Note, BChE staining was limited to a few scattered cortical neurons (insets B,D,F,H) and did not label pathological structures in these neurodegenerative diseases. Scale bars = 250 μ m, insets 50 μ m (Macdonald et al., 2017)

The objective of this thesis was to examine clinicopathological correlates and the specificity of neurodegeneration-associated proteins in tauopathy and aging.

Cholinesterase expression, particularly BChE, was further evaluated as a potential biomarker for AD compared to octogenarians and older, and PSP to validate its use as a sensitive and specific diagnostic target for the disease.

We hypothesized that neuropathological aggregates would not correlate well with clinical outcomes in tauopathy and aging, nor would they be specific to neurodegenerative disease when compared to aged individuals. Additionally, we hypothesized that BChE would be sensitive and specific to AD-associated neuropathology.

1.7. Chapter Overviews

The following three chapters outline work to address the objective of this thesis, to identify clinicopathological correlates in tauopathy and aging and to evaluate the specificity and sensitivity of BChE as a biomarker for AD.

Chapter 2 describes and compares neuropathological and cholinesterase expression in several regions vital to cognition within human cognitively normal octogenarians and older and AD brains. This study sought to establish the abundance of neuropathology in a very old population and identify if AChE and BChE associate with plaque pathology differently than previous studies in a younger normal population (Macdonald et al., 2017).

Chapter 3 describes neuropathological and cholinesterase expression in the rostral prefrontal cortex, a region implicated in executive function in the tauopathies PSP and AD, and in cognitively normal human brains. This study sought to evaluate the

specificity of AChE and BChE to AD associated neuropathology relative to the tau-positive glial aggregates characteristic of PSP.

In Chapter 4, we described a novel Canadian family with a rare *MAPT* mutation. Clinical and neuropathological findings are compared within the family and to three previously reported families with the same mutation. This study sought to examine clinicopathological correlates in tauopathy with a known cause.

Chapter 5 consolidates the findings of the previous chapters and offers a discussion of future directions pertaining to the association of neuropathology with neurodegeneration and evaluating the role of BChE in AD. The significance of this thesis will then be contextualised within current literature and discussed.

1.8. Authorship

All work included herein was predominantly investigated, curated, analyzed, visualized, and written by the student.

CHAPTER 2 Clinicopathological Correlates in Aging: Neuropathology and Cholinesterase Expression in Octogenarians and Older

2.1. Publication Status

Published manuscript presented with permission.

S.P. Maxwell, M.K. Cash, S. Darvesh. Neuropathology and cholinesterase expression in the brains of octogenarians and older. *Chem. Biol. Interact.* 364. DOI:

10.1016/j.cbi.2022.110065

2.2. Overview

The following chapter examines expression of neuropathological aggregates and cholinesterases in the rostral prefrontal cortex and hippocampal formation of cognitively normal octogenarians and older compared to Alzheimer's disease to explore the concept of neuropathological resiliency.

2.3. Abstract

A subset of octogenarians and older maintain normal cognitive function (CNOO) despite high prevalence and incidence of cognitive decline attributed to neurodegeneration or aging in the population. The rostral prefrontal cortex (rPFC) and hippocampal formation are brain regions integral to cognition, namely attention and memory, facilitated in part by cholinergic innervation. We hypothesized that preserved cholinergic neurotransmission in these regions contributes to intact cognition in the CNOO. To test this, we evaluated the burden of neuropathological and cholinesterase-associated protein aggregates in the rPFC and hippocampal formation. Tissues from age- and sex-matched CNOO and Alzheimer's disease (AD) rPFC and hippocampal formation were stained for β -amyloid ($A\beta$), tau, α -synuclein, phosphorylated TAR DNA-binding

protein 43 (pTDP-43), acetylcholinesterase (AChE), and butyrylcholinesterase (BChE). The relative abundance of neuropathological aggregates was semi-quantitatively scored. Deposition of A β plaques, tau neurofibrillary tangles (NFT) and pTDP-43 inclusions were comparable between CNOO and AD cases. Intraneuronal A β and tau-positive thorny astrocytes consistent with aging-related tau astrogliopathy, were also noted in the rPFC. Abundance of BChE-positive plaque pathology was significantly higher in AD than in CNOO cases in most regions of interest, followed closely by abundance of AChE-positive plaque pathology. BChE and AChE activities were also associated with varied NFT morphologies. CNOO cases maintained cognition despite a high neuropathological burden in the rPFC and hippocampal formation. BChE-positive and, to a lesser extent, AChE-positive pathologies were significantly lower in most regions in the CNOO compared to AD. This suggests a specificity of cholinesterase-associated neuropathology with AD. We conclude that while CNOO have cholinesterase-associated neuropathology in the rPFC and hippocampal formation, abundance in this population is significantly lower compared to AD which may contribute to their intact cognition.

2.4. Introduction

Successful aging, as defined by Rowe and Kahn (Rowe and Kahn, 1997), requires the absence of disease and disease-related disability, high cognitive and physical function, and active engagement with life. The global population of the oldest-old, defined as individuals at least 80 years and older, is projected to triple between 2015 and 2050 (He et al., 2016). However, this population has the highest prevalence of age-related neurodegenerative disorders (Hou et al., 2019), such as Alzheimer's disease (AD) (Alzheimer's Association, 2021), as well as age-related cognitive decline separate from

pathological neurodegenerative processes (Murman, 2015). Given that a decline in cognitive function correlates with a lower quality of life (Hussenoeder et al., 2020), it is vital to understand how certain individuals age successfully.

A subset of the oldest-old, the cognitively normal octogenarians and older (CNOO), do not exhibit cognitive decline (Qiu and Fratiglioni, 2018). The prevailing hypotheses for successful brain aging in this population relies on cognitive reserve (Stern, 2002). β -amyloid ($A\beta$) (Jansen et al., 2015), tau (Nelson et al., 2012), α -synuclein (Mikolaenko et al., 2005), and phosphorylated TAR DNA-binding protein 43 (pTDP-43) (Nascimento et al., 2018) aggregates are common in normal older adult brains. Therefore, mechanism(s) must exist to compensate for pathological changes allowing for neural processes, such as cognitive function, to be maintained (Stern, 2002). Protective lifestyle factors which may affect cognitive reserve have been identified including education, exercise, social interaction, and several others (Livingston et al., 2020). Higher education, for example, has been correlated with increased functional connectivity in older adults (Chen et al., 2019). However, the mechanism(s) by which other neuroprotective factors act to increase cognitive reserve have not been elucidated. Frailty, a collective decline in physiological function, also influences clinical outcomes in the oldest-old with less frail individuals having a lower incidence of dementia despite high neuropathological load (Wallace et al., 2020).

The rostral prefrontal cortex (rPFC; Raz et al., 1997) and hippocampus (Nobis et al., 2019; Schuff et al., 1999) have been identified as regions that undergo volume loss in the aging brain. These regions are also implicated in many facets of cognition, such as memory (Preston and Eichenbaum, 2013; Squire, 1992) and executive function

(Funahashi, 2017; Reuben et al., 2011; Rossi et al., 2009). While hippocampal atrophy has been consistently observed in AD (De Leon et al., 1997; Jack et al., 1999) and is a predictor of conversion from mild cognitive impairment to AD (Jack et al., 1999), the rPFC is an understudied area under both physiological and pathological conditions.

Both the rPFC and hippocampus are richly innervated by cholinergic projections, with the rPFC receiving cholinergic innervation from the nucleus basalis of Meynert and the hippocampus receiving major cholinergic input from the medial septal nucleus and vertical limb of the diagonal band nucleus (Mesulam et al., 1983; Mesulam and Geula, 1988). Cholinergic neurotransmission is vital to cognition, as cholinergic dysfunction leads to cognitive and behavioural disturbances in AD (Coyle et al., 1983). This includes the loss of the neurotransmitter, acetylcholine, and reduced activity of its synthesizing enzyme, choline acetyltransferase and its hydrolyzing enzyme, acetylcholinesterase (AChE) (Davies and Maloney, 1976; Perry et al., 1978; Wilcock et al., 1982). Butyrylcholinesterase (BChE), an enzyme which co-regulates acetylcholine hydrolysis with AChE, has increased or unchanged activity in AD (S. Darvesh et al., 2010; Perry et al., 1978). AChE and BChE activities are associated with A β plaques and tau neurofibrillary tangles (NFTs) in AD (S. Darvesh et al., 2010; Geula and Mesulam, 1995; Macdonald et al., 2017). However, increased cortical BChE activity has been shown to have preferential accumulation in fibrillar plaques in AD compared to diffuse plaques typically observed in cognitively normal brains (Darvesh et al., 2012; Macdonald et al., 2017; Mesulam and Geula, 1994). The importance of cholinergic signalling is further demonstrated by the effectiveness of cholinesterase inhibitors in improving cognitive function and, consequentially, daily living in AD patients (Birks, 2006).

Based on the above observations, we hypothesized that preservation of the cholinergic system in the rPFC and hippocampal formation is one means by which cognition is maintained in the CNOO. We examined and compared the neuropathological load and cholinesterase involvement within the rPFC and hippocampal formation of CNOO and AD brains to test the hypothesis that cholinergic preservation is a potential mechanism of optimal cognitive aging. Neuropathological burden of A β , tau, α -synuclein, and pTDP-43, as well as AChE and BChE activities, were assessed in the rPFC and hippocampal formation in these two groups.

2.5. Materials and Methods

2.5.1. Brain Tissues

Post-mortem brain tissues were obtained from the Maritime Brain Tissue Bank (Halifax, Nova Scotia, Canada) with approval from the Nova Scotia Health Research Ethics Board. These included sex- and age- matched brains from 10 CNOO and 10 AD cases. In this study, CNOO cases were defined as individuals who were 80 years and older with no clinical history of dementia, and AD cases fulfilled clinical (McKhann et al., 2011) and neuropathological (Montine et al., 2012) diagnostic criteria for AD. Demographic details of all cases are summarized in Table 2.1.

Brains were bisected at the midline during autopsy with half of the brain used for neuropathological diagnosis by a neuropathologist, and the other half sent to the Maritime Brain Tissue Bank. The latter half, once received by the Maritime Brain Tissue Bank, was cut into 1-2 cm coronal slabs, then immersion fixed in 10% formalin in 0.1 M

Table 2.1 Demographic details

	Case	Sex	Age (y)	Brain Weight (g)	Braak Stage (Braak et al., 2006)	CERAD Plaque Score (Mirra et al., 1991)
Cognitively Normal Octogenarians and Older (CNOO)	CNOO1	F	82	1240	IV	Sparse
	CNOO2	F	86	1430	IV	Moderate
	CNOO3	F	89	1294	III	Sparse-Moderate
	CNOO4	F	96	1303	III	Moderate-Frequent
	CNOO5	F	109	1065	VI	Moderate-Frequent
	CNOO6	M	89	1365	II	Sparse
	CNOO7	M	91	1195	II	Sparse
	CNOO8	M	92	1386	III	Moderate-frequent
	CNOO9	M	93	1650	III	Moderate-frequent
	CNOO10	M	101	1126	II	Sparse
Alzheimer's disease (AD)	AD1	F	87	1030	VI	Frequent
	AD2	F	91	1210	VI	Frequent
	AD3	F	92	1009	IV	Frequent
	AD4	F	93	990	V	Frequent
	AD5	F	99	1024	V	Frequent
	AD6	M	86	1440	VI	Frequent
	AD7	M	92	1230	IV	Frequent
	AD8	M	90	1350	VI	Frequent
	AD9	M	92	1149	VI	Frequent
	AD10	M	98	1066	V	Frequent

phosphate buffer (PB; pH 7.4) at 4 °C for 1-7 days. Tissue blocks from the rPFC and hippocampal formation were cryoprotected in increasing concentrations of sucrose, ranging from 10% to 40% in PB, for approximately 2 days at each concentration. Tissue was stored in 40% sucrose in PB with 0.6% sodium azide at 4 °C prior to sectioning. Note, hippocampal tissue was unavailable for case CNOO7 due to excessive white matter degeneration.

The cryoprotected tissue blocks from the rPFC and hippocampal formation were cut with a Leica SM2000R microtome (Leica Microsystems Inc., Nussloch, Germany) with a Physitemp freezing stage and BFS-40MPA controller (Physitemp Instruments LLC, Clifton, NJ, United States) in 50 µm coronal sections. Sections were stored in 40% sucrose with 0.6% sodium azide in PB at -20 °C until they were required for staining experiments ranging from 10% to 40% in PB, for approximately 2 days at each concentration. Tissue was stored in 40% sucrose in PB with 0.6% sodium azide at 4 °C prior to sectioning. Note, hippocampal tissue was unavailable for case CNOO7 due to excessive white matter degeneration.

2.5.2. Immunohistochemical staining

Standard immunohistochemical techniques were employed using specific primary antibodies (Table 2.2) to detect A β plaques, tau NFTs and neuropil threads (NTs), α -synuclein Lewy bodies and neurites, and pTDP-43 cytoplasmic inclusions and dystrophic neurites.

All tissue sections were rinsed in PB for 30 min. Sections to be stained for A β underwent antigen retrieval which included a rinse with 0.5 M PB for 5 min, followed by

Table 2.2 Antibodies used for immunohistochemical staining

Antibody	Host Animal	Dilution	Manufacturer	Catalogue Number
Polyclonal anti-amyloid- β -peptide	Rabbit	1:400	Invitrogen, Rockford, IL, United States	71-5800
Polyclonal anti-human tau	Rabbit	1:16,000	DakoCytomation, Santa Clara, CA, United States	A0024
Monoclonal anti- α -synuclein	Mouse	1:200	Invitrogen, Frederick, MD, United States	18-0215
Monoclonal anti-TAR DNA-binding protein 43, phospho-Ser409/410 (Clone 11-9)	Mouse	1:48,000	Cosmo Bio, Tokyo, Japan	CAC-TIP-PTD-M01

a rinse in distilled water (dH₂O) for 15 min, gentle agitation in 95% formic acid for 2 min, then five rinses in dH₂O for 1 min, and a final rinse in PB for 30 min. All sections were placed in 0.3% hydrogen peroxide (H₂O₂) in PB for 30 min to quench endogenous peroxidase activity after which they were rinsed in PB for 30 min. Sections to be stained for α -synuclein and pTDP-43 underwent antigen retrieval, which included incubation in 0.01 M citrate buffer (pH 6.0) at 80 °C for 30 min followed by a 30 min rinse in PB. All sections were incubated overnight (16-18 h) in PB with 0.1% Triton X-100, normal goat serum (1:100) and the appropriate primary antibody at room temperature. Afterwards, sections were rinsed for 30 min in PB and incubated in PB with 0.1% Triton X-100, normal goat serum (1:1000) and the corresponding biotinylated secondary antibody (1:500) at room temperature for 1 h. Sections were then rinsed in PB for 30 min and incubated in PB with 0.1% Triton X-100 and the Vectastain Elite ABC kit (1:182; PK-6100, Vector Laboratories, Burlingame, CA, United States) according to manufacturer's instructions at room temperature for 1 h. After rinsing in PB for 30 min, sections were developed in 1.39 mM 3,3'-diaminobenzidine tetrahydrochloride (DAB) in PB for 5 min. For every mL of DAB, 50 μ L of 0.3% H₂O₂ in PB was added to each section. The reaction was stopped by rinsing sections in 0.01 M acetate buffer (pH 3.3) for 30 min. In control experiments, no staining was observed when the primary antibody was omitted. All sections were mounted on slides and coverslipped for examination with brightfield microscopy.

2.5.3. Histochemical staining

A thionin stain for Nissl substance was used to visualize cytoarchitecture of the rPFC and hippocampal formation as well as a counterstain for immunohistochemically

stained α -synuclein and pTDP-43 sections as previously described (Hamodat et al., 2017).

Histochemical staining to visualize AChE and BChE activities was performed using a modified (Darvesh et al., 2010) Karnovsky-Roots method (Karnovsky and Roots, 1964). All reagents were purchased from Sigma-Aldrich (St. Louis, MO, United States). Tissue sections were rinsed in 0.1 M maleate buffer (MB; pH 7.4) for 30 min, then placed in 0.15% H₂O₂ in MB for 30 min to quench endogenous peroxidase activity. Following a 30 min rinse in MB, the sections were incubated in the Karnovsky-Roots solution between 3 and 120 h depending on the fixation time of individual cases. The solution contained 0.5 mM sodium citrate, 0.47 mM cupric sulphate, 0.05 mM potassium ferricyanide, 0.8 mM butyrylthiocholine iodide (BChE substrate), and 0.01 mM BW 284 C 51 [1,5-bis (4-allyl dimethylammoniumphenyl) pentan-3-one dibromide] (AChE-specific inhibitor) in MB at pH 6.8 or 8.0. A pH of 6.8 was used to visualize cholinesterase activity associated with neuropathological structures while a pH of 8.0 was used to visualize cholinesterase activity associated with normal neural structures including neurons and glia for parcellation of cytoarchitecture (Geula and Mesulam, 1989a). Sections were rinsed for 30 min in dH₂O before being placed in 0.1% cobalt chloride in dH₂O for 10 min. Following a rinse for 30 min in PB, the tissue was incubated in 1.39 mM DAB in PB for 5 min. Sections were developed with the addition of 50 μ L of 0.15% H₂O₂ in PB per mL of DAB solution. To stop the reaction, sections were rinsed in 0.01 M acetate buffer (pH 3.3) for 30 min.

Histochemical procedures for the visualization of AChE activity were like that of BChE except 0.4 mM acetylthiocholine iodide (AChE substrate) was used in the presence of 0.06 nM ethopropazine (BChE-specific inhibitor).

Control experiments were carried out to ensure specificity of AChE and BChE staining as described previously (Darvesh et al., 2010). All sections were mounted on slides and coverslipped for examination with brightfield microscopy.

2.5.4. Data analysis

Sections containing the rPFC and hippocampal formation were analyzed and photographed with a Zeiss Axio Scan.Z1 slide scanner with Zen 3.1 Blue Edition software (Carl Zeiss Canada Ltd, Toronto, Canada). Photomicrographs were colour balanced, brightness adjusted and assembled using Adobe Photoshop (CS 5, Version 12.0, San Diego, CA, United States).

Regions of interest were parcellated using sections stained for Nissl substance with thionin and cholinesterase activity at pH 8.0. After, the abundance, morphology and distribution of pathology stained with A β , tau, α -synuclein, pTDP-43, and for AChE and BChE activity at pH 6.8 was examined in the rPFC of the middle frontopolar gyrus (Fig. 2.1), herein referred to as rPFC, dentate gyrus (DG), hippocampus (cornu Ammonis (CA1-3)), subicular complex (subiculum, presubiculum (PrS), and parasubiculum (PaS)), and entorhinal cortex (EC). Unless specified, descriptions of pathological load in the hippocampal formation are typically provided for the region identified as the hippocampal body (Ding and Van Hoesen, 2015). In cases where both the hippocampal body and head (Ding and Van Hoesen, 2015) were present, we found the hippocampal

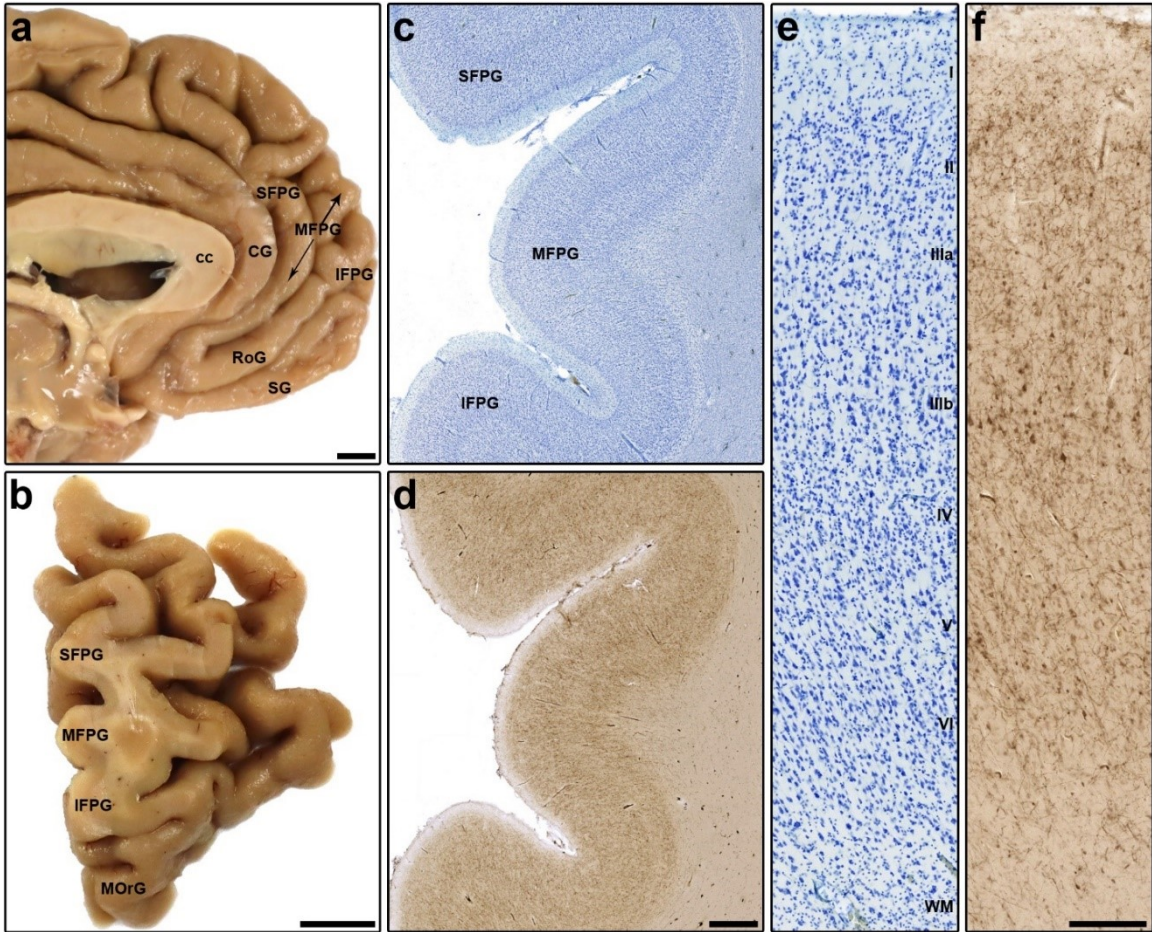


Figure 2.1 Photomicrographs of the medial (a) and coronal (b) views of the middle frontopolar gyrus (MFPG) in the frontal lobe of the human brain, and the rostral prefrontal cortex (rPFC) at the level of the MFPG (c, d) stained for Nissl substance with thionin (c, e) and acetylcholinesterase (AChE; d, f) to demonstrate cytoarchitecture of the region. Note, the granularity of the cortex and sublaminated layer III as distinct characteristics of the rPFC (e), and moderately stained AChE-positive fibers in layers I, II, III and V (f). Scale bars = 1 cm (a, b), 1 mm (d), and 250 μ m (f). Abbreviations: corpus callosum, cc; cingulate gyrus, CG; inferior frontopolar gyrus, IFPG; middle frontopolar gyrus, MFPG; medial orbital gyrus, MOrG; rostral gyrus, RoG; superior frontopolar gyrus, SFPG; straight gyrus, SG; white matter, WM

head generally reflected a similar pathological deposition as in the hippocampal body. Regional abundance of A β , AChE, and BChE plaques, tau NFTs and NTs, Lewy bodies and neurites, and pTDP-43 cytoplasmic inclusions and dystrophic neurites was analyzed and scored for each case using a semi-quantitative neuropathological approach as described previously: 0, no pathology; 1, sparse pathology; 2, moderate pathology; 3, frequent pathology (Hamodat et al., 2017).

Mean neuropathological scores for A β , AChE, and BChE plaques, tau NFTs, and pTDP-43 cytoplasmic inclusions were compared between the CNOO and AD groups in each region of interest via an independent T-test. Significant differences between mean neuropathological scores were denoted as follows: * $p < 0.05$; ** $p < 0.01$; *** $p < 0.001$. Mean neuropathological scores were also compared between sexes in the CNOO and AD groups, as well as between the CNOO and AD groups within each sex (Supplementary Information, Supplementary Tables A.1-A.4). All statistical comparisons were performed using SPSS (IBM Corp, Armonk, NY, United States).

2.6. Results

Sections stained for Nissl substance using thionin, as well as AChE activity at pH 8.0 was used to parcellate the rPFC (Fig. 2.1), and hippocampal formation (Fig. 2.2). This permitted the neuropathological scoring of A β -, AChE- and BChE-positive plaques, tau NFTs, α -synuclein Lewy bodies, and pTDP-43 neuronal cytoplasmic inclusions (NCIs) within each region of interest.

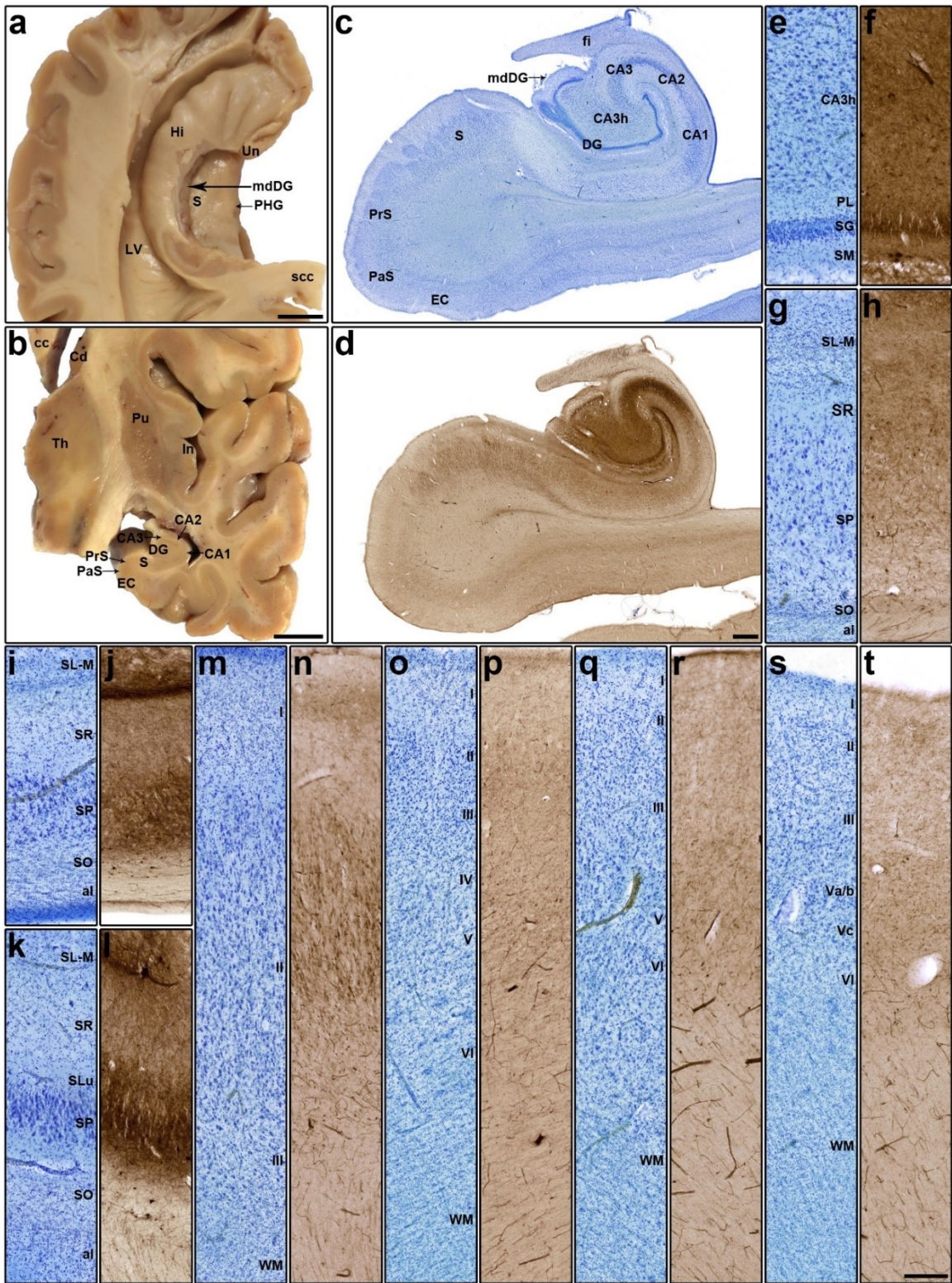


Figure 2.2 Photomicrographs of horizontal (a) and coronal (b) views of the hippocampal formation in the temporal lobe of the human brain. Sections stained for Nissl substance with thionin (c, e, g, i, k, m, o, q, s) and acetylcholinesterase (d, f, h, j, l, n, p, r, t) depict the hippocampal formation (c, d) and lamination of each subregion including dentate gyrus (e, f), cornu Ammonis (CA) 1 (g, h), CA2 (i, j), CA3 (k, l), subiculum (m, n), presubiculum (o, p), parasubiculum (q, r), and entorhinal cortex (s, t). Note, the fimbria has been removed in (a) to identify the rounded protrusions of the margo denticulatus of the dentate gyrus (mdDG). Scale bars = 1 cm (a, b), 1 mm (d) 250 μ m (t). Abbreviations: alveus, al; Cornu ammonis, CA; CA3 (hilar extent), CA3h; dentate gyrus, DG; entorhinal cortex, EC; fimbria, fi; hippocampus, HI; lateral ventricle, LV; margo denticulatus of the dentate gyrus, mdDG; parasubiculum, PaS; parahippocampal gyrus, PHG; polymorphic layer, PL; presubiculum, PrS; subiculum, S; splenium of corpus callosum, scc; stratum granulosum, SG; stratum lacunosum-moleculare, SL-M; stratum lucidum, SLu; stratum moleculare of the dentate gyrus; SM-DG; stratum oriens, SO; stratum pyramidale, SP; stratum radiatum, SR; uncus, un; white matter, WM.

2.6.1. Parcellation of the rostral prefrontal cortex (rPFC)

Cytoarchitectural organization of the rPFC in humans was first described by Brodmann (Brodmann, 2006), then adopted and further subdivided by Ongür *et al.* (Öngür *et al.*, 2003). Brodmann's area 10, or frontopolar area, approximates the rPFC and is comprised of the anterior quarter of the superior and middle frontal gyri on the lateral aspect of the brain, bounded by the callosomarginal gyrus medially and the superior rostral sulcus inferomedially (Fig 2.1a, b; Brodmann, 2006). Ongür *et al.* roughly adopted Brodmann's area 10 but extended it further on the medial surface and subdivided it into three regions: 10m occupying the most caudal medial frontal surface, 10r rostral to 10m, and 10p occupying the frontal pole (Öngür *et al.*, 2003). Nissl substance staining of all three regions reveals a neocortex with relatively thick granular layers and a sublaminated layer III. The subdivisions of Brodmann's area 10 differ in the thickness of granular layers II and IV, and in the development of layer III regarding the number of large pyramidal neurons (Öngür *et al.*, 2003). We examined 10p, based on Ongür *et al.*'s description of a six layered cortex with thick layers II and IV and a well-developed sublaminated layer III (Fig. 2.1c and e) with moderately stained AChE-positive fibers in layers I, II, III and V (Fig. 2.1d and f; Öngür *et al.*, 2003).

2.6.2. Parcellation of the hippocampal formation

Parcellation of the hippocampal formation (Fig. 2.2a, b) was originally described by Ramón y Cajal (Cajal, 1995), except for the parasubiculum, which was first described by Brodmann (Brodmann, 2006). Later, parcellation of the hippocampal formation was extended by Insausti and Amaral (Insausti and Amaral, 2012), Insausti *et al.* (Insausti *et al.*, 2017), and Ding and Van Hoesen (Ding and Van Hoesen, 2015). Sections stained for

Nissl substance (Fig. 2.2c), and AChE at pH 8.0 (Fig. 2.2d) were used to demarcate regions of the hippocampal formation (Darvesh et al., 1998; Ding and Van Hoesen, 2015; Green and Mesulam, 1988) which is comprised of the DG, hippocampus, subicular complex, and EC.

The DG consists of the molecular, granular, and polymorphic layers (Fig. 2.2e and f). The superficial, medial aspect of the DG is known as margo denticulatus (Fig. 2.2a and c; Klingler, 1948). The margo denticulatus is a topographical feature of the DG, so named because of the tooth-like or serrated projections that protrude along its medial surface (Fig. 2.2a). It is important to distinguish margo denticulatus from the hilar aspect as we observed differential distribution of pathology in the DG.

The hippocampus is divided into layers consisting of the alveus fiber tract, stratum oriens, stratum pyramidale, stratum lucidum, stratum radiatum, and stratum lacunosum-moleculare from the most superficial to deepest layer (Fig. 2.2g-l; Ding and Van Hoesen, 2015; Insausti and Amaral, 2012). Stratum pyramidale was originally subdivided into four regions, namely CA1-4 (Lorente De Nó, 1934), although more recent examination of the cytoarchitecture and connectivity in the region has suggested it should be divided into three regions, CA1-3 (Fig. 2.2c, d; Insausti and Amaral, 2012), which we adopted herein.

The subicular complex is comprised of the subiculum, presubiculum, and parasubiculum (Fig. 2.2c and d) We adopted the division of the subiculum into molecular (I), pyramidal (II) and polymorphic (III) cell layers (Fig. 2.2m and n; Bakst and Amaral, 1984; Kobayashi and Amaral, 1999). Laminar distribution in the presubiculum (Fig. 2.2o and p) has also been iterative with the most recent understanding resulting in a six-

layered structure divided into a molecular layer (I), rounded pyramidal layers (II and III), lamina dissecans (IV), deep layers V and VI (Fig. 2.2i and j; Insausti et al., 2017). The parasubiculum (Fig. 2.2q and r) is identical in layer composition to the presubiculum with the exception of a discontinuous lamina dissecans at this level (Insausti et al., 2017).

Finally, the EC (Fig. 2.2c, d) was originally designated as a singular region, area 28, by Brodmann (Brodmann, 2006). Later, Brodmann's parcellation of the EC was adopted and expanded by Green and Mesulam (Green and Mesulam, 1988) and Insausti *et al.* (Insausti et al., 2017). Sections stained for Nissl substance with thionin (Fig. 2.2c) and for AChE activity (Fig. 2.2d) correlated with Brodmann area 28b (Brodmann, 2006), also known as the caudal limiting subfield, which is bordered medially by the lower lip of the hippocampal fissure and laterally by the posterior transentorhinal cortex (Insausti et al., 2017). At this level, the EC is composed of five layers (Fig. 2.2s, t). A thick molecular layer I surrounds layer II which is composed of distinct cell islands containing pyramidal neurons and stellate cells (Insausti et al., 2017; Witter et al., 2017). Layer III is a radially oriented external pyramidal layer (Insausti et al., 2017). In this extent of the EC, lamina dissecans (IV) is absent (Insausti et al., 2017), thus layers III and V are fused together. Layer V, the internal pyramidal layer, is comprised of larger, radially oriented pyramidal neurons with sublaminar layers Va and b indistinguishable at this level while Vc increases in width (Insausti et al., 2017). A homogenous layer VI contains a mixture of multipolar and pyramidal neurons (Canto et al., 2008; Insausti et al., 2017).

2.6.3. Rostral Prefrontal Cortex Pathology

Overall, a frequent abundance of A β plaques was observed in the rPFC of all CNOO and AD cases (Table 2.3), with the greatest deposition of plaques observed in

Table 2.3 Statistical analysis of the mean neuropathological aggregate scores in regions of interest related to cognitive function in cognitively normal octogenarians and older (CNOO) compared to Alzheimer’s disease (AD) brains

Region	A β Plaques			Tau Neurofibrillary Tangles			pTDP-43 Neuronal Cytoplasmic Inclusions			AChE Plaques			BChE Plaques		
	CNOO Mean Score (SD)	AD Mean Score (SD)	p value	CNOO Mean Score (SD)	AD Mean Score (SD)	p value	CNOO Mean Score (SD)	AD Mean Score (SD)	p value	CNOO Mean Score (SD)	AD Mean Score (SD)	p value	CNOO Mean Score (SD)	AD Mean Score (SD)	p value
rPFC ^a	3.00 (0)	3.00 (0)	1	0.70 (0.68)	2.10 (0.88)	<0.001***	0 (0)	0.40 (0.97)	0.223	2.20 (1.32)	3.00 (0)	0.087	2.30 (1.25)	3.00 (0)	0.111
DG	1.78 (1.48)	2.50 (0.85)	0.222	1.67 (0.87)	2.40 (0.84)	0.079	0.89 (1.36)	1.10 (1.37)	0.741	1.13 (1.36)	2.22 (0.97)	0.072	0.89 (1.27)	3.00 (0)	0.001**
CA1	1.44 (1.33)	2.50 (0.85)	0.063	2.78 (0.67)	3.00 (0)	0.347	0.89 (1.27)	1.10 (1.29)	0.724	1.00 (1.32)	2.00 (0.94)	0.073	0.89 (1.17)	3.00 (0)	<0.001***
CA2	0.44 (0.72)	0.90 (0.99)	0.275	1.78 (1.09)	2.50 (0.71)	0.102	0 (0)	0.50 (0.71)	0.052	0.14 (0.38)	1.13 (0.35)	<0.001***	0.22 (0.44)	1.40 (1.08)	0.008**
CA3	1.11 (1.45)	1.10 (0.99)	0.985	1.11 (0.78)	2.50 (0.85)	0.002**	0.33 (0.5)	0.50 (0.71)	0.565	0.29 (0.49)	1.25 (0.71)	0.01*	0.78 (0.97)	1.60 (1.08)	0.1
S	1.78 (1.39)	2.70 (0.68)	0.098	2.22 (0.97)	3.00 (0)	0.043*	0.78 (1.09)	1.20 (1.31)	0.46	1.11 (1.45)	2.10 (0.74)	0.094	0.78 (0.97)	2.70 (0.48)	<0.001***
PrS	2.33 (1.32)	3.00 (0)	0.169	1.89 (0.78)	2.80 (0.42)	0.005**	0.44 (0.53)	0.50 (0.97)	0.881	1.22 (1.39)	2.60 (0.84)	0.023*	1.56 (1.24)	3.00 (0)	0.008**
PaS	1.78 (1.30)	3.00 (0)	0.023*	1.89 (0.93)	2.67 (0.71)	0.063	0.22 (0.44)	0.50 (0.93)	0.457	0.78 (1.09)	2.50 (0.93)	0.003**	1.00 (0.87)	2.78 (0.44)	<0.001***
EC	2.33 (1.32)	3.00 (0)	0.169	2.78 (0.67)	3.00 (0)	0.347	0.33 (0.50)	1.20 (1.40)	0.093	1.11 (1.27)	2.40 (0.84)	0.017*	1.44 (1.13)	3.00 (0)	0.003**

^aRegions: CA, cornu Ammonis; DG, dentate gyrus; EC, entorhinal cortex; PaS parasubiculum; PrS, presubiculum; rPFC, rostral prefrontal cortex; S, subiculum

laminar layers III-V, and lesser deposition in remaining layers (Fig. 2.3a and b). Additionally, three CNOO cases had A β -positive neurons comprised of several morphologically distinct neuronal subtypes (e.g., multipolar and bipolar neurons) located predominantly in the middle laminar layers (III-V; Fig. 2.3b).

The rPFC was spared of tau NFTs in all but two CNOO cases and was variably affected in all AD cases. Thus, a significant difference in deposition was noted between the two groups ($p = 0.001$; Table 2.3). In CNOO and AD cases with tau neuropathology, NFT deposition was most abundant in layers III-V, with sparse deposition in remaining layers (Fig. 2.3c, d). NTs were deposited in a similar pattern to NFT deposition in both groups. Tau neuritic plaques, consisting of tau aggregates in dystrophic neurites (DNs) surrounding A β plaques (He et al., 2018), were present in one AD (layer V) and one CNOO (spanning III-V) case (not shown). Tau-positive thorn-shaped astrocytes morphologically consistent with aging-related tau astroglialopathy (ARTAG; Kovacs et al., 2016b) were observed in the white matter at the level of the middle frontopolar gyrus of two CNOO cases (Fig. 2.4a).

α -Synuclein and pTDP-43 deposits were not observed in the CNOO rPFC. Sparse α -synuclein aggregates, including extracellular Lewy body-like inclusions, a Lewy body and a Lewy neurite (Alafuzoff et al., 2009; McKeith et al., 2005), were observed in two AD cases (not shown). Two AD cases had pTDP-43 NCIs and DNs, one sparse and one frequent in abundance (Table 2.3; not shown).

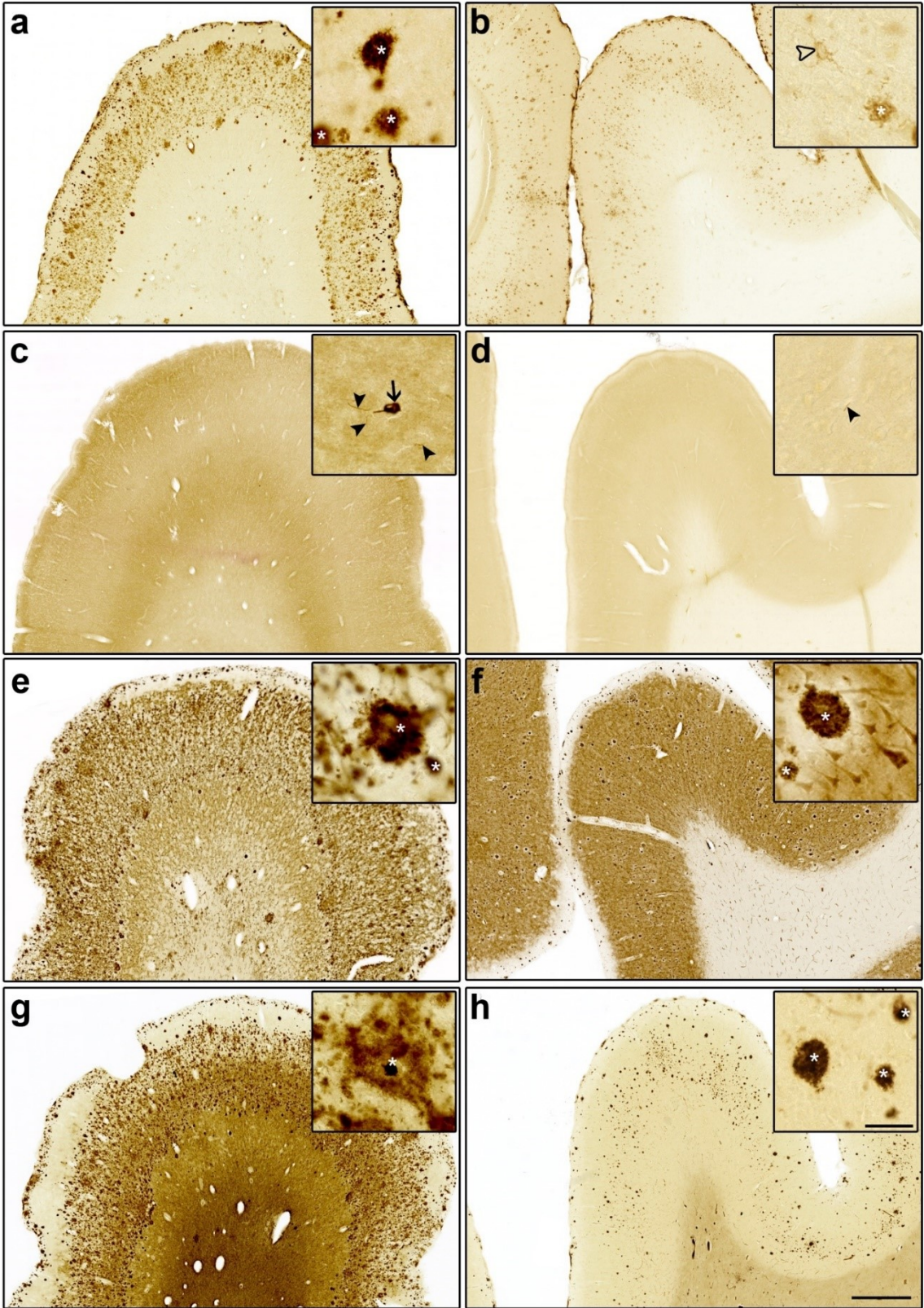


Figure 2.3 Photomicrographs of neuropathological deposits in the Alzheimer's disease (a, c, e, g) and cognitively normal octogenarian and older (b, d, f, h) rostral prefrontal cortex, stained for β -amyloid (a, b), tau (c, d), acetylcholinesterase (e, f), and butyrylcholinesterase (g, h). Note, plaques are denoted by white asterisks, tau neurofibrillary tangles by arrows, tau neuropil threads by arrowheads, and intraneuronal β -amyloid by an open arrowhead. Scale bars = 1 mm, inset 50 μ m.

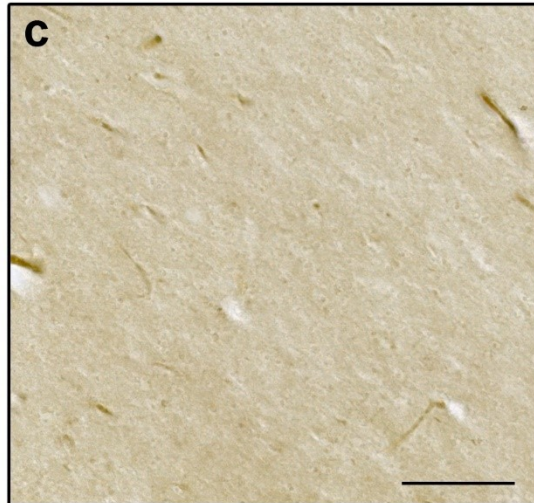
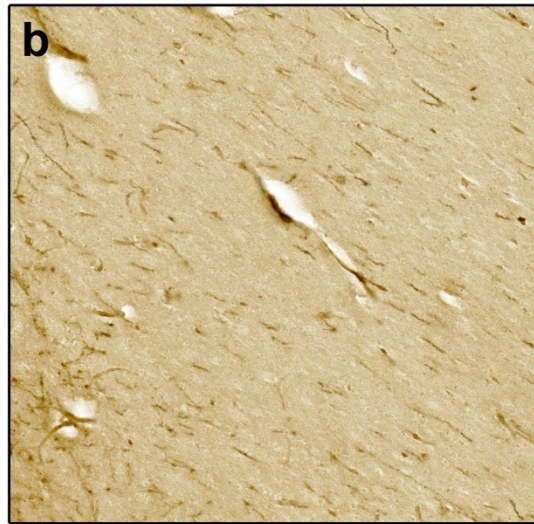
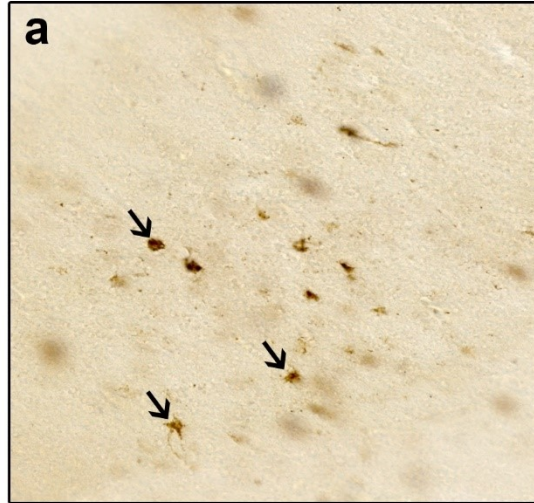


Figure 2.4 Photomicrographs of tau staining of thorn-shaped astrocytes (arrows) morphologically consistent with aging-related tau astrogliopathy in the white matter of the rostral prefrontal cortex at the level of the medial frontopolar gyrus (a). The thorn-shaped astrocytes were not stained for acetylcholinesterase (b) or butyrylcholinesterase (b) in the same region. Scale bar = 100 μm .

AChE- and BChE-positive plaque load in the rPFC was not significantly different in CNOO compared to AD cases (Table 2.3). All cases with cholinesterase-positive plaques had frequent deposition in layers III-V (Fig. 2.3e-h). Remaining layers of the rPFC also had frequent cholinesterase-positive plaque deposition, albeit to a lesser degree than in layers III-V, in AD cases and sparse to moderate cholinesterase-positive plaque deposition in CNOO cases. Of cases that had A β plaques in the rPFC, only CNOO7 did not have cholinesterase-positive plaques. Additionally, AChE and BChE activities did not appear to associate with A β -positive neurons as noted above in three CNOO cases (Fig. 2.3f and h). Likewise, of the cases with ARTAG, neither AChE nor BChE activity associated with tau thorn-shaped astrocytes in the white matter (Fig. 2.4b and c).

2.6.4. Dentate Gyrus Pathology

In the DG, A β plaques were predominantly located in the molecular layer of both CNOO and AD cases with deposition in remaining layers ranging from absent to sparse. The margo denticulatus of the DG had a greater abundance of A β plaques regardless of deposition elsewhere in the DG in all AD cases (Fig. 2.5a) and in three CNOO cases (Fig. 2.5b). A β plaques in the margo denticulatus were primarily confined to the molecular layer, although in AD cases with frequent plaque abundance, plaque deposition occasionally extended into the granular and polymorphic layers.

Tau NFT deposition in the DG of AD and CNOO cases was not significantly different although CNOO cases tended to have a lower tau neuropathological burden ($p = 0.079$; Table 2.3). There was no distinct laminar distribution of NFTs that unified AD or CNOO cases. However, NT distribution was consistently greater in the molecular and polymorphic layers than in the granular layer of all cases (Fig. 2.5c and d). Tau-positive

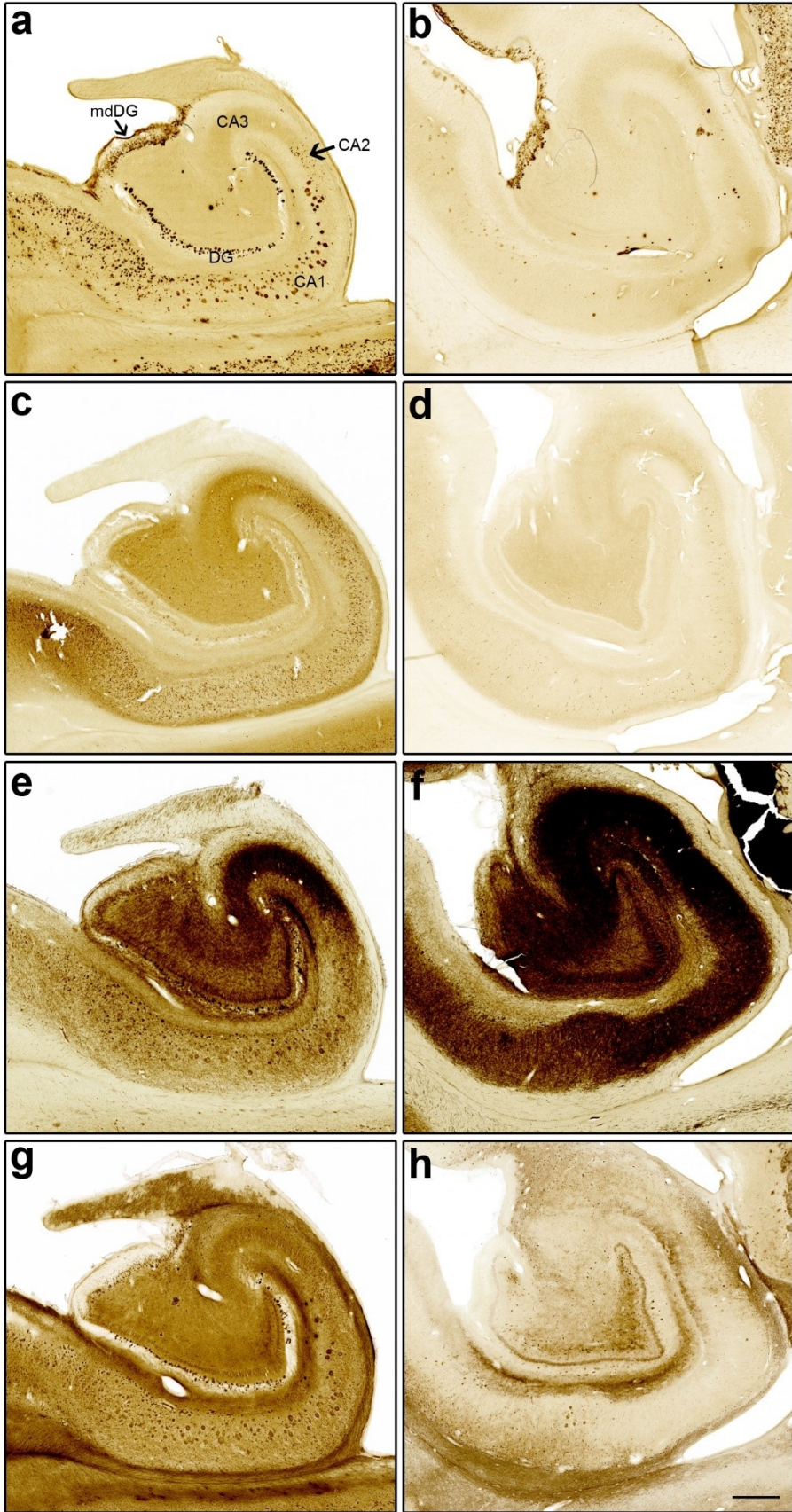


Figure 2.5 Photomicrographs of neuropathological deposits in the Alzheimer's disease (a, c, e, g) and cognitively normal octogenarian and older (b, d, f, h) dentate gyrus (DG) and cornu Ammonis 1-3 (CA1-3) stained for β -amyloid (a, b), tau (c, d), acetylcholinesterase (e, f), and butyrylcholinesterase (g, h). Note, deposition of β -amyloid plaques at the surface of the margo denticulatus of the dentate gyrus (mdDG; a, b) is not fully recapitulated by cholinesterase staining (e-h). Scale bar = 1 mm.

neuritic plaques were commonly observed in the molecular and polymorphic layers in AD cases but were less abundant in CNOO cases (not shown).

α -Synuclein pathology was absent in the AD and CNOO DG, except for a single α -synuclein-positive astrocytic star-like inclusion, as shown previously (Terada et al., 2000), in the polymorphic layer of a CNOO case (not shown).

In the DG, pTDP-43-positive NCIs were predominantly observed in the granular layer with infrequent, sparse NCIs in the molecular or polymorphic layers (Fig. 2.6a, c, f). Scattered to sparse DNPs were identified in all layers of the DG.

AChE-positive plaque pathology in the DG was not observed in all cases due to dark, AChE-positive neuropil in this region (Fig. 2.5f). However, in cases where pathology could be discerned, AChE-positive plaque burden was not significantly different between AD and CNOO cases ($p = 0.072$; Table 2.3). In those cases, the molecular layer had the greatest abundance of AChE-positive plaques (Fig. 2.5e and f). Remaining layers had no or sparse AChE-positive plaques. Few AChE-positive plaque deposits were noted at the margo denticulatus, particularly in the superficial aspect of the molecular layer (Fig 2.5e and f).

BChE-positive plaque load was significantly higher in the DG of AD cases compared to CNOO cases ($p = 0.001$; Table 2.3). Like AChE, the molecular layer had the greatest deposition of BChE-positive plaques, with absent or sparse BChE-positive plaques in remaining layers (Fig. 2.5g and h). BChE-positive pathology also did not recapitulate $A\beta$ plaque deposition in the margo denticulatus (Fig. 2.5g and h)

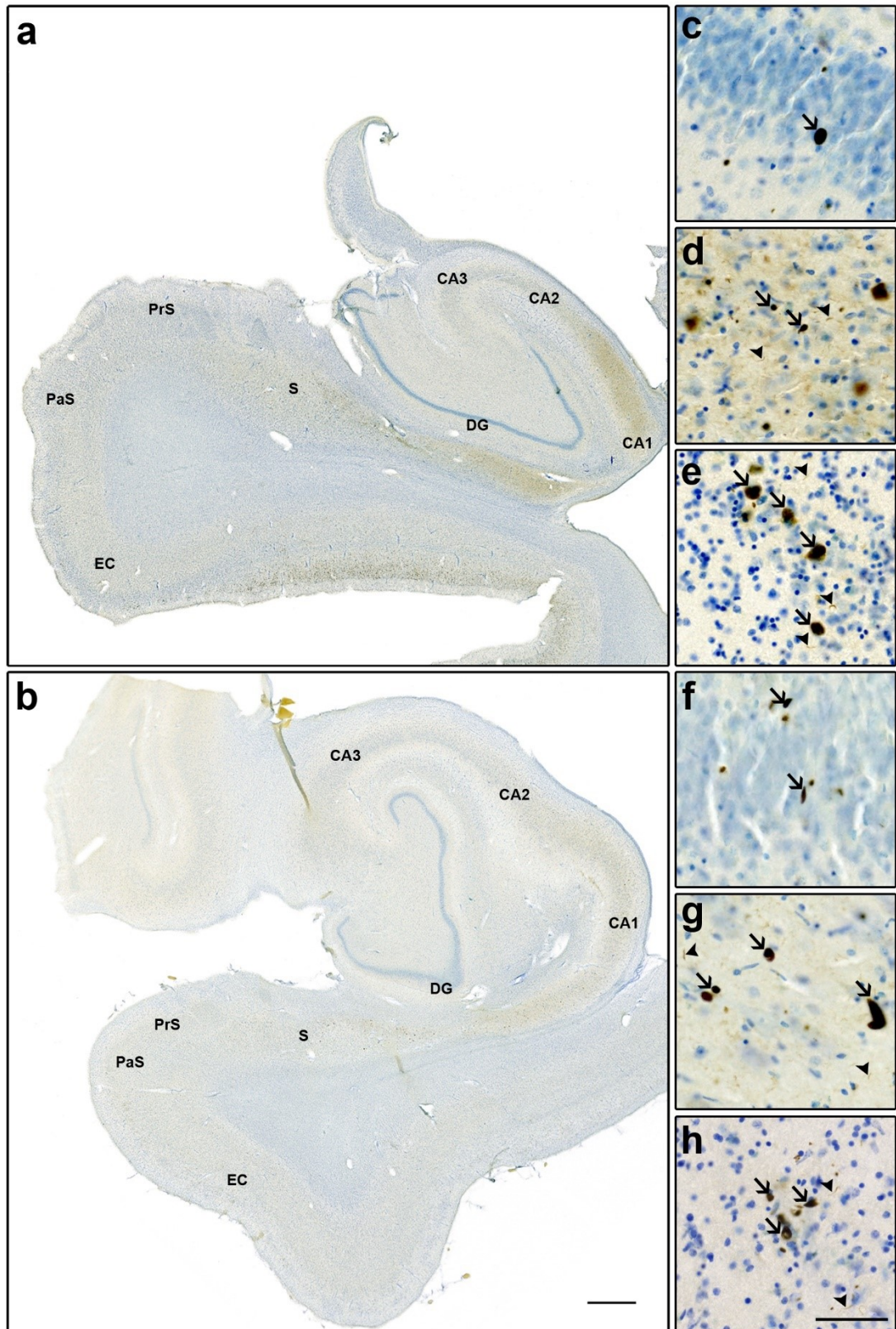


Figure 2.6 Photomicrographs of the Alzheimer's disease (a, c-e) and cognitively normal octogenarian or older (b, f-h) hippocampal formation stained for phosphorylated TAR DNA-binding protein 43 (pTDP-43) and counter stained for Nissl substance with thionin. Higher power examples of neuronal cytoplasmic inclusions (arrows) and dystrophic neurites (arrowheads) are noted in the granular layer of the dentate gyrus (c, f), cornu Ammonis 1 (CA1) (d, g), and layer II of the entorhinal cortex (e, h). Scale bars = 1 mm (low power), and 50 μ m (high power). Abbreviations: cornu Ammonis, CA; dentate gyrus, DG; entorhinal cortex, EC; parasubiculum, PaS; presubiculum, PrS; subiculum, S.

2.6.5. Hippocampal Pathology

In the hippocampus, CA1 had the most abundant A β plaque load overall (Table 2.3) with deposition increasing in abundance from the dorsal extent to the ventral extent, followed by the stratum radiatum underlying CA1-3 in CNOO and AD cases (Fig. 2.5a and b). CA2 had the lowest plaque abundance in both CNOO and AD cases, and was the region most frequently spared of A β plaques (Table 2.3). Similarly, CA3 was often spared of A β plaques in both groups, but when A β pathology was present, it was often greater in the hilar region (Table 2.3). Sparse plaques were observed in remaining layers over- and underlying CA1-3. In addition to plaque pathology, A β -positive NFTs, described elsewhere (Lacosta et al., 2017; Perry et al., 1992), were commonly observed in the pyramidal neurons of CA1 and CA2 in both AD and, to a lesser extent, CNOO cases (not shown).

Regarding tau pathology, CA1-3 was consistently the most affected region in the hippocampus (Fig. 2.5c and d). CA1 had the greatest abundance of NFTs in both groups. CA2 was intermediately affected by NFT pathology compared to CA1 and CA3 in CNOO cases, whereas NFT abundance was similar in CA2 and CA3 in AD cases (Table 2.3). CA3 was the only region of the hippocampus where tau NFT deposition in AD was significantly greater than in CNOO cases ($p = 0.002$; Table 2.3). Tau NFT deposition in the CA3 of most AD and CNOO cases was comparable in the hilar and dorsal extent. Deposition of tau NTs mirrored that of NFTs, including in CA1 where an increase in abundance was noted from the dorsal extent to the ventral extent. Tau-positive neuritic plaques were most common in CA1 and CA3 and rarely noted in CA2 of AD and CNOO cases.

CA1 was the most prominent region of α -synuclein deposition in the form of extracellular Lewy body-like inclusions and α -synuclein-positive astrocytes. However, neuropathological load was sparse overall in both groups (not shown).

pTDP-43-positive NCIs and DNPs were found predominantly in CA1-3, with the greatest abundance of NCIs in CA1 followed by CA3 in CNOO and AD cases (Fig. 2.6a, b, d, g). NCIs were only identified in CA2 of AD cases (Fig. 2.6a). Scattered neuronal nuclear inclusions were observed in CA3 of one AD case (not shown). Sparse pTDP-43 pathology was noted in remaining layers underlying CA1-3 (Fig. 2.6a and b).

Like the DG, abundant AChE-positive neuropil prevented quantification of neuropathology in some regions of the hippocampus. In cases where pathology could be identified, AChE-positive plaque abundance was significantly lower in CNOO compared to AD cases in both CA2 ($p = <0.001$) and CA3 ($p = 0.01$) but was comparable in CA1 ($p = 0.073$; Table 2.3). AChE-positive plaques were most abundant in CA1-3, mirroring that of A β -plaque deposition (Fig. 2.5e, f). CA1 had the greatest AChE-positive plaque load, while the hilar region of CA3 had greater AChE-positive plaque burden than in its dorsal extent. CA2 had the lowest AChE-positive plaque burden in both AD and CNOO cases. Overall, sparse AChE-plaque deposition was noted in remaining layers over- and underlying CA1-3. AChE-positive NFTs were observed throughout the hippocampus of AD cases, and particularly in CA1 and CA2 of three CNOO cases.

The greatest deposition of BChE-positive plaques was noted in CA1-3 (Fig. 2.5g and h), however, overall abundance was significantly lower in CNOO compared to AD cases in both CA1 ($p = <0.001$) and CA2 ($p = 0.008$; Table 2.3). Distribution of BChE-positive plaques in the hippocampus mirrored that of AChE-positive plaques staining,

including plaque distribution in CA3 where BChE-positive plaque burden was greater in the hilar extent than in the dorsal extent. As noted above with A β and AChE staining, CA2 was the region with the lowest BChE-positive plaque deposition. BChE-positive NFTs were common throughout CA1 and CA2 in AD cases but were not observed in CNOO cases (Fig. 2.5g and h).

2.6.6. Subicular Complex Pathology

The subiculum contained comparable levels of A β deposition in AD and CNOO cases with similar patterns of distribution (Table 2.3). Namely, plaque abundance was highest in layer II with occasional plaques in remaining layers (Fig. 2.7a and d). A β -positive NFTs were also common in the pyramidal cells of layer II of the subiculum in AD cases, while they were only occasionally observed in CNOO cases.

In the PrS, A β pathology was most abundant in layers II and III (Fig. 2.7a, d). All AD cases as well as the majority of CNOO cases had frequent A β plaques in these layers (Table 2.3). Most AD and two CNOO cases had diffuse lake-like staining in this region as depicted in an AD case (Fig. 2.7a and b), while remaining AD and CNOO cases had multiple, tightly packed plaques spanning layers II and III, as noted in a CNOO case (Fig. 2.7d and e). A β plaques were typically absent in layer I in CNOO cases, while sparse deposits were noted in AD cases. In layers IV-VI the abundance of A β plaques was sparse in CNOO cases and moderate in AD cases. Occasional A β -positive NFTs were observed in layers V and VI of the PrS in several AD cases.

The PaS was the only region where A β deposition in the CNOO was significantly lower than in AD ($p = 0.023$; Table 2.3). In both AD and CNOO cases, A β plaque

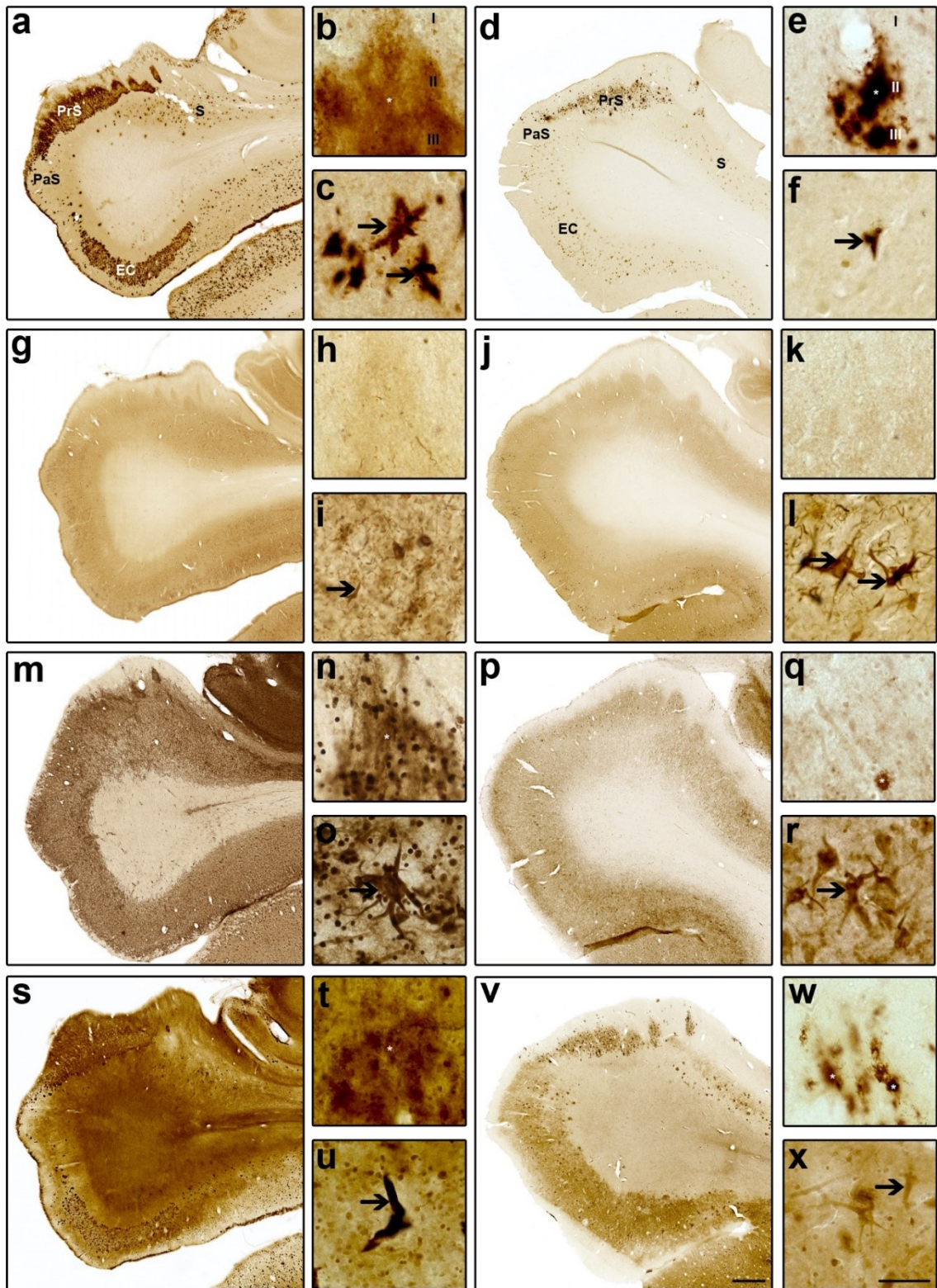


Figure 2.7 Low powered photomicrographs of neuropathological deposits in the Alzheimer's disease (a-c, g-i, m-o, s-u) and cognitively normal octogenarian or older (d-f, j-l, p-r, v-x) subiculum (S), presubiculum (PrS), parasubiculum (PaS) and entorhinal cortex (EC) stained for β -amyloid ($A\beta$; a-f), tau (g-l), acetylcholinesterase (AChE; m-r), and butyrylcholinesterase (BChE; s-x). Higher powered photomicrographs of the border between layers I and II of the PrS (b, e, h, k, n, q, t, w) shows (b, e) lake-like staining of $A\beta$ (*) in both groups that is recapitulated by AChE (h, q) and BChE (t, w) staining. High powered photomicrographs also show examples of extracellular neurofibrillary tangles (arrows) in layers II and III of the EC stained with $A\beta$ (c, f) and tau (i, l), and for AChE (o, r) and BChE (u, x). Scale bars = 1 mm (low power), 50 μ m (high power).

deposits from layers II and III of the PrS often extended into layer I of the PaS (Fig. 2.7a and d). After layer I, layers II and III of the PaS typically exhibited the greatest deposition of A β plaques, while V and VI exhibited sparser deposition in both groups. A β -positive extracellular NFTs (eNFTs), described previously (Lacosta et al., 2017; Perry et al., 1992), were often observed in layer II of the PaS in both AD and CNOO cases. Occasional A β -positive NFTs were also noted in AD cases.

Regarding tau pathology, the subiculum had the greatest abundance of NFTs in both groups within the subicular complex. However, tau NFTs were more frequent in AD than CNOO cases ($p = 0.043$; Table 2.3), with the greatest deposition of NFTs and NTs in layer II and sparse deposition in remaining layers (Fig. 2.7g and j). Tau-positive neuritic plaques were occasionally observed in layer II of AD cases (not shown).

In the PrS, tau NFT deposition was significantly greater in AD compared to CNOO cases ($p = 0.005$; Table 2.3). Within this region, tau NFTs were primarily observed in layers II, III, V, and VI in all cases (Fig. 2.7g and j). The abundance and distribution of tau NTs mirrored that of NFTs except for layer IV which often had dense NTs but only occasional NFTs.

Abundance of tau NFTs in the PaS was not significantly different in CNOO compared to AD cases ($p = 0.063$; Table 2.3). Tau pathology was most abundant in layers II and III in both CNOO and AD cases, particularly in layer III, followed by layers V and VI (Fig. 2.7g and j). Tau-positive eNFTs were often observed in layers II and III of the PaS in both groups.

The subiculum was the region where α -synuclein-positive neuropathology was most observed albeit sparsely with no discernible patterns of deposition between groups

or layers (not shown). Lewy bodies, axonal spheroids, Lewy neurites, and astrocytic star-like inclusions were all observed in the region. α -Synuclein-positive neuropathology was also observed in the PrS of two AD cases and the PaS of one CNOO case.

The subiculum was the most affected region by pTDP-43-positive neuropathology (Table 2.3; Fig. 2.6a and b). pTDP-43-positive NCIs and DNs were found predominantly in layer II, with little to no deposition in remaining layers. In the PrS, sparse NCIs and DNs were typically noted in layer II and particularly layer III. In the PaS, sparse pTDP-43 pathology was typically observed in layers II and III of CNOO cases, and in layers I-V of AD cases. In all cases, sparse DNs were observed in all layers of the PaS.

AChE-positive plaque burden was comparable in the subiculum between CNOO and AD cases ($p = 0.094$; Table 2.3). However, there was significantly less deposition of AChE-positive plaques in the PrS ($p = 0.023$) and PaS ($p = 0.003$) in CNOO compared to AD cases (Table 2.3). Laminar distribution in the subicular complex was similar in both groups (Fig. 2.7m and p). AChE-positive plaques and NFTs were predominantly observed in layer II of the subiculum in both AD and CNOO cases. In the PrS, AChE-positive lake-like staining was observed in layers II and III (Fig. 2.7m, n, p, q) with distinct AChE-positive plaques noted in layers V and VI. AChE-positive NFTs were also noted in the PrS in AD and CNOO cases, but with less abundance than in the rest of the subicular complex. In the PaS, AChE-positive plaque burden was greatest overall in layers II and III with occasional spillover from lake-like staining into layer I, and decreased deposition was noted in remaining layers. AChE-positive NFTs and eNFTs were common in layers II and III of the PaS of AD cases and were identified in layer II in one CNOO case.

BChE-positive plaque burden was significantly lower in the subiculum ($p = <0.001$), PrS ($p = 0.008$) and PaS ($p = 0.003$) of CNOO cases compared to AD cases, with deposition patterns resembling that of AChE (Table 2.3; Fig. 2.7s and v). BChE-positive plaques and NFTs in the subiculum were mostly limited to layer II with occasional BChE-positive pathology in remaining layers. In the PrS, BChE-positive lake-like staining was observed in layers II and III (Fig. 2.7s, t, v, w) with sparse BChE-positive plaque deposition in remaining layers. BChE-positive NFTs were occasionally observed in the deeper layers of the PrS of AD cases. Lake-like staining occasionally extended into layer I of the PaS. Like AChE-positive plaque pathology, BChE-positive plaques were most common in layers II and III and with decreased deposition in layers V and VI of the PaS. Both BChE-positive NFTs and eNFTs were observed in layer II of the PaS in several AD cases and one CNOO case.

2.6.7. Entorhinal Cortex Pathology

All AD cases and the majority of CNOO cases had frequent A β plaque deposition in the EC with similar patterns of laminar distribution in both groups (Fig. 2.7a and d). A β plaques were most frequently observed spanning layer III to the superficial extent of V, often appearing as an island of tightly packed plaques midspan. This was particularly evident in AD cases (Fig. 2.7a). In comparison, A β plaque load was typically less in layers I, Vc and especially VI, and was comprised of more defined compact or dense-cored plaques (Fig. 2.7a and d). A β -positive eNFTs were commonly observed in layer II in both groups (Fig. 2.7c and f).

Both groups had comparable tau NFT burden in the EC ($p = 0.347$; Table 2.3). Deposition of tau NFTs was most abundant in layer II followed closely by layers III and

V (Fig. 2.7g and j). Tau eNFTs were predominantly observed in layer II (Fig. 2.7i and l). Overall, moderate deposition of NFTs were noted in layer VI, while tau NFTs in layer I were typically absent in CNOO cases and sparse in AD cases. Tau NTs were most abundant in layers II-V.

Sparse α -synuclein-positive neuropathology was only observed in the EC of one AD case (not shown).

pTDP-43-positive NCIs were most abundant in layer II of the EC (Fig. 2.6a, c, d, f) in both groups. NCIs were observed in remaining layers of the EC, albeit to a lesser extent. DNPs were scattered to sparse in all layers of AD cases but were often absent in CNOO cases. In AD cases with a frequent pTDP-43-positive neuropathology, it was noted that NCIs were preferentially deposited from midspan to the lateral extent of the EC, with sparser deposition in the medial extent.

The EC had significantly less AChE-positive plaque pathology in CNOO than AD cases ($p = 0.017$; Table 2.3). AChE-positive plaque load was greatest in layers III-V, often appearing as an island of tightly packed plaques midspan of the EC (Fig. 2.7m and p). Additionally, layer II often had a significant burden of AChE-positive plaques and eNFTs in both groups (Fig. 2.7o and r).

BChE-positive plaque pathology was significantly lower in the EC of CNOO compared to AD cases ($p = 0.003$; Table 2.3) with the highest deposition in layers III-V resembling a tightly packed island of plaques (Fig. 2.7s and v). BChE-positive eNFTs were commonly observed in layer II of the EC in both groups (Fig. 2.7u and x).

2.7. Discussion

Cognitive decline as a result of either neurodegeneration or aging (Alzheimer's Association, 2021; Hou et al., 2019; Murman, 2015) is highly prevalent in octogenarians and older. A subset of octogenarians and older maintain normal cognitive function (Qiu and Fratiglioni, 2018), however, the mechanism(s) by which their cognition remains intact is unknown. AChE and BChE have been demonstrated to associate with A β plaque pathology predominantly in AD compared to cognitively normal cases (Macdonald et al., 2017). We compared the association of AChE and BChE activity with neuropathology in the rPFC and hippocampal formation of CNOO and AD cases to evaluate cholinesterase expression as a potential mechanism of cognitive preservation in CNOO.

A semi-quantitative approach was used in this study allow for the scoring of all neuropathological aggregates with the same methodology. While this technique lacks the specificity of a quantitative approach, such as percentage of area stained (Darvesh et al., 2012; Macdonald et al., 2017), it allowed for the exclusion of normal, physiological staining such as AChE activity associated with neurons and neuropil. Subjectivity was combatted by having independent scoring completed by two researchers, with a final score reached by consensus.

Through immunohistochemical staining, we examined several neuropathologies associated with neurodegenerative disorders. Neuropathological aggregates, including A β plaques, tau NFTs and NTs, and pTDP-43 NCIs and DNs were observed in CNOO cases with an abundance comparable to AD cases in the majority of examined regions (Table 3) while α -synuclein deposition was not significant in either group in the regions examined.

Prior studies evaluated the prevalence of neuropathological aggregates in people without dementia. Regarding AD-associated neuropathology, up to 30% of cognitively normal adults over the age of 65 have been found to have A β plaques in their brain (Katzman et al., 1988), often with a burden comparable to AD in some regions (Macdonald et al., 2017). Despite their common occurrence, however, A β plaque accumulation is not always observed in cases of extreme old age (Neltner et al., 2016). In our study, all CNOO cases had A β plaque deposition in the rPFC, while two cases lacked deposition in the hippocampal formation. Tau NFTs, on the other hand, were observed in every case across multiple studies of oldest-old brains (Neltner et al., 2016), a result which was also observed in this study.

The CNOO cases examined herein, also had intracellular A β deposition in addition to extracellular AD-associated plaque pathology. Intraneuronal A β has been documented in AD, Down syndrome, and cognitively normal human brains (Gouras et al., 2000; Wegiel et al., 2007). However, the A β -positive neurons were predominantly observed in temporal structures, such as the dentate gyrus, hippocampus, and entorhinal cortex, in the cytoplasm (Gouras et al., 2000; Wegiel et al., 2007) and pyramidal neurons of the cortex (Wegiel et al., 2007). We observed intraneuronal A β accumulation outlining the cell body and apical dendrites of several morphologically distinct neuronal subtypes in the rPFC. This may represent a separate protein sequestering phenomenon that should be further examined.

Additionally, we observed tau deposition in the white matter at the level of the rPFC that was morphologically consistent with thorn-shaped astrocytes in the clinically non-specific neuropathology of ARTAG (Kovacs et al., 2016b). Morphologically

identical thorn-shaped astrocytes are also observed in chronic traumatic encephalopathy (Ameen-Ali et al., 2022; Forrest et al., 2019), but our cases were cognitively normal and lacked the clinical history required for a diagnosis of chronic traumatic encephalopathy. The association of tau-positive thorn-shaped astrocytes with blood-brain barrier dysfunction in chronic traumatic encephalopathy may imply a similar role in ARTAG despite a lack of clinically significant changes (Ameen-Ali et al., 2022). Uptake and phagocytosis of pathologic tau by astrocytes may represent one neuroprotective mechanism to prevent neuronal accumulation of tau (Kovacs, 2018).

pTDP-43 aggregates, associated with frontotemporal dementia, amyotrophic lateral sclerosis (Neumann et al., 2006), and limbic-predominant age-related TDP-43 encephalopathy (Nelson et al., 2019), were common in the hippocampal formation of our CNOO cases (Table 2.3; Fig. 2.5). pTDP-43 deposition has been reported to occur in up to 74% of AD cases (Josephs et al., 2014a, 2014b; McAleese et al., 2017) and up to 40% of normal cases (McAleese et al., 2017; Nascimento et al., 2018; Uchino et al., 2015). In this study, 50% of AD cases and 44% of CNOO cases examined had pTDP-43 pathology. The mean of age of our cohort (92.8 years) was greater than that of previous studies (McAleese et al., 2017; Nascimento et al., 2018; Uchino et al., 2015) which reaffirms that the incidence of pTDP-43 deposition increases with age (Geser et al., 2010), with the greatest incidence observed in octogenarians and older.

The deposition of α -synuclein pathologies in AD and normal brains has been reported (Markesbery et al., 2009). However, in other studies which examined the brains of cognitively normal nonagenarians and older, α -synuclein deposits were the least common neuropathological aggregate (Neltner et al., 2016). These findings were also

observed in our study and may be attributed, in part, to not examining regions such as the amygdala and brainstem where deposition is more common in cognitively normal older individuals (Markesbery et al., 2009).

In addition to a significant presence of neuropathology in our cases, regional differences in neuropathological distribution should be considered. We observed similar patterns of distribution between both AD and CNOO cases. In our cases, we consistently observed frequent A β in the rPFC but with more variable deposition in the hippocampal formation. Meanwhile, greater deposition of tau and pTDP-43 was often noted in the hippocampal formation than in the rPFC, particularly in CNOO cases. In part, differences in pathological burden can be attributed to stage of pathological protein deposition. In AD, A β plaque deposition is thought to occur earliest in the neocortex and spread inward (Thal et al., 2002), whereas deposition of tau and pTDP-43 begins subcortically in the limbic system and spreads outward (Braak et al., 2006; Braak and Braak, 1991; Josephs et al., 2016, 2014a). Tau aggregation first occurs in the transentorhinal cortex and EC (Kaufman et al., 2018) in layer II neurons that are vulnerable due their unique expression profiles for A β , and tau processing and microtubule dynamics (Roussarie et al., 2020). Regions investigated herein demonstrated a similar pattern of deposition, and therefore encompassed both early- and late-stage aggregate deposition for all examined proteins.

The principal cells of the neocortex, hippocampus, subicular complex, and EC are pyramidal neurons. Susceptibility to intracellular protein aggregates results in a subsequent loss of pyramidal neurons in AD (Mann, 1996), with CA1, subiculum and EC identified as the most strongly affected (Hyman et al., 1984; Morrison and Hof, 2002; Price et al., 1991). Our study reflects this pattern of neuropathological distribution with

the greatest burden occurring in the pyramidal cell-containing laminar layers of the hippocampus, subiculum, and EC in both AD and CNOO cases.

In contrast, the PrS has been reported to be relatively spared of both NFTs (Ball, 1977; Hirano and Zimmerman, 1962; Hyman et al., 1984) and fibrillar A β plaques (Wisniewski et al., 1998) despite having principal pyramidal neurons. The PrS was not spared of significant AD-associated neuropathology in our study. While the PrS had lake-like A β deposition in layers II and III, a finding that has been well documented (Kalus et al., 1989; Wisniewski et al., 1998), cored and compact plaque deposits were often present in deeper layers of both groups. There was moderate to frequent NFT burden in AD cases and sparse to moderate NFT burden in CNOO cases. While deposition of A β plaques and NFTs in the PrS is not insignificant overall, the resiliency of layer II and III pyramidal neurons to the development of fibrillar cored and compact plaques is a notable regional difference and should be further examined to identify potential mechanisms of resistance to A β neuropathology.

The DG has also been described as relatively spared of pathology in AD (Ball, 1977; Hirano and Zimmerman, 1962; Hyman et al., 1986, 1984). However, in this study, AD cases had moderate to frequent abundance of A β plaques and NFTs, and CNOO case burden was not significantly different. The margo denticulatus (Klingler, 1948), so named due to its toothed appearance, is an anatomical feature of the DG visible at the medial, extra-ventricular aspect of the hippocampal body (Fig. 2.2a; Destrieux et al., 2013; Duvernoy et al., 2013; Klingler, 1948). We observed preferential A β plaque accumulation at the margo denticulatus, particularly in the molecular layer (Fig. 2.5a and b). This phenomenon had been previously described by Braak and Braak (Braak and

Braak, 1991) as “fluffy material” and the deposition appears to be morphologically similar to the diffuse lake-like deposits in layers II of the PrS and PaS (Fig. 2.7a, b, d, e; Kalus et al., 1989; Wisniewski et al., 1998). The superficial molecular layer of the DG is innervated by fibers originating predominantly in layer II of the EC via the perforant pathway which synapse on dendritic projections from granular neurons in the adjacent layer (Duvernoy et al., 2013; Witter et al., 2000). The cytoarchitecture and connectivity of the molecular layer of the DG at the margo denticulatus is not described as varying from the rest of the structure (Duvernoy et al., 2013). Further investigation is needed to understand why this region appears to be more vulnerable to A β deposition. Additionally, while the granular layer often only had sparse deposition of A β and tau aggregates, it had the highest laminar deposition of pTDP-43-positive NCIs within the structure (Fig. 2.6c and f). pTDP-43 aggregates in the granular layer of the DG are a common feature of frontotemporal dementia (Higashi et al., 2007; Neumann et al., 2006), however, reports of pTDP-43 NCIs associated with AD have been variable (Amador-Ortiz et al., 2007; Higashi et al., 2007; Hu et al., 2008; Kadokura et al., 2009). In our study, all cases with pTDP-43 aggregates had NCIs present in the granular layer of the DG with most AD cases having frequent deposition.

Both the rPFC and the hippocampal formation are innervated by cholinergic projections located in the basal forebrain (Mesulam et al., 1983; Mesulam and Geula, 1988) which are involved in cognition. Loss of cholinergic innervation is, in part, responsible for cognitive decline in AD (Coyle et al., 1983). Burden of tau NFTs, and not A β plaques, has been suggested to correlate with AD cognitive decline (Arriagada et al., 1992). It has been demonstrated that the cholinergic neurons of the basal forebrain are

vulnerable to tau NFTs and α -synuclein Lewy bodies, and resistant to pTDP-43 pathology (Geula et al., 2021). As pTDP-43 neuropathology in AD has been associated with worse performance on cognitive tests (Josephs et al., 2008) and a more rapid decline in cognition (Wilson et al., 2013), pTDP-43-associated neurodegeneration may be attributed to a different mechanism than loss of cholinergic neurons. Our CNOO cases had a NFT burden comparable to AD cases in five regions of interest in the hippocampal formation. Intrinsic cortical cholinergic neurons have not been confirmed in the human rPFC or hippocampal formation (Blusztajn and Rinnofer, 2016; Levey et al., 1984). However, the significant burden of tau NFTs that we observe in regions that are connected to the basal forebrain would suggest that NFT deposition has progressed to subcortical regions like the basal forebrain, yet the CNOO show some level of resistance to NFT deposition not observed in AD.

SuperAgers, defined as octogenarians and older with episodic memory scores comparable to the average scores of individuals 50-60 years of age (Harrison et al., 2012), have been found to have reduced neuronal AChE activity (Janeczek et al., 2018) and less AD pathology compared to peers with episodic memory scores considered average for their age (Rogalski et al., 2013). The retrospective nature of our study means we do not have cognitive testing values for our CNOO cases. However, all CNOO cases lacked any history of cognitive complaints. Overall, there was reduced plaque load associated with AChE activity in our CNOO cases as compared to AD cases. AChE activity associated with normal physiological processes amongst our cases should be assessed in the future. Moreover, our CNOO cases had A β plaque and tau NFT burdens comparable to AD cases in the majority of regions examined. The excellent memory

performance of SuperAgers may, in part, be attributable to both increased availability of acetylcholine and lack of toxic neuropathology. Our cases, however, may have a more modest increase in acetylcholine availability, but maintained cognition despite significant neuropathological burden of A β plaques, tau NFTs, and pTDP-43 NCIs. Therefore, while the brains of SuperAgers are well preserved, our CNOO cases may have compensated for neuropathological changes.

Loss of cholinergic transmission through selective death of basal forebrain cholinergic neurons in AD led to the cholinergic hypothesis (Bartus, 2000), and subsequently, the use of cholinesterase inhibitors for modest symptomatic relief in AD through increased acetylcholine availability (Birks, 2006). Decreased AChE activity and increased BChE activity in the cerebral cortex, as well as the presence of cholinesterase-positive A β plaques, are characteristic features of AD (Darvesh et al., 2010; Geula and Mesulam, 1989a; Macdonald et al., 2017). AChE and BChE activities associate with a subset of A β plaques (Darvesh et al., 2010; Geula and Mesulam, 1989a, 1995; Macdonald et al., 2017), with BChE having been implicated in plaque maturation from a benign to a neurotoxic species (Darvesh et al., 2012; Guillozet et al., 1997; Mesulam and Geula, 1994). In our study, AChE and BChE appeared to predominantly associate with compact or cored plaques and not diffuse appearing plaques in regions such as the margo denticulatus, with the exception of lake-like deposition in the subicular complex (Fig. 2.5 and 2.7). As we have shown previously, BChE specificity for plaques in AD compared to those observed in normal brains indicates that this enzyme may be a more sensitive biomarker for AD diagnosis and management (Macdonald et al., 2017). AChE and BChE expressions were reflected in both distribution and relative abundance of plaques. Seven

of nine regions of interest had significantly lower BChE-positive plaque abundance in the CNOO than in AD which further demonstrated the specificity of BChE for plaque pathology in AD (Table 2.3). Although AChE-positive plaque abundance was also lower in five of nine regions in CNOO compared to AD, normal neuronal and neuropil expression in the cerebral cortex precludes its use as an effective diagnostic target for AD. Neuronal AChE activity decreases in most brain regions in AD, and less dramatically with age, but plaque associated activity in AD increases (Darvesh et al., 2010; Geula and Mesulam, 1989a, 1995, 1989b; Janeczek et al., 2018). Although the mechanism is unknown, decreased neuronal AChE activity has been proposed as an example of neuroplasticity, to bolster cholinergic neurotransmission through increasing synaptic availability of acetylcholine (Janeczek et al., 2018). AChE activity associated with plaques was more specific to AD cases consistent with previous studies (Geula and Mesulam, 1989a), although quantifying normal AChE activity was beyond the scope of this study. Neuronal AChE activity in CNOO cases should be compared to younger cognitively normal cases in the future to determine if they also demonstrate an age-related decline.

While AChE and BChE activities in our cases appeared specific to AD-associated plaque pathology, it did not readily identify between NFTs in the CNOO and AD. While AChE and BChE-positive NFTs have been observed previously in AD, it was only in a small fraction of NFTs (Geula and Mesulam, 1995; Hamodat et al., 2017). The exceptions being a few studies (Gomez-Ramos et al., 1992; Mesulam and Asuncion Morán, 1987) which found co-localization of NFTs with cholinesterases in AD and normal temporal structures, such as the EC, similar to our findings, but this was prior to

the characterization of eNFTs and A β -positive NFT species. We observed that NFTs and eNFTs in the hippocampal formation in both CNOO and AD cases were frequently recapitulated by AChE (Fig. 2.7p and r) and BChE activities (Fig. 2.7u and x). In turn, no cholinesterase-positive NFTs were observed in the rPFC. Relatively low fixation times to prevent loss of cholinesterase activity (Morán and Gómez-Ramos, 1992) may have been ideal for visualization of eNFTs which also appear to be sensitive to fixation conditions (Perry et al., 1992). As NFTs in this region can be A β -positive, tau-positive, or both (Lacosta et al., 2017; Perry et al., 1992; Schwab et al., 1998; Schwab and McGeer, 2000), it still remains unclear which species may be associated with cholinesterase activity. The unique association of AChE and BChE with this subset of NFTs in the hippocampal formation may implicate cholinesterase involvement in NFT formation and should be further explored.

Additionally, it has been demonstrated that BChE does not associate with tau pathology indicative of corticobasal degeneration and frontotemporal dementia, infarcts in vascular dementia, or α -synuclein pathology in dementia with Lewy bodies (Macdonald et al., 2017). BChE and AChE activities did not appear to associate with intraneuronal A β , tau-positive thorn-shaped astrocytes, or pTDP-43 and α -synuclein aggregates in this study.

Females are more likely to be diagnosed with dementia (Alzheimer's Association, 2021) and those with AD are more likely to progress to the most severe stages of the disease with the lowest cognitive scores and greatest NFT burden, but not A β burden, at the time of death (Filon et al., 2016). In this study, female CNOO cases had greater NFT abundance in the rPFC, and BChE-positive plaque abundance in the PrS (Appendix A,

Supplementary Data, Table A.1). We observed no sex differences in neuropathological burden amongst AD cases (Appendix A, Supplementary Data, Table A.2). Our pilot study is limited by a relatively small sample size. In future studies of CNOO and AD, a larger sample size may lower deviation between groups presenting more clear differences in neuropathological burden between the sexes.

In conclusion, the CNOO maintained cognition despite a significant burden of neuropathological aggregates in regions vital for cognitive function recapitulating similar patterns of deposition as noted in AD brains. The presence of a variety of neuropathological proteins in CNOO brains should be indicative of the need to avoid assumptions of clinical significance based on neuropathology alone. Neuropathological aggregation may be necessary for the diagnosis of neurodegenerative diseases, however, it is not sufficient and alternative mechanisms of neurodegeneration and resiliency must be explored on a molecular rather than solely a structural level. The unusual sequestering of A β in neurons and tau and α -synuclein in astrocytes may be indicative of protective mechanisms in the CNOO. Plaque-associated cholinesterase activity was lower in most regions examined in the CNOO compared to AD cases. BChE-activity, not AChE, was more specific to AD plaque pathology further demonstrating its potential as a biomarker and therapeutic target. Both cholinesterases, however, associated with a subset of NFTs in the hippocampal formation. Regional differences in the association of cholinesterases with NFTs and diffuse plaques in the hippocampal formation should be further explored.

2.8. Acknowledgements

This work was supported in part by the Canadian Institutes of Health Research (PJT- 153319), Alzheimer's Society of Canada (Research Program Master's Award),

Alzheimer's Society of Nova Scotia (Phyllis Horton Student Research Award), Dalhousie University Faculty of Medicine (Graduate Studentship), Dalhousie Medical Research Foundation (Irene MacDonald Sobey Endowed Chair in Curative Approaches to Alzheimer's Disease, The Durland Breakthrough Fund, The Clare Durland Fund in Alzheimer's Disease Research, and Weizmann Canada Studentship in Medical Neuroscience).

CHAPTER 3 Clinicopathological Correlates in Sporadic Tauopathy: Neuropathology and Cholinesterase Expression in Progressive Supranuclear Palsy

3.1. Publication Status

Manuscript in preparation.

S.P. Maxwell, M.K. Cash, S. Darvesh. (2022). Cholinesterases do not associate with tau pathology in progressive supranuclear palsy.

3.2. Overview

The following chapter evaluates if acetylcholinesterase or butyrylcholinesterase associate with tau pathology in progressive supranuclear palsy.

3.3. Abstract

Progressive supranuclear palsy (PSP) is a progressive neurodegenerative disorder characterized clinically by supranuclear gaze palsy, postural instability, and Parkinsonism motor symptoms, and neuropathologically by neuronal and glial tau aggregation. Despite prominent motor symptoms, frontal lobe symptoms, such as cognitive and behavioural impairment, are common features of PSP. Executive function, the cognitive processes that allow for planning and executing activities required for daily life, are particularly impaired in PSP. The aim of this study was to evaluate neuropathological and cholinesterase expression in the rostral prefrontal cortex (rPFC), a region implicated in executive function, from PSP compared to another prominent tauopathy, Alzheimer's disease (AD), and cognitively normal (CN) human brains. Tissues from age- and sex-matched PSP, Alzheimer's disease (AD), and CN rPFC were stained immunohistochemically for β -amyloid ($A\beta$), and tau, as well as histochemically for acetylcholinesterase and butyrylcholinesterase (BChE) activity. Abundance of

neuropathological aggregates was scored semi-quantitatively. PSP cases had a low burden of AD-associated neuropathologies comparable to CN cases. As described previously, tufted astrocytes (TAs) and oligodendrocytic coiled bodies (CBs) were highly specific to PSP cases. Cholinesterases predominantly associated with A β pathology in AD, and did not associate with neurofibrillary tangles, TAs and CBs in PSP cases. This supports the use of BChE as a sensitive and specific biomarker of AD and implies that frontal lobe function in PSP must be impaired through alternate means than cholinesterase expression.

3.4. Introduction

Progressive supranuclear palsy (PSP) is a neurodegenerative disorder characterized by atypical parkinsonism typically accompanied with mild dementia (Nath et al., 2001). Steele, Richardson, and Olszewski, first described and characterized the clinical presentation of PSP, which encompassed cases with a clinical course that did not conform to known neurodegenerative diseases, such as multiple systems atrophy or Alzheimer's disease (AD; Steele et al., 1964). The neuropathological hallmarks of PSP include neurofibrillary tangles (NFTs), tau tufted astrocytes (TAs) and tau oligodendrocytic coiled bodies (CBs) composed of predominantly of 4-repeat N-terminal microtubule-binding domain containing (4R) tau aggregates (Arai et al., 2001; Arima et al., 1997; Nishimura et al., 1992; Powell et al., 1974). Inclusion criteria for a neuropathological diagnosis of PSP mandates findings of NFTs and/or neuropil threads (NTs) in the basal ganglia and brainstem (Hauw et al., 1994). Identification of TAs and CBs are also highly characteristic of PSP although they are not currently included in the diagnostic criteria (Dickson, 1999; Litvan et al., 1996b).

Despite being considered predominantly a disorder of motor function, frontal lobe features such as cognitive decline and behavioural symptoms are common features of PSP and should be considered in management of the disease (Rittman et al., 2016). Cognitive impairment is present at onset in approximately 10% of PSP cases (Bensimon et al., 2009), and the majority of cases progress to experience dementia during the disease course (Daniel et al., 1995; Pillon et al., 1991; Viscidi et al., 2021). It has been proposed that cognitive decline in PSP is predominantly due to executive dysfunction, whereby the individuals exhibit difficulty in task initiation and perseverance, conceptualization, lexical fluency, conflicting instructions, go-no go tests and prehension behaviour (Gerstenecker et al., 2013). On cognitive tests, PSP patients perform worse on tests of frontal lobe function, such as the Frontal Assessment Battery, with milder deficits in other cognitive domains, such as memory (Brown et al., 2010; Gerstenecker et al., 2013).

The rostral prefrontal cortex (rPFC) has been implicated in executive function, namely in working memory and attention (Benoit et al., 2012; Funahashi, 2017). The rPFC's role in executive function is thought to, in part, be attributed to cholinergic modulation from the basal forebrain (Croxson et al., 2011). The role of the cholinergic system in executive function is further supported by the deficits observed with selective atrophy of basal forebrain cholinergic neurons in Alzheimer's disease (AD; Coyle et al., 1983; Whitehouse et al., 1981). Loss of basal forebrain cholinergic neurons has also been observed in PSP, although to a lesser degree than AD (Kasashima and Oda, 2003; Tagliavini et al., 1983), and may contribute to cognitive decline (Warren et al., 2005). Despite sharing similar findings of cholinergic dysfunction, cholinesterase inhibitors offer modest improvement in symptoms of AD (Birks, 2006), but have mixed results in

PSP clinical trials (Fabbrini et al., 2001; Litvan et al., 2001). One study reported no improvement in cognitive test scores with the cholinesterase inhibitor donepezil (Fabbrini et al., 2001), while another study reported a mild improvement in cognitive test scores, but worsening motor symptoms (Litvan et al., 2001). While changes in cholinesterase expression in the AD brain have been characterized (Darvesh et al., 2010; Geula and Mesulam, 1989a, 1995), similar characterization of cholinesterase-associated neuropathology in PSP has not been undertaken.

Thus, we hypothesized that cholinesterase expression would not associate with neuropathology in the rPFC of PSP compared to AD and cognitively normal (CN) brains. We examined and compared the abundance of neuropathological aggregates associated with the pathophysiology of PSP, as well as comorbid AD neuropathology, in the rPFC of all three groups to test the hypothesis that cholinesterase expression is specific to AD plaque pathology and does not associate with tau aggregates in PSP.

3.5. Materials and Methods

3.5.1. Brain Tissues

The rPFC at the level of the medial frontopolar gyrus from PSP (N=10), sporadic AD (N=10), and cognitively normal (CN; N=10) sex- and age-matched brains from the Maritime Brain Tissue Bank (Halifax, NS, Canada) were utilized in this study with approval from the Nova Scotia Health Authority Research Ethics Board. Case demographics are summarized in Table 3.1. Clinical and neuropathological reports for

Table 3.1 Case demographic details

	Case	Age (y)	Sex	Brain Weight (g)	PSP Criteria Met? ^a	Braak Stage ^b	CERAD Plaque Score ^c
Progressive Supranuclear Palsv (PSP)	PSP1	70	F	1338	Yes	N/A	Moderate
	PSP2	80	F	1200	Yes	N/A	None
	PSP3	81	F	1478	Yes	N/A	Sparse
	PSP4	67	F	1140	Yes	N/A	None
	PSP5	88	F	1208	Yes	N/A	Moderate
	PSP6	66	M	1500	Yes	N/A	Sparse
	PSP7	82	M	1125	Yes	N/A	None
	PSP8	83	M	1340	Yes	N/A	None
	PSP9	84	M	1600	Yes	N/A	Sparse
	PSP10	93	M	1391	Yes	III	Sparse
Alzheimer's disease (AD)	AD1	70	F	1079	No	VI	Frequent
	AD2	84	F	1175	No	V	Moderate-Frequent
	AD3	87	F	1030	No	VI	Frequent
	AD4	91	F	1138	No	V	Moderate
	AD5	92	F	1009	No	IV	Frequent
	AD6	58	M	1470	No	VI	Frequent
	AD7	67	M	1350	No	IV	Moderate-Frequent
	AD8	71	M	1340	No	IV	Moderate-Frequent
	AD9	86	M	1440	No	VI	Moderate
	AD10	92	M	1230	No	IV	Frequent
Cognitively Normal (CN)	CN1	71	F	1250	No	I	Sparse
	CN2	80	F	1300	No	II	None
	CN3	83	F	1235	No	II	Sparse-Moderate
	CN4	90	F	1290	No	IV	Moderate
	CN5	109	F	1056	No	VI	Moderate-Frequent
	CN6	55	M	1500	No	0	None
	CN7	63	M	1360	No	0	None
	CN8	69	M	1320	No	II	Sparse
	CN9	72	M	1380	No	0	None
	CN10	91	M	1195	No	II	Sparse

^a(Hauw et al., 1994)

^b(Braak et al., 2006; Braak and Braak, 1995)

^c(Mirra et al., 1991)

each brain were reviewed to optimize diagnostic accuracy. PSP and AD cases received their respective diagnoses from a neuropathologist, whereas CN control cases had no reported clinical history of dementia regardless of neuropathological findings. Typical PSP diagnostic criteria necessitates very high NFT density in the pallidum, subthalamic nucleus and substantia nigra, high to very high NFT density in the pontine tegmentum, and low to high NFT density in the oculomotor nucleus, striatum, pontine nuclei, and medulla including the dentate nucleus (Hauw et al., 1994). NFT density should be absent or low in the hippocampus, entorhinal cortex, prefrontal and precentral cortices, and other association cortices, as NFT deposition in these regions is characteristic of AD (Hauw et al., 1994). AD cases met neuropathological criteria for AD (Braak et al., 2006; Braak and Braak, 1995; Mirra et al., 1991; Montine et al., 2012). CN cases had Braak stages ranging from 0 to VI and Consortium to Establish a Registry for AD (CERAD) plaque scores ranging from none to moderate-frequent (Table 3.1). No genotyping was available.

Human brain hemisections were immersion fixed in 10% formalin in 0.1M phosphate buffer (pH 7.4; PB) at 4°C between 1-7 days, cryoprotected and stored in phosphate buffer (PB) with 40% sucrose and 0.6% sodium azide. The rPFC at the frontal pole was removed and cut into 50 µm sections using a Leica SM2000R microtome (Leica Microsystems Inc., Nussloch, Germany) with a Physitemp freezing stage and PFS 30TC or PFS-40MPA controller (Physitemp Instruments, Inc., Clifton, NJ, United States). Adjacent brain tissue sections from all brains were stained using immunohistochemical techniques with specific antibodies for A β and tau, as well as histochemical techniques for Nissl substance with thionin, and BChE and AChE activity.

3.5.2. Immunohistochemistry

Standard immunohistochemical staining procedures were performed with primary antibodies for A β (polyclonal rabbit anti-A β ; 1:400; Cat. No. 71-5800, Life Technologies, Rockford, IL, USA), and pan tau (polyclonal rabbit anti-human tau; 1:16000; Cat. No. A0024; DakoCytomation, Glostrup, Denmark) to detect A β plaques and tau NFTs, NTs, TAs, and CBs, respectively.

Sections were rinsed in 0.1 M PB (pH 7.4) for 30 min. Sections to be stained for A β were rinsed for 5 min in 0.05 M PB followed by a 15 min rinse in dH₂O. These sections were gently agitated in 95% formic acid for 2 min to improve staining, then underwent five 1 min rinses in dH₂O and a 30 min rinse in 0.1 M PB. The endogenous peroxidase activity of all immunohistochemically stained sections was quenched in 0.3% hydrogen peroxide in 0.1 M PB for 30 min and then rinsed in 0.1 M PB for an additional 30 min. All sections were then incubated in 0.1 M PB containing 0.1% Triton X-100 and the respective primary antibody overnight (16 h) at room temperature. Following a rinse in 0.1 M PB for 30 min, sections were incubated in 0.1 M PB with 0.1% Triton X-100, biotinylated goat α rabbit secondary antibody (1:500; Cat. No. BA-1000, Vector Laboratories, Burlingame, CA, United States), and normal goat serum (1:1000) for 1 h at room temperature. The tissue was rinsed for 30 min in 0.1 M PB, then incubated for 1 h at room temperature in 0.1 M PB with 0.1% Triton X-100 and the Vectastain Elite ABC kit (1:182; Cat. No. PK-6100, Vector Laboratories, Burlingame, CA, United States), according to the manufacturer's instructions. Sections were rinsed for 30 min in 0.1 M PB and developed in a solution of 0.1 M PB containing 1.39 mM 3,3'-diaminobenzidine (DAB). After a 5 min incubation, 50 μ L of 0.1 M PB containing 0.3% hydrogen peroxide

was added per mL of DAB solution. The tissue was incubated for approximately 5 min, then the reaction was stopped by rinsing sections in 0.01 M acetate buffer (pH 3.3). In control experiments, no staining was observed when the primary antibodies were omitted. All sections were mounted on slides, air dried, and coverslipped for examination with brightfield microscopy.

3.5.3. Histochemical staining

Thionin stain for Nissl substance was used to visual cytoarchitecture of the rPFC, as done previously (Hamodat et al., 2017).

AChE and BChE histochemical staining was performed using a modified Karnovsky-Roots method (Darvesh et al., 2010; Karnovsky and Roots, 1964) using reagents purchased from Sigma-Aldrich (St. Louis, MO, United States). Incubation in Karnovsky-Roots solution with a pH of 6.8 was used to visualize AChE and BChE activity associated with neuropathological aggregates, whereas staining for AChE at pH 8.0 was used to visualize normal, physiological neuronal and structures for parcellation of the rPFC. First, tissue sections were rinsed in 0.1 M maleate buffer (MB, pH 7.4) for 30 min. Endogenous activity was then quenched in 0.15% hydrogen peroxide in MB for 30 min and rinsed in MB for an additional 30 min. Sections were incubated between 3.5 to 6 h to achieve optimal staining in 0.1 M MB (pH 6.8 or 8.0) containing 0.5 mM sodium citrate, 0.47 mM cupric sulfate, 0.5 mM potassium ferricyanide, as well as specific AChE and BChE substrates and inhibitors. To visualize BChE activity, 0.8 mM butyrylthiocholine iodide was used in conjunction with the AChE inhibitor 0.01 mM BW 284C 51. To visualize AChE activity, 0.4 mM of acetylthiocholine iodide was used in conjunction with the BChE inhibitor 0.06 mM ethopropazine. Following incubation in

Karnovsky-Roots solution, all sections were rinsed with dH₂O for 30 min then placed in 0.1% cobalt chloride solution in dH₂O for 10 min. After another rinse in dH₂O for 30 min, sections were placed in 0.1 M PB containing 1.39 mM DAB. Following a 5 min incubation, 50 µL of 0.3% hydrogen peroxide in 0.1 M PB was added per mL of DAB solution and the reaction was carried out for approximately 5 min. Sections were then washed in 0.01 M acetate buffer (pH 3.3), mounted on slides, air dried, coverslipped, and examined with brightfield microscopy. Control experiments were performed as previously described (Darvesh et al., 2010).

3.5.4. Data analysis

rPFC sections were analyzed and imaged with a Zeiss Axio Scan Z1 slide scanner with Zen 3.1 Blue Edition software (Carl Zeiss Canada Ltd, Toronto, Canada).

Photomicrographs were colour balanced, brightness adjusted and assembled into figures using Adobe Photoshop (CC 2022, Version 12.0, San Diego, CA, United States).

The rPFC was parcellated using sections stained for Nissl substance with thionin and AChE activity at pH 8.0. Neuropathological aggregates in the rPFC at the level of the medial frontopolar gyrus were semi-quantitatively scored using modified CERAD criteria (Mirra et al., 1991) described previously: 0, pathology absent; 1, sparse pathology; 2, moderate pathology; 3, frequent pathology (Hamodat et al., 2017). Neuropathological diagnosis of PSP requires subcortical NFT deposition (Hauw et al., 1994), and tau TAs and CBs are also often characteristic of PSP (Dickson, 1999; Litvan et al., 1996b), therefore the abundance of NFTs, TAs and CBs were scored in each case. To encompass AD diagnostic criteria A β plaques were additionally scored (Mirra et al., 1991), as well as AChE- and BChE-positive neuropathology at pH 6.8.

Mean abundance of A β plaques, tau-positive NFTs, tau-positive TAs, tau-positive CBs, as well as AChE- and BChE- positive pathology were compared between PSP, AD, and CN groups via one-way analysis of variance (ANOVA) with Bonferroni *post-hoc* tests. Significant differences between individual groups were concluded at a level of $p < 0.05$ accounting for a Bonferroni correction after three comparisons. Significant difference is denoted as follows: * $p < 0.05$; ** $p < 0.01$ *** $p < 0.001$. All statistical analysis was performed using SPSS (IBM corp, Armonk, NY, United States).

3.6. Results

Parcellation of the rPFC at the level of the medial frontopolar gyrus was confirmed using sections stained for Nissl substance with thionin and AChE activity at pH 8.0. Cytoarchitectural features of the six layers described by Öngür *et al.* (2003) as Area 10p, expanded from Brodmann's Area 10 (Brodmann, 2006), were used to confirm that neuropathological analysis was undertaken in the rPFC. For additional information on the parcellation of the rPFC refer to previous chapter.

Deposition of tau NFTs were significantly different between groups ($p = < 0.001$), in part due to greater NFT abundance in AD compared to both PSP and CN cases (Fig. 3.1A). NFT abundance was comparable between PSP and CN cases. NFT abundance was greatest in layers III and V in all groups (Fig. 3.2A).

Tau TAs were only observed in nine PSP cases with sparse to moderate frequency (Fig. 3.1B), resulting in statistically different abundance between groups (Fig. 3.2A; $p = < 0.001$). TAs were predominantly found in layers III and V of the rPFC, although in cases with the greatest abundance, they were often identified in every cortical layer.

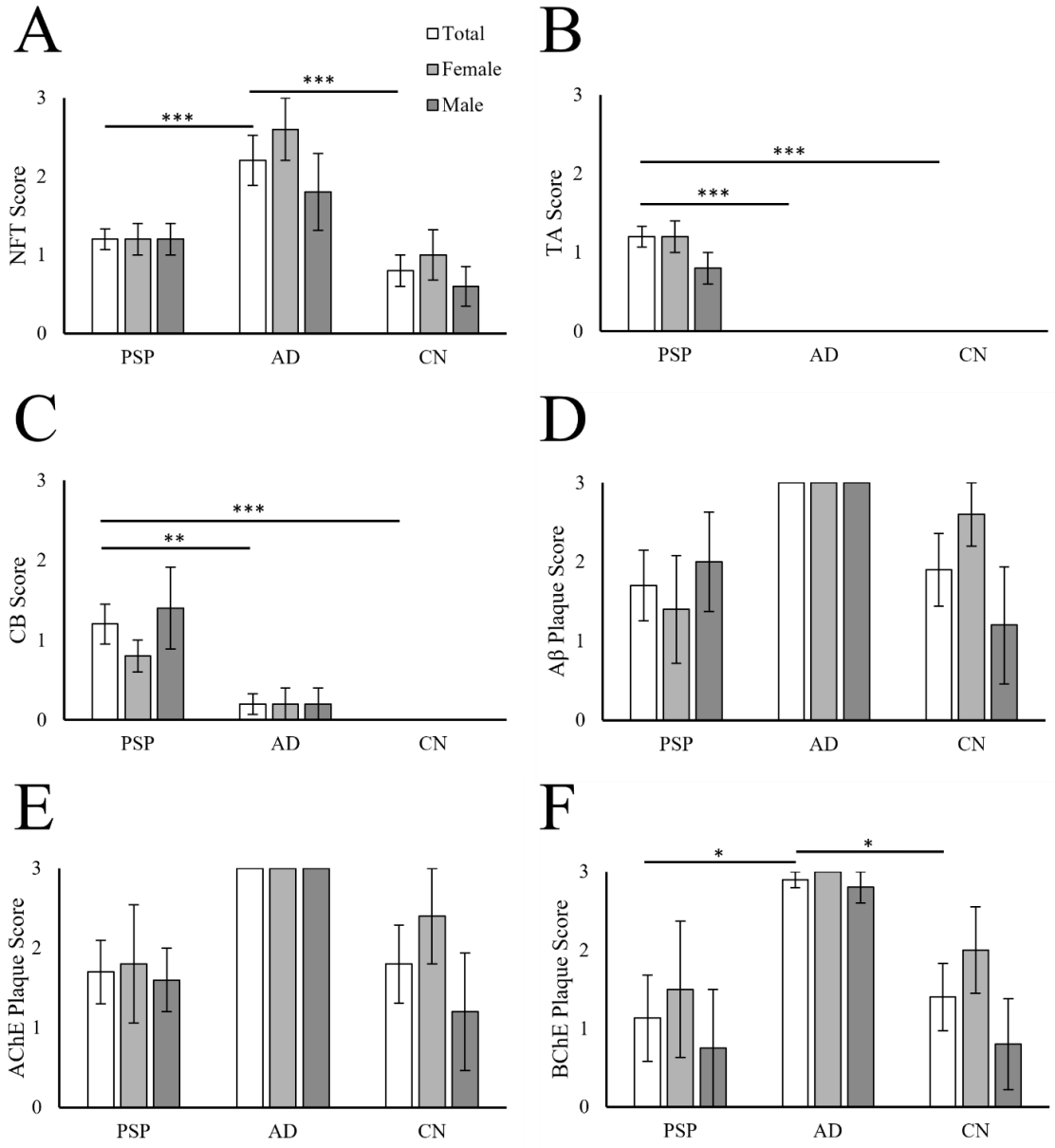


Figure 3.1 Comparison of mean abundance scores of tau neurofibrillary tangles (NFT; A), tufted astrocytes (TA; B) and oligodendroglial coiled bodies (CB; C), as well as β -amyloid (A β ; D), acetylcholinesterase (AChE; E) and butyrylcholinesterase (BChE; F) plaques in the rostral prefrontal cortex of progressive supranuclear palsy (PSP), Alzheimer's disease (AD), and cognitively normal (CN) brains. In AD, BChE pathology was significantly greater compared to PSP and CN cases. While AD cases had significantly greater NFT abundance than PSP, both PSP and AD had greater deposition than CN. Deposition of TAs and CBs, both hallmarks of PSP, were highly specific to PSP cases. No statistically significant sex differences were observed within each group. Error bars represent standard error of means. Lack of error bars in the AD groups in D and E are a result of no variance. Bonferroni corrected p values were used with significance denoted as follows: *p<0.05; **p<0.01; ***p<0.001.

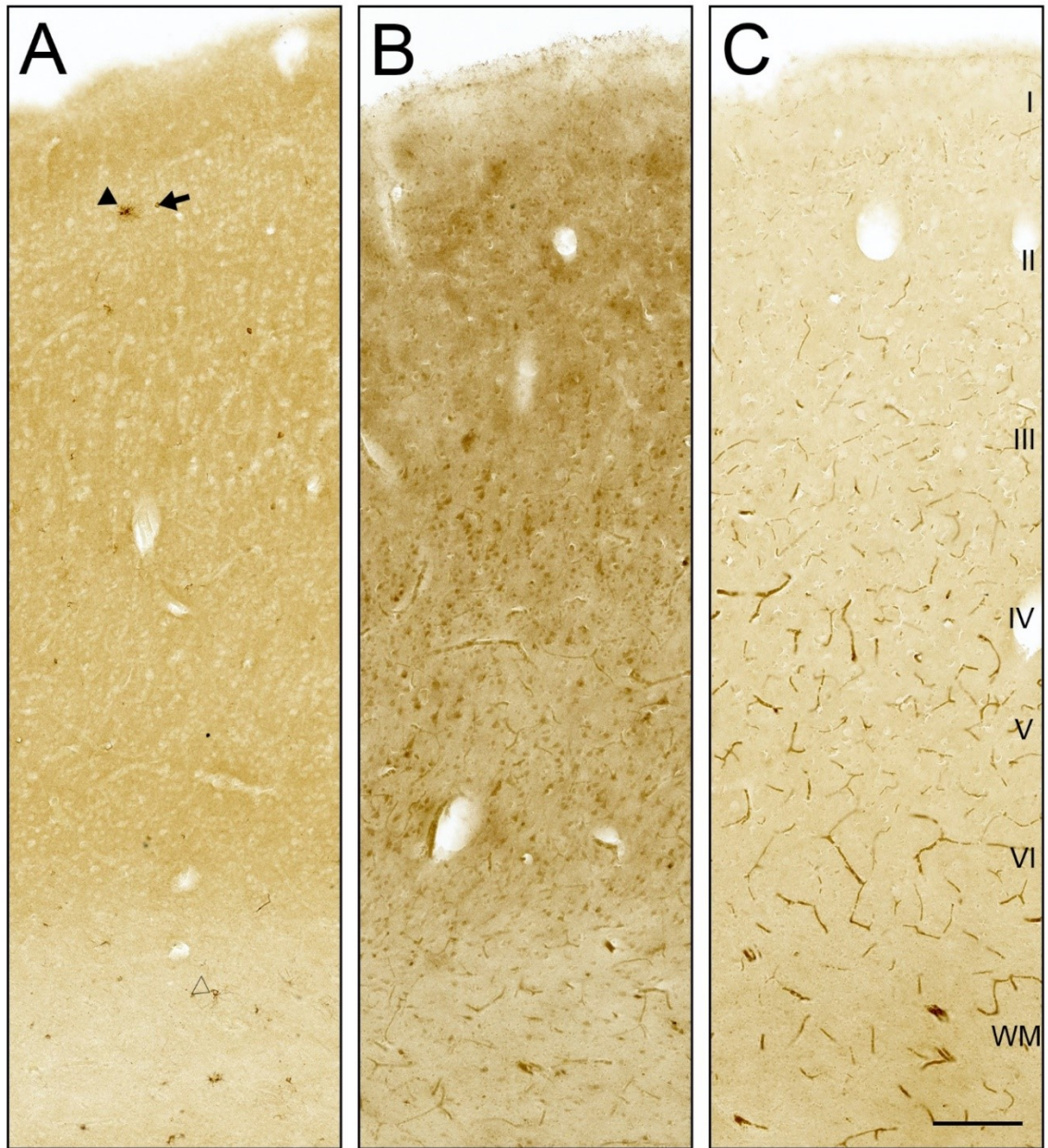


Figure 3.2 Photomicrographs depicting a cross-section of the six-layered rostral prefrontal cortex at the medial frontopolar gyrus stained with tau (A), acetylcholinesterase (AChE; B), and butyrylcholinesterase (BChE; C) in a representative progressive supranuclear palsy (PSP) case. Note, the tau-positive neuropathological hallmarks of PSP: tufted astrocytes (arrowhead) and neurofibrillary tangles (arrow) in the gray matter, and oligodendrocytic coiled bodies (open arrowhead) in the white matter (WM). AChE and BChE do not recapitulate tau staining of PSP neuropathology, only faint AChE-positive neuronal staining (B) and BChE-positive blood vessels (C) are present in the cortex. Scale bar = 200 μ M.

The abundance of tau-positive aggregates morphologically consistent with oligodrocytic CBs (Arima et al., 1997) was different between groups (Fig. 3.1C; $p=0.003$) and CBs were predominantly observed in the white matter adjacent to the medial frontopolar gyrus in all but two PSP cases (Fig. 3.2A). A singular CB was present in two AD cases (Fig. 3.1C). Sparse white matter NTs were often observed in PSP cases as well.

Other tau pathologies like AD neuritic plaques (He et al., 2018) and thorn-shaped astrocytes morphologically consistent with aging-related tau astrogliopathy (ARTAG; Kovacs et al., 2016) were observed.

Mean A β plaque abundance significantly differed between the three groups ($p=0.042$), but *post hoc* pairwise comparison revealed no specific differences (Fig. 3.1D). In PSP and CN cases, sparse to moderate A β plaque deposition was often observed predominantly in layers III and V (Fig. 3.3A, G). Females CN cases tended to have greater plaque abundance, however, no significant sex differences in A β plaque abundance were observed (Fig. 3.1D). Contrastingly, most AD cases had frequent deposition in all laminar layers across both sexes (Fig. 3.3D).

AChE-positive plaque abundance and distribution in all groups closely resembled that of A β (Fig. 3.3B, E, H), and similarly, abundance was significantly different between the three groups ($p=0.031$). However, *post hoc* pairwise comparison revealed no specific differences (Fig. 3.1E). PSP and CN cases had overall sparse to moderate deposition, with female CN cases tending to have greater abundance than their male counterparts. However, no significant sex differences in AChE plaque abundance were observed within any group (Fig. 3.1E). In all AD cases, AChE-positive plaque abundance was overall

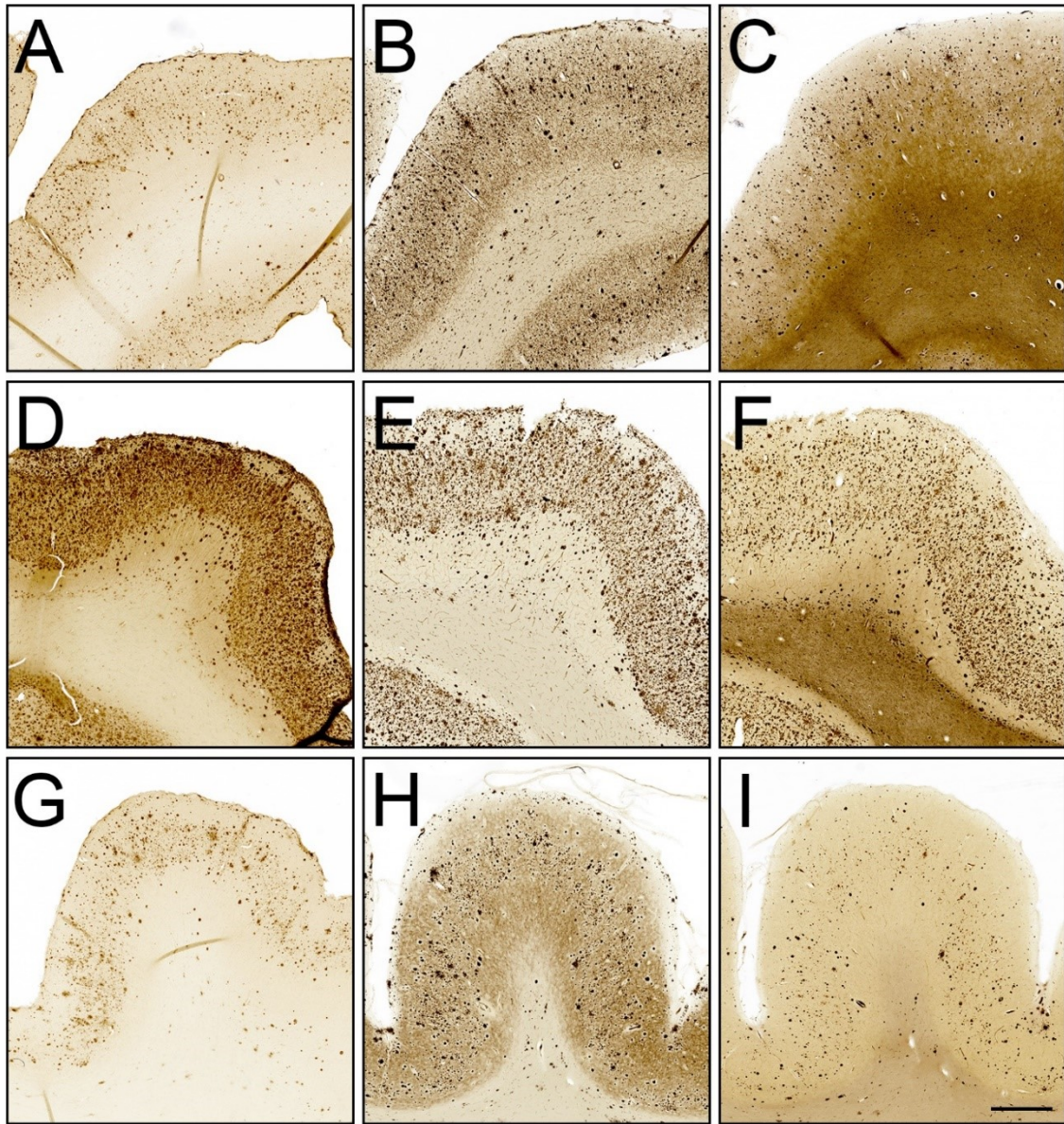


Figure 3.3 Photomicrographs of the medial frontopolar gyrus in the rostral prefrontal cortex rPFC stained for β -amyloid ($A\beta$; A, D, G), acetylcholinesterase (AChE; B, E, H), and butyrylcholinesterase (BChE; C, F, I) to visualize plaque pathology in progressive supranuclear palsy (PSP; A-C), Alzheimer's disease (AD; D-F) and cognitively normal (CN; G-I) brains. Note, only a subset of plaques are recapitulated by AChE and BChE staining in PSP and CN rPFC while the majority of plaques appear AChE- and BChE-positive in AD. Scale bar = 1 mm.

frequent, but abundance decreased within laminar layers, particularly in layer VI (Fig. 3.3E). No AChE-staining that appeared morphologically consistent with NFTs, TAs or CBs was observed (Fig. 3.2B) Additionally, AChE staining did not recapitulate AD neuritic plaques or ARTAG thorn-shaped astrocyte.

BChE-positive plaque abundance was significantly different between groups ($p=0.006$), in part, due to statistically greater abundance noted in AD cases compared to both PSP and CN cases (Fig. 3.1F; Fig. 3.3). Two PSP cases were omitted from statistical analysis due to lack of BChE staining which may be a results of technical issues such as fixation or post-mortem interval. The majority of PSP cases had no BChE-positive plaque pathology, with the exception of two cases with frequent deposition (Fig. 3.3C). Both PSP and CN cases had sparse to moderate deposition overall, with abundance trending greater in females (Fig. 3.1F). In AD, BChE-positive plaque pathology was overall moderate to frequent in all layers (Fig. 3.3F). No BChE-staining that appeared morphologically consistent with NFTs, TAs or CBs was observed (Fig. 3.2C). Additionally, BChE staining did not recapitulate AD neuritic plaques or ARTAG thorn-shaped astrocytes.

3.7. Discussion

Subcortical tau NFTs are required for the diagnosis of PSP, while TAs and CBs are also highly characteristic of the disease despite not currently being including in the diagnostic criteria (Dickson, 1999; Hauw et al., 1994; Litvan et al., 1996b). In the rPFC in PSP cases, NFT abundance was comparable to CN cases and significantly lower than deposition in AD cases (Fig. 3.1A). Low NFT burden in the prefrontal cortex is consistent with the expected distribution of NFTs in the PSP diagnostic criteria (Hauw et

al., 1994). Deposition of tau in TAs and CBs were highly specific to PSP cases compared to AD and CN cases, although neither were present in the rPFC of every PSP case. Examination of more regions may reveal tau-positive glial pathology elsewhere. CBs were present in two AD cases, however, and have been reported in early onset AD (Umahara et al., 2002). The two AD cases with CBs were diagnosed at 56 and 65 years of age respectively. As onset of symptoms likely began earlier in the latter case, both AD cases with CBs in our study could be identified as early-onset consistent with previous findings. Overall, PSP cases displayed a neuropathological burden of tau aggregates in the rPFC consistent in prevalence with current diagnostic criteria (Hauw et al., 1994; Litvan et al., 1996b).

PSP cases had an overall low neuropathological burden of A β plaques and tau NFTs in the rPFC comparable to the abundance observed in CN cases. This supports the theory that frontal lobe symptoms, such as executive dysfunction, arise from subcortical disruption of cholinergic circuits, such as through selective loss of striatal cholinergic interneurons striatum or altered cholinergic receptor expression rather than direct impairment of the frontal cortex (Warren et al., 2005).

We observed no statistically significant sex differences within groups (Fig. 3.1). In PSP, the existence of phenotypic sex differences has been disputed (Baba et al., 2006; Mahale et al., 2022), and sex differences in neuropathological burden or distribution has not been reported. However, females are reported to have greater neuropathological burden at autopsy than males in AD (Barnes et al., 2005). In this study, female AD cases, on average, had greater NFT burden than male AD cases, however, the difference was not significant. Relatively low sample size and semi-quantitative measures may not be

sensitive enough to capture differences in pathological burden between the sexes in severe disease in the current study. Females AD cases, on average, had greater NFT burden than male cases, the difference was not significant.

While changes in cholinesterase expression are well documented in AD, whether cholinesterases associate with neuropathology in PSP has not been examined. Both AChE and BChE had been shown to associate with A β plaque pathology (Darvesh et al., 2010; Geula and Mesulam, 1989a, 1995; Macdonald et al., 2017). We have previously shown that BChE, in particular, associates specifically with A β plaque pathology predominantly observed in AD compared to CN cases, and not with tau pathology in frontotemporal dementia or corticobasal degeneration, vascular infarcts, or α -synuclein pathology (Macdonald et al., 2017). Herein, we demonstrated that neither AChE nor BChE appear to associate with NFTs, TAs, or CBs in PSP. Additionally, cholinesterase-positive plaque burden in PSP cases was comparable to CN cases. While sample size should be increased in the future, these findings further support the use of BChE as a potential sensitive and specific diagnostic biomarker for AD (DeBay and Darvesh, 2020). While some imaging strategies under development for PSP diagnosis are promising, such as diffusion weighting MRI to identify focal white matter damage, heterogeneity in PSP neuropathology limit their reliability (Whitwell et al., 2017). Alternate biomarkers of PSP pathophysiology that span its multiple presentations, must be identified in order to reliably diagnose PSP.

3.8. Acknowledgements

This work was supported in part by the Canadian Institutes of Health Research (PJT-153319), Alzheimer Society of Canada (Research Program Master's Award),

Alzheimer Society of Nova Scotia (Phyllis Horton Student Research Award), Dalhousie University Faculty of Medicine (Graduate Studentship), Dalhousie Medical Research Foundation (Irene MacDonald Sobey Endowed Chair in Curative Approaches to Alzheimer's Disease, The Durland Breakthrough Fund, The Clare Durland Fund in Alzheimer's Disease Research, and Weizmann Canada Studentship in Medical Neuroscience).

CHAPTER 4 Clinicopathological Correlates in Heritable Tauopathy: A Family with the Rare IVS10+14 *MAPT* Mutation

4.1. Publication Status

Published manuscript presented with permission.

S.P. Maxwell, M.K. Cash, K. Rockwood, J. Fisk, S. Darvesh. (2021). Clinical and neuropathological variability in the rare IVS10 + 14 tau mutation. *Neurobiol. Aging*. 101: 298.e1-298.e10. DOI: 10.1016/j.neurobiolaging.2021.01.004

4.2. Overview

The current chapter presents the clinical and neuropathological data of a new family with the IVS10 +14 *MAPT* mutation and reviews instances of the mutation in other families for the purpose of comparing symptomology and neuropathology. This research was published as an article in *Neurobiology of Aging* (Maxwell et al., 2021) and appears in this chapter in its original published form.

4.3. Abstract

Mutations in the microtubule-associated protein tau gene are known to cause progressive neurodegenerative disorders with variable clinical and neuropathological phenotypes, including the intronic 10 + 14 (IVS10 + 14) splice site mutation. Three families have been reported with the IVS10 + 14 microtubule-associated protein tau mutation. Here, we describe the clinical and neuropathological data from an additional family. Neuropathological data were available for 2 of the 3 cases, III-4, and III-5. While III-5 had widespread tau deposition and atrophy, III-4 exhibited more mild neuropathological changes except for the substantia nigra. The previously reported

families that express the IVS10 + 14 mutation exhibited significant interfamilial heterogeneity, with symptoms including amyotrophy, dementia, disinhibition, parkinsonism, and breathing problems. In addition to expressing many of these symptoms, members of this fourth family experienced profound sensory abnormalities and sleep disturbance. Although there were probable clinicopathological correlates for the symptoms expressed by the earlier families and III-5 from our cohort, pathology in III-4 did not appear sufficient to explain symptom severity. This indicates the need to explore alternate mechanisms of tau-induced brain dysfunction.

4.4. Introduction

Tau is a microtubule-associated protein classically described as a regulator of cytoskeletal integrity through tubulin stabilization and polymerization (Weingarten et al., 1975). In addition, tau is involved in axonal transport (Baird and Bennett, 2013; Scholz and Mandelkow, 2014), synaptic plasticity and function (Biundo et al., 2018; Boehm, 2013; Spires-Jones and Hyman, 2014), and nucleic acid protection (Sultan et al., 2011; Violet et al., 2015, 2014). In the human central nervous system, tau is predominantly expressed in neurons, however, low levels are also expressed in astrocytes and oligodendrocytes (Binder et al., 1985; Müller et al., 1997; Papasozomenos and Binder, 1987).

Tauopathies are a family of neurodegenerative disorders characterized by the abnormal deposition of tau protein. While the majority of primary tauopathy cases are sporadic, approximately one-third have an autosomal dominant pattern of inheritance, with 10% of primary tauopathy cases attributed to microtubule-associated protein tau (*MAPT*) encoding gene mutations (Rohrer and Warren, 2011). *MAPT*, located on the long

arm of chromosome 17, is comprised of 16 exons which are used to produce 6 tau isoforms via alternate splicing mechanisms (Fig. 4.1A; Neve et al., 1986; Andreadis et al., 1995). The 58 identified pathogenic *MAPT* mutations represent a wide range of clinical and neuropathological phenotypes (Fig. 4.1B). About one-third of *MAPT* mutations affect alternate splicing of exon 10 (Niblock and Gallo, 2012). The IVS10 + 14 mutation is a rare point mutation in intron 10 of *MAPT* that has been previously identified in 3 unrelated families, 1 of Irish and 2 of Japanese descent (Hutton et al., 1998; Kutoku et al., 2012; Omoto et al., 2012). This point mutation occurs in the stem's intron splicing silencer region of the stem-loop structure at the exon-intron 10 interface, resulting in increased production of the 4-repeat isoforms of tau (Grover et al., 1999; Hutton et al., 1998; Varani et al., 1999).

The phenotype of IVS10 + 14 and other *MAPT* mutations show high inter- and intra-familial heterogeneity (Benussi et al., 2015; Kutoku et al., 2012; Lynch et al., 1994; Omoto et al., 2012). Despite the shared mutation, the clinical presentations amongst the 3 families are distinct (Lynch et al., 1994; Omoto et al., 2012; Sima et al., 1996). Here, we describe a fourth family from which 3 siblings expressed the IVS10 + 14 *MAPT* mutation and review the clinical and neuropathological presentations of the previously documented cases. By comparing the clinical and neuropathological presentations of the mutation amongst known families, we sought to gain insights into phenotypic variability despite an identical *MAPT* mutation.

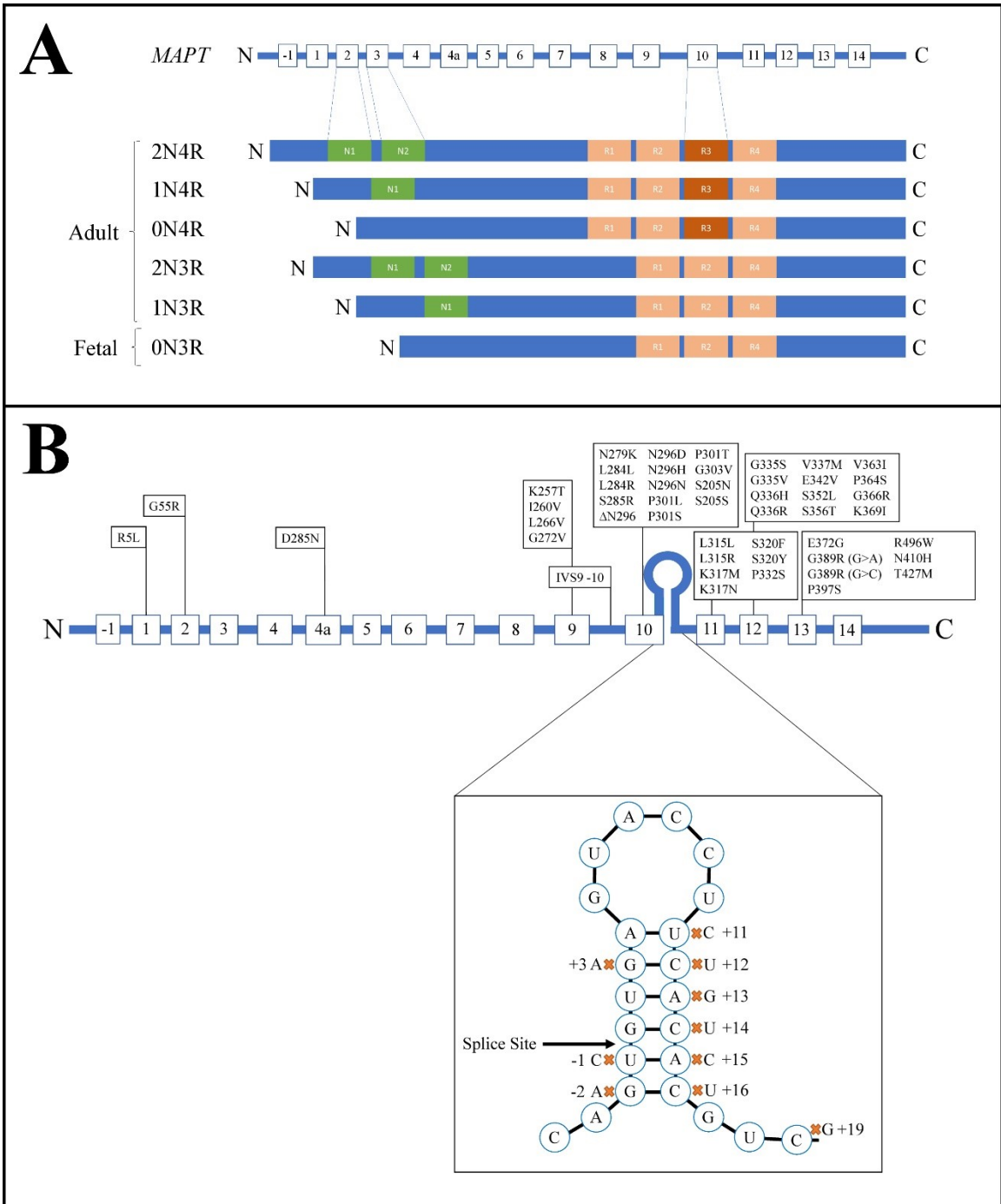


Figure 4.1 Diagrams illustrating the tau protein isoforms in the human brain (A; adapted from (Andreadis et al., 1995; Neve et al., 1986) and presently identified pathogenic microtubule-associated protein tau (*MAPT*) gene mutations (B; adapted from the Alzforum Mutation Database). Six tau isoforms are expressed in the human brain through alternate splicing of exons 2, 3, and 10 (A). Five isoforms are expressed in the adult brain, whereas the shortest isoform is only expressed in the fetal brain. The N-terminal projection domain contains exons 2 and 3 (green), and exon 10 comprises the second repeat region in the microtubule tubule binding domain (red). Fifty-eight *MAPT* mutations have been identified, which result in a pathogenic phenotype (B). A third of *MAPT* mutations affect alternate splicing of exon 10, including the IVS10 + 14 mutation located in the stem-loop structure of intron 10.

4.5. Methods

Clinical and neuropathological records from a Caucasian family of 3 siblings (III-3, III-4, III-5) with the IVS10 + 14 *MAPT* mutation were obtained from the Maritime Brain Tissue Bank with approval from the Nova Scotia Health Ethics Board. Demographic details and the availability of clinical and neuropathological tests are summarized in Table 4.1.

Summary reports of neuropsychological assessments were available for III-3, III-4, and III-5. Test data were available for III-4, including Wechsler Adult Intelligence Scale-Revised AIS-R (vocabulary, comprehension, similarities, mental arithmetic, picture completion, picture arrangement, block design, and digits symbol subtests), Wechsler Memory Scale-Revised (logical memory, digit span, and visual memory span), Rey-Osterrieth figure (copy and delayed recall), the California Verbal Learning Test, Boston Naming Test, Token Test, verbal fluency (ie, words beginning with letters F, A, and S, and animal naming), Benton Facial Recognition, and the Wisconsin Card Sorting Test (Lezak et al., 2004). The Mini-Mental State Examination (MMSE; Folstein et al., 1975) was completed for III-4 and III-5.

Postmortem brain tissues of III-4 and III-5 were examined at autopsy.

Stained neuropathological sections for were only available for III-5. Brain tissue sections from the anterior cingulate cortex, temporal lobe, basal ganglia, hippocampus, amygdala, midbrain, pons, cerebellum, and pineal gland were stained for hematoxylin and eosin and Luxol fast blue, and immunohistochemically for tau (Dako, A0024, 1:200). The anterior cingulate cortex was additionally stained with Bielchowsky silver stain and immunohistochemically stained for β -amyloid (Dako, M0872, 1:25). All sections were

Table 4.1 Case demographics data and availability of clinical and neuropathological testing

	Case		
	III-3	III-4	III-5
Sex	F	M	M
Age at onset (y)	37	45	39
Disease duration (y)	5	10	9
Neuropsychological assessment	Yes	Yes	Yes
MMSE	No	Yes	Yes
CT/MRI	Yes	Yes	Yes
SPECT	No	Yes	No
EEG	Yes	No	No
EMG/nerve conduction studies	Yes	Yes	No
Autopsy	Yes	Yes	Yes
Neuropathological assessment	No	Yes	Yes

analyzed using brightfield microscopy. Representative tissue sections were photographed using a Zeiss Axio Scan.Z1 slide scanner with Zen 3.1 software (Blue Edition, Carl Zeiss Canada Ltd; Toronto, Canada). The photomicrographs were assembled using Corel Paintshop Pro 2020 (Corel Corp; Ottawa, Canada).

4.6. Results

4.6.1. Clinical descriptions

We identified 3 siblings, all of whom presented with cognitive and behavioural dysfunction in the 1990s. Their maternal grandmother was reported to have suffered from a very rapid and progressive dementia. Their mother had died at age 55 years after experiencing a period of rapid decline in cognitive function throughout her 40s and a particularly stark deficit in recent memory. For their mother, pneumoencephalography showed brain atrophy, leading to a diagnosis of “diffuse organic brain disease and presenile dementia”.

The eldest sibling, III-3, presented with memory complaints, dysphagia, dysphoria, sleep abnormalities, loss of appetite, and hyposexuality at age 37. Sensory complaints included loss of smell and taste and occasional diplopia. She also experienced arm, neck, and back pain. An initial computed tomography (CT) scan and electroencephalogram (EEG) were normal. A neuropsychological assessment summary report showed no evidence of loss in intellectual ability but impairment in performing tasks requiring attention and concentration. In follow-up the next year, she demonstrated impaired mobility and balance, slow gait, and an extended, rigid neck, leading to frequent falls. She had become more withdrawn, depressed, and lost her voice.

Neuropsychological reassessment was reported as indicating a similar pattern of

cognitive abilities as had been shown previously. An EEG indicated mild abnormalities with nonspecific, bilateral frontotemporal theta dysrhythmia, thought to be consistent with metabolic or hypoxic encephalopathy. Electromyography and nerve conduction studies indicated diffuse motor denervation in proximal and distal muscles. A biopsy of the right gastrocnemius muscle showed amyotrophy, indicating denervation atrophy. III-3 died at age 42 years after a disease duration of approximately 5 years.

The middle sibling, III-4, had the most insidious onset and reported poor memory and loss of taste and smell 2 years before their initial examination at age 45 years. He was also greatly troubled by impaired sleep, which he attributed to dysesthesias in both his arms; this he described as “deep pain” in his muscles. His wife described him as awake throughout the night while pacing and rubbing the backs of his forearms. His MMSE was within the normal range at 29/30. Neuropsychological assessment showed impaired new learning, difficulties in object naming and verbal fluency, and intact executive, receptive languages, and visuospatial abilities. A perfusion single-photon emission computed tomography (SPECT) scan did not indicate patterns consistent with Alzheimer’s disease (AD) or frontotemporal dementia (FTD). Two years later, he developed trouble with recent memory for events, as well as parkinsonian symptoms, including bilateral cogwheel rigidity, mild bradykinesia, decreased fine finger movements in his right hand, reduced bilateral arm swing when walking, and a slight flexed posture. He also had a positive glabellar tap response. Magnetic resonance imaging (MRI) showed marked bilateral atrophy of the mesial temporal structures. Electromyography showed a mild right median and possible right ulnar sensory neuropathy. In a follow-up appointment, he presented with further cognitive deficits, particularly in memory, as well as leg pain.

Repeat neuropsychological testing demonstrated impairment in executive abilities as well as the memory and word-finding difficulties noted previously. An MRI scan noted bilateral anterior temporal atrophy, and a SPECT scan showed medial temporal hypoperfusion with some decreased perfusion in the parieto-temporal cortex. During this period of clinical decline, various pharmacologic and non-pharmacologic treatments for his dysesthesia were prescribed without success. Patient III-4 died at age 55 years having progressed to akinetic mutism after a disease duration of 10 years.

The youngest sibling, III-5, presented with memory problems, arm pain, and motor features of parkinsonism at age 39 years. He demonstrated a deterioration of functional and cognitive abilities. A summary of the neuropsychological report indicated relatively intact attention and concentration but severely compromised memory and new learning ability, cognitively inflexibility, as well as word-finding and word fluency deficits. His MMSE was 23/30. CT and MRI scans were unremarkable. One year later, he had developed further cognitive decline and behavioural changes, including progressive language deterioration, impulsivity, indecisiveness, repetitive behaviour, and disinhibition. III-5 died at age 49 years having progressed to akinetic mutism after a disease duration of 9 years.

Both III-4 and III-5 tested negative for known mutations associated with prion protein disease, fatal familial insomnia, and familial AD. However, post-mortem genotyping of a blood sample from case III-4 revealed the IVS10 + 14 *MAPT* mutation. Genetic testing was not performed for III-3 and III-5.

4.6.2. Pathology

4.6.2.1. Gross Findings

At autopsy of III-3 there was marked muscle wasting and flexion contractures. The brain and spinal cord had a normal external appearance.

The brain of III-4 had an unfixed weight of 1530 g, and the right hemisphere was retained for neuropathological examination. External inspection of the right hemisphere revealed no abnormalities of the superior sagittal sinus, dura, or leptomeninges, and there was no evidence of focal lesions or an aneurysm. Mild generalized cerebral atrophy and atherosclerosis were noted. The brainstem and cerebellum were unremarkable, and there was no evidence of uncal or tonsillar herniation. Coronal sections revealed no focal lesions, and there was mild generalized atrophy. White matter, subcortical structures, and cerebral ventricles appeared normal. An examination of the axial sections of the brain stem showed moderate depigmentation of the substantia nigra. Finally, sagittal sections of the cerebellum and serial sections of the spinal cord were unremarkable.

The brain of III-5 had an unfixed weight of 1250 g. External inspection of the brain revealed no leptomeningeal or vascular abnormalities, and there was no evidence of uncal or tonsillar herniation. There was mild frontotemporal atrophy. Coronal sections showed no evidence of focal lesions. Cortical changes were limited to mild, bilateral cortical thinning over the frontotemporal regions. Throughout the brain the white matter was atrophic bilaterally. The cerebral ventricles were mildly dilated with a left side predominance. Deep grey structures also showed atrophy predominantly on the left side. The amygdala and globus pallidus were atrophic. Axial midbrain sections showed a loss

of pigmentation in the substantia nigra and locus coeruleus. The medulla and cerebellum were unremarkable. The spinal cord was not examined.

4.6.2.2. Microscopic findings

Microscopic findings for III-3 were unavailable.

Sections from the brain of patient III-4 were stained histochemically with hematoxylin and eosin and Luxol fast blue, as well as immunohistochemically for tau. Tissue sections showed pathology in the cerebral cortex and neuronal degeneration of the amygdala, substantia nigra, and spinal cord. The anterior cingulate cortex had numerous scattered, swollen chromatolytic neurons with amorphous, eosinophilic inclusions, which were rare in remaining neocortical regions. Significant neuronal loss was not observed. The hippocampus, thalamus, and mammillary bodies were preserved. The amygdala was moderately affected with scattered swollen neurons and patchy neuronal loss and gliosis, whereas the caudate nucleus, globus pallidus, subthalamic nucleus, nucleus basalis of Meynert, and hypothalamus were normal. In the brainstem, the substantia nigra showed marked neuronal loss and rare neurons with pale, neuromelanin. Morphologically, these inclusions had a subtle fibrillary appearance. The pons, medulla and cerebellum were unremarkable. The spinal cord had scattered, swollen neurons in the ventral and dorsal horns, and nucleus thoracicus. However, white matter in the spinal cord was well preserved with no Wallerian degeneration or axonal spheroids. Likewise, dorsal and ventral roots were well preserved. Pathology that is characteristic of AD, Pick's disease, Lewy body dementia or cerebral amyloid angiopathy was absent.

Ultrastructural examination of the inclusions in the cortex of III-4 showed loose aggregates of granular material without straight or paired helical filaments. Tau

immunohistochemistry revealed tau-positive inclusions in neurons and glia with variable distribution between and within structures. In the cortex, tau-positive neuronal inclusions were common with the highest density in the parahippocampal gyrus. Tau-positive inclusions were common in the subiculum, and in the hippocampus, where these inclusions were common in CA1, occasional in CA2, and scattered in CA3 and granular layer of the dentate gyrus. Tau-positive neurons were frequent in the hypothalamus, particularly in the paraventricular nucleus, and were moderate in the amygdala, mamillary bodies, and the thalamus. The distribution of tau-positive neurons was strikingly variable in the basal ganglia with the greatest density in the nucleus accumbens, followed by the caudate head, subthalamic nucleus, putamen, and globus pallidus. The nucleus basalis of Meynert had moderate neuronal tau deposition. In the brainstem, tau-positive neurons were frequent in the substantia nigra, moderate in the periaqueductal grey, dorsal raphe, locus coeruleus, and reticular formation of the medulla, and sparse in the red nucleus, basis pontis and remaining nuclei of the medulla. Tau-positive neurons were absent in the cerebellar cortex and deep cerebellar nuclei, but scattered tau-positive inclusions were noted the in the dorsal and ventral portions of the spinal column.

In the white matter of III-4, tau immunohistochemistry revealed tau-positive glia, oligodendrocytes and astrocytes. In the cerebral cortex, glial inclusions were sparse in layers I and II, with a sharp increase in layer III. There was a dense, uniform distribution of tau-positive glia throughout layers III to VI of the cerebral cortex, through to the subcortical white matter. The distribution of tau-positive glia was generally reduced in deep grey structures including the thalamus and putamen, except for the caudate nucleus

where deposition increased dramatically amongst the striatopallidal fibres. Some white matter tracts were less affected than others. For example, the fornix had frequent tau-positive glia, whereas the white matter in the amygdala had a more moderate deposition. In the brainstem and cerebellum, only sparse tau-positive glia were noted.

As noted in the neuropathological report, the neuropathological examination of III-4 did not conform to the classical descriptions of either neurofibrillary tangles or Pick bodies.

The brain of III-5 was primarily characterized by widespread cerebral cortical and subcortical neuronal loss and gliosis. Specifically, the cerebral cortex had scattered, swollen eosinophilic neurons resembling chromatolysis. Neuronal loss and gliosis were patchy, and spongiosis was focal in the cerebral cortex, particularly in the superficial layers (Fig. 4.2). Subcortical structures also showed neuronal loss, particularly in the hippocampus and the caudate nucleus. Gliosis was most prominent in the pyramidal layer of the hippocampus. The striatum was mildly affected, whereas the medial border of the globus pallidus was pale and vacuolated (Fig. 4.2). The substantia nigra had severe neuronal loss, whereas the remaining neurons were swollen with pale eosinophilic material (Fig. 2). The locus coeruleus showed neuronal loss whereas the basis pontis was well preserved. The cerebellar cortex was unremarkable, but deep cerebellar nuclei showed mild neuronal loss with granular accumulation identified as grumose degeneration, which included swollen neurons with central chromatolysis and granular deposits composed of the altered axon terminals of Purkinje cells (Fig. 4.2).

Tau immunostaining showed widespread tau accumulation in both neurons and white matter glia in the cerebral cortex, hippocampus, amygdala, striatum, thalamus, red

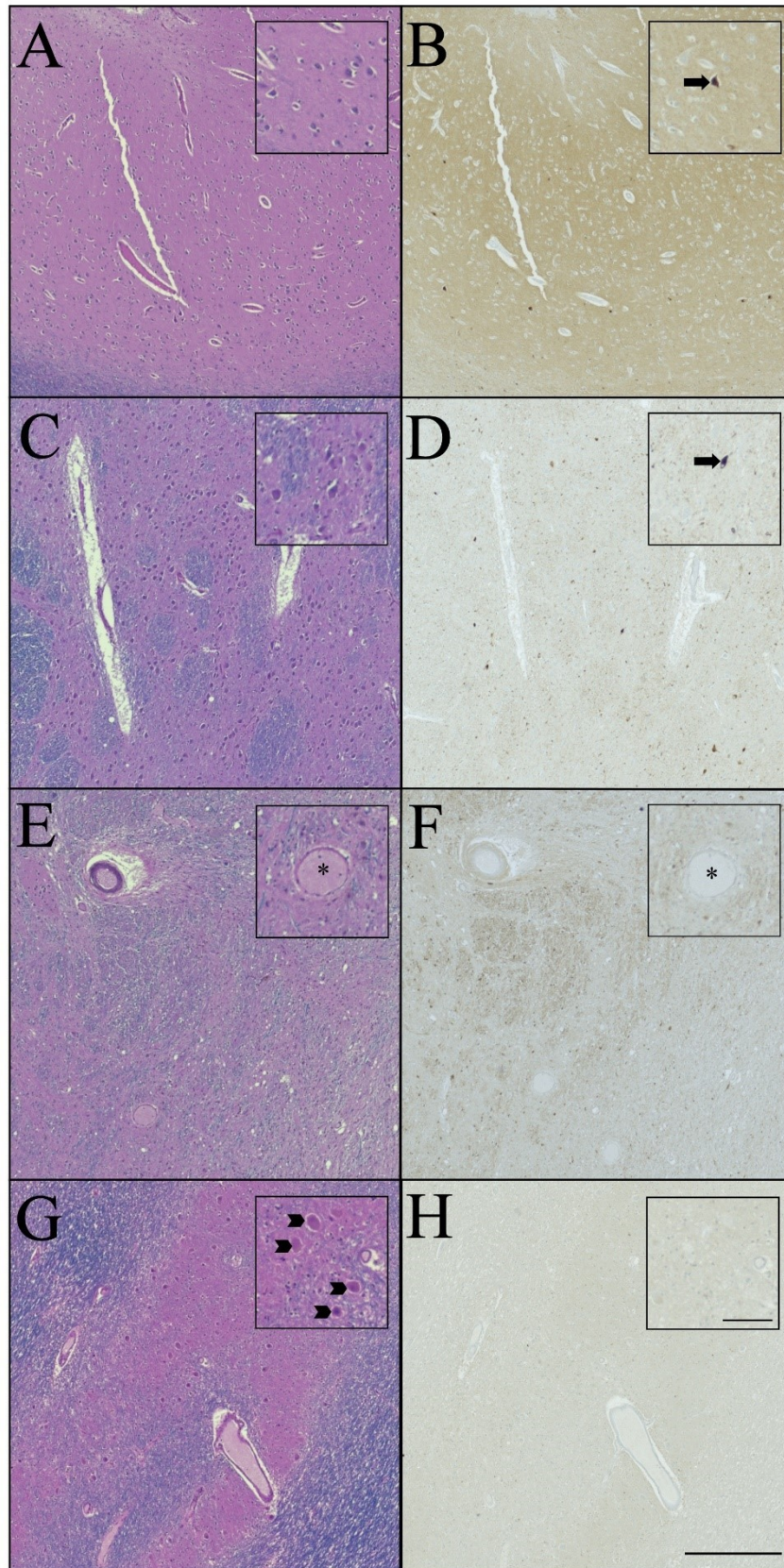


Figure 4.2 Photomicrographs of the anterior cingulate gyrus (A, B), substantia nigra (C, D), medial globus pallidus (E, F), and dentate nucleus of the cerebellum (G, H) from a case (III-5) of familial tauopathy with the IVS10 + 14 microtubule-associated protein tau (*MAPT*) mutation stained with hematoxylin–eosin and Luxol fast blue (A, C, E, G), and immunohistochemically for tau (B, D, F, H). Note, patchy neuronal loss and gliosis with scattered, swollen eosinophilic neurons in the anterior cingulate gyrus (A), severe neuronal loss with swollen eosinophilic inclusions exclusively in neurons in the substantia nigra (C), vacuolation (asterisk) in the medial globus pallidus (E), and mild neuronal loss and grumose degeneration (arrow heads) in the dentate nucleus of the cerebellum (G). There is widespread accumulation of tau in neurons (arrows) and white matter glia (B, D, F, H). Scale bar = 500 μm ; scale bar for insets = 50 μm .

nucleus, and substantia nigra (Fig. 4.2). The remaining neurons of the substantia nigra had rare neurofibrillary tangles, whereas the locus coeruleus had no tau-positive inclusions. The morphology of tau-immunopositive neurons was identified as irregular or ballooned, with some neurons exhibiting a spherical appearance. The pathologic hallmarks characteristic of Pick's disease or Lewy body dementia were absent, and β -amyloid plaques and neurofibrillary tangles characteristic of AD were scarce.

The neuropathological observations for III-5 were interpreted as being most consistent with corticobasal ganglionic degeneration.

4.7. Discussion

We report the clinical and neuropathological presentations of 3 siblings in a family with the rare IVS10 + 14 *MAPT* mutation. As it is recurrent in reports of siblings in families affected with familial FTD (Gabryelewicz et al., 2010), imaging and clinical features can both be common and divergent (Gabryelewicz et al., 2010; Greaves and Rohrer, 2019; Sellami et al., 2018). As reported below, both intra- and inter-familial phenotypic heterogeneity is well demonstrated in reports of all 4 families with the IVS10 + 14 *MAPT* mutation. This makes the case for routine genotyping and individualized outcome measurement in patients with uncommon features and a family history compatible with a rare FTD (Boxer et al., 2020).

4.7.1. Previously reported families

Lynch et al. first described the clinical presentation of an Irish family with the IVS10 + 14 *MAPT* mutation composed of 33 members, 13 affected by the disease, and 12 with sufficient clinical data (1994). This family presented with a heterogenous grouping of symptoms, which were referred to as 'disinhibition-dementia-parkinsonism-

amyotrophy complex', or DDPAC. Disease onset was reported to be approximately 45 years of age, following on what the family described as insidious personality changes characterized by disinhibition that included hyper-religiosity, alcoholism, hypersexuality, hyperphagia, aggression, irritability, "childish" egocentric behaviour, and kleptomania. Later in the disease course, dementia and parkinsonism with bradykinesia and postural instability developed. One case uniquely presented with prominent amyotrophy, thought to be linked to tau-induced peripheral axonopathy (Lynch et al., 1994; Probst et al., 2000). CT and MRI brain scans were reported as showing ventricular dilation with moderate to severe cortical atrophy, particularly in the frontal lobes (Lynch et al., 1994). Although memory was significantly affected, language and orientation were relatively preserved until later in the disease. At the end stage of the disease, all affected family members were akinetic and mute (Lynch et al., 1994; Wilhelmsen et al., 1994).

Pedigree analysis suggested that this family was affected by a highly penetrant autosomal dominant pattern of inheritance (Lynch et al., 1994) and the causative mutation was later identified as a point mutation in intron 10 of *MAPT*, changing cytosine to tyrosine 14 base pairs after the 3' end of exon 10 (Clark et al., 1998; Wilhelmsen et al., 1994).

Although the severity of the neuropathology identified in members of this family with the IVS10 + 14 *MAPT* mutation was variable between cases, its distribution remained relatively consistent (Lynch et al., 1994; Sima et al., 1996; Wilhelmsen et al., 1994). All examined brains showed moderate to severe neuronal loss and gliosis that was particularly evident in the anterior cingulate cortex, as well as frontal, temporal, and occipital association cortices with stark boundaries between affected and spared cortical

regions. Subcortical areas, including the substantia nigra, nucleus accumbens, and amygdala, were affected but to a lesser degree than the cerebral cortex. The hippocampus was relatively spared with the exception of degeneration of the afferent perforant tract, which had marked gliosis visualized by glial fibrillary protein counterstained with phosphotungstic acid-hematoxylin (Sima et al., 1996). This deterioration was thought to be a secondary result of the neuronal loss and dense gliosis observed in the entorhinal cortex. In 2 available spinal cords, there was asymmetrical neuronal loss in the anterior horn that varied by level. Tau immunoreactivity and Bielschowsky silver staining revealed argyrophilic, tau-positive intraneuronal inclusions in the cerebral cortex and white matter oligodendroglial coiled bodies. In addition, scattered ballooned neurons were observed in all cases with variable tau immunoreactivity. An insignificant deposition of AD-type neurofibrillary tangles and β -amyloid plaques were observed.

A second family with the IVS10 + 14 *MAPT* mutation comprised of 2 Japanese sisters was later reported (Omoto et al., 2012). Both sisters were described as exhibiting progressive behavioural changes and asymmetrical parkinsonism that did not respond to levodopa at disease onset. Their mother had also suffered from levodopa unresponsive parkinsonism, which progressed to akinetic mutism. These sisters later developed memory loss, disorientation, and cyanosis. Polysomnography indicated central hypoventilation with hypoxia. An MRI scan of the eldest sister showed mild atrophy of the midbrain tegmentum. The finding of decreased 5-hydroxyindole acetic acid, a major serotonin metabolite, in the cerebrospinal fluid was taken to suggest low serotonin concentration. Her symptoms and biochemical examination mimicked that of Perry's syndrome, a rare progressive brain disorder caused by mutation of the *DCTN1* gene

(Farrer et al., 2009). However, the possible diagnosis of Perry's syndrome was later dismissed by genetic and neuropathologic examination (Mishima et al., 2018). Although symptoms of both sisters improved with ventilation, the eldest sister died from apnea 22 months after disease onset (Omoto et al., 2012). Genotyping of both sisters revealed the causative IVS10 + 14 mutation.

Unlike the first identified family, disease-associated changes in the second family reported by Omoto et al. primarily affected the brainstem and subcortical regions (2012). They observed severe neuronal loss and gliosis in the globus pallidus, subthalamic nucleus, dentate nucleus of the cerebellum, substantia nigra, and midbrain tegmentum, particularly in the dorsal raphe nucleus. A profound loss of serotonergic neurons was noted in the dorsal raphe nucleus responsible for the generation of respiratory rhythm (Alvarenga et al., 2005; Omoto et al., 2012). Microscopic findings included 4-repeat tau-positive globose tangles, neuropil threads and oligodendroglial coiled bodies resembling progressive supranuclear palsy pathology in morphology and tau isoform composition (Omoto et al., 2012). The observed neuropathology did not support Perry's syndrome due to a lack of Tau DNA-binding protein 43-positive inclusions (Mishima et al., 2018; Omoto et al., 2012).

A second Japanese family with the IVS10 + 14 *MAPT* mutation consisted of 3 sisters with the shared symptom of dementia at the onset but otherwise variable clinical presentations (Kutoku et al., 2012). The youngest sister was admitted for isolated amnesic problems with otherwise preserved cognition. Brain MRI revealed mild brain atrophy in the frontal and temporal lobes. [¹²³I]iodoamphetamine SPECT scans showed hypoperfusion of the hippocampus, superior parietal lobe, and posterior cingulate gyrus

contributing to a provisional diagnosis of amnesic mild cognitive impairment. Over a 5-year period, she experienced progressive behavioural changes (aggression, overindulging in candy), parkinsonism, and worsening dementia. DNA analysis identified the causative IVS10 + 14 *MAPT* mutation. A review of her family medical history revealed 2 elder sisters who also received medical care for progressive dementia and genotyping confirmed the presence of the same mutation in these 2 siblings. The eldest sister had been diagnosed with FTD with associated behavioural changes, including alcoholism, without parkinsonism. The other sister had presented with memory disturbance that progressed to include parkinsonism.

Neuropathological data from this second Japanese family was not reported (Kutoku et al., 2012).

4.7.2. Clinicopathological correlates

Herein, we report 3 cases from a single family with a rare point mutation in intron 10 of *MAPT*; however, our data must be interpreted with caution. For example, neuropathological reports were only available for cases III-4 and III-5. Clinical and neuropathological information was obtained through a chart review, leading to information gaps. Sex differences could not be examined because of small cohort sizes, unequal distribution of sex, and the deidentification of sex to maintain patient anonymity in the Lynch et al. cohort (1994; Wilhelmsen et al., 1994). However, consistent with reports from other families, we found clinical presentations with predominant prefrontal behavioural features (withdrawal, impulsivity, indecisiveness, repetitive behaviour, and disinhibition), motor findings (parkinsonism and amyotrophy), and cognitive decline (memory, attention, and language; Table 4.2). Our cohort also exhibited the additional

Table 4.2 Clinical features of the IVS10 + 14 *MAPT* mutation expressed by number of cases in each cohort

Clinical Characteristics	Cohort			
	(Lynch et al., 1994)	(Omoto et al., 2012)	(Kutoku et al., 2012)	Current cohort
Cohort size	12	2	3	3
Cognitive				
Dementia	12	1	3	3
Executive dysfunction	0	0	0	2
Motor				
Parkinsonism	12	2	2	3
Behavioral				
Apathy	12	1	0	3
Disinhibition	12	0	2	1
Sensory				
Limb pain	0	0	0	3
Sensory loss	1	0	0	2
Sleep				
Sleep disturbance	2	0	0	2
Other				
Cyanosis	0	1	0	0

features of profound sensory findings, and 2 cases experienced sleep disturbances.

Below, we will compare the clinicopathological correlates of the IVS10 + 14 *MAPT* mutation across all known families.

Disruption of frontal-subcortical neurocircuitry affecting the dorsolateral prefrontal, orbitofrontal, and anterior cingulate circuits is associated with executive dysfunction, disinhibition, and apathy, respectively (Bonelli and Cummings, 2007). All reported cases of the IVS10 + 14 *MAPT* mutation experienced progressive dementia and changes in behaviour (Kutoku et al., 2012; Lynch et al., 1994; Omoto et al., 2012) with symptoms that can, in part, be attributed to pathology in 1 or more areas involved in these frontal-subcortical circuits.

The dorsolateral circuit mediates executive function, which includes the ability to form and execute goal-oriented plans effectively (Bonelli and Cummings, 2007; Lezak et al., 2004). Impaired concentration and attention were observed in 2 of our cases but were not noted in the other families (Kutoku et al., 2012; Lynch et al., 1994; Omoto et al., 2012). As executive dysfunction often precedes functional cognitive decline, it is likely that it contributed to the demented phenotype reported in all cases (Baudic et al., 2006; Carlson et al., 2009; Clark et al., 2012). The first reported family had severe atrophy of the prefrontal cortex and moderate involvement of the globus pallidus, whereas the dorsal part of the basal ganglia and dorsomedial thalamus were relatively spared (Sima et al., 1996). The second family described by Omoto et al. (2012) had severe neuronal loss and gliosis of the globus pallidus. Although both III-4 and III-5, in our cohort, had mild, generalized frontal atrophy, III-5 had preserved executive function despite having severe atrophy and vacuolation of the globus pallidus, neuronal loss in the caudate nucleus and

widespread tau pathology in the cerebral cortex, striatum and thalamus. Contrastingly, the dorsolateral prefrontal circuit of III-4, who experienced executive dysfunction, was relatively preserved aside from significant tau-positive glial inclusions in the striatopallidal fibers of the caudate nucleus. Thus, while the observed pathology was sufficient to explain the executive dysfunction noted in 2 previously reported families, it was insufficient to explain the severity of symptoms in our cohort.

Dysfunction of the orbitofrontal circuit mediates behavioural disinhibition (Bonelli and Cummings, 2007; Starkstein and Kremer, 2001), including impulsivity and addiction. All cases reported by Lynch et al. (1994) and Kutoku et al. (2012), one described by Omoto et al. (2012), and our case, III-5, exhibited behaviours that can be attributed to disinhibition (Table 4.2). Neuronal loss and gliosis was identified in the orbitofrontal cortex, globus pallidus, and caudate nucleus of the first reported family (Sima et al., 1996). Despite experiencing appetite loss usually associated with orbitofrontal damage, the case described by Omoto et al. (2012) did not have notable cortical atrophy but did have severe neuronal loss and gliosis in the globus pallidus. The disinhibition experienced by III-5 in our cohort could be attributed to severe atrophy of the frontal cortex and deep grey structures, including the caudate and globus pallidus.

Impairment of the anterior cingulate circuit mediates apathy or loss of motivation (Bonelli and Cummings, 2007). Akinetic mutism is a wakeful state of severe apathy with indifference to pain, thirst and hunger, absence of initiative and speech, and failure to respond to questions or commands (Ackermann and Ziegler, 1995; Mega and Cohenour, 1997). All cases described by Lynch et al. (1994) and 2 of our cases (III-4 and III-5) experienced apathy culminating in akinetic mutism (Table 4.2). Our case III-3 and one of

the sisters described by Omoto et al. (2012) also experienced apathy (Table 4.2). The brains of the first reported family exhibited severe pathologic changes of the anterior cingulate cortex and ventral regions of the basal ganglia (Sima et al., 1996) associated with the circuit (Bonelli and Cummings, 2007; Selemon and Goldman-Rakic, 1985). Regarding our cases, III-4 demonstrated severe cortical pathology in the anterior cingulate cortex, whereas the basal ganglia was preserved. In contrast, case III-5 noted milder pathologic changes in the anterior cingulate cortex, as well as neuronal loss in the caudate nucleus, and atrophy of the globus pallidus with microscopic vacuolation. Only the globus pallidus was affected in the case described by Omoto et al. (2012). A lack of neuropathological data for case III-3 prevents a further clinicopathological correlation.

With the exception of one case described by Kutoku et al. (2012), all cases experienced parkinsonian motor symptoms (Table 4.2; Lynch et al., 1994; Omoto et al., 2012). Parkinsonism is driven by the loss of dopaminergic neurons, especially of the substantia nigra (Bernheimer et al., 1973), which results in an imbalance in basal ganglia output and cumulates in increased inhibition of the thalamus, suppressing movement (McGregor and Nelson, 2019). All cases that experienced parkinsonism exhibited depigmentation and neuronal loss of the substantia nigra consistent with their symptoms (Omoto et al., 2012; Sima et al., 1996). In addition, III-5 had grumose degeneration of the deep cerebellar nuclei. It has been proposed that grumose degeneration contributes to the features of postural instability and frequent falls in progressive supranuclear palsy because of its disruption of the dentatorubrothalamic tract (Hauw et al., 1994; Ishizawa et al., 2000; Litvan et al., 1996a). Therefore, grumose degeneration may have contributed to the parkinsonism exhibited by III-5.

Breathing issues that progressed to pronounced cyanosis was a unique feature of the second family reported and was attributed to atrophy of the dorsal raphe nucleus (Table 4.2; Omoto et al., 2012). Our case III-3 was noted to have abnormalities consistent with hypoxic encephalopathy indicated by EEG, but without neuropathological findings, a cause is not discernable. Respiratory centers were preserved in all other cases, although III-5 and the Lynch et al. (1994) cohort did demonstrate neuronal loss in the locus coeruleus (Sima et al., 1996).

Case III-4 was observed to have the unique motor symptom of impaired sleep and arm dysesthesias, which is consistent with the “restless arms” variant of restless leg syndrome (RLS; Ruppert, 2019). Although the pathophysiology of RLS remains unknown, it has been determined that gross structural brain abnormalities are not a pathologic feature of RLS, rather, the pathophysiology is likely neurochemical or receptor-based (Bucher et al., 1996; Koo et al., 2016; Pittock et al., 2004). Dopaminergic dysfunction in the form of altered post- and pre-synaptic activity of the nigrostriatal system likely contributes to idiopathic RLS (Connor et al., 2009). However, leg restlessness that occurs as a symptom of Parkinson’s disease is likely related to localized dopaminergic neuronal loss in the substantia nigra (Peeraully and Tan, 2012). The incidence of RLS is also high in patients with spinal cord injury (de Mello et al., 1996; Hartmann et al., 1999; Nilsson et al., 2011; Salminen et al., 2013; Telles et al., 2011; Yokota et al., 1991). This is thought to result from changes in dopaminergic signaling in the spinal cord because of the effectiveness of dopaminergic medication in treating RLS symptoms following spinal cord injury (Giummarra and Bradshaw, 2010; Kumru et al., 2016; Nishida et al., 2013). In the case of III-4’s unique presentation of RLS symptoms,

possible contributing factors may have included dopaminergic neuronal loss in the substantia nigra, in combination with altered dopaminergic signalling as a result of extensive tau pathology, particularly in the striatum, as well as loss of dopaminergic innervated spinal cord neurons.

One member of the family described by Lynch et al. (1994) had clinical amyotrophy with muscle wasting as did our case III-3. Although III-4 had pathologic changes in the ventral horn, the spinal cord and ventral roots were normal. The spinal cord was unavailable for III-5. However, all 3 siblings in our cohort described muscle pain (Table 4.2), and while the dorsal horn was preserved in III-4, there were swollen neurons and tau-positive inclusions present. Some cases with the IVS10 + 14 tau mutation had neurofilament-positive axonal spheroids in the anterior horn of the spinal cord (Sima et al., 1996), a characteristic shared with sporadic and familial amyotrophic lateral sclerosis (ALS; Carpenter, 1968; Hirano et al., 1984; Munoz et al., 1988; Rouleau et al., 1996). Neurofilament accumulation is thought to slow axonal transport, impairing axonal, and resulting in axonal degeneration (Collard et al., 1995). While ALS is characterized by neurofilament pathology, amyotrophy in Guamanian ALS and parkinsonism-dementia complex is caused by tau deposits in the spinal cord (Matsumoto et al., 1990). Animal models expressing certain tau mutations also display an amyotrophic phenotype with either neurofilament or tau accumulation in the spinal cord (Ishihara et al., 1999; Lewis et al., 2000; Probst et al., 2000; Spittaels et al., 1999).

Sleep disturbance was a clinical feature in 2 of our cases (Table 4.2). Although III-4's sleep problems can be partly attributed to discomfort from nighttime predominant RLS symptoms (Bogan, 2006), the source of sleep disturbance in III-3 is not clear

because of a lack of neuropathological data. III-4 did not have severe pathology in other sleep centers such as the basal forebrain, hypothalamus, or brainstem (Hauw et al., 2011), aside from the substantia nigra, suggesting that neuropathological changes in brain sleep centers alone were not sufficient to explain his sleep abnormalities. The basal ganglia has recently been implicated in sleep-wake regulation (Lazarus et al., 2013), but aside from increased tau deposition in some structures, there was not discernable atrophy in the basal ganglia of III-4. Two family members described by Lynch et al. (1994) also experienced sleep disturbance in the form of somnolence (Table 4.2). The brains of this family exhibited moderate neuronal loss in the hypothalamus and mild loss in the locus coeruleus, both of which contained tau-positive neuronal inclusions (Sima et al., 1996), potentially contributing to their somnolescent phenotype (Hauw et al., 2011; Von Economo, 1968, 1930).

Sensory dysfunction in the form of loss of smell and taste was a unique feature in 2 of our 3 cases (III-3 and III-4; Table 4.2). Most individuals that experience smell disorders also experience taste disorders (Deems et al., 1991). The association between loss of taste and smell is hypothesized to be a result of either central nervous system interactions between chemical senses (Landis et al., 2010) or comorbidities (Stinton et al., 2010). The olfactory pathway begins in the olfactory epithelium with projections to the olfactory bulb, which then projects to the primary olfactory gyrus via the olfactory tract and then to the primary olfactory cortex (e.g. olfactory tubercle and piriform) (Hamodat et al., 2017; Price, 1990; Shipley and Reyes, 1991). The gustatory pathway begins at the chemo-receptive first order neurons of the tongue, which synapse with primary sensory neurons. The pathway end in the regions responsible for perceiving and distinguishing

tastes, the gustatory complex, the anterior insula in the temporal lobe, and the frontal opercular region (Kobayashi, 2006) via the medulla and thalamus (Iannilli and Gudziol, 2019). Neuropathologic data were unavailable for III-3, and the only neuropathologic changes noted in the brain of III-4 potentially related to olfaction and gustation was mild generalized cortical atrophy, which appears insufficient to explain the severity of his sensory loss.

Phenotypic variability, even in patients with the same mutation, is not unique to the IVS10 + 14 *MAPT* mutation nor tauopathies. It has been observed previously with other FTD variants (Greaves and Rohrer, 2019), including progranulin gene deletion, which results in a TAR DNA-binding protein 43 proteinopathy (g.2988_2989delCA, P439_R44ofsX6; (Gabryelewicz et al., 2010). One brother presented with predominant parkinsonism, apathy, and somnolence and progressed to develop cognitive, behavioural, and psychiatric features, whereas the other presented with progressive, nonfluent aphasia and progressed to develop behavioural and motor features. The challenges of this variability in clinical trials have been a recent focus, leading to the suggestion that in addition to biomarkers, individualized outcome measures may facilitate efficient evaluation of disease treatment (Boxer et al., 2020). Consider that this newly described family, although 2 affected members (III-3 and III-4) had early loss of taste and smell, and 2 complained of arm pain (III-4 and III-5), no presenting feature was common to all. Even some shared features (e.g. dysphoria, gait abnormalities, impaired memory) varied in their timing of onset (from a presenting feature to a later one) and in salience (e.g. impaired sleep, when present understandably became the main focus). Other symptoms were present only in one affected member but still important to them and their care

partners. Coupled with the relative rarity of familial tauopathies, these are pragmatic issues for clinical trials in the area and especially for progress in the development of disease-modifying therapies.

4.8. Conclusion

Each family with the IVS10 + 14 *MAPT* mutation shows striking intrafamilial and interfamilial phenotypic variability despite sharing the same causative mutation. Our cases contribute the additional symptoms of sleep disturbance and sensory abnormalities to the potential clinical profile of the IVS10 + 14 *MAPT* mutation. This mutation demonstrates the lack of a clear genotype-phenotype correlation. Alternative mechanisms must influence disease pathogenesis, including gene interactions, epigenetics, and stochasticity, to explain phenotypic variability in heritable diseases (Kammenga, 2017). Importantly, our cases illustrate that neuropathology is not always sufficient to explain the presence and severity of clinical symptoms, the exception in this example being motor symptoms and atrophy of the substantia nigra. Likewise, the focal areas of increased tau deposition identified in III-4 were not associated with gross structural changes or neuronal loss, and it is known that tau is capable of inducing cognitive impairment through both neuronal loss and synaptic dysfunction (Di et al., 2016). The widespread and variable tau pathology in individuals with the IVS10 + 14 *MAPT* mutation seems to correlate with clinical symptoms in all reported cases except III-4. The severity of the syndrome exhibited by III-4 from our cohort seem disproportionate to the observed pathology indicating the need to explore alternate mechanisms of tau-induced changes in the brain in addition to the observable structural alterations.

4.9. Acknowledgements

We would like to thank Drs. Rob Macaulay, Alex Easton and Sidney Croul for their expertise and assistance in obtaining the neuropathological data in preparation of this manuscript, and Kosuke Kanayama for his help with literature translation. This work was supported in part by the Canadian Institutes of Health Research (PJT- 153319), Alzheimer Society of Canada (Research Program Master's Award), Alzheimer Society of Nova Scotia (Phyllis Horton Student Research Award), Dalhousie University Faculty of Medicine (Graduate Studentship), Dalhousie Medical Research Foundation (Irene MacDonald Sobey Endowed Chair in Curative Approaches to Alzheimer's Disease and The Durland Breakthrough Fund).

CHAPTER 5 Conclusions

5.1. Overview

This final chapter will briefly review the conclusions of the previous three chapters, then consolidate and contextualize their findings regarding clinopathological correlation in aging and neurodegeneration. Future work will be proposed to explore additional neuropathologic and cholinergic changes in the aging and disease process and the significance of the presented work will be addressed.

5.2. General Conclusions

Chapter 1 provided a review of the tau and its role in disease, as well as the clinical and neuropathological presentation of the most common tauopathy, Alzheimer's disease (AD). The present strategies used for the clinical and neuropathological diagnosis of AD were outlined, as well as the strategies being employed to develop novel biomarker assays and neuroimaging techniques for diagnostics, and therapeutics. Cholinergic dysfunction and its correlation with cognitive decline in AD was highlighted, with a focus on cholinesterase expression. Cholinesterase inhibitors are one of the only available treatments for AD that have demonstrable, positive clinical outcomes. Meanwhile, clinical trials targeting the clearance of AD-associated pathology have exhibited no clinical benefit. Finally, I reviewed our previous work demonstrating that butyrylcholinesterase (BChE) is a sensitive and specific biomarker of AD compared to current targets such as β -amyloid ($A\beta$), with the potential to be used as a target for diagnosis using neuroimaging techniques.

Chapter 2 described the abundance of neuropathological and cholinesterase-associated aggregates in cognitively normal octogenarians and older (CNOO) compared to AD in the rostral prefrontal cortex (rPFC) and the hippocampal formation, two regions

vital to cognitive function. This work demonstrated the high prevalence and abundance of protein aggregates associated with neurodegeneration in older brains. Even in cases with very high A β plaque load, BChE expression was noted to be significantly lower in CNOO than in AD cases. Cholinesterases were also observed to associate with a subset of tau neurofibrillary tangles (NFTs) in both groups, which may imply cholinesterase involvement in tangle formation. Regarding potential mechanisms of cognitive preservation, low cholinesterase expression in CNOO cases compared to AD cases may indicate greater acetylcholine availability for cholinergic neurotransmission. Differential protein sequestering strategies, such as intraneuronal A β and astrocytic tau uptake, may represent an additional neuroprotective mechanism in the CNOO. These findings indicate that while neuropathological aggregates may be necessary for the pathophysiology of AD and other neurodegenerative disorders, they are not sufficient to cause neurodegeneration, as neuropathology can be highly abundant in cognitive normal (CN) brains.

In Chapter 3, we examined and compared neuropathological and cholinesterase expression in the rPFC in progressive supranuclear palsy (PSP), AD, and CN brains. Both AD and PSP experience executive dysfunction, a cognitive process partially attributed to the rPFC. It was demonstrated that PSP brains tend to have a low abundance of AD-associated neuropathology, and glial tau aggregates are highly specific to PSP compared to AD and CN. BChE maintained specificity to plaques in AD, and neither AChE nor BChE associated with tau pathology in PSP. These findings support the use of BChE as a biomarker for AD, as well as indicate that low acetylcholine availability in the rPFC due to cholinesterase expression is not likely a major contributor to executive dysfunction in PSP.

Chapter 4 described a new family comprised of three siblings exhibiting the rare IVS10 + 14 *MAPT* mutation that caused early-onset, rapid deterioration of cognitive, behavioural, and motor systems. Our study was limited by a lack of genetic testing on all siblings, necessitating the assumption that two of the siblings also expressed the IVS10+14 *MAPT* mutation, availability of clinical and neuropathological tests, and availability of histochemical and synaptic staining. Comparison of our cases to the three previously reported families revealed a high degree of intra- and inter-familial heterogeneity in clinical and neuropathological presentation that was still present when there was a unifying, causal mutation. Unlike sporadic cases of tauopathy described in the preceding chapters, the cause of heritable tauopathy is known, however, that does not indicate that symptomology or patterns of tau deposition can be predicted. Nor does it indicate that clinical presentation will correlate with post-mortem examination of neuropathology, as indicated by one case in our cohort who exhibited severe symptoms that did not seem attributable to the relatively mild neuropathologic changes observed. These findings indicate a need to expand the scope of clinicopathological correlation beyond burden of neurodegeneration associate proteins, such as through examining changes in protein expression at the molecular level. It also demonstrates that even with a shared causal mutation, heterogeneity can result from several factors including genetic, epigenetic, sex, and stochastic differences. For example, the tau H1C haplotype confers a greater risk of developing sporadic tauopathy (Myers et al., 2005), and epigenetic factors such as chronic stress is associated with increased tau aggregation (Carroll et al., 2011). These differences may account for the clinical and neuropathological intra- and inter-familial variability observed.

It is also pertinent to discuss the importance of sex differences in the context of neurodegenerative disease research and this thesis. Sex differences in AD specifically have been well characterized, with females having a greater lifetime risk of developing AD (Plassman et al., 2007), and the prevalence and effect of risk factors for AD, such as depression or APOE genotype, vary by sex (Duarte-Guterman et al., 2021; Mielke, 2018). Clinically, AD females experience greater cognitive decline than males (Duarte-Guterman et al., 2021; Henderson and Buckwalter, 1994). Neuropathologically, AD females have greater neuropathological burden (Barnes et al., 2005), reduced hippocampal volumes (Apostolova et al., 2006), and greater overall brain atrophy (Hua et al., 2010) than age-matched males. Sex differences have not been as well characterized in other neurodegenerative disease. For example, only sex differences in clinical presentation have been examined in PSP (Baba et al., 2006). Continued characterization of sex differences in neurodegeneration and aging is vital to account for one potential cause of clinical and neuropathological heterogeneity.

This thesis examined sex differences in Chapters 2 and 3 in the context of aging and PSP, while they could not be examined in Chapter 4 due to limited sample size in our cohort and inconsistent reporting of sex in previous cohorts. While there were regional sex differences of tau in the rPFC and BChE plaques in the presubiculum of CNOO cases (Appendix A, Supplementary Data, Table A.1), no sex differences were observed between male and female AD cases (Appendix A, Supplementary Data, Table A.2). Likewise, no sex differences were observed in neuropathological burden in PSP, AD or CN cases in Chapter 3 (Fig. 3.1). Small sample size and a lack of sensitivity of semi-quantitative analysis likely contributed to a lack of observed sex differences herein.

5.3. Future work and Significance

A β - and tau-targeted approaches in AD have resulted in multiple failed clinical trials of antibodies that clear neuropathological burden, but fail to produce clinically meaningful results in humans (Giacobini and Gold, 2013; Sandusky-Beltran and Sigurdsson, 2020). For example, the A β -targeting aducanumab reduces A β plaque burden in the brain (Sevigny et al., 2016). Recently, aducanumab was approved for use in AD despite unclear drug eligibility, concerning side effects and a lack of evidence that the drug produced a significant clinical benefit during clinical trials (Fleck, 2021; Knopman et al., 2021). All that the approval of aducanumab has provided is false hope to desperate patients and squandered health care resources (Fleck, 2021). Clearing AD neuropathology is evidently not sufficient to prevent AD disease progression. This thesis has demonstrated that neuropathological changes do not always correlate with clinical phenotype. Thus, alternative avenues for diagnostic and therapeutic approaches to AD must be explored.

Cholinergic dysfunction is implicated in several neurodegenerative disorders, such as AD, Parkinson's disease and PSP, which share localized loss of cholinergic neurons (Bartus et al., 1982; Pasquini et al., 2021; Warren et al., 2005). However, we have demonstrated that altered cholinesterase expression, particularly of BChE, appears to be specific to AD herein, and previously (Macdonald et al., 2017). At present, BChE provides a target for the diagnosis of AD during life, which could lead to better clinical management of the disease course for patients, caregivers, and physicians. It could also provide more accurate patient selection for AD-focused clinical trials. In the future, when

more treatments or curative approaches are available, accurate diagnostics will be required to determine drug eligibility.

In addition to supporting research into novel therapeutics, the use of cholinesterase inhibitors (ChIs) should also be re-evaluated. It has been demonstrated that ChIs are both under prescribed and prescribed sub-optimally regarding length of prescription and dosage (Giacobini et al., 2022). It has been decades since the last ChI was developed. The first ChI, tacrine, predominantly inhibits acetylcholinesterase (AChE; Darvesh et al., 2003b), but the clinical benefit remains controversial and it is no longer available due to severe side effects (Qizilbash et al., 1998). The currently available ChIs inhibit both AChE and BChE to varying degrees (Darvesh et al., 2003b). The development of a BChE specific inhibitor may provide further insight into BChE's role in AD pathophysiology, and may be an effective, novel therapeutic.

AD is only one of many tauopathies. Herein, we also presented an examination of neuropathology in PSP. Like AD, diagnosis of PSP is complicated by clinical heterogeneity and non-specific neuropathological features, such as the presence of tau or white matter atrophy (Whitwell et al., 2017). There are also no drugs available that are specific to PSP treatment, although ChIs and drugs used in Parkinson's disease have been tested with mixed results (Fabbrini et al., 2001; Kompoliti et al., 1998; Litvan et al., 2001). Disease features which are specific to PSP pathophysiology, as BChE appears to AD, must be identified to develop more targeted diagnostics and therapeutics for PSP.

Through highlighting the limitations of neuropathological targets in tauopathy, this thesis sought to shift the focus on alternative mechanisms of cognitive dysfunction,

such as cholinesterase expression, that have demonstrable diagnostic and therapeutic potential.

REFERENCES

- Ackermann, H., Ziegler, W., 1995. [Akinetic mutism--a review of the literature]. *Fortschr. Neurol. Psychiatr.* 63, 59–67. <https://doi.org/10.1055/s-2007-996603>
- Ahmed, Z., Bigio, E.H., Budka, H., Dickson, D.W., Ferrer, I., Ghetti, B., Giaccone, G., Hatanpaa, K.J., Holton, J.L., Josephs, K.A., Powers, J., Spina, S., Takahashi, H., White, C.L., Revesz, T., Kovacs, G.G., 2013. Globular glial tauopathies (GGT): consensus recommendations. *Acta Neuropathol. (Berl.)* 126, 537–544. <https://doi.org/10.1007/s00401-013-1171-0>
- Alafuzoff, I., Ince, P.G., Arzberger, T., Al-Sarraj, S., Bell, J., Bodi, I., Bogdanovic, N., Bugiani, O., Ferrer, I., Gelpi, E., Gentleman, S., Giaccone, G., Ironside, J.W., Kavantzias, N., King, A., Korkolopoulou, P., Kovács, G.G., Meyronet, D., Monoranu, C., Parchi, P., Parkkinen, L., Patsouris, E., Roggendorf, W., Rozemuller, A., Stadelmann-Nessler, C., Streichenberger, N., Thal, D.R., Kretschmar, H., 2009. Staging/typing of Lewy body related alpha-synuclein pathology: a study of the BrainNet Europe Consortium. *Acta Neuropathol. (Berl.)* 117, 635–652. <https://doi.org/10.1007/s00401-009-0523-2>
- Albert, M.S., DeKosky, S.T., Dickson, D., Dubois, B., Feldman, H.H., Fox, N.C., Gamst, A., Holtzman, D.M., Jagust, W.J., Petersen, R.C., Snyder, P.J., Carrillo, M.C., Thies, B., Phelps, C.H., 2011. The diagnosis of mild cognitive impairment due to Alzheimer's disease: Recommendations from the National Institute on Aging-Alzheimer's Association workgroups on diagnostic guidelines for Alzheimer's disease. *Alzheimers Dement. J. Alzheimers Assoc.* 7, 270–279. <https://doi.org/10.1016/j.jalz.2011.03.008>
- Alladi, S., Xuereb, J., Bak, T., Nestor, P., Knibb, J., Patterson, K., Hodges, J.R., 2007. Focal cortical presentations of Alzheimer's disease. *Brain J. Neurol.* 130, 2636–2645. <https://doi.org/10.1093/brain/awm213>
- Alonso, A. del C., Li, B., Grundke-Iqbal, I., Iqbal, K., 2008. Mechanism of tau-induced neurodegeneration in Alzheimer disease and related tauopathies. *Curr. Alzheimer Res.* 5, 375–384. <https://doi.org/10.2174/156720508785132307>
- Alonso, A. del C., Li, B., Grundke-Iqbal, I., Iqbal, K., 2006. Polymerization of hyperphosphorylated tau into filaments eliminates its inhibitory activity. *Proc. Natl. Acad. Sci. U. S. A.* 103, 8864–8869. <https://doi.org/10.1073/pnas.0603214103>
- Alonso, A., Zaidi, T., Novak, M., Grundke-Iqbal, I., Iqbal, K., 2001. Hyperphosphorylation induces self-assembly of tau into tangles of paired helical filaments/straight filaments. *Proc. Natl. Acad. Sci. U. S. A.* 98, 6923–6928. <https://doi.org/10.1073/pnas.121119298>

- Alonso, A.C., Zaidi, T., Grundke-Iqbal, I., Iqbal, K., 1994. Role of abnormally phosphorylated tau in the breakdown of microtubules in Alzheimer disease. *Proc. Natl. Acad. Sci. U. S. A.* 91, 5562–5566. <https://doi.org/10.1073/pnas.91.12.5562>
- Alquezar, C., Arya, S., Kao, A.W., 2021. Tau Post-translational Modifications: Dynamic Transformers of Tau Function, Degradation, and Aggregation. *Front. Neurol.* 11.
- Alvarenga, R.M., Pires, J.G.P., Futuro Neto, H.A., 2005. Functional mapping of the cardiorespiratory effects of dorsal and median raphe nuclei in the rat. *Braz. J. Med. Biol. Res.* 38, 1719–1727. <https://doi.org/10.1590/S0100-879X2005001100022>
- Alzheimer, A., 2006. Concerning a unique disease of the cerebral cortex, in: Jucker, M., Beyreuther, K., Haass, C., Nitsch, R.M., Christen, Y. (Eds.), *Alzheimer: 100 Years and Beyond, Research and Perspectives in Alzheimer's Disease*. Springer Berlin Heidelberg, pp. 3–11. https://doi.org/10.1007/978-3-540-37652-1_1
- Alzheimer's Association, 2021. 2021 Alzheimer's disease facts and figures. *Alzheimers Dement.* 17, 327–406. <https://doi.org/10.1002/alz.12328>
- Amador-Ortiz, C., Lin, W.-L., Ahmed, Z., Personett, D., Davies, P., Duara, R., Graff-Radford, N.R., Hutton, M.L., Dickson, D.W., 2007. TDP-43 immunoreactivity in hippocampal sclerosis and Alzheimer's disease. *Ann. Neurol.* 61, 435–445. <https://doi.org/10.1002/ana.21154>
- Ameen-Ali, K.E., Bretzin, A., Lee, E.B., Folkerth, R., Hazrati, L.-N., Iacono, D., Keene, C.D., Kofler, J., Kovacs, G.G., Nolan, A., Perl, D.P., Priemer, D.S., Smith, D.H., Wiebe, D.J., Stewart, W., CONNECT-TBI Investigators, 2022. Detection of astrocytic tau pathology facilitates recognition of chronic traumatic encephalopathy neuropathologic change. *Acta Neuropathol. Commun.* 10, 50. <https://doi.org/10.1186/s40478-022-01353-4>
- Andreadis, A., 2005. Tau gene alternative splicing: expression patterns, regulation and modulation of function in normal brain and neurodegenerative diseases. *Biochim. Biophys. Acta BBA - Mol. Basis Dis., The Biology and Pathobiology of Tau* 1739, 91–103. <https://doi.org/10.1016/j.bbadis.2004.08.010>
- Andreadis, A., Broderick, J.A., Kosik, K.S., 1995. Relative exon affinities and suboptimal splice site signals lead to non-equivalence of two cassette exons. *Nucleic Acids Res.* 23, 3585–3593. <https://doi.org/10.1093/nar/23.17.3585>
- Andreadis, A., Brown, W.M., Kosik, K.S., 1992. Structure and novel exons of the human tau gene. *Biochemistry* 31, 10626–10633. <https://doi.org/10.1021/bi00158a027>
- Andreadis, A., Wagner, B.K., Broderick, J.A., Kosik, K.S., 1996. A tau promoter region without neuronal specificity. *J. Neurochem.* 66, 2257–2263. <https://doi.org/10.1046/j.1471-4159.1996.66062257.x>

- Andreasen, N., Hesse, C., Davidsson, P., Minthon, L., Wallin, A., Winblad, B., Vanderstichele, H., Vanmechelen, E., Blennow, K., 1999. Cerebrospinal Fluid β -Amyloid(1-42) in Alzheimer Disease: Differences Between Early- and Late-Onset Alzheimer Disease and Stability During the Course of Disease. *Arch. Neurol.* 56, 673–680. <https://doi.org/10.1001/archneur.56.6.673>
- Apostolova, L.G., Dinov, I.D., Dutton, R.A., Hayashi, K.M., Toga, A.W., Cummings, J.L., Thompson, P.M., 2006. 3D comparison of hippocampal atrophy in amnesic mild cognitive impairment and Alzheimer's disease. *Brain J. Neurol.* 129, 2867–2873. <https://doi.org/10.1093/brain/awl274>
- Arai, T., Ikeda, K., Akiyama, H., Shikamoto, Y., Tsuchiya, K., Yagishita, S., Beach, T., Rogers, J., Schwab, C., McGeer, P.L., 2001. Distinct isoforms of tau aggregated in neurons and glial cells in brains of patients with Pick's disease, corticobasal degeneration and progressive supranuclear palsy. *Acta Neuropathol. (Berl.)* 101, 167–173. <https://doi.org/10.1007/s004010000283>
- Arima, K., Nakamura, M., Sunohara, N., Ogawa, M., Anno, M., Izumiyama, Y., Hirai, S., Ikeda, K., 1997. Ultrastructural characterization of the tau-immunoreactive tubules in the oligodendroglial perikarya and their inner loop processes in progressive supranuclear palsy. *Acta Neuropathol. (Berl.)* 93, 558–566. <https://doi.org/10.1007/s004010050652>
- Armstrong, M.J., Litvan, I., Lang, A.E., Bak, T.H., Bhatia, K.P., Borroni, B., Boxer, A.L., Dickson, D.W., Grossman, M., Hallett, M., Josephs, K.A., Kertesz, A., Lee, S.E., Miller, B.L., Reich, S.G., Riley, D.E., Tolosa, E., Tröster, A.I., Vidailhet, M., Weiner, W.J., 2013. Criteria for the diagnosis of corticobasal degeneration. *Neurology* 80, 496–503. <https://doi.org/10.1212/WNL.0b013e31827f0fd1>
- Arriagada, P.V., Growdon, J.H., Hedley-Whyte, E.T., Hyman, B.T., 1992. Neurofibrillary tangles but not senile plaques parallel duration and severity of Alzheimer's disease. *Neurology* 42, 631–631. <https://doi.org/10.1212/WNL.42.3.631>
- Baba, Y., Putzke, J.D., Whaley, N.R., Wszolek, Z.K., Uitti, R.J., 2006. Progressive supranuclear palsy: phenotypic sex differences in a clinical cohort. *Mov. Disord. Off. J. Mov. Disord. Soc.* 21, 689–692. <https://doi.org/10.1002/mds.20769>
- Baird, F.J., Bennett, C.L., 2013. Microtubule defects & Neurodegeneration. *J. Genet. Syndr. Gene Ther.* 4, 203. <https://doi.org/10.4172/2157-7412.1000203>
- Bakst, I., Amaral, D.G., 1984. The distribution of acetylcholinesterase in the hippocampal formation of the monkey. *J. Comp. Neurol.* 225, 344–371. <https://doi.org/10.1002/cne.902250304>
- Ball, M.J., 1977. Neuronal loss, neurofibrillary tangles and granulovacuolar degeneration in the hippocampus with ageing and dementia. *Acta Neuropathol. (Berl.)* 37, 111–118. <https://doi.org/10.1007/BF00692056>

- Baralle, F.E., Giudice, J., 2017. Alternative splicing as a regulator of development and tissue identity. *Nat. Rev. Mol. Cell Biol.* 18, 437–451.
<https://doi.org/10.1038/nrm.2017.27>
- Barnes, L.L., Wilson, R.S., Bienias, J.L., Schneider, J.A., Evans, D.A., Bennett, D.A., 2005. Sex differences in the clinical manifestations of Alzheimer disease pathology. *Arch. Gen. Psychiatry* 62, 685–691.
<https://doi.org/10.1001/archpsyc.62.6.685>
- Bartus, R.T., 2000. On Neurodegenerative Diseases, Models, and Treatment Strategies: Lessons Learned and Lessons Forgotten a Generation Following the Cholinergic Hypothesis. *Exp. Neurol.* 163, 495–529. <https://doi.org/10.1006/exnr.2000.7397>
- Bartus, R.T., Dean, R.L., Beer, B., Lippa, A.S., 1982. The cholinergic hypothesis of geriatric memory dysfunction. *Science* 217, 408–414.
<https://doi.org/10.1126/science.7046051>
- Baudic, S., Barba, G.D., Thibaudet, M.C., Smagghe, A., Remy, P., Traykov, L., 2006. Executive function deficits in early Alzheimer’s disease and their relations with episodic memory. *Arch. Clin. Neuropsychol.* 21, 15–21.
<https://doi.org/10.1016/j.acn.2005.07.002>
- Benoit, R.G., Gilbert, S.J., Frith, C.D., Burgess, P.W., 2012. Rostral Prefrontal Cortex and the Focus of Attention in Prospective Memory. *Cereb. Cortex* 22, 1876–1886.
<https://doi.org/10.1093/cercor/bhr264>
- Bensimon, G., Ludolph, A., Agid, Y., Vidailhet, M., Payan, C., Leigh, P.N., NNIPPS Study Group, 2009. Riluzole treatment, survival and diagnostic criteria in Parkinson plus disorders: the NNIPPS study. *Brain J. Neurol.* 132, 156–171.
<https://doi.org/10.1093/brain/awn291>
- Benson, D.F., Davis, R.J., Snyder, B.D., 1988. Posterior Cortical Atrophy. *Arch. Neurol.* 45, 789–793. <https://doi.org/10.1001/archneur.1988.00520310107024>
- Benussi, A., Padovani, A., Borroni, B., 2015. Phenotypic Heterogeneity of Monogenic Frontotemporal Dementia. *Front. Aging Neurosci.* 7.
<https://doi.org/10.3389/fnagi.2015.00171>
- Berger, A., 2002. Magnetic resonance imaging. *BMJ* 324, 35.
- Bernheimer, H., Birkmayer, W., Hornykiewicz, O., Jellinger, K., Seitelberger, F., 1973. Brain dopamine and the syndromes of Parkinson and Huntington Clinical, morphological and neurochemical correlations. *J. Neurol. Sci.* 20, 415–455.
[https://doi.org/10.1016/0022-510X\(73\)90175-5](https://doi.org/10.1016/0022-510X(73)90175-5)

- Bertrand, D., Wallace, T.L., 2020. A Review of the Cholinergic System and Therapeutic Approaches to Treat Brain Disorders, in: Shoaib, M., Wallace, T.L. (Eds.), Behavioral Pharmacology of the Cholinergic System, Current Topics in Behavioral Neurosciences. Springer International Publishing, Cham, pp. 1–28. https://doi.org/10.1007/7854_2020_141
- Bieniek, K.F., Cairns, N.J., Crary, J.F., Dickson, D.W., Folkerth, R.D., Keene, C.D., Litvan, I., Perl, D.P., Stein, T.D., Vonsattel, J.-P., Stewart, W., Dams-O'Connor, K., Gordon, W.A., Tripodis, Y., Alvarez, V.E., Mez, J., Alosco, M.L., McKee, A.C., 2021. The Second NINDS/NIBIB Consensus Meeting to Define Neuropathological Criteria for the Diagnosis of Chronic Traumatic Encephalopathy. *J. Neuropathol. Exp. Neurol.* 80, 210–219. <https://doi.org/10.1093/jnen/nlab001>
- Bigbee, J.W., Sharma, K.V., Gupta, J.J., Dupree, J.L., 1999. Morphogenic role for acetylcholinesterase in axonal outgrowth during neural development. *Environ. Health Perspect.* 107, 81–87.
- Binder, L.I., Frankfurter, A., Rebhun, L.I., 1985. The distribution of tau in the mammalian central nervous system. *J. Cell Biol.* 101, 1371–1378. <https://doi.org/10.1083/jcb.101.4.1371>
- Birks, J., 2006. Cholinesterase inhibitors for Alzheimer's disease. *Cochrane Database Syst. Rev.* CD005593. <https://doi.org/10.1002/14651858.CD005593>
- Biundo, F., Del Prete, D., Zhang, H., Arancio, O., D'Adamio, L., 2018. A role for tau in learning, memory and synaptic plasticity. *Sci. Rep.* 8, 3184. <https://doi.org/10.1038/s41598-018-21596-3>
- Black, M.M., Cochran, J.M., Kurdyla, J.T., 1984. Solubility properties of neuronal tubulin: evidence for labile and stable microtubules. *Brain Res.* 295, 255–263. [https://doi.org/10.1016/0006-8993\(84\)90974-0](https://doi.org/10.1016/0006-8993(84)90974-0)
- Blennow, K., Wallin, A., Agren, H., Spenger, C., Siegfried, J., Vanmechelen, E., 1995. Tau protein in cerebrospinal fluid: a biochemical marker for axonal degeneration in Alzheimer disease? *Mol. Chem. Neuropathol.* 26, 231–245. <https://doi.org/10.1007/BF02815140>
- Blennow, K., Zetterberg, H., 2018. Biomarkers for Alzheimer's disease: current status and prospects for the future. *J. Intern. Med.* 284, 643–663. <https://doi.org/10.1111/joim.12816>
- Blokland, A., 1995. Acetylcholine: a neurotransmitter for learning and memory? *Brain Res. Rev.* 21, 285–300. [https://doi.org/10.1016/0165-0173\(95\)00016-X](https://doi.org/10.1016/0165-0173(95)00016-X)
- Blusztajn, J.K., Rinnofner, J., 2016. Intrinsic Cholinergic Neurons in the Hippocampus: Fact or Artifact? *Front. Synaptic Neurosci.* 8, 6. <https://doi.org/10.3389/fnsyn.2016.00006>

- Bodakuntla, S., Jijumon, A.S., Villablanca, C., Gonzalez-Billault, C., Janke, C., 2019. Microtubule-Associated Proteins: Structuring the Cytoskeleton. *Trends Cell Biol.* 29, 804–819. <https://doi.org/10.1016/j.tcb.2019.07.004>
- Boehm, J., 2013. A “danse macabre”: tau and Fyn in STEP with amyloid beta to facilitate induction of synaptic depression and excitotoxicity. *Eur. J. Neurosci.* 37, 1925–1930. <https://doi.org/10.1111/ejn.12251>
- Bogan, R.K., 2006. Effects of restless legs syndrome (RLS) on sleep. *Neuropsychiatr. Dis. Treat.* 2, 513–519.
- Bonelli, R.M., Cummings, J.L., 2007. Frontal-subcortical circuitry and behavior. *Dialogues Clin. Neurosci.* 9, 141–151.
- Boxer, A.L., Gold, M., Feldman, H., Boeve, B.F., Dickinson, S.L.-J., Fillit, H., Ho, C., Paul, R., Pearlman, R., Sutherland, M., Verma, A., Arneric, S.P., Alexander, B.M., Dickerson, B.C., Dorsey, E.R., Grossman, M., Huey, E.D., Irizarry, M.C., Marks, W.J., Masellis, M., McFarland, F., Niehoff, D., Onyike, C.U., Paganoni, S., Panzara, M.A., Rockwood, K., Rohrer, J.D., Rosen, H., Schuck, R.N., Soares, H.D., Tatton, N., 2020. New directions in clinical trials for frontotemporal lobar degeneration: Methods and outcome measures. *Alzheimers Dement. J. Alzheimers Assoc.* 16, 131–143. <https://doi.org/10.1016/j.jalz.2019.06.4956>
- Braak, H., Alafuzoff, I., Arzberger, T., Kretschmar, H., Del Tredici, K., 2006. Staging of Alzheimer disease-associated neurofibrillary pathology using paraffin sections and immunocytochemistry. *Acta Neuropathol. (Berl.)* 112, 389–404. <https://doi.org/10.1007/s00401-006-0127-z>
- Braak, H., Braak, E., 1995. Staging of Alzheimer’s disease-related neurofibrillary changes. *Neurobiol. Aging* 16, 271–278; discussion 278-284. [https://doi.org/10.1016/0197-4580\(95\)00021-6](https://doi.org/10.1016/0197-4580(95)00021-6)
- Braak, H., Braak, E., 1991. Neuropathological staging of Alzheimer-related changes. *Acta Neuropathol. (Berl.)* 82, 239–259. <https://doi.org/10.1007/BF00308809>
- Bramblett, G.T., Goedert, M., Jakes, R., Merrick, S.E., Trojanowski, J.Q., Lee, V.M., 1993. Abnormal tau phosphorylation at Ser396 in Alzheimer’s disease recapitulates development and contributes to reduced microtubule binding. *Neuron* 10, 1089–1099. [https://doi.org/10.1016/0896-6273\(93\)90057-x](https://doi.org/10.1016/0896-6273(93)90057-x)
- Brandt, R., Léger, J., Lee, G., 1995. Interaction of tau with the neural plasma membrane mediated by tau’s amino-terminal projection domain. *J. Cell Biol.* 131, 1327–1340. <https://doi.org/10.1083/jcb.131.5.1327>

- Brickman, A.M., Manly, J.J., Honig, L.S., Sanchez, D., Reyes-Dumeyer, D., Lantigua, R.A., Lao, P.J., Stern, Y., Vonsattel, J.P., Teich, A.F., Airey, D.C., Proctor, N.K., Dage, J.L., Mayeux, R., 2021. Plasma p-tau181, p-tau217, and other blood-based Alzheimer's disease biomarkers in a multi-ethnic, community study. *Alzheimers Dement. J. Alzheimers Assoc.* 17, 1353–1364. <https://doi.org/10.1002/alz.12301>
- Brion, J.P., Smith, C., Couck, A.M., Gallo, J.M., Anderton, B.H., 1993. Developmental changes in tau phosphorylation: fetal tau is transiently phosphorylated in a manner similar to paired helical filament-tau characteristic of Alzheimer's disease. *J. Neurochem.* 61, 2071–2080. <https://doi.org/10.1111/j.1471-4159.1993.tb07444.x>
- Brodmann, K., 2006. Brodmann's localisation in the cerebral cortex: the principles of comparative localisation in the cerebral cortex based on cytoarchitectonics. Springer, New York, NY.
- Broomfield, C.A., Maxwell, D.M., Solana, R.P., Castro, C.A., Finger, A.V., Lenz, D.E., 1991. Protection by butyrylcholinesterase against organophosphorus poisoning in nonhuman primates. *J. Pharmacol. Exp. Ther.* 259, 633–638.
- Brown, R.G., Lacomblez, L., Landwehrmeyer, B.G., Bak, T., Uttner, I., Dubois, B., Agid, Y., Ludolph, A., Bensimon, G., Payan, C., Leigh, N.P., for the NNIPPS Study Group, 2010. Cognitive impairment in patients with multiple system atrophy and progressive supranuclear palsy. *Brain* 133, 2382–2393. <https://doi.org/10.1093/brain/awq158>
- Bucher, S.F., Trenkwalder, C., Oertel, W.H., 1996. Reflex studies and MRI in the restless legs syndrome. *Acta Neurol. Scand.* 94, 145–150. <https://doi.org/10.1111/j.1600-0404.1996.tb07045.x>
- Buee, L., Bussiere, T., Buee-Scherrer, V., Delacourte, A., Hof, P.R., 2000. Tau protein isoforms, phosphorylation and role in neurodegenerative disorders. *Brain Res. Rev.* 36.
- Butner, K.A., Kirschner, M.W., 1991. Tau protein binds to microtubules through a flexible array of distributed weak sites. *J. Cell Biol.* 115, 717–730. <https://doi.org/10.1083/jcb.115.3.717>
- Buxbaum, J.D., Oishi, M., Chen, H.I., Pinkas-Kramarski, R., Jaffe, E.A., Gandy, S.E., Greengard, P., 1992. Cholinergic agonists and interleukin 1 regulate processing and secretion of the Alzheimer beta/A4 amyloid protein precursor. *Proc. Natl. Acad. Sci. U. S. A.* 89, 10075–10078. <https://doi.org/10.1073/pnas.89.21.10075>
- Caceres, A., Kosik, K.S., 1990. Inhibition of neurite polarity by tau antisense oligonucleotides in primary cerebellar neurons. *Nature* 343, 461–463. <https://doi.org/10.1038/343461a0>

- Cairns, N.J., Bigio, E.H., Mackenzie, I.R.A., Neumann, M., Lee, V.M.-Y., Hatanpaa, K.J., White, C.L., Schneider, J.A., Grinberg, L.T., Halliday, G., Duyckaerts, C., Lowe, J.S., Holm, I.E., Tolnay, M., Okamoto, K., Yokoo, H., Murayama, S., Woulfe, J., Munoz, D.G., Dickson, D.W., Ince, P.G., Trojanowski, J.Q., Mann, D.M.A., Consortium for Frontotemporal Lobar Degeneration, 2007. Neuropathologic diagnostic and nosologic criteria for frontotemporal lobar degeneration: consensus of the Consortium for Frontotemporal Lobar Degeneration. *Acta Neuropathol. (Berl.)* 114, 5–22. <https://doi.org/10.1007/s00401-007-0237-2>
- Cajal, S.R. y, 1995. *Histology of the Nervous System of Man and Vertebrates*. Oxford University Press.
- Canto, C.B., Wouterlood, F.G., Witter, M.P., 2008. What Does the Anatomical Organization of the Entorhinal Cortex Tell Us? *Neural Plast.* 2008, e381243. <https://doi.org/10.1155/2008/381243>
- Carlson, M.C., Xue, Q.-L., Zhou, J., Fried, L.P., 2009. Executive Decline and Dysfunction Precedes Declines in Memory: The Women’s Health and Aging Study II. *J. Gerontol. A. Biol. Sci. Med. Sci.* 64A, 110–117. <https://doi.org/10.1093/gerona/gln008>
- Carpenter, S., 1968. Proximal axonal enlargement in motor neuron disease. *Neurology* 18, 841–851. <https://doi.org/10.1212/wnl.18.9.841>
- Carroll, J.C., Iba, M., Bangasser, D.A., Valentino, R.J., James, M.J., Brunden, K.R., Lee, V.M.-Y., Trojanowski, J.Q., 2011. Chronic Stress Exacerbates Tau Pathology, Neurodegeneration, and Cognitive Performance through a Corticotropin-Releasing Factor Receptor-Dependent Mechanism in a Transgenic Mouse Model of Tauopathy. *J. Neurosci.* 31, 14436–14449. <https://doi.org/10.1523/JNEUROSCI.3836-11.2011>
- Cash, M.K., Rockwood, K., Fisk, J.D., Darvesh, S., 2021. Clinicopathological correlations and cholinesterase expression in early-onset familial Alzheimer’s disease with the presenilin 1 mutation, Leu235Pro. *Neurobiol. Aging* 103, 31–41. <https://doi.org/10.1016/j.neurobiolaging.2021.02.025>
- Castillo-Carranza, D.L., Guerrero-Muñoz, M.J., Sengupta, U., Hernandez, C., Barrett, A.D.T., Dineley, K., Kaye, R., 2015. Tau Immunotherapy Modulates Both Pathological Tau and Upstream Amyloid Pathology in an Alzheimer’s Disease Mouse Model. *J. Neurosci.* 35, 4857–4868. <https://doi.org/10.1523/JNEUROSCI.4989-14.2015>
- Chen, J., Kanai, Y., Cowan, N.J., Hirokawa, N., 1992. Projection domains of MAP2 and tau determine spacings between microtubules in dendrites and axons. *Nature* 360, 674–677. <https://doi.org/10.1038/360674a0>

- Chen, V.P., Gao, Y., Geng, L., Parks, R.J., Pang, Y.-P., Brimijoin, S., 2015. Plasma butyrylcholinesterase regulates ghrelin to control aggression. *Proc. Natl. Acad. Sci.* 112, 2251–2256. <https://doi.org/10.1073/pnas.1421536112>
- Chen, Y., Qi, D., Qin, T., Chen, K., Ai, M., Li, X., Li, H., Zhang, J., Mao, H., Yang, Y., Zhang, Z., 2019. Brain Network Connectivity Mediates Education-related Cognitive Performance in Healthy Elderly Adults. *Curr. Alzheimer Res.* 16, 19–28. <https://doi.org/10.2174/1567205015666181022094158>
- Clark, C.M., Schneider, J.A., Bedell, B.J., Beach, T.G., Bilker, W.B., Mintun, M.A., Pontecorvo, M.J., Hefti, F., Carpenter, A.P., Flitter, M.L., Krautkramer, M.J., Kung, H.F., Coleman, R.E., Doraiswamy, P.M., Fleisher, A.S., Sabbagh, M.N., Sadowsky, C.H., Reiman, E.M., Zehntner, S.P., Skovronsky, D.M., 2011. Use of Florbetapir-PET for Imaging β -Amyloid Pathology. *JAMA* 305, 275–283. <https://doi.org/10.1001/jama.2010.2008>
- Clark, L.N., Poorkaj, P., Wszolek, Z., Geschwind, D.H., Nasreddine, Z.S., Miller, B., Li, D., Payami, H., Awert, F., Markopoulou, K., Andreadis, A., D’Souza, I., Lee, V.M.-Y., Reed, L., Trojanowski, J.Q., Zhukareva, V., Bird, T., Schellenberg, G., Wilhelmsen, K.C., 1998. Pathogenic implications of mutations in the tau gene in pallido-ponto-nigral degeneration and related neurodegenerative disorders linked to chromosome 17. *Proc. Natl. Acad. Sci.* 95, 13103–13107. <https://doi.org/10.1073/pnas.95.22.13103>
- Clark, L.R., Schiehser, D.M., Weissberger, G.H., Salmon, D.P., Delis, D.C., Bondi, M.W., 2012. Specific Measures of Executive Function Predict Cognitive Decline in Older Adults. *J. Int. Neuropsychol. Soc.* 18, 118–127. <https://doi.org/10.1017/S1355617711001524>
- Cleveland, D.W., Hwo, S.Y., Kirschner, M.W., 1977. Physical and chemical properties of purified tau factor and the role of tau in microtubule assembly. *J. Mol. Biol.* 116, 227–247. [https://doi.org/10.1016/0022-2836\(77\)90214-5](https://doi.org/10.1016/0022-2836(77)90214-5)
- Coleman, R.E., 2005. Positron emission tomography diagnosis of Alzheimer’s disease. *Neuroimaging Clin. N. Am.* 15, 837–846, x. <https://doi.org/10.1016/j.nic.2005.09.007>
- Collard, J.-F., Côté, F., Julien, J.-P., 1995. Defective axonal transport in a transgenic mouse model of amyotrophic lateral sclerosis. *Nature* 375, 61–64. <https://doi.org/10.1038/375061a0>
- Collins, S.J., Ahlskog, J.E., Parisi, J.E., Maraganore, D.M., 1995. Progressive supranuclear palsy: neuropathologically based diagnostic clinical criteria. *J. Neurol. Neurosurg. Psychiatry* 58, 167–173. <https://doi.org/10.1136/jnnp.58.2.167>

- Connor, J.R., Wang, X.-S., Allen, R.P., Beard, J.L., Wiesinger, J.A., Felt, B.T., Earley, C.J., 2009. Altered dopaminergic profile in the putamen and substantia nigra in restless leg syndrome. *Brain J. Neurol.* 132, 2403–2412. <https://doi.org/10.1093/brain/awp125>
- Couchie, D., Mavilia, C., Georgieff, I.S., Liem, R.K., Shelanski, M.L., Nunez, J., 1992. Primary structure of high molecular weight tau present in the peripheral nervous system. *Proc. Natl. Acad. Sci. U. S. A.* 89, 4378–4381.
- Coyle, J.T., Price, D.L., DeLong, M.R., 1983. Alzheimer's Disease: A Disorder of Cortical Cholinergic Innervation. *Science* 219, 1184–1190. <https://doi.org/10.1126/science.6338589>
- Crary, J.F., Trojanowski, J.Q., Schneider, J.A., Abisambra, J.F., Abner, E.L., Alafuzoff, I., Arnold, S.E., Attems, J., Beach, T.G., Bigio, E.H., Cairns, N.J., Dickson, D.W., Gearing, M., Grinberg, L.T., Hof, P.R., Hyman, B.T., Jellinger, K., Jicha, G.A., Kovacs, G.G., Knopman, D.S., Kofler, J., Kukull, W.A., Mackenzie, I.R., Masliah, E., McKee, A., Montine, T.J., Murray, M.E., Neltner, J.H., Santa-Maria, I., Seeley, W.W., Serrano-Pozo, A., Shelanski, M.L., Stein, T., Takao, M., Thal, D.R., Toledo, J.B., Troncoso, J.C., Vonsattel, J.P., White, C.L., Wisniewski, T., Woltjer, R.L., Yamada, M., Nelson, P.T., 2014. Primary age-related tauopathy (PART): a common pathology associated with human aging. *Acta Neuropathol. (Berl.)* 128, 755–766. <https://doi.org/10.1007/s00401-014-1349-0>
- Croxson, P.L., Kyriazis, D.A., Baxter, M.G., 2011. Cholinergic modulation of a specific memory function of prefrontal cortex. *Nat. Neurosci.* 14, 1510–1512. <https://doi.org/10.1038/nn.2971>
- Dani, J.A., Bertrand, D., 2007. Nicotinic acetylcholine receptors and nicotinic cholinergic mechanisms of the central nervous system. *Annu. Rev. Pharmacol. Toxicol.* 47, 699–729. <https://doi.org/10.1146/annurev.pharmtox.47.120505.105214>
- Daniel, S.E., de Bruin, V.M., Lees, A.J., 1995. The clinical and pathological spectrum of Steele-Richardson-Olszewski syndrome (progressive supranuclear palsy): a reappraisal. *Brain J. Neurol.* 118 (Pt 3), 759–770. <https://doi.org/10.1093/brain/118.3.759>
- Darvesh, S., 2016. Butyrylcholinesterase as a Diagnostic and Therapeutic Target for Alzheimer's Disease. *Curr. Alzheimer Res.* 13, 1173–1177.
- Darvesh, S., Cash, M.K., Reid, G.A., Martin, E., Mitnitski, A., Geula, C., 2012. Butyrylcholinesterase is Associated with β -Amyloid Plaques in the Transgenic APPSWE/PSEN1dE9 Mouse Model of Alzheimer Disease. *J. Neuropathol. Exp. Neurol.* 71, 2–14. <https://doi.org/10.1097/NEN.0b013e31823cc7a6>
- Darvesh, Sultan, Grantham, D., Hopkins, D., 1998. Distribution of butyrylcholinesterase in human amygdala and hippocampal formation. *J. Comp. Neurol.* 393, 374–90. [https://doi.org/10.1002/\(SICI\)1096-9861\(19980413\)393:33.0.CO;2-Z](https://doi.org/10.1002/(SICI)1096-9861(19980413)393:33.0.CO;2-Z)

- Darvesh, S., Grantham, D.L., Hopkins, D.A., 1998. Distribution of butyrylcholinesterase in the human amygdala and hippocampal formation. *J. Comp. Neurol.* 393, 374–390.
- Darvesh, S., Hopkins, D.A., 2003. Differential distribution of butyrylcholinesterase and acetylcholinesterase in the human thalamus. *J. Comp. Neurol.* 463, 25–43. <https://doi.org/10.1002/cne.10751>
- Darvesh, S., Hopkins, D.A., Geula, C., 2003a. Neurobiology of butyrylcholinesterase. *Nat. Rev. Neurosci.* 4, 131–138. <https://doi.org/10.1038/nrn1035>
- Darvesh, S., Leach, L., Black, S.E., Kaplan, E., Freedman, M., 2005. The behavioural neurology assessment. *Can. J. Neurol. Sci. J. Can. Sci. Neurol.* 32, 167–177. <https://doi.org/10.1017/s0317167100003930>
- Darvesh, S., LeBlanc, A.M., Macdonald, I.R., Reid, G.A., Bhan, V., Macaulay, R.J., Fisk, J.D., 2010. Butyrylcholinesterase activity in multiple sclerosis neuropathology. *Chem. Biol. Interact.*, 10th International Meeting on Cholinesterases 187, 425–431. <https://doi.org/10.1016/j.cbi.2010.01.037>
- Darvesh, S., Reid, G.A., Martin, E., 2010. Biochemical and histochemical comparison of cholinesterases in normal and Alzheimer brain tissues. *Curr. Alzheimer Res.* 7, 386–400. <https://doi.org/10.2174/156720510791383868>
- Darvesh, S., Walsh, R., Kumar, R., Caines, A., Roberts, S., Magee, D., Rockwood, K., Martin, E., 2003b. Inhibition of Human Cholinesterases by Drugs Used to Treat Alzheimer Disease. *Alzheimer Dis. Assoc. Disord.* 17, 117–126.
- Davies, P., Maloney, A.J., 1976. Selective loss of central cholinergic neurons in Alzheimer's disease. *Lancet* 2, 1403. [https://doi.org/10.1016/s0140-6736\(76\)91936-x](https://doi.org/10.1016/s0140-6736(76)91936-x)
- De Ferrari, G.V., Canales, M.A., Shin, I., Weiner, L.M., Silman, I., Inestrosa, N.C., 2001. A Structural Motif of Acetylcholinesterase That Promotes Amyloid β -Peptide Fibril Formation. *Biochemistry* 40, 10447–10457. <https://doi.org/10.1021/bi0101392>
- De Leon, M.J., George, A.E., Golomb, J., Tarshish, C., Convit, A., Kluger, A., De Santi, S., McRae, T., Ferris, S.H., Reisberg, B., Ince, C., Rusinek, H., Bobinski, M., Quinn, B., Miller, D.C., Wisniewski, H.M., 1997. Frequency of hippocampal formation atrophy in normal aging and Alzheimer's disease. *Neurobiol. Aging* 18, 1–11. [https://doi.org/10.1016/s0197-4580\(96\)00213-8](https://doi.org/10.1016/s0197-4580(96)00213-8)
- de Mello, M.T., Lauro, F.A., Silva, A.C., Tufik, S., 1996. Incidence of periodic leg movements and of the restless legs syndrome during sleep following acute physical activity in spinal cord injury subjects. *Spinal Cord* 34, 294–296. <https://doi.org/10.1038/sc.1996.53>

- Deardorff, W.J., Grossberg, G.T., 2016. A fixed-dose combination of memantine extended-release and donepezil in the treatment of moderate-to-severe Alzheimer's disease. *Drug Des. Devel. Ther.* 10, 3267–3279. <https://doi.org/10.2147/DDDT.S86463>
- DeBay, D., Darvesh, S., 2020. Butyrylcholinesterase as a biomarker in Alzheimer's disease. pp. 263–280. <https://doi.org/10.1016/B978-0-12-815854-8.00017-3>
- DeBay, D.R., Reid, G.A., Pottie, I.R., Martin, E., Bowen, C.V., Darvesh, S., 2017. Targeting butyrylcholinesterase for preclinical single photon emission computed tomography (SPECT) imaging of Alzheimer's disease. *Alzheimers Dement. Transl. Res. Clin. Interv.* 3, 166–176. <https://doi.org/10.1016/j.trci.2017.01.005>
- Deems, D.A., Doty, R.L., Settle, R.G., Moore-Gillon, V., Shaman, P., Mester, A.F., Kimmelman, C.P., Brightman, V.J., Snow, J.B., 1991. Smell and taste disorders, a study of 750 patients from the University of Pennsylvania Smell and Taste Center. *Arch. Otolaryngol. Head Neck Surg.* 117, 519–528. <https://doi.org/10.1001/archotol.1991.01870170065015>
- Delaby, C., Estellés, T., Zhu, N., Arranz, J., Barroeta, I., Carmona-Iragui, M., Illán-Gala, I., Santos-Santos, M.Á., Altuna, M., Sala, I., Sánchez-Saudinós, M.B., Videla, L., Valldeneu, S., Subirana, A., Tondo, M., Blanco-Vaca, F., Lehmann, S., Belbin, O., Blesa, R., Fortea, J., Lleó, A., Alcolea, D., 2022. The A β 1–42/A β 1–40 ratio in CSF is more strongly associated to tau markers and clinical progression than A β 1–42 alone. *Alzheimers Res. Ther.* 14, 1–11. <https://doi.org/10.1186/s13195-022-00967-z>
- Destrieux, C., Bourry, D., Velut, S., 2013. Surgical anatomy of the hippocampus. *Neurochirurgie.* 59, 149–158. <https://doi.org/10.1016/j.neuchi.2013.08.003>
- Dhiman, K., Gupta, V.B., Villemagne, V.L., Eratne, D., Graham, P.L., Fowler, C., Bourgeat, P., Li, Q., Collins, S., Bush, A.I., Rowe, C.C., Masters, C.L., Ames, D., Hone, E., Blennow, K., Zetterberg, H., Martins, R.N., 2020. Cerebrospinal fluid neurofilament light concentration predicts brain atrophy and cognition in Alzheimer's disease. *Alzheimers Dement. Diagn. Assess. Dis. Monit.* 12, e12005. <https://doi.org/10.1002/dad2.12005>
- Di, J., Cohen, L.S., Corbo, C.P., Phillips, G.R., El Idrissi, A., Alonso, A.D., 2016. Abnormal tau induces cognitive impairment through two different mechanisms: synaptic dysfunction and neuronal loss. *Sci. Rep.* 6, 20833. <https://doi.org/10.1038/srep20833>
- Dickson, D.W., 1999. Neuropathologic differentiation of progressive supranuclear palsy and corticobasal degeneration. *J. Neurol.* 246, II6–II15. <https://doi.org/10.1007/BF03161076>

- Dickson, D.W., Bergeron, C., Chin, S.S., Duyckaerts, C., Horoupian, D., Ikeda, K., Jellinger, K., Lantos, P.L., Lippa, C.F., Mirra, S.S., Tabaton, M., Vonsattel, J.P., Wakabayashi, K., Litvan, I., Office of Rare Diseases of the National Institutes of Health, 2002. Office of Rare Diseases neuropathologic criteria for corticobasal degeneration. *J. Neuropathol. Exp. Neurol.* 61, 935–946.
- Ding, S.-L., Van Hoesen, G.W., 2015. Organization and Detailed Parcellation of Human Hippocampal Head and Body Regions Based on a Combined Analysis of Cyto- and Chemoarchitecture. *J. Comp. Neurol.* 523, 2233–2253. <https://doi.org/10.1002/cne.23786>
- Dixit, R., Ross, J.L., Goldman, Y.E., Holzbaur, E.L.F., 2008. Differential Regulation of Dynein and Kinesin Motor Proteins by Tau. *Science* 319, 1086–1089. <https://doi.org/10.1126/science.1152993>
- Drechsel, D.N., Hyman, A.A., Cobb, M.H., Kirschner, M.W., 1992. Modulation of the dynamic instability of tubulin assembly by the microtubule-associated protein tau. *Mol. Biol. Cell* 3, 1141–1154. <https://doi.org/10.1091/mbc.3.10.1141>
- Drubin, D.G., Feinstein, S.C., Shooter, E.M., Kirschner, M.W., 1985. Nerve growth factor-induced neurite outgrowth in PC12 cells involves the coordinate induction of microtubule assembly and assembly-promoting factors. *J. Cell Biol.* 101, 1799–1807. <https://doi.org/10.1083/jcb.101.5.1799>
- Du, A., Xie, J., Guo, K., Yang, L., Wan, Y., OuYang, Q., Zhang, Xuejin, Niu, X., Lu, L., Wu, J., Zhang, Xuejun, 2015. A novel role for synaptic acetylcholinesterase as an apoptotic deoxyribonuclease. *Cell Discov.* 1, 15002. <https://doi.org/10.1038/celldisc.2015.2>
- Duarte-Guterman, P., Albert, A.Y., Barha, C.K., Galea, L.A.M., 2021. Sex influences the effects of APOE genotype and Alzheimer’s diagnosis on neuropathology and memory. <https://doi.org/10.1101/2020.06.25.20139980>
- Dubois, B., Villain, N., Frisoni, G.B., Rabinovici, G.D., Sabbagh, M., Cappa, S., Bejanin, A., Bombois, S., Epelbaum, S., Teichmann, M., Habert, M.-O., Nordberg, A., Blennow, K., Galasko, D., Stern, Y., Rowe, C.C., Salloway, S., Schneider, L.S., Cummings, J.L., Feldman, H.H., 2021. Clinical diagnosis of Alzheimer’s disease: recommendations of the International Working Group. *Lancet Neurol.* 20, 484–496. [https://doi.org/10.1016/S1474-4422\(21\)00066-1](https://doi.org/10.1016/S1474-4422(21)00066-1)
- Duvernoy, H., Cattin, Françoise, Risold, P.-Y., 2013. Structure, Functions, and Connections, in: Duvernoy, H.M., Cattin, Françoise, Risold, P.-Y. (Eds.), *The Human Hippocampus: Functional Anatomy, Vascularization and Serial Sections with MRI*. Springer, Berlin, Heidelberg, pp. 5–38. https://doi.org/10.1007/978-3-642-33603-4_3

- Duysen, E.G., Stribley, J.A., Fry, D.L., Hinrichs, S.H., Lockridge, O., 2002. Rescue of the acetylcholinesterase knockout mouse by feeding a liquid diet; phenotype of the adult acetylcholinesterase deficient mouse. *Brain Res. Dev. Brain Res.* 137, 43–54. [https://doi.org/10.1016/s0165-3806\(02\)00367-x](https://doi.org/10.1016/s0165-3806(02)00367-x)
- English, B.A., Jones, C.K., 2012. Chapter 14 - Cholinergic Neurotransmission, in: Robertson, D., Biaggioni, I., Burnstock, G., Low, P.A., Paton, J.F.R. (Eds.), *Primer on the Autonomic Nervous System (Third Edition)*. Academic Press, San Diego, pp. 71–74. <https://doi.org/10.1016/B978-0-12-386525-0.00014-7>
- Erkinjuntti, T., Hokkanen, L., Sulkava, R., Palo, J., 1988. The blessed dementia scale as a screening test for dementia. *Int. J. Geriatr. Psychiatry* 3, 267–273. <https://doi.org/10.1002/gps.930030406>
- Esmaeli-Azad, B., McCarty, J.H., Feinstein, S.C., 1994. Sense and antisense transfection analysis of tau function: tau influences net microtubule assembly, neurite outgrowth and neuritic stability. *J. Cell Sci.* 107 (Pt 4), 869–879.
- Fabbrini, G., Barbanti, P., Bonifati, V., Colosimo, C., Gasparini, M., Vanacore, N., Meco, G., 2001. Donepezil in the treatment of progressive supranuclear palsy. *Acta Neurol. Scand.* 103, 123–5. <https://doi.org/10.1034/j.1600-0404.2001.103002123.x>
- Falke, E., Nissanov, J., Mitchell, T.W., Bennett, D.A., Trojanowski, J.Q., Arnold, S.E., 2003. Subicular dendritic arborization in Alzheimer’s disease correlates with neurofibrillary tangle density. *Am. J. Pathol.* 163, 1615–1621. [https://doi.org/10.1016/S0002-9440\(10\)63518-3](https://doi.org/10.1016/S0002-9440(10)63518-3)
- Farias, G.A., Muñoz, J.P., Garrido, J., Maccioni, R.B., 2002. Tubulin, actin, and tau protein interactions and the study of their macromolecular assemblies. *J. Cell. Biochem.* 85, 315–324. <https://doi.org/10.1002/jcb.10133>
- Farrer, M.J., Hulihan, M.M., Kachergus, J.M., Dächsel, J.C., Stoessl, A.J., Grantier, L.L., Calne, S., Calne, D.B., Lechevalier, B., Chapon, F., Tsuboi, Y., Yamada, T., Gutmann, L., Elibol, B., Bhatia, K.P., Wider, C., Vilariño-Güell, C., Ross, O.A., Brown, L.A., Castanedes-Casey, M., Dickson, D.W., Wszolek, Z.K., 2009. DCTN1 mutations in Perry syndrome. *Nat. Genet.* 41, 163–165. <https://doi.org/10.1038/ng.293>
- Feany, M.B., Ksiazak-Reding, H., Liu, W.K., Vincent, I., Yen, S.H., Dickson, D.W., 1995. Epitope expression and hyperphosphorylation of tau protein in corticobasal degeneration: differentiation from progressive supranuclear palsy. *Acta Neuropathol. (Berl.)* 90, 37–43. <https://doi.org/10.1007/BF00294457>
- Ferreira-Vieira, T.H., Guimaraes, I.M., Silva, F.R., Ribeiro, F.M., 2016. Alzheimer’s Disease: Targeting the Cholinergic System. *Curr. Neuropharmacol.* 14, 101–115. <https://doi.org/10.2174/1570159X13666150716165726>

- Filon, J.R., Intorcchia, A.J., Sue, L.I., Vazquez Arreola, E., Wilson, J., Davis, K.J., Sabbagh, M.N., Belden, C.M., Caselli, R.J., Adler, C.H., Woodruff, B.K., Rapsack, S.Z., Ahern, G.L., Burke, A.D., Jacobson, S., Shill, H.A., Driver-Dunckley, E., Chen, K., Reiman, E.M., Beach, T.G., Serrano, G.E., 2016. Gender Differences in Alzheimer Disease: Brain Atrophy, Histopathology Burden, and Cognition. *J. Neuropathol. Exp. Neurol.* 75, 748–754. <https://doi.org/10.1093/jnen/nlw047>
- Fleck, L.M., 2021. Alzheimer's and Aducanumab: Unjust Profits and False Hopes. *Hastings Cent. Rep.* 51, 9–11. <https://doi.org/10.1002/hast.1264>
- Folstein, M.F., Folstein, S.E., McHugh, P.R., 1975. Mini-mental state: A practical method for grading the cognitive state of patients for the clinician. *J. Psychiatr. Res.* 12, 189–198. [https://doi.org/10.1016/0022-3956\(75\)90026-6](https://doi.org/10.1016/0022-3956(75)90026-6)
- Forlenza, O.V., Spink, J.M., Dayanandan, R., Anderton, B.H., Olesen, O.F., Lovestone, S., 2000. Muscarinic agonists reduce tau phosphorylation in non-neuronal cells via GSK-3beta inhibition and in neurons. *J. Neural Transm. Vienna Austria* 1996 107, 1201–1212. <https://doi.org/10.1007/s007020070034>
- Forrest, S.L., Kril, J.J., Wagner, S., Hönigschnabl, S., Reiner, A., Fischer, P., Kovacs, G.G., 2019. Chronic Traumatic Encephalopathy (CTE) Is Absent From a European Community-Based Aging Cohort While Cortical Aging-Related Tau Astroglipathy (ARTAG) Is Highly Prevalent. *J. Neuropathol. Exp. Neurol.* 78, 398–405. <https://doi.org/10.1093/jnen/nlz017>
- François, M., Leifert, W., Martins, R., Thomas, P., Fenech, M., 2014. Biomarkers of Alzheimer's disease risk in peripheral tissues; focus on buccal cells. *Curr. Alzheimer Res.* 11, 519–531. <https://doi.org/10.2174/1567205011666140618103827>
- Freedman, M., Leach, L., Carmela Tartaglia, M., Stokes, K.A., Goldberg, Y., Spring, R., Nourhaghghi, N., Gee, T., Strother, S.C., Alhaj, M.O., Borrie, M., Darvesh, S., Fernandez, A., Fischer, C.E., Fogarty, J., Greenberg, B.D., Gyenes, M., Herrmann, N., Keren, R., Kirstein, J., Kumar, S., Lam, B., Lena, S., McAndrews, M.P., Naglie, G., Partridge, R., Rajji, T.K., Reichmann, W., Uri Wolf, M., Verhoeff, N.P.L.G., Wasserman, J.L., Black, S.E., Tang-Wai, D.F., 2018. The Toronto Cognitive Assessment (TorCA): normative data and validation to detect amnesic mild cognitive impairment. *Alzheimers Res. Ther.* 10. <https://doi.org/10.1186/s13195-018-0382-y>
- Frisoni, G.B., Fox, N.C., Jack, C.R., Scheltens, P., Thompson, P.M., 2010. The clinical use of structural MRI in Alzheimer disease. *Nat. Rev. Neurol.* 6, 67–77. <https://doi.org/10.1038/nrneurol.2009.215>
- Funahashi, S., 2017. Working Memory in the Prefrontal Cortex. *Brain Sci.* 7, 49. <https://doi.org/10.3390/brainsci7050049>

- Gabryelewicz, T., Masellis, M., Berdyski, M., Bilbao, J.M., Rogaeva, E., George-Hyslop, P.S., Barczak, A., Czyzewski, K., Barcikowska, M., Wszolek, Z., Black, S.E., Zekanowski, C., 2010. Intra-familial clinical heterogeneity due to FTL-DU with TDP-43 proteinopathy caused by a novel deletion in progranulin gene (PGRN). *J. Alzheimers Dis.* 22, 1123–1133. <https://doi.org/10.3233/JAD-2010-101413>
- Galton, C.J., Patterson, K., Xuereb, J.H., Hodges, J.R., 2000. Atypical and typical presentations of Alzheimer's disease: a clinical, neuropsychological, neuroimaging and pathological study of 13 cases. *Brain* 123, 484–498. <https://doi.org/10.1093/brain/123.3.484>
- Gamblin, T.C., 2005. Potential structure/function relationships of predicted secondary structural elements of tau. *Biochim. Biophys. Acta BBA - Mol. Basis Dis., The Biology and Pathobiology of Tau* 1739, 140–149. <https://doi.org/10.1016/j.bbadis.2004.08.013>
- Ganguli, M., Jia, Y., Hughes, T.F., Snitz, B.E., Chang, C.-C.H., Berman, S.B., Sullivan, K.J., Kamboh, M.I., 2019. Mild Cognitive Impairment that Does Not Progress to Dementia: A Population-Based Study. *J. Am. Geriatr. Soc.* 67, 232–238. <https://doi.org/10.1111/jgs.15642>
- Genever, P.G., Birch, M.A., Brown, E., Skerry, T.M., 1999. Osteoblast-derived acetylcholinesterase: a novel mediator of cell-matrix interactions in bone? *Bone* 24, 297–303. [https://doi.org/10.1016/S8756-3282\(98\)00187-2](https://doi.org/10.1016/S8756-3282(98)00187-2)
- Georgieff, I.S., Liem, R.K., Couchie, D., Mavilia, C., Nunez, J., Shelanski, M.L., 1993. Expression of high molecular weight tau in the central and peripheral nervous systems. *J. Cell Sci.* 105 (Pt 3), 729–737.
- Gerstenecker, A., Mast, B., Duff, K., Ferman, T.J., Litvan, I., 2013. Executive Dysfunction Is the Primary Cognitive Impairment in Progressive Supranuclear Palsy. *Arch. Clin. Neuropsychol.* 28, 104–113. <https://doi.org/10.1093/arclin/acs098>
- Geser, F., Robinson, J.L., Malunda, J.A., Xie, S.X., Clark, C.M., Kwong, L.K., Moberg, P.J., Moore, E.M., Van Deerlin, V.M., Lee, V.M.-Y., Arnold, S.E., Trojanowski, J.Q., 2010. Pathological 43-kDa Transactivation Response DNA-Binding Protein in Older Adults With and Without Severe Mental Illness. *Arch. Neurol.* 67, 1238–1250. <https://doi.org/10.1001/archneurol.2010.254>
- Geula, C., Dunlop, S.R., Ayala, I., Kawles, A.S., Flanagan, M.E., Gefen, T., Mesulam, M.-M., 2021. Basal forebrain cholinergic system in the dementias: Vulnerability, resilience, and resistance. *J. Neurochem.* 158, 1394–1411. <https://doi.org/10.1111/jnc.15471>

- Geula, C., Mesulam, M., 1989a. Special properties of cholinesterases in the cerebral cortex of Alzheimer's disease. *Brain Res.* 498, 185–189. [https://doi.org/10.1016/0006-8993\(89\)90419-8](https://doi.org/10.1016/0006-8993(89)90419-8)
- Geula, C., Mesulam, M.M., 1995. Cholinesterases and the pathology of Alzheimer disease. *Alzheimer Dis. Assoc. Disord.* 9 Suppl 2, 23–28. <https://doi.org/10.1097/00002093-199501002-00005>
- Geula, C., Mesulam, M.M., 1989b. Cortical cholinergic fibers in aging and Alzheimer's disease: a morphometric study. *Neuroscience* 33, 469–481. [https://doi.org/10.1016/0306-4522\(89\)90399-0](https://doi.org/10.1016/0306-4522(89)90399-0)
- Giacobini, E., Cuello, A., Fisher, A., 2022. Reimagining cholinergic therapy for Alzheimer's disease. *Brain*. <https://doi.org/10.1093/brain/awac096>
- Giacobini, E., Gold, G., 2013. Alzheimer disease therapy—moving from amyloid- β to tau. *Nat. Rev. Neurol.* 9, 677–686. <https://doi.org/10.1038/nrneurol.2013.223>
- Giummarra, M.J., Bradshaw, J.L., 2010. The phantom of the night: restless legs syndrome in amputees. *Med. Hypotheses* 74, 968–972. <https://doi.org/10.1016/j.mehy.2009.12.009>
- Goedert, M., Jakes, R., 1990. Expression of separate isoforms of human tau protein: correlation with the tau pattern in brain and effects on tubulin polymerization. *EMBO J.* 9, 4225–4230. <https://doi.org/10.1002/j.1460-2075.1990.tb07870.x>
- Goedert, M., Spillantini, M.G., Crowther, R.A., 1992. Cloning of a big tau microtubule-associated protein characteristic of the peripheral nervous system. *Proc. Natl. Acad. Sci. U. S. A.* 89, 1983–1987. <https://doi.org/10.1073/pnas.89.5.1983>
- Goedert, M., Spillantini, M.G., Jakes, R., Rutherford, D., Crowther, R.A., 1989a. Multiple isoforms of human microtubule-associated protein tau: sequences and localization in neurofibrillary tangles of Alzheimer's disease. *Neuron* 3, 519–526. [https://doi.org/10.1016/0896-6273\(89\)90210-9](https://doi.org/10.1016/0896-6273(89)90210-9)
- Goedert, M., Spillantini, M.G., Potier, M.C., Ulrich, J., Crowther, R.A., 1989b. Cloning and sequencing of the cDNA encoding an isoform of microtubule-associated protein tau containing four tandem repeats: differential expression of tau protein mRNAs in human brain. *EMBO J.* 8, 393–399.
- Gomez-Ramos, P., Mufson, E.J., Moran, M.A., 1992. Ultrastructural localization of acetylcholinesterase in neurofibrillary tangles, neuropil threads and senile plaques in aged and Alzheimer's brain. *Brain Res.* 569, 229–237. [https://doi.org/10.1016/0006-8993\(92\)90634-1](https://doi.org/10.1016/0006-8993(92)90634-1)
- Gong, C.-X., Liu, F., Grundke-Iqbal, I., Iqbal, K., 2006. Dysregulation of protein phosphorylation/dephosphorylation in Alzheimer's disease: a therapeutic target. *J. Biomed. Biotechnol.* 2006, 31825. <https://doi.org/10.1155/JBB/2006/31825>

- Goode, B.L., Feinstein, S.C., 1994. Identification of a novel microtubule binding and assembly domain in the developmentally regulated inter-repeat region of tau. *J. Cell Biol.* 124, 769–782. <https://doi.org/10.1083/jcb.124.5.769>
- Gouras, G.K., Tsai, J., Naslund, J., Vincent, B., Edgar, M., Checler, F., Greenfield, J.P., Haroutunian, V., Buxbaum, J.D., Xu, H., Greengard, P., Relkin, N.R., 2000. Intraneuronal A β 42 Accumulation in Human Brain. *Am. J. Pathol.* 156, 15–20. [https://doi.org/10.1016/s0002-9440\(10\)64700-1](https://doi.org/10.1016/s0002-9440(10)64700-1)
- Greaves, C.V., Rohrer, J.D., 2019. An update on genetic frontotemporal dementia. *J. Neurol.* 266, 2075–2086. <https://doi.org/10.1007/s00415-019-09363-4>
- Green, R.C., Mesulam, M.M., 1988. Acetylcholinesterase fiber staining in the human hippocampus and parahippocampal gyrus. *J. Comp. Neurol.* 273, 488–499. <https://doi.org/10.1002/cne.902730405>
- Grinberg, L.T., Heinsen, H., 2009. Argyrophilic grain disease: an update about a frequent cause of dementia. *Dement. Neuropsychol.* 3, 2–7. <https://doi.org/10.1590/S1980-57642009DN30100002>
- Grover, A., Houlden, H., Baker, M., Adamson, J., Lewis, J., Prihar, G., Pickering-Brown, S., Duff, K., Hutton, M., 1999. 5' splice site mutations in tau associated with the inherited dementia FTDP-17 affect a stem-loop structure that regulates alternative splicing of exon 10. *J. Biol. Chem.* 274, 15134–15143. <https://doi.org/10.1074/jbc.274.21.15134>
- Grundke-Iqbal, I., Iqbal, K., Quinlan, M., Tung, Y.C., Zaidi, M.S., Wisniewski, H.M., 1986a. Microtubule-associated protein tau. A component of Alzheimer paired helical filaments. *J. Biol. Chem.* 261, 6084–6089.
- Grundke-Iqbal, I., Iqbal, K., Tung, Y.C., Quinlan, M., Wisniewski, H.M., Binder, L.I., 1986b. Abnormal phosphorylation of the microtubule-associated protein tau (tau) in Alzheimer cytoskeletal pathology. *Proc. Natl. Acad. Sci. U. S. A.* 83, 4913–4917. <https://doi.org/10.1073/pnas.83.13.4913>
- Guillozet, A.L., Smiley, J.F., Mash, D.C., Mesulam, M.M., 1997. Butyrylcholinesterase in the life cycle of amyloid plaques. *Ann. Neurol.* 42, 909–918. <https://doi.org/10.1002/ana.410420613>
- Guillozet, A.L., Weintraub, S., Mash, D.C., Mesulam, M.M., 2003. Neurofibrillary tangles, amyloid, and memory in aging and mild cognitive impairment. *Arch. Neurol.* 60, 729–736. <https://doi.org/10.1001/archneur.60.5.729>
- Gustke, N., Trinczek, B., Biernat, J., Mandelkow, E.M., Mandelkow, E., 1994. Domains of tau protein and interactions with microtubules. *Biochemistry* 33, 9511–9522. <https://doi.org/10.1021/bi00198a017>

- Hamodat, H., Cash, M.K., Fisk, J.D., Darvesh, S., 2017. Cholinesterases in normal and Alzheimer's disease primary olfactory gyrus. *Neuropathol. Appl. Neurobiol.* 43, 571–583. <https://doi.org/10.1111/nan.12423>
- Hampel, H., O'Bryant, S.E., Molinuevo, J.L., Zetterberg, H., Masters, C.L., Lista, S., Kiddle, S.J., Batrla, R., Blennow, K., 2018. Blood-based biomarkers for Alzheimer's disease: mapping the road to the clinic. *Nat. Rev. Neurol.* 14, 639–652. <https://doi.org/10.1038/s41582-018-0079-7>
- Harel, M., Sussman, J.L., Krejci, E., Bon, S., Chanal, P., Massoulié, J., Silman, I., 1992. Conversion of acetylcholinesterase to butyrylcholinesterase: modeling and mutagenesis. *Proc. Natl. Acad. Sci. U. S. A.* 89, 10827–10831. <https://doi.org/10.1073/pnas.89.22.10827>
- Harrison, T.M., Weintraub, S., Mesulam, M.-M., Rogalski, E., 2012. Superior Memory and Higher Cortical Volumes in Unusually Successful Cognitive Aging. *J. Int. Neuropsychol. Soc.* 18, 1081–1085. <https://doi.org/10.1017/S1355617712000847>
- Hartmann, M., Pfister, R., Pfadenhauer, K., 1999. Restless legs syndrome associated with spinal cord lesions. *J. Neurol. Neurosurg. Psychiatry* 66, 688–689. <https://doi.org/10.1136/jnnp.66.5.688a>
- Hauw, J.J., Daniel, S.E., Dickson, D., Horoupian, D.S., Jellinger, K., Lantos, P.L., McKee, A., Tabaton, M., Litvan, I., 1994. Preliminary NINDS neuropathologic criteria for Steele-Richardson-Olszewski syndrome (progressive supranuclear palsy). *Neurology* 44, 2015–2019. <https://doi.org/10.1212/wnl.44.11.2015>
- Hauw, J.-J., Haussler-Hauw, C., De Girolami, U., Hasboun, D., Seilhean, D., 2011. Neuropathology of Sleep Disorders: A Review. *J. Neuropathol. Exp. Neurol.* 70, 243–252. <https://doi.org/10.1097/NEN.0b013e318211488e>
- Hawkins, R.D., Gunter, J.M., 1946. Studies on cholinesterase. *Biochem. J.* 40, 192–197.
- He, H.J., Wang, X.S., Pan, R., Wang, D.L., Liu, M.N., He, R.Q., 2009. The proline-rich domain of tau plays a role in interactions with actin. *BMC Cell Biol.* 10, 81. <https://doi.org/10.1186/1471-2121-10-81>
- He, W., Goodkind, D., Kowal, P., 2016. An Aging World: 2015 (No. P95/16-1). United States Census Bureau.
- He, Z., Guo, J.L., McBride, J.D., Narasimhan, S., Kim, H., Changolkar, L., Zhang, B., Gathagan, R.J., Yue, C., Dengler, C., Stieber, A., Nitla, M., Coulter, D.A., Abel, T., Brunden, K.R., Trojanowski, J.Q., Lee, V.M.-Y., 2018. Amyloid- β plaques enhance Alzheimer's brain tau-seeded pathologies by facilitating neuritic plaque tau aggregation. *Nat. Med.* 24, 29–38. <https://doi.org/10.1038/nm.4443>
- Health Quality Ontario, 2014. The Appropriate Use of Neuroimaging in the Diagnostic Work-Up of Dementia. *Ont. Health Technol. Assess. Ser.* 14, 1–64.

- Hedreen, J.C., Struble, R.G., Whitehouse, P.J., Price, D.L., 1984. Topography of the magnocellular basal forebrain system in human brain. *J. Neuropathol. Exp. Neurol.* 43, 1–21. <https://doi.org/10.1097/00005072-198401000-00001>
- Henderson, V.W., Buckwalter, J.G., 1994. Cognitive deficits of men and women with Alzheimer's disease. *Neurology* 44, 90–96. <https://doi.org/10.1212/wnl.44.1.90>
- Higashi, S., Iseki, E., Yamamoto, R., Minegishi, M., Hino, H., Fujisawa, K., Togo, T., Katsuse, O., Uchikado, H., Furukawa, Y., Kosaka, K., Arai, H., 2007. Concurrence of TDP-43, tau and α -synuclein pathology in brains of Alzheimer's disease and dementia with Lewy bodies. *Brain Res.* 1184, 284–294. <https://doi.org/10.1016/j.brainres.2007.09.048>
- Himmler, A., Drechsel, D., Kirschner, M.W., Martin, D.W., 1989. Tau consists of a set of proteins with repeated C-terminal microtubule-binding domains and variable N-terminal domains. *Mol. Cell. Biol.* 9, 1381–1388. <https://doi.org/10.1128/mcb.9.4.1381>
- Hippius, H., Neundörfer, G., 2003. The discovery of Alzheimer's disease. *Dialogues Clin. Neurosci.* 5, 101–108.
- Hirano, A., Nakano, I., Kurland, L.T., Mulder, D.W., Holley, P.W., Saccomanno, G., 1984. Fine structural study of neurofibrillary changes in a family with amyotrophic lateral sclerosis. *J. Neuropathol. Exp. Neurol.* 43, 471–480. <https://doi.org/10.1097/00005072-198409000-00002>
- Hirano, A., Zimmerman, H.M., 1962. Alzheimer's Neurofibrillary Changes: A Topographic Study. *Arch. Neurol.* 7, 227–242. <https://doi.org/10.1001/archneur.1962.04210030065009>
- Hirokawa, N., Shiomura, Y., Okabe, S., 1988. Tau proteins: the molecular structure and mode of binding on microtubules. *J. Cell Biol.* 107, 1449–1459. <https://doi.org/10.1083/jcb.107.4.1449>
- Ho, T.N.T., Abraham, N., Lewis, R.J., 2020. Structure-Function of Neuronal Nicotinic Acetylcholine Receptor Inhibitors Derived From Natural Toxins. *Front. Neurosci.* 14.
- Hong, M., Zhukareva, V., Vogelsberg-Ragaglia, V., Wszolek, Z., Reed, L., Miller, B.I., Geschwind, D.H., Bird, T.D., McKeel, D., Goate, A., Morris, J.C., Wilhelmsen, K.C., Schellenberg, G.D., Trojanowski, J.Q., Lee, V.M., 1998. Mutation-specific functional impairments in distinct tau isoforms of hereditary FTDP-17. *Science* 282, 1914–1917. <https://doi.org/10.1126/science.282.5395.1914>
- Hou, Y., Dan, X., Babbar, M., Wei, Y., Hasselbalch, S.G., Croteau, D.L., Bohr, V.A., 2019. Ageing as a risk factor for neurodegenerative disease. *Nat. Rev. Neurol.* 15, 565–581. <https://doi.org/10.1038/s41582-019-0244-7>

- Hu, W.T., Josephs, K.A., Knopman, D.S., Boeve, B.F., Dickson, D.W., Petersen, R.C., Parisi, J.E., 2008. Temporal lobar predominance of TDP-43 neuronal cytoplasmic inclusions in Alzheimer disease. *Acta Neuropathol. (Berl.)* 116, 215–220. <https://doi.org/10.1007/s00401-008-0400-4>
- Hua, X., Hibar, D.P., Lee, S., Toga, A.W., Jack, C.R., Weiner, M.W., Thompson, P.M., 2010. Sex and age differences in atrophic rates: an ADNI study with N=1368 MRI scans. *Neurobiol. Aging* 31, 1463–1480. <https://doi.org/10.1016/j.neurobiolaging.2010.04.033>
- Hussenoeder, F.S., Conrad, I., Roehr, S., Fuchs, A., Pentzek, M., Bickel, H., Moesch, E., Weyerer, S., Werle, J., Wiese, B., Mamone, S., Brettschneider, C., Hesel, K., Kleineidam, L., Kaduszkiewicz, H., Eisele, M., Maier, W., Wagner, M., Scherer, M., König, H.-H., Riedel-Heller, S.G., 2020. Mild cognitive impairment and quality of life in the oldest old: a closer look. *Qual. Life Res.* 29, 1675–1683. <https://doi.org/10.1007/s11136-020-02425-5>
- Hutton, M., Lendon, C.L., Rizzu, P., Baker, M., Froelich, S., Houlden, H., Pickering-Brown, S., Chakraverty, S., Isaacs, A., Grover, A., Hackett, J., Adamson, J., Lincoln, S., Dickson, D., Davies, P., Petersen, R.C., Stevens, M., de Graaff, E., Wauters, E., van Baren, J., Hillebrand, M., Joosse, M., Kwon, J.M., Nowotny, P., Che, L.K., Norton, J., Morris, J.C., Reed, L.A., Trojanowski, J., Basun, H., Lannfelt, L., Neystat, M., Fahn, S., Dark, F., Tannenberg, T., Dodd, P.R., Hayward, N., Kwok, J.B., Schofield, P.R., Andreadis, A., Snowden, J., Craufurd, D., Neary, D., Owen, F., Oostra, B.A., Hardy, J., Goate, A., van Swieten, J., Mann, D., Lynch, T., Heutink, P., 1998. Association of missense and 5'-splice-site mutations in tau with the inherited dementia FTDP-17. *Nature* 393, 702–705. <https://doi.org/10.1038/31508>
- Hwang, S.C., Jhon, D.-Y., Bae, Y.S., Kim, J.H., Rhee, S.G., 1996. Activation of Phospholipase C- γ by the Concerted Action of Tau Proteins and Arachidonic Acid. *J. Biol. Chem.* 271, 18342–18349. <https://doi.org/10.1074/jbc.271.31.18342>
- Hyman, B.T., Trojanowski, J.Q., 1997. Consensus recommendations for the postmortem diagnosis of Alzheimer disease from the National Institute on Aging and the Reagan Institute Working Group on diagnostic criteria for the neuropathological assessment of Alzheimer disease. *J. Neuropathol. Exp. Neurol.* 56, 1095–1097. <https://doi.org/10.1097/00005072-199710000-00002>
- Hyman, B.T., Van Hoesen, G.W., Damasio, A.R., Barnes, C.L., 1984. Alzheimer's disease: cell-specific pathology isolates the hippocampal formation. *Science* 225, 1168–1170. <https://doi.org/10.1126/science.6474172>
- Hyman, B.T., Van Hoesen, G.W., Kromer, L.J., Damasio, A.R., 1986. Perforant pathway changes and the memory impairment of Alzheimer's disease. *Ann. Neurol.* 20, 472–481. <https://doi.org/10.1002/ana.410200406>

- Iannilli, E., Gudziol, V., 2019. Gustatory pathway in humans: A review of models of taste perception and their potential lateralization. *J. Neurosci. Res.* 97, 230–240. <https://doi.org/10.1002/jnr.24318>
- Ingelsson, M., Fukumoto, H., Newell, K.L., Growdon, J.H., Hedley-Whyte, E.T., Frosch, M.P., Albert, M.S., Hyman, B.T., Irizarry, M.C., 2004. Early Abeta accumulation and progressive synaptic loss, gliosis, and tangle formation in AD brain. *Neurology* 62, 925–931. <https://doi.org/10.1212/01.wnl.0000115115.98960.37>
- Insausti, R., Amaral, D.G., 2012. Hippocampal Formation, in: Mai, J.K., Paxinos, G. (Eds.), *The Human Nervous System*. Academic Press, Amsterdam, Netherlands, pp. 896–942. <https://doi.org/10.1016/B978-0-12-374236-0.10024-0>
- Insausti, R., Muñoz-López, M., Insausti, A.M., Artacho-Pérula, E., 2017. The Human Periallocortex: Layer Pattern in Presubiculum, Parasubiculum and Entorhinal Cortex. A Review. *Front. Neuroanat.* 11. <https://doi.org/10.3389/fnana.2017.00084>
- Iqbal, K., Grundke-Iqbal, I., Zaidi, T., Merz, P.A., Wen, G.Y., Shaikh, S.S., Wisniewski, H.M., Alafuzoff, I., Winblad, B., 1986. Defective brain microtubule assembly in Alzheimer's disease. *Lancet Lond. Engl.* 2, 421–426. [https://doi.org/10.1016/s0140-6736\(86\)92134-3](https://doi.org/10.1016/s0140-6736(86)92134-3)
- Ishiguro, K., Shiratsuchi, A., Sato, S., Omori, A., Arioka, M., Kobayashi, S., Uchida, T., Imahori, K., 1993. Glycogen synthase kinase 3 beta is identical to tau protein kinase I generating several epitopes of paired helical filaments. *FEBS Lett.* 325, 167–172. [https://doi.org/10.1016/0014-5793\(93\)81066-9](https://doi.org/10.1016/0014-5793(93)81066-9)
- Ishihara, T., Hong, M., Zhang, B., Nakagawa, Y., Lee, M.K., Trojanowski, J.Q., Lee, V.M.-Y., 1999. Age-Dependent Emergence and Progression of a Tauopathy in Transgenic Mice Overexpressing the Shortest Human Tau Isoform. *Neuron* 24, 751–762. [https://doi.org/10.1016/S0896-6273\(00\)81127-7](https://doi.org/10.1016/S0896-6273(00)81127-7)
- Ishii, M., Kurachi, Y., 2006. Muscarinic Acetylcholine Receptors. *Curr. Pharm. Des.* 12, 3573–81.
- Ishizawa, K., Lin, W.-L., Tiseo, P., Honer, W.G., Davies, P., Dickson, D.W., 2000. A Qualitative and Quantitative Study of Grumose Degeneration in Progressive Supranuclear Palsy. *J. Neuropathol. Exp. Neurol.* 59, 513–524. <https://doi.org/10.1093/jnen/59.6.513>
- Ismail, Z., Black, S.E., Camicioli, R., Chertkow, H., Herrmann, N., Laforce Jr., R., Montero-Odasso, M., Rockwood, K., Rosa-Neto, P., Seitz, D., Sivananthan, S., Smith, E.E., Soucy, J.-P., Vedel, I., Gauthier, S., Participants, the C., 2020. Recommendations of the 5th Canadian Consensus Conference on the diagnosis and treatment of dementia. *Alzheimers Dement.* 16, 1182–1195. <https://doi.org/10.1002/alz.12105>

- Jack, C.R., Petersen, R.C., Xu, Y.C., O'Brien, P.C., Smith, G.E., Ivnik, R.J., Boeve, B.F., Waring, S.C., Tangalos, E.G., Kokmen, E., 1999. Prediction of AD with MRI-based hippocampal volume in mild cognitive impairment. *Neurology* 52, 1397–1403. <https://doi.org/10.1212/wnl.52.7.1397>
- Jadhav, S., Cubinkova, V., Zimova, I., Brezovakova, V., Madari, A., Cigankova, V., Zilka, N., 2015. Tau-mediated synaptic damage in Alzheimer's disease. *Transl. Neurosci.* 6, 214–226. <https://doi.org/10.1515/tnsci-2015-0023>
- Janeczek, M., Gefen, T., Samimi, M., Kim, G., Weintraub, S., Bigio, E., Rogalski, E., Mesulam, M.-M., Geula, C., 2018. Variations in Acetylcholinesterase Activity within Human Cortical Pyramidal Neurons Across Age and Cognitive Trajectories. *Cereb. Cortex N. Y. NY* 28, 1329–1337. <https://doi.org/10.1093/cercor/bhx047>
- Jansen, W.J., Ossenkoppele, R., Knol, D.L., Tijms, B.M., Scheltens, P., Verhey, F.R.J., Visser, P.J., Amyloid Biomarker Study Group, Aalten, P., Aarsland, D., Alcolea, D., Alexander, M., Almdahl, I.S., Arnold, S.E., Baldeiras, I., Barthel, H., van Berckel, B.N.M., Bibeau, K., Blennow, K., Brooks, D.J., van Buchem, M.A., Camus, V., Cavedo, E., Chen, K., Chetelat, G., Cohen, A.D., Drzezga, A., Engelborghs, S., Fagan, A.M., Fladby, T., Fleisher, A.S., van der Flier, W.M., Ford, L., Förster, S., Fortea, J., Foskett, N., Frederiksen, K.S., Freund-Levi, Y., Frisoni, G.B., Froelich, L., Gabryelewicz, T., Gill, K.D., Gkatzima, O., Gómez-Tortosa, E., Gordon, M.F., Grimmer, T., Hampel, H., Hausner, L., Hellwig, S., Herukka, S.-K., Hildebrandt, H., Ishihara, L., Ivanoiu, A., Jagust, W.J., Johannsen, P., Kandimalla, R., Kapaki, E., Klimkiewicz-Mrowiec, A., Klunk, W.E., Köhler, S., Koglin, N., Kornhuber, J., Kramberger, M.G., Van Laere, K., Landau, S.M., Lee, D.Y., de Leon, M., Lisetti, V., Lleó, A., Madsen, K., Maier, W., Marcusson, J., Mattsson, N., de Mendonça, A., Meulenbroek, O., Meyer, P.T., Mintun, M.A., Mok, V., Molinuevo, J.L., Møllergård, H.M., Morris, J.C., Mroczko, B., Van der Mussele, S., Na, D.L., Newberg, A., Nordberg, A., Nordlund, A., Novak, G.P., Paraskevas, G.P., Parnetti, L., Perera, G., Peters, O., Popp, J., Prabhakar, S., Rabinovici, G.D., Ramakers, I.H.G.B., Rami, L., Resende de Oliveira, C., Rinne, J.O., Rodrigue, K.M., Rodríguez-Rodríguez, E., Roe, C.M., Rot, U., Rowe, C.C., Rütger, E., Sabri, O., Sanchez-Juan, P., Santana, I., Sarazin, M., Schröder, J., Schütte, C., Seo, S.W., Soetewey, F., Soininen, H., Spuru, L., Struyfs, H., Teunissen, C.E., Tsolaki, M., Vandenberghe, R., Verbeek, M.M., Villemagne, V.L., Vos, S.J.B., van Waalwijk van Doorn, L.J.C., Waldemar, G., Wallin, A., Wallin, Å.K., Wiltfang, J., Wolk, D.A., Zboch, M., Zetterberg, H., 2015. Prevalence of cerebral amyloid pathology in persons without dementia: a meta-analysis. *JAMA* 313, 1924–1938. <https://doi.org/10.1001/jama.2015.4668>
- Jeganathan, S., von Bergen, M., Mandelkow, E.-M., Mandelkow, E., 2008. The Natively Unfolded Character of Tau and Its Aggregation to Alzheimer-like Paired Helical Filaments. *Biochemistry* 47, 10526–10539. <https://doi.org/10.1021/bi800783d>

- Jenkins, S.M., W. Johnson, G.V., 1998. Tau complexes with phospholipase C- γ in situ. *NeuroReport* 9, 67–71.
- Jiao, B., Liu, H., Guo, L., Liao, X., Zhou, Y., Weng, L., Xiao, X., Zhou, Lu, Wang, X., Jiang, Y., Yang, Q., Zhu, Y., Zhou, Lin, Zhang, W., Wang, J., Yan, X., Tang, B., Shen, L., 2021. Performance of Plasma Amyloid β , Total Tau, and Neurofilament Light Chain in the Identification of Probable Alzheimer's Disease in South China. *Front. Aging Neurosci.* 13.
- Josephs, K.A., 2017. Current Understanding of Neurodegenerative Diseases Associated With the Protein Tau. *Mayo Clin. Proc.* 92, 1291–1303. <https://doi.org/10.1016/j.mayocp.2017.04.016>
- Josephs, K.A., Murray, M.E., Whitwell, J.L., Parisi, J.E., Petrucelli, L., Jack, C.R., Petersen, R.C., Dickson, D.W., 2014a. Staging TDP-43 pathology in Alzheimer's disease. *Acta Neuropathol. (Berl.)* 127, 441–450. <https://doi.org/10.1007/s00401-013-1211-9>
- Josephs, K.A., Murray, M.E., Whitwell, J.L., Tosakulwong, N., Weigand, S.D., Petrucelli, L., Liesinger, A.M., Petersen, R.C., Parisi, J.E., Dickson, D.W., 2016. Updated TDP-43 in Alzheimer's disease staging scheme. *Acta Neuropathol. (Berl.)* 131, 571–585. <https://doi.org/10.1007/s00401-016-1537-1>
- Josephs, K.A., Whitwell, J.L., Knopman, D.S., Hu, W.T., Stroh, D.A., Baker, M., Rademakers, R., Boeve, B.F., Parisi, J.E., Smith, G.E., Ivnik, R.J., Petersen, R.C., Jack, C.R., Dickson, D.W., 2008. Abnormal TDP-43 immunoreactivity in AD modifies clinicopathologic and radiologic phenotype. *Neurology* 70, 1850–1857. <https://doi.org/10.1212/01.wnl.0000304041.09418.b1>
- Josephs, K.A., Whitwell, J.L., Weigand, S.D., Murray, M.E., Tosakulwong, N., Liesinger, A.M., Petrucelli, L., Senjem, M.L., Knopman, D.S., Boeve, B.F., Ivnik, R.J., Smith, G.E., Jack, C.R., Parisi, J.E., Petersen, R.C., Dickson, D.W., 2014b. TDP-43 is a key player in the clinical features associated with Alzheimer's disease. *Acta Neuropathol. (Berl.)* 127, 811–824. <https://doi.org/10.1007/s00401-014-1269-z>
- Jung, D., Filliol, D., Mieke, M., Rendon, A., 1993. Interaction of brain mitochondria with microtubules reconstituted from brain tubulin and MAP2 or TAU. *Cell Motil.* 24, 245–255. <https://doi.org/10.1002/cm.970240405>
- Jurica, M.S., Moore, M.J., 2003. Pre-mRNA splicing: awash in a sea of proteins. *Mol. Cell* 12, 5–14. [https://doi.org/10.1016/s1097-2765\(03\)00270-3](https://doi.org/10.1016/s1097-2765(03)00270-3)
- Kadokura, A., Yamazaki, T., Lemere, C.A., Takatama, M., Okamoto, K., 2009. Regional distribution of TDP-43 inclusions in Alzheimer disease (AD) brains: Their relation to AD common pathology. *Neuropathology* 29, 566–573. <https://doi.org/10.1111/j.1440-1789.2009.01017.x>

- Kahlson, M.A., Colodner, K.J., 2016. Glial Tau Pathology in Tauopathies: Functional Consequences. *J. Exp. Neurosci.* 9, 43–50. <https://doi.org/10.4137/JEN.S25515>
- Kalus, P., Braak, H., Braak, E., Bohl, J., 1989. The presubicular region in Alzheimer's disease: topography of amyloid deposits and neurofibrillary changes. *Brain Res.* 494, 198–203. [https://doi.org/10.1016/0006-8993\(89\)90164-9](https://doi.org/10.1016/0006-8993(89)90164-9)
- Kammenga, J.E., 2017. The background puzzle: how identical mutations in the same gene lead to different disease symptoms. *FEBS J.* 284, 3362–3373. <https://doi.org/10.1111/febs.14080>
- Kampers, T., Friedhoff, P., Biernat, J., Mandelkow, E.-M., Mandelkow, E., 1996. RNA stimulates aggregation of microtubule-associated protein tau into Alzheimer-like paired helical filaments. *FEBS Lett.* 399, 344–349. [https://doi.org/10.1016/S0014-5793\(96\)01386-5](https://doi.org/10.1016/S0014-5793(96)01386-5)
- Karnovsky, M.J., Roots, L., 1964. A “direct-coloring” thiocholine method for cholinesterases. *J. Histochem. Cytochem. Off. J. Histochem. Soc.* 12, 219–221. <https://doi.org/10.1177/12.3.219>
- Kasashima, S., Oda, Y., 2003. Cholinergic neuronal loss in the basal forebrain and mesopontine tegmentum of progressive supranuclear palsy and corticobasal degeneration. *Acta Neuropathol. (Berl.)* 105, 117–124.
- Katz, D.I., Bernick, C., Dodick, D.W., Mez, J., Mariani, M.L., Adler, C.H., Alosco, M.L., Balcer, L.J., Banks, S.J., Barr, W.B., Brody, D.L., Cantu, R.C., Dams-O'Connor, K., Geda, Y.E., Jordan, B.D., McAllister, T.W., Peskind, E.R., Petersen, R.C., Wethe, J.V., Zafonte, R.D., Foley, É.M., Babcock, D.J., Koroshetz, W.J., Tripodis, Y., McKee, A.C., Shenton, M.E., Cummings, J.L., Reiman, E.M., Stern, R.A., 2021. National Institute of Neurological Disorders and Stroke Consensus Diagnostic Criteria for Traumatic Encephalopathy Syndrome. *Neurology* 96, 848–863. <https://doi.org/10.1212/WNL.00000000000011850>
- Katzman, R., Terry, R., DeTeresa, R., Brown, T., Davies, P., Fuld, P., Renbing, X., Peck, A., 1988. Clinical, pathological, and neurochemical changes in dementia: A subgroup with preserved mental status and numerous neocortical plaques. *Ann. Neurol.* 23, 138–144. <https://doi.org/10.1002/ana.410230206>
- Kaufman, S.K., Del Tredici, K., Thomas, T.L., Braak, H., Diamond, M.I., 2018. Tau seeding activity begins in the transentorhinal/entorhinal regions and anticipates phospho-tau pathology in Alzheimer's disease and PART. *Acta Neuropathol. (Berl.)* 136, 57–67. <https://doi.org/10.1007/s00401-018-1855-6>
- Kenessey, A., Yen, S.H., 1993. The extent of phosphorylation of fetal tau is comparable to that of PHF-tau from Alzheimer paired helical filaments. *Brain Res.* 629, 40–46. [https://doi.org/10.1016/0006-8993\(93\)90478-6](https://doi.org/10.1016/0006-8993(93)90478-6)

- Klingler, J., 1948. Die makroskopische Anatomie der Ammonsformation. Denkschr. Schweiz. Naturforschenden Ges. 78, 1–78.
- Knopman, D.S., Jones, D.T., Greicius, M.D., 2021. Failure to demonstrate efficacy of aducanumab: An analysis of the EMERGE and ENGAGE trials as reported by Biogen, December 2019. *Alzheimers Dement.* 17, 696–701.
<https://doi.org/10.1002/alz.12213>
- Knopman, D.S., Petersen, R.C., 2014. Mild Cognitive Impairment and Mild Dementia: A Clinical Perspective. *Mayo Clin. Proc.* 89, 1452–1459.
<https://doi.org/10.1016/j.mayocp.2014.06.019>
- Kobayashi, M., 2006. Functional Organization of the Human Gustatory Cortex. *J. Oral Biosci.* 48, 244–260. [https://doi.org/10.1016/S1349-0079\(06\)80007-1](https://doi.org/10.1016/S1349-0079(06)80007-1)
- Kobayashi, Y., G.Amaral, D., 1999. Chapter IV Chemical neuroanatomy of the hippocampal formation and the perirhinal and parahippocampal cortices, in: Bloom, F.E., Björklund, A., Hökfelt (Eds.), *Handbook of Chemical Neuroanatomy*. Elsevier Science, pp. 285–401.
- Kompoliti, K., Goetz, C.G., Litvan, I., Jellinger, K., Verny, M., 1998. Pharmacological Therapy in Progressive Supranuclear Palsy. *Arch. Neurol.* 55, 1099–1102.
<https://doi.org/10.1001/archneur.55.8.1099>
- Koo, B.B., Bagai, K., Walters, A.S., 2016. Restless Legs Syndrome: Current Concepts about Disease Pathophysiology. *Tremor Hyperkinetic Mov.* 6.
<https://doi.org/10.7916/D83J3D2G>
- Kornblihtt, A.R., Schor, I.E., Alló, M., Dujardin, G., Petrillo, E., Muñoz, M.J., 2013. Alternative splicing: a pivotal step between eukaryotic transcription and translation. *Nat. Rev. Mol. Cell Biol.* 14, 153–165.
<https://doi.org/10.1038/nrm3525>
- Kosik, K.S., Orecchio, L.D., Bakalis, S., Neve, R.L., 1989. Developmentally regulated expression of specific tau sequences. *Neuron* 2, 1389–1397.
[https://doi.org/10.1016/0896-6273\(89\)90077-9](https://doi.org/10.1016/0896-6273(89)90077-9)
- Kovacs, G.G., 2018. Understanding the Relevance of Aging-Related Tau Astroglipathy (ARTAG). *Neuroglia* 1, 339–350. <https://doi.org/10.3390/neuroglia1020023>

- Kovacs, G.G., Ferrer, I., Grinberg, L.T., Alafuzoff, I., Attems, J., Budka, H., Cairns, N.J., Cray, J.F., Duyckaerts, C., Ghetti, B., Halliday, G.M., Ironside, J.W., Love, S., Mackenzie, I.R., Munoz, D.G., Murray, M.E., Nelson, P.T., Takahashi, H., Trojanowski, J.Q., Ansorge, O., Arzberger, T., Baborie, A., Beach, T.G., Bieniek, K.F., Bigio, E.H., Bodi, I., Dugger, B.N., Feany, M., Gelpi, E., Gentleman, S.M., Giaccone, G., Hatanpaa, K.J., Heale, R., Hof, P.R., Hofer, M., Hortobágyi, T., Jellinger, K., Jicha, G.A., Ince, P., Kofler, J., Kövari, E., Kril, J.J., Mann, D.M., Matej, R., McKee, A.C., McLean, C., Milenkovic, I., Montine, T.J., Murayama, S., Lee, E.B., Rahimi, J., Rodriguez, R.D., Rozemüller, A., Schneider, J.A., Schultz, C., Seeley, W., Seilhean, D., Smith, C., Tagliavini, F., Takao, M., Thal, D.R., Toledo, J.B., Tolnay, M., Troncoso, J.C., Vinters, H.V., Weis, S., Wharton, S.B., White, C.L., Wisniewski, T., Woulfe, J.M., Yamada, M., Dickson, D.W., 2016b. Aging-related tau astrogliopathy (ARTAG): harmonized evaluation strategy. *Acta Neuropathol. (Berl.)* 131, 87–102. <https://doi.org/10.1007/s00401-015-1509-x>
- Krestova, M., Garcia-Sierra, F., Bartos, A., Ricny, J., Ripova, D., 2012. Structure and Pathology of Tau Protein in Alzheimer Disease. *Int. J. Alzheimers Dis.* 2012, 731526. <https://doi.org/10.1155/2012/731526>
- Kumru, H., Albu, S., Vidal, J., Barrio, M., Santamaria, J., 2016. Dopaminergic treatment of restless legs syndrome in spinal cord injury patients with neuropathic pain. *Spinal Cord Ser. Cases* 2, 16022. <https://doi.org/10.1038/scsandc.2016.22>
- Kutoku, Y., Miyazaki, Y., Yamashita, Y., Kuwano, R., Murakami, T., Sunada, Y., 2012. [FTDP-17 presenting amnesic MCI as an initial symptom: case report]. *Rinsho Shinkeigaku* 52, 73–78. <https://doi.org/10.5692/clinicalneuro.52.73>
- Lacosta, A.-M., Insua, D., Badi, H., Pesini, P., Sarasa, M., 2017. Neurofibrillary Tangles of A β x-40 in Alzheimer's Disease Brains. *J. Alzheimers Dis. JAD* 58, 661–667. <https://doi.org/10.3233/JAD-170163>
- Landau, S.M., Breault, C., Joshi, A.D., Pontecorvo, M., Mathis, C.A., Jagust, W.J., Mintun, M.A., Alzheimer's Disease Neuroimaging Initiative, 2013. Amyloid- β imaging with Pittsburgh compound B and florbetapir: comparing radiotracers and quantification methods. *J. Nucl. Med. Off. Publ. Soc. Nucl. Med.* 54, 70–77. <https://doi.org/10.2967/jnumed.112.109009>
- Landis, B.N., Scheibe, M., Weber, C., Berger, R., Brämerson, A., Bende, M., Nordin, S., Hummel, T., 2010. Chemosensory interaction: acquired olfactory impairment is associated with decreased taste function. *J. Neurol.* 257, 1303–1308. <https://doi.org/10.1007/s00415-010-5513-8>

- Larrimore, K.E., Kannan, L., Kendle, R.P., Jamal, T., Barcus, M., Stefanko, K., Kilbourne, J., Brimijoin, S., Zhan, C.-G., Neisewander, J., Mor, T.S., 2020. A plant-derived cocaine hydrolase prevents cocaine overdose lethality and attenuates cocaine-induced drug seeking behavior. *Prog. Neuropsychopharmacol. Biol. Psychiatry* 102, 109961. <https://doi.org/10.1016/j.pnpbp.2020.109961>
- Lazarus, M., Chen, J.-F., Urade, Y., Huang, Z.-L., 2013. Role of the basal ganglia in the control of sleep and wakefulness. *Curr. Opin. Neurobiol.* 23, 780–785. <https://doi.org/10.1016/j.conb.2013.02.001>
- Lee, G., Kwei, S., Newman, S., Olmsted, J., Liu, Y., 1996. A new molecular interactor for tau protein. *Mol. Biol. Cell* 7, 3316–3316.
- Lee, G., Neve, R.L., Kosik, K.S., 1989. The microtubule binding domain of tau protein. *Neuron* 2, 1615–1624. [https://doi.org/10.1016/0896-6273\(89\)90050-0](https://doi.org/10.1016/0896-6273(89)90050-0)
- Lee, G., Newman, S.T., Gard, D.L., Band, H., Panchamoorthy, G., 1998. Tau interacts with src-family non-receptor tyrosine kinases. *J. Cell Sci.* 111, 3167–3177.
- Lee, V.M., Goedert, M., Trojanowski, J.Q., 2001. Neurodegenerative tauopathies. *Annu. Rev. Neurosci.* 24, 1121–1159. <https://doi.org/10.1146/annurev.neuro.24.1.1121>
- Lerner, M.R., Boyle, J.A., Mount, S.M., Wolin, S.L., Steitz, J.A., 1980. Are snRNPs involved in splicing? *Nature* 283, 220–224. <https://doi.org/10.1038/283220a0>
- Leuzinger, W., 1969. Structure and function of acetylcholinesterase. *Prog. Brain Res.* 31, 241–245. [https://doi.org/10.1016/S0079-6123\(08\)63242-2](https://doi.org/10.1016/S0079-6123(08)63242-2)
- Leuzy, A., Chiotis, K., Lemoine, L., Gillberg, P.-G., Almkvist, O., Rodriguez-Vieitez, E., Nordberg, A., 2019. Tau PET imaging in neurodegenerative tauopathies—still a challenge. *Mol. Psychiatry* 24, 1112–1134. <https://doi.org/10.1038/s41380-018-0342-8>
- Levey, A.I., Wainer, B.H., Rye, D.B., Mufson, E.J., Mesulam, M.-M., 1984. Choline acetyltransferase-immunoreactive neurons intrinsic to rodent cortex and distinction from acetylcholinesterase-positive neurons. *Neuroscience* 13, 341–353. [https://doi.org/10.1016/0306-4522\(84\)90234-3](https://doi.org/10.1016/0306-4522(84)90234-3)
- Lewis, J., McGowan, E., Rockwood, J., Melrose, H., Nacharaju, P., Van Slegtenhorst, M., Gwinn-Hardy, K., Paul Murphy, M., Baker, M., Yu, X., Duff, K., Hardy, J., Corral, A., Lin, W.L., Yen, S.H., Dickson, D.W., Davies, P., Hutton, M., 2000. Neurofibrillary tangles, amyotrophy and progressive motor disturbance in mice expressing mutant (P301L) tau protein. *Nat. Genet.* 25, 402–405. <https://doi.org/10.1038/78078>
- Lezak, M.D., Howieson, D.B., Loring, D.W., Hannay, H.J., Fischer, J.S., 2004. *Neuropsychological assessment*, 4th ed., Neuropsychological assessment, 4th ed. Oxford University Press, New York, NY, US.

- Li, B., Duysen, E.G., Carlson, M., Lockridge, O., 2008. The butyrylcholinesterase knockout mouse as a model for human butyrylcholinesterase deficiency. *J. Pharmacol. Exp. Ther.* 324, 1146–1154. <https://doi.org/10.1124/jpet.107.133330>
- Litvan, I., Agid, Y., Calne, D., Campbell, G., Dubois, B., Duvoisin, R.C., Goetz, C.G., Golbe, L.I., Grafman, J., Growdon, J.H., Hallett, M., Jankovic, J., Quinn, N.P., Tolosa, E., Zee, D.S., 1996a. Clinical research criteria for the diagnosis of progressive supranuclear palsy (Steele-Richardson-Olszewski syndrome): report of the NINDS-SPSP international workshop. *Neurology* 47, 1–9. <https://doi.org/10.1212/wnl.47.1.1>
- Litvan, I., Hauw, J.J., Bartko, J.J., Lantos, P.L., Daniel, S.E., Horoupian, D.S., McKee, A., Dickson, D., Baner, C., Tabaton, M., Jellinger, K., Anderson, D.W., 1996b. Validity and Reliability of the Preliminary NINDS Neuropathologic Criteria for Progressive Supranuclear Palsy and Related Disorders. *J. Neuropathol. Exp. Neurol.* 55, 97–105. <https://doi.org/10.1097/00005072-199601000-00010>
- Litvan, I., Phipps, M., Pharr, V.L., Hallett, M., Grafman, J., Salazar, A., 2001. Randomized placebo-controlled trial of donepezil in patients with progressive supranuclear palsy. *Neurology* 57, 467–473. <https://doi.org/10.1212/wnl.57.3.467>
- Liu, A.K.L., Lim, E.J., Ahmed, I., Chang, R.C. -C., Pearce, R.K.B., Gentleman, S.M., 2018. Review: Revisiting the human cholinergic nucleus of the diagonal band of Broca. *Neuropathol. Appl. Neurobiol.* 44, 647–662. <https://doi.org/10.1111/nan.12513>
- Liu, C., Götz, J., 2013. Profiling Murine Tau with 0N, 1N and 2N Isoform-Specific Antibodies in Brain and Peripheral Organs Reveals Distinct Subcellular Localization, with the 1N Isoform Being Enriched in the Nucleus. *PLoS ONE* 8. <https://doi.org/10.1371/journal.pone.0084849>
- Liu, F., Grundke-Iqbal, I., Iqbal, K., Gong, C.-X., 2005. Contributions of protein phosphatases PP1, PP2A, PP2B and PP5 to the regulation of tau phosphorylation. *Eur. J. Neurosci.* 22, 1942–1950. <https://doi.org/10.1111/j.1460-9568.2005.04391.x>
- Livingston, G., Selbaek, G., Rockwood, K., Huntley, J.D., Sommerlad, A., Mukadam, N., 2020. Cognitive reserve and resilience: Possible mechanisms of dementia prevention. *Alzheimers Dement.* 16, e037931. <https://doi.org/10.1002/alz.037931>
- Lockridge, O., Norgren, R.B., Johnson, R.C., Blake, T.A., 2016. Naturally Occurring Genetic Variants of Human Acetylcholinesterase and Butyrylcholinesterase and Their Potential Impact on the Risk of Toxicity from Cholinesterase Inhibitors. *Chem. Res. Toxicol.* 29, 1381–1392. <https://doi.org/10.1021/acs.chemrestox.6b00228>
- Lorente De Nó, R., 1934. Studies on the structure of the cerebral cortex. II. Continuation of the study of the ammonic system. *J. Für Psychol. Neurol.* 46, 113–177.

- Luck, T., Luppia, M., Wiese, B., Maier, W., van den Bussche, H., Eisele, M., Jessen, F., Weeg, D., Weyerer, S., Pentzek, M., Leicht, H., Koehler, M., Tebarth, F., Olbrich, J., Eifflaender-Gorfer, S., Fuchs, A., Koenig, H.-H., Riedel-Heller, S.G., AgeCoDe Study Group, 2012. Prediction of incident dementia: impact of impairment in instrumental activities of daily living and mild cognitive impairment-results from the German study on ageing, cognition, and dementia in primary care patients. *Am. J. Geriatr. Psychiatry Off. J. Am. Assoc. Geriatr. Psychiatry* 20, 943–954. <https://doi.org/10.1097/JGP.0b013e31825c09bc>
- Lynch, T., Sano, M., Marder, K.S., Bell, K.L., Foster, N.L., Defendini, R.F., Sima, A.A., Keohane, C., Nygaard, T.G., Fahn, S., 1994. Clinical characteristics of a family with chromosome 17-linked disinhibition-dementia-parkinsonism-amyotrophy complex. *Neurology* 44, 1878–1884.
- Lyon, A.M., Tesmer, J.J.G., 2013. Structural Insights into Phospholipase C- β Function. *Mol. Pharmacol.* 84, 488–500. <https://doi.org/10.1124/mol.113.087403>
- Macdonald, I., Pottie, I., Joy, E.E., Matte, G., Burrell, S., Mawko, G., Martin, E., Darvesh, S., 2010. IC-P-051: Synthesis and Evaluation of Butyrylcholinesterase Ligands for Neuroimaging Alzheimer's Disease. *Alzheimers Dement.* 6, S23–S23. <https://doi.org/10.1016/j.jalz.2010.05.066>
- Macdonald, I.R., Maxwell, S.P., Reid, G.A., Cash, M.K., DeBay, D.R., Darvesh, S., 2017. Quantification of Butyrylcholinesterase Activity as a Sensitive and Specific Biomarker of Alzheimer's Disease. *J. Alzheimers Dis. JAD* 58, 491–505. <https://doi.org/10.3233/JAD-170164>
- Magdesian, M.H., Carvalho, M.M.V.F., Mendes, F.A., Saraiva, L.M., Juliano, M.A., Juliano, L., Garcia-Abreu, J., Ferreira, S.T., 2008. Amyloid- β Binds to the Extracellular Cysteine-rich Domain of Frizzled and Inhibits Wnt/ β -Catenin Signaling*. *J. Biol. Chem.* 283, 9359–9368. <https://doi.org/10.1074/jbc.M707108200>
- Mahale, R.R., Krishnan, S., Divya, K.P., Jisha, V.T., Kishore, A., 2022. Gender differences in progressive supranuclear palsy. *Acta Neurol. Belg.* 122, 357–362. <https://doi.org/10.1007/s13760-021-01599-0>
- Mandelkow, E.-M., Biernat, J., Drewes, G., Gustke, N., Trinczek, B., Mandelkow, E., 1995. Tau domains, phosphorylation, and interactions with microtubules. *Neurobiol. Aging, The Schmitt Symposium: The Cytoskeleton and Alzheimer's Disease* 16, 355–362. [https://doi.org/10.1016/0197-4580\(95\)00025-A](https://doi.org/10.1016/0197-4580(95)00025-A)
- Manly, J.J., Tang, M.-X., Schupf, N., Stern, Y., Vonsattel, J.-P.G., Mayeux, R., 2008. Frequency and Course of Mild Cognitive Impairment in a Multiethnic Community. *Ann. Neurol.* 63, 494–506. <https://doi.org/10.1002/ana.21326>

- Mann, D.M., 1996. Pyramidal nerve cell loss in Alzheimer's disease. *Neurodegener. J. Neurodegener. Disord. Neuroprotection Neuroregeneration* 5, 423–427. <https://doi.org/10.1006/neur.1996.0057>
- Manoharan, I., Boopathy, R., Darvesh, S., Lockridge, O., 2007. A medical health report on individuals with silent butyrylcholinesterase in the Vysya community of India. *Clin. Chim. Acta Int. J. Clin. Chem.* 378, 128–135. <https://doi.org/10.1016/j.cca.2006.11.005>
- Markesbery, W.R., Jicha, G.A., Liu, H., Schmitt, F.A., 2009. Lewy Body Pathology in Normal Elderly Subjects. *J. Neuropathol. Exp. Neurol.* 68, 816–822. <https://doi.org/10.1097/NEN.0b013e3181ac10a7>
- Martin, L., Latypova, X., Terro, F., 2011. Post-translational modifications of tau protein: implications for Alzheimer's disease. *Neurochem. Int.* 58, 458–471. <https://doi.org/10.1016/j.neuint.2010.12.023>
- Martin, L., Latypova, X., Wilson, C.M., Magnaudeix, A., Perrin, M.-L., Yardin, C., Terro, F., 2013. Tau protein kinases: involvement in Alzheimer's disease. *Ageing Res. Rev.* 12, 289–309. <https://doi.org/10.1016/j.arr.2012.06.003>
- Matsumoto, S., Hirano, A., Goto, S., 1990. Spinal cord neurofibrillary tangles of Guamanian amyotrophic lateral sclerosis and parkinsonism-dementia complex: an immunohistochemical study. *Neurology* 40, 975–979. <https://doi.org/10.1212/wnl.40.6.975>
- Matsuzono, K., Hishikawa, N., Ohta, Y., Yamashita, T., Deguchi, K., Nakano, Y., Abe, K., 2015. Combination Therapy of Cholinesterase Inhibitor (Donepezil or Galantamine) plus Memantine in the Okayama Memantine Study. *J. Alzheimers Dis. JAD* 45, 771–780. <https://doi.org/10.3233/JAD-143084>
- Maxwell, S.P., Cash, M.K., Rockwood, K., Fisk, J.D., Darvesh, S., 2021. Clinical and neuropathological variability in the rare IVS10 + 14 tau mutation. *Neurobiol. Aging* 101, 298.e1–298.e10. <https://doi.org/10.1016/j.neurobiolaging.2021.01.004>
- McAleese, K.E., Walker, L., Erskine, D., Thomas, A.J., McKeith, I.G., Attems, J., 2017. TDP-43 pathology in Alzheimer's disease, dementia with Lewy bodies and ageing. *Brain Pathol. Zurich Switz.* 27, 472–479. <https://doi.org/10.1111/bpa.12424>
- McGregor, M.M., Nelson, A.B., 2019. Circuit Mechanisms of Parkinson's Disease. *Neuron* 101, 1042–1056. <https://doi.org/10.1016/j.neuron.2019.03.004>

- McKeith, I.G., Dickson, D.W., Lowe, J., Emre, M., O'Brien, J.T., Feldman, H., Cummings, J., Duda, J.E., Lippa, C., Perry, E.K., Aarsland, D., Arai, H., Ballard, C.G., Boeve, B., Burn, D.J., Costa, D., Del Ser, T., Dubois, B., Galasko, D., Gauthier, S., Goetz, C.G., Gomez-Tortosa, E., Halliday, G., Hansen, L.A., Hardy, J., Iwatsubo, T., Kalaria, R.N., Kaufer, D., Kenny, R.A., Korczyn, A., Kosaka, K., Lee, V.M.Y., Lees, A., Litvan, I., Londos, E., Lopez, O.L., Minoshima, S., Mizuno, Y., Molina, J.A., Mukaetova-Ladinska, E.B., Pasquier, F., Perry, R.H., Schulz, J.B., Trojanowski, J.Q., Yamada, M., Consortium on DLB, 2005. Diagnosis and management of dementia with Lewy bodies: third report of the DLB Consortium. *Neurology* 65, 1863–1872. <https://doi.org/10.1212/01.wnl.0000187889.17253.b1>
- McKhann, G., Drachman, D., Folstein, M., Katzman, R., Price, D., Stadlan, E.M., 1984. Clinical diagnosis of Alzheimer's disease: report of the NINCDS-ADRDA Work Group under the auspices of Department of Health and Human Services Task Force on Alzheimer's Disease. *Neurology* 34, 939–944. <https://doi.org/10.1212/wnl.34.7.939>
- McKhann, G.M., Knopman, D.S., Chertkow, H., Hyman, B.T., Jack, C.R., Kawas, C.H., Klunk, W.E., Koroshetz, W.J., Manly, J.J., Mayeux, R., Mohs, R.C., Morris, J.C., Rossor, M.N., Scheltens, P., Carrillo, M.C., Thies, B., Weintraub, S., Phelps, C.H., 2011. The diagnosis of dementia due to Alzheimer's disease: Recommendations from the National Institute on Aging-Alzheimer's Association workgroups on diagnostic guidelines for Alzheimer's disease. *Alzheimers Dement. J. Alzheimers Assoc.* 7, 263–269. <https://doi.org/10.1016/j.jalz.2011.03.005>
- McMillan, P., Korvatska, E., Poorkaj, P., Evstafjeva, Z., Robinson, L., Greenup, L., Leverenz, J., Schellenberg, G.D., D'Souza, I., 2008. Tau isoform regulation is region- and cell-specific in mouse brain. *J. Comp. Neurol.* 511, 788–803. <https://doi.org/10.1002/cne.21867>
- Mega, M.S., Cohenour, R.C., 1997. Akinetic mutism: disconnection of frontal-subcortical circuits. *Neuropsychiatry. Neuropsychol. Behav. Neurol.* 10, 254–259.
- Mendel, B., Mundell, D.B., Rudney, H., 1943. Studies on cholinesterase. *Biochem. J.* 37, 473–476.
- Mendez, M.F., Mastri, A.R., Zander, B.A., Frey, W.H., 1992. A clinicopathological study of CT scans in Alzheimer's disease. *J. Am. Geriatr. Soc.* 40, 476–478. <https://doi.org/10.1111/j.1532-5415.1992.tb02014.x>
- Mesulam, M., Guillozet, A., Shaw, P., Quinn, B., 2002. Widely spread butyrylcholinesterase can hydrolyze acetylcholine in the normal and Alzheimer brain. *Neurobiol. Dis.* 9, 88–93. <https://doi.org/10.1006/nbdi.2001.0462>

- Mesulam, M.M., Asuncion Morán, M., 1987. Cholinesterases within neurofibrillary tangles related to age and Alzheimer's disease. *Ann. Neurol.* 22, 223–228. <https://doi.org/10.1002/ana.410220206>
- Mesulam, M.M., Geula, C., 1994. Butyrylcholinesterase reactivity differentiates the amyloid plaques of aging from those of dementia. *Ann. Neurol.* 36, 722–727. <https://doi.org/10.1002/ana.410360506>
- Mesulam, M.M., Geula, C., 1991. Acetylcholinesterase-rich neurons of the human cerebral cortex: cytoarchitectonic and ontogenetic patterns of distribution. *J. Comp. Neurol.* 306, 193–220. <https://doi.org/10.1002/cne.903060202>
- Mesulam, M.-M., Geula, C., 1988. Nucleus basalis (Ch4) and cortical cholinergic innervation in the human brain: Observations based on the distribution of acetylcholinesterase and choline acetyltransferase. *J. Comp. Neurol.* 275, 216–240. <https://doi.org/10.1002/cne.902750205>
- Mesulam, M.-M., Mufson, E.J., Levey, A.I., Wainer, B.H., 1983. Cholinergic innervation of cortex by the basal forebrain: Cytochemistry and cortical connections of the septal area, diagonal band nuclei, nucleus basalis (Substantia innominata), and hypothalamus in the rhesus monkey. *J. Comp. Neurol.* 214, 170–197. <https://doi.org/10.1002/cne.902140206>
- Mielke, M.M., 2018. Sex and Gender Differences in Alzheimer's Disease Dementia. *Psychiatr. Times* 35, 14–17.
- Miklossy, J., Qing, H., Radenovic, A., Kis, A., Vileno, B., László, F., Miller, L., Martins, R.N., Waeber, G., Mooser, V., Bosman, F., Khalili, K., Darbinian, N., McGeer, P.L., 2010. Beta amyloid and hyperphosphorylated tau deposits in the pancreas in type 2 diabetes. *Neurobiol. Aging* 31, 1503–1515. <https://doi.org/10.1016/j.neurobiolaging.2008.08.019>
- Mikolaenko, I., Pletnikova, O., Kawas, C.H., O'Brien, R., Resnick, S.M., Crain, B., Troncoso, J.C., 2005. Alpha-Synuclein Lesions in Normal Aging, Parkinson Disease, and Alzheimer Disease: Evidence from the Baltimore Longitudinal Study of Aging (BLSA). *J. Neuropathol. Exp. Neurol.* 64, 156–162. <https://doi.org/10.1093/jnen/64.2.156>
- Mirra, S.S., Heyman, A., McKeel, D., Sumi, S.M., Crain, B.J., Brownlee, L.M.Bc., Vogel, F.S., Hughes, J.P.M., Belle, G. van, Berg, L., participating neuropathologists, 1991. The Consortium to Establish a Registry for Alzheimer's Disease (CERAD): Part II. Standardization of the neuropathologic assessment of Alzheimer's disease. *Neurology* 41, 479–486. <https://doi.org/10.1212/wnl.41.4.479>

- Mishima, T., Fujioka, S., Tomiyama, H., Yabe, I., Kurisaki, R., Fujii, N., Neshige, R., Ross, O.A., Farrer, M.J., Dickson, D.W., Wszolek, Z.K., Hattori, N., Tsuboi, Y., 2018. Establishing diagnostic criteria for Perry syndrome. *J. Neurol. Neurosurg. Psychiatry* 89, 482–487. <https://doi.org/10.1136/jnnp-2017-316864>
- Montine, T.J., Phelps, C.H., Beach, T.G., Bigio, E.H., Cairns, N.J., Dickson, D.W., Duyckaerts, C., Frosch, M.P., Masliah, E., Mirra, S.S., Nelson, P.T., Schneider, J.A., Thal, D.R., Trojanowski, J.Q., Vinters, H.V., Hyman, B.T., 2012. National Institute on Aging-Alzheimer's Association guidelines for the neuropathologic assessment of Alzheimer's disease: a practical approach. *Acta Neuropathol. (Berl.)* 123, 1–11. <https://doi.org/10.1007/s00401-011-0910-3>
- Morán, M.A., Gómez-Ramos, P., 1992. Cholinesterase histochemistry in the human brain: effect of various fixation and storage conditions. *J. Neurosci. Methods* 43, 49–54. [https://doi.org/10.1016/0165-0270\(92\)90066-m](https://doi.org/10.1016/0165-0270(92)90066-m)
- Morishima-Kawashima, M., Hasegawa, M., Takio, K., Suzuki, M., Yoshida, H., Watanabe, A., Titani, K., Ihara, Y., 1995. Hyperphosphorylation of tau in PHF. *Neurobiol. Aging* 16, 365–371; discussion 371–380. [https://doi.org/10.1016/0197-4580\(95\)00027-c](https://doi.org/10.1016/0197-4580(95)00027-c)
- Morris, J.C., Heyman, A., Mohs, R.C., Hughes, J.P., van Belle, G., Fillenbaum, G., Mellits, E.D., Clark, C., 1989. The Consortium to Establish a Registry for Alzheimer's Disease (CERAD). Part I. Clinical and neuropsychological assessment of Alzheimer's disease. *Neurology* 39, 1159–1165. <https://doi.org/10.1212/wnl.39.9.1159>
- Morrison, J.H., Hof, P.R., 2002. Selective vulnerability of corticocortical and hippocampal circuits in aging and Alzheimer's disease. *Prog. Brain Res.* 136, 467–486. [https://doi.org/10.1016/s0079-6123\(02\)36039-4](https://doi.org/10.1016/s0079-6123(02)36039-4)
- Müller, R., Heinrich, M., Heck, S., Blohm, D., Richter-Landsberg, C., 1997. Expression of microtubule-associated proteins MAP2 and tau in cultured rat brain oligodendrocytes. *Cell Tissue Res.* 288, 239–249. <https://doi.org/10.1007/s004410050809>
- Munoz, D.G., Greene, C., Perl, D.P., Selkoe, D.J., 1988. Accumulation of phosphorylated neurofilaments in anterior horn motoneurons of amyotrophic lateral sclerosis patients. *J. Neuropathol. Exp. Neurol.* 47, 9–18. <https://doi.org/10.1097/00005072-198801000-00002>
- Murman, D.L., 2015. The Impact of Age on Cognition. *Semin. Hear.* 36, 111–121. <https://doi.org/10.1055/s-0035-1555115>
- Myers, A.J., Kaleem, M., Marlowe, L., Pittman, A.M., Lees, A.J., Fung, H.C., Duckworth, J., Leung, D., Gibson, A., Morris, C.M., de Silva, R., Hardy, J., 2005. The H1c haplotype at the MAPT locus is associated with Alzheimer's disease. *Hum. Mol. Genet.* 14, 2399–2404. <https://doi.org/10.1093/hmg/ddi241>

- Nascimento, C., Di Lorenzo Alho, A.T., Conceição Amaral, C.B., Paraizo Leite, R.E., Nitrini, R., Jacob-Filho, W., Pasqualucci, C.A., Kastehelmi Hokkanen, S.R., Hunter, S., Keage, H., Kovacs, G.G., Grinberg, L.T., Suemoto, C.K., 2018. Prevalence of TDP-43 proteinopathy in cognitively normal older adults: systematic review and meta-analysis. *Neuropathol. Appl. Neurobiol.* 44, 286–297. <https://doi.org/10.1111/nan.12430>
- Nasreddine, Z.S., Phillips, N.A., Bédirian, V., Charbonneau, S., Whitehead, V., Collin, I., Cummings, J.L., Chertkow, H., 2005. The Montreal Cognitive Assessment, MoCA: A Brief Screening Tool For Mild Cognitive Impairment. *J. Am. Geriatr. Soc.* 53, 695–699. <https://doi.org/10.1111/j.1532-5415.2005.53221.x>
- Nath, U., Ben-Shlomo, Y., Thomson, R.G., Morris, H.R., Wood, N.W., Lees, A.J., Burn, D.J., 2001. The prevalence of progressive supranuclear palsy (Steele-Richardson-Olszewski syndrome) in the UK. *Brain J. Neurol.* 124, 1438–1449. <https://doi.org/10.1093/brain/124.7.1438>
- Nelson, P.T., Alafuzoff, I., Bigio, E.H., Bouras, C., Braak, H., Cairns, N.J., Castellani, R.J., Crain, B.J., Davies, P., Tredici, K.D., Duyckaerts, C., Frosch, M.P., Haroutunian, V., Hof, P.R., Hulette, C.M., Hyman, B.T., Iwatsubo, T., Jellinger, K.A., Jicha, G.A., Kövari, E., Kukull, W.A., Leverenz, J.B., Love, S., Mackenzie, I.R., Mann, D.M., Masliah, E., McKee, A.C., Montine, T.J., Morris, J.C., Schneider, J.A., Sonnen, J.A., Thal, D.R., Trojanowski, J.Q., Troncoso, J.C., Wisniewski, T., Woltjer, R.L., Beach, T.G., 2012. Correlation of Alzheimer Disease Neuropathologic Changes With Cognitive Status: A Review of the Literature. *J. Neuropathol. Exp. Neurol.* 71, 362–381. <https://doi.org/10.1097/NEN.0b013e31825018f7>
- Nelson, P.T., Dickson, D.W., Trojanowski, J.Q., Jack, C.R., Boyle, P.A., Arfanakis, K., Rademakers, R., Alafuzoff, I., Attems, J., Brayne, C., Coyle-Gilchrist, I.T.S., Chui, H.C., Fardo, D.W., Flanagan, M.E., Halliday, G., Hokkanen, S.R.K., Hunter, S., Jicha, G.A., Katsumata, Y., Kawas, C.H., Keene, C.D., Kovacs, G.G., Kukull, W.A., Levey, A.I., Makkinejad, N., Montine, T.J., Murayama, S., Murray, M.E., Nag, S., Rissman, R.A., Seeley, W.W., Sperling, R.A., White III, C.L., Yu, L., Schneider, J.A., 2019. Limbic-predominant age-related TDP-43 encephalopathy (LATE): consensus working group report. *Brain* 142, 1503–1527. <https://doi.org/10.1093/brain/awz099>
- Neltner, J.H., Abner, E.L., Jicha, G.A., Schmitt, F.A., Patel, E., Poon, L.W., Gearing, M., Green, R.C., Davey, A., Johnson, M.A., Jazwinski, S.M., Kim, S., Davis, D., Woodard, J.L., Kryscio, R.J., Van Eldik, L.J., Nelson, P.T., 2016. Brain pathologies in extreme old age. *Neurobiol. Aging* 37, 1–11. <https://doi.org/10.1016/j.neurobiolaging.2015.10.009>

- Neumann, M., Sampathu, D.M., Kwong, L.K., Truax, A.C., Micsenyi, M.C., Chou, T.T., Bruce, J., Schuck, T., Grossman, M., Clark, C.M., McCluskey, L.F., Miller, B.L., Masliah, E., Mackenzie, I.R., Feldman, H., Feiden, W., Kretzschmar, H.A., Trojanowski, J.Q., Lee, V.M.-Y., 2006. Ubiquitinated TDP-43 in frontotemporal lobar degeneration and amyotrophic lateral sclerosis. *Science* 314, 130–133. <https://doi.org/10.1126/science.1134108>
- Neve, R.L., Harris, P., Kosik, K.S., Kurnit, D.M., Donlon, T.A., 1986. Identification of cDNA clones for the human microtubule-associated protein tau and chromosomal localization of the genes for tau and microtubule-associated protein 2. *Mol. Brain Res.* 1, 271–280. [https://doi.org/10.1016/0169-328X\(86\)90033-1](https://doi.org/10.1016/0169-328X(86)90033-1)
- Newman, E., Gupta, K., Climer, J., Monaghan, C., Hasselmo, M., 2012. Cholinergic modulation of cognitive processing: insights drawn from computational models. *Front. Behav. Neurosci.* 6.
- Niblock, M., Gallo, J.-M., 2012. Tau alternative splicing in familial and sporadic tauopathies. *Biochem. Soc. Trans.* 40, 677–680. <https://doi.org/10.1042/BST20120091>
- Nicolet, Y., Lockridge, O., Masson, P., Fontecilla-Camps, J.C., Nachon, F., 2003. Crystal structure of human butyrylcholinesterase and of its complexes with substrate and products. *J. Biol. Chem.* 278, 41141–41147. <https://doi.org/10.1074/jbc.M210241200>
- Nilsson, S., Levi, R., Nordström, A., 2011. Treatment-resistant sensory motor symptoms in persons with SCI may be signs of restless legs syndrome. *Spinal Cord* 49, 754–756. <https://doi.org/10.1038/sc.2010.164>
- Nishida, S., Hitsumoto, A., Namba, K., Usui, A., Inoue, Y., 2013. Persistence of secondary restless legs syndrome in a phantom limb caused by end-stage renal disease. *Intern. Med. Tokyo Jpn.* 52, 815–818. <https://doi.org/10.2169/internalmedicine.52.9013>
- Nishimura, M., Namba, Y., Ikeda, K., Oda, M., 1992. Glial fibrillary tangles with straight tubules in the brains of patients with progressive supranuclear palsy. *Neurosci. Lett.* 143, 35–38. [https://doi.org/10.1016/0304-3940\(92\)90227-X](https://doi.org/10.1016/0304-3940(92)90227-X)
- Nobis, L., Manohar, S.G., Smith, S.M., Alfaro-Almagro, F., Jenkinson, M., Mackay, C.E., Husain, M., 2019. Hippocampal volume across age: Nomograms derived from over 19,700 people in UK Biobank. *NeuroImage Clin.* 23, 101904. <https://doi.org/10.1016/j.nicl.2019.101904>
- Noble, W., Hanger, D.P., Miller, C.C.J., Lovestone, S., 2013. The Importance of Tau Phosphorylation for Neurodegenerative Diseases. *Front. Neurol.* 4, 83. <https://doi.org/10.3389/fneur.2013.00083>

- Nunez, J., Fischer, I., 1997. Microtubule-associated proteins (MAPs) in the peripheral nervous system during development and regeneration. *J. Mol. Neurosci.* 8, 207–222. <https://doi.org/10.1007/BF02736834>
- Oddo, S., LaFerla, F.M., 2006. The role of nicotinic acetylcholine receptors in Alzheimer's disease. *J. Physiol.-Paris, The World of the Synapse: Molecular Basis, Pathologies and Drug Discovery* 99, 172–179. <https://doi.org/10.1016/j.jphysparis.2005.12.080>
- Olivera, S., Henley, J.M., Rodriguez-Ithurralde, D., 2003. AMPA receptor potentiation by acetylcholinesterase is age-dependently upregulated at synaptogenesis sites of the rat brain. *Int. J. Dev. Neurosci.* 21, 49–61. [https://doi.org/10.1016/S0736-5748\(02\)00083-7](https://doi.org/10.1016/S0736-5748(02)00083-7)
- Omoto, M., Suzuki, S., Ikeuchi, T., Ishihara, T., Kobayashi, T., Tsuboi, Y., Ogasawara, J., Koga, M., Kawai, M., Iwaki, T., Kanda, T., 2012. Autosomal dominant tauopathy with parkinsonism and central hypoventilation. *Neurology* 78, 762–764. <https://doi.org/10.1212/WNL.0b013e318248e531>
- Öngür, D., Ferry, A.T., Price, J.L., 2003. Architectonic subdivision of the human orbital and medial prefrontal cortex. *J. Comp. Neurol.* 460, 425–449. <https://doi.org/10.1002/cne.10609>
- Panda, D., Goode, B.L., Feinstein, S.C., Wilson, L., 1995. Kinetic Stabilization of Microtubule Dynamics at Steady State by Tau and Microtubule-Binding Domains of Tau. *Biochemistry* 34, 11117–11127. <https://doi.org/10.1021/bi00035a017>
- Panda, D., Samuel, J.C., Massie, M., Feinstein, S.C., Wilson, L., 2003. Differential regulation of microtubule dynamics by three- and four-repeat tau: Implications for the onset of neurodegenerative disease. *Proc. Natl. Acad. Sci. U. S. A.* 100, 9548–9553. <https://doi.org/10.1073/pnas.1633508100>
- Papasozomenos, S.C., Binder, L.I., 1987. Phosphorylation determines two distinct species of Tau in the central nervous system. *Cell Motil. Cytoskeleton* 8, 210–226. <https://doi.org/10.1002/cm.970080303>
- Paraoanu, L.E., Steinert, G., Klaczinski, J., Becker-Röck, M., Bytyqi, A., Layer, P.G., 2006. On functions of cholinesterases during embryonic development. *J. Mol. Neurosci.* MN 30, 201–204. <https://doi.org/10.1385/JMN:30:1:201>
- Park, S.E., Kim, N.D., Yoo, Y.H., 2004. Acetylcholinesterase Plays a Pivotal Role in Apoptosome Formation. *Cancer Res.* 64, 2652–2655. <https://doi.org/10.1158/0008-5472.CAN-04-0649>
- Pasi, M., Poggesi, A., Pantoni, L., 2011. The use of CT in dementia. *Int. Psychogeriatr.* 23, S6–S12. <https://doi.org/10.1017/S1041610211000950>

- Pasquini, J., Brooks, D.J., Pavese, N., 2021. The Cholinergic Brain in Parkinson's Disease. *Mov. Disord. Clin. Pract.* 8, 1012–1026. <https://doi.org/10.1002/mdc3.13319>
- Peeraully, T., Tan, E.-K., 2012. Linking restless legs syndrome with Parkinson's disease: clinical, imaging and genetic evidence. *Transl. Neurodegener.* 1, 6. <https://doi.org/10.1186/2047-9158-1-6>
- Pei, J.J., Braak, E., Braak, H., Grundke-Iqbal, I., Iqbal, K., Winblad, B., Cowburn, R.F., 1999. Distribution of active glycogen synthase kinase 3beta (GSK-3beta) in brains staged for Alzheimer disease neurofibrillary changes. *J. Neuropathol. Exp. Neurol.* 58, 1010–1019. <https://doi.org/10.1097/00005072-199909000-00011>
- Pemberton, H.G., Collij, L.E., Heeman, F., Bollack, A., Shekari, M., Salvadó, G., Alves, I.L., Garcia, D.V., Battle, M., Buckley, C., Stephens, A.W., Bullich, S., Garibotto, V., Barkhof, F., Gispert, J.D., Farrar, G., on behalf of the AMYPAD consortium, 2022. Quantification of amyloid PET for future clinical use: a state-of-the-art review. *Eur. J. Nucl. Med. Mol. Imaging* 49, 3508–3528. <https://doi.org/10.1007/s00259-022-05784-y>
- Perry, E.K., Perry, R.H., Blessed, G., Tomlinson, B.E., 1978. Changes in brain cholinesterases in senile dementia of Alzheimer type. *Neuropathol. Appl. Neurobiol.* 4, 273–277.
- Perry, G., Cras, P., Siedlak, S.L., Tabaton, M., Kawai, M., 1992. Beta protein immunoreactivity is found in the majority of neurofibrillary tangles of Alzheimer's disease. *Am. J. Pathol.* 140, 283–290.
- Petersen, R.C., 2004. Mild cognitive impairment as a diagnostic entity. *J. Intern. Med.* 256, 183–194. <https://doi.org/10.1111/j.1365-2796.2004.01388.x>
- Petersen, R.C., 2003. *Mild Cognitive Impairment: Aging to Alzheimer's Disease*. Oxford University Press.
- Pillon, B., Dubois, B., Ploska, A., Agid, Y., 1991. Severity and specificity of cognitive impairment in Alzheimer's, Huntington's, and Parkinson's diseases and progressive supranuclear palsy. *Neurology* 41, 634–643. <https://doi.org/10.1212/WNL.41.5.634>
- Pittock, S.J., Parrett, T., Adler, C.H., Parisi, J.E., Dickson, D.W., Ahlskog, J.E., 2004. Neuropathology of primary restless leg syndrome: Absence of specific τ - and α -synuclein pathology. *Mov. Disord.* 19, 695–699. <https://doi.org/10.1002/mds.20042>

- Plassman, B.L., Langa, K.M., Fisher, G.G., Heeringa, S.G., Weir, D.R., Ofstedal, M.B., Burke, J.R., Hurd, M.D., Potter, G.G., Rodgers, W.L., Steffens, D.C., Willis, R.J., Wallace, R.B., 2007. Prevalence of dementia in the United States: the aging, demographics, and memory study. *Neuroepidemiology* 29, 125–132. <https://doi.org/10.1159/000109998>
- Powell, H.C., London, G.W., Lampert, P.W., 1974. Neurofibrillary Tangles in Progressive Supranuclear Palsy. *Electron Microscopic Observations. J. Neuropathol. Exp. Neurol.* 33, 98–106. <https://doi.org/10.1097/00005072-197401000-00007>
- Preston, A.R., Eichenbaum, H., 2013. Interplay of hippocampus and prefrontal cortex in memory. *Curr. Biol.* 23, R764–R773. <https://doi.org/10.1016/j.cub.2013.05.041>
- Price, J.L., 1990. Olfactory System, in: Paxinos, G. (Ed.), *The Human Nervous System*. Academic Press, San Diego, pp. 979–998.
- Price, J.L., Davis, P.B., Morris, J.C., White, D.L., 1991. The distribution of tangles, plaques and related immunohistochemical markers in healthy aging and Alzheimer's disease. *Neurobiol. Aging* 12, 295–312. [https://doi.org/10.1016/0197-4580\(91\)90006-6](https://doi.org/10.1016/0197-4580(91)90006-6)
- Probst, A., Götz, J., Wiederhold, K.H., Tolnay, M., Mistl, C., Jaton, A.L., Hong, M., Ishihara, T., Lee, V.M.-Y., Trojanowski, J.Q., Jakes, R., Crowther, R.A., Spillantini, M.G., Bürki, K., Goedert, M., 2000. Axonopathy and amyotrophy in mice transgenic for human four-repeat tau protein. *Acta Neuropathol. (Berl.)* 99, 469–481. <https://doi.org/10.1007/s004010051148>
- Qiu, C., Fratiglioni, L., 2018. Aging without Dementia is Achievable: Current Evidence from Epidemiological Research. *J. Alzheimers Dis.* 62, 933–942. <https://doi.org/10.3233/JAD-171037>
- Qizilbash, N., Whitehead, A., Higgins, J., Wilcock, G., Schneider, L., Farlow, M., for the Dementia Trialists' Collaboration, 1998. Cholinesterase Inhibition for Alzheimer Disease. A Meta-analysis of the Tacrine Trials. *JAMA* 280, 1777–1782. <https://doi.org/10.1001/jama.280.20.1777>
- Radić, Z., Pickering, N.A., Vellom, D.C., Camp, S., Taylor, P., 1993. Three distinct domains in the cholinesterase molecule confer selectivity for acetyl- and butyrylcholinesterase inhibitors. *Biochemistry* 32, 12074–12084. <https://doi.org/10.1021/bi00096a018>
- Rahmim, A., Zaidi, H., 2008. PET versus SPECT: strengths, limitations and challenges. *Nucl. Med. Commun.* 29, 193–207. <https://doi.org/10.1097/MNM.0b013e3282f3a515>

- Ravaglia, G., Forti, P., Montesi, F., Lucicesare, A., Pisacane, N., Rietti, E., Dalmonte, E., Bianchin, M., Mecocci, P., 2008. Mild cognitive impairment: epidemiology and dementia risk in an elderly Italian population. *J. Am. Geriatr. Soc.* 56, 51–58. <https://doi.org/10.1111/j.1532-5415.2007.01503.x>
- Raz, N., Gunning, F.M., Head, D., Dupuis, J.H., McQuain, J., Briggs, S.D., Loken, W.J., Thornton, A.E., Acker, J.D., 1997. Selective aging of the human cerebral cortex observed in vivo: differential vulnerability of the prefrontal gray matter. *Cereb. Cortex* 7, 268–282. <https://doi.org/10.1093/cercor/7.3.268>
- Reid, G.A., Darvesh, S., 2015. Butyrylcholinesterase-knockout reduces brain deposition of fibrillar β -amyloid in an Alzheimer mouse model. *Neuroscience* 298, 424–435. <https://doi.org/10.1016/j.neuroscience.2015.04.039>
- Reuben, A., Brickman, A.M., Muraskin, J., Steffener, J., Stern, Y., 2011. Hippocampal atrophy relates to fluid intelligence decline in the elderly. *J. Int. Neuropsychol. Soc.* 17, 56–61. <https://doi.org/10.1017/S135561771000127X>
- Rittman, T., Coyle-Gilchrist, I.T., Rowe, J.B., 2016. Managing cognition in progressive supranuclear palsy. *Neurodegener. Dis. Manag.* 6, 499–508. <https://doi.org/10.2217/nmt-2016-0027>
- Rogalski, E.J., Gefen, T., Shi, J., Samimi, M., Bigio, E., Weintraub, S., Geula, C., Mesulam, M.-M., 2013. Youthful Memory Capacity in Old Brains: Anatomic and Genetic Clues from the Northwestern SuperAging Project. *J. Cogn. Neurosci.* 25, 29–36. https://doi.org/10.1162/jocn_a_00300
- Rohrer, J.D., Warren, J.D., 2011. Phenotypic signatures of genetic frontotemporal dementia. *Curr. Opin. Neurol.* 24, 542–549. <https://doi.org/10.1097/WCO.0b013e32834cd442>
- Rösler, T.W., Tayanian Marvian, A., Brendel, M., Nykänen, N.-P., Höllerhage, M., Schwarz, S.C., Hopfner, F., Koeglsperger, T., Respondek, G., Schweyer, K., Levin, J., Villemagne, V.L., Barthel, H., Sabri, O., Müller, U., Meissner, W.G., Kovacs, G.G., Höglinger, G.U., 2019. Four-repeat tauopathies. *Prog. Neurobiol.* 180, 101644. <https://doi.org/10.1016/j.pneurobio.2019.101644>
- Rossi, A.F., Pessoa, L., Desimone, R., Ungerleider, L.G., 2009. The prefrontal cortex and the executive control of attention. *Exp. Brain Res.* 192, 489–497. <https://doi.org/10.1007/s00221-008-1642-z>
- Rotundo, R.L., Ruiz, C.A., Marrero, E., Kimbell, L.M., Rossi, S.G., Rosenberry, T., Darr, A., Tsoulfas, P., 2008. Assembly and regulation of acetylcholinesterase at the vertebrate neuromuscular junction. *Chem. Biol. Interact.* 175, 26–29. <https://doi.org/10.1016/j.cbi.2008.05.025>

- Rouleau, G.A., Clark, A.W., Rooke, K., Pramatarova, A., Krizus, A., Suchowersky, O., Julien, J.P., Figlewicz, D., 1996. SOD1 mutation is associated with accumulation of neurofilaments in amyotrophic lateral sclerosis. *Ann. Neurol.* 39, 128–131. <https://doi.org/10.1002/ana.410390119>
- Roussarie, J.-P., Yao, V., Rodriguez-Rodriguez, P., Oughtred, R., Rust, J., Plautz, Z., Kasturia, S., Albornoz, C., Wang, W., Schmidt, E.F., Dannenfeller, R., Tadych, A., Brichta, L., Barnea-Cramer, A., Heintz, N., Hof, P.R., Heiman, M., Dolinski, K., Flajolet, M., Troyanskaya, O.G., Greengard, P., 2020. Selective Neuronal Vulnerability in Alzheimer’s Disease: A Network-Based Analysis. *Neuron* 107, 821-835.e12. <https://doi.org/10.1016/j.neuron.2020.06.010>
- Rowe, J.W., Kahn, R.L., 1997. Successful aging. *Gerontologist* 37, 433–440. <https://doi.org/10.1093/geront/37.4.433>
- Roy, B., Haupt, L.M., Griffiths, L.R., 2013. Review: Alternative Splicing (AS) of Genes As An Approach for Generating Protein Complexity. *Curr. Genomics* 14, 182–194. <https://doi.org/10.2174/1389202911314030004>
- Ruppert, E., 2019. Restless arms syndrome: prevalence, impact, and management strategies. *Neuropsychiatr. Dis. Treat.* 15, 1737–1750. <https://doi.org/10.2147/NDT.S161583>
- Sadot, E., Marx, R., Barg, J., Behar, L., Ginzburg, I., 1994. Complete sequence of 3’-untranslated region of Tau from rat central nervous system. Implications for mRNA heterogeneity. *J. Mol. Biol.* 241, 325–331. <https://doi.org/10.1006/jmbi.1994.1508>
- Salminen, A.V., Manconi, M., Rimpilä, V., Luoto, T.M., Koskinen, E., Ferri, R., Ohman, J., Polo, O., 2013. Disconnection between periodic leg movements and cortical arousals in spinal cord injury. *J. Clin. Sleep Med. JCSM Off. Publ. Am. Acad. Sleep Med.* 9, 1207–1209. <https://doi.org/10.5664/jcsm.3174>
- Samimi, N., Sharma, G., Kimura, T., Matsubara, T., Huo, A., Chiba, K., Saito, Y., Murayama, S., Akatsu, H., Hashizume, Y., Hasegawa, M., Farjam, M., Shahpasand, K., Ando, K., Hisanaga, S.-I., 2021. Distinct phosphorylation profiles of tau in brains of patients with different tauopathies. *Neurobiol. Aging* 108, 72–79. <https://doi.org/10.1016/j.neurobiolaging.2021.08.011>
- Sandusky-Beltran, L.A., Sigurdsson, E.M., 2020. Tau immunotherapies: Lessons learned, current status and future considerations. *Neuropharmacology* 175, 108104. <https://doi.org/10.1016/j.neuropharm.2020.108104>
- Santacruz, K., Lewis, J., Spire, T., Paulson, J., Kotilinek, L., Ingelsson, M., Guimaraes, A., DeTure, M., Ramsden, M., McGowan, E., Forster, C., Yue, M., Orne, J., Janus, C., Mariash, A., Kuskowski, M., Hyman, B., Hutton, M., Ashe, K.H., 2005. Tau suppression in a neurodegenerative mouse model improves memory function. *Science* 309, 476–481. <https://doi.org/10.1126/science.1113694>

- Schmidt, R., Hofer, E., Bouwman, F.H., Buerger, K., Cordonnier, C., Fladby, T., Galimberti, D., Georges, J., Heneka, M.T., Hort, J., Laczó, J., Molinuevo, J.L., O'Brien, J.T., Religa, D., Scheltens, P., Schott, J.M., Sorbi, S., 2015. EFNS-ENS/EAN Guideline on concomitant use of cholinesterase inhibitors and memantine in moderate to severe Alzheimer's disease. *Eur. J. Neurol.* 22, 889–898. <https://doi.org/10.1111/ene.12707>
- Scholz, T., Mandelkow, E., 2014. Transport and diffusion of Tau protein in neurons. *Cell. Mol. Life Sci.* 71, 3139–3150. <https://doi.org/10.1007/s00018-014-1610-7>
- Schröder, H., Grösche, M., Adler, M., Spengler, M., Niemeyer, C.M., 2017. Immuno-PCR with digital readout. *Biochem. Biophys. Res. Commun.* 488, 311–315. <https://doi.org/10.1016/j.bbrc.2017.04.162>
- Schuff, N., Amend, D.L., Knowlton, R., Norman, D., Fein, G., Weiner, M.W., 1999. Age-related metabolite changes and volume loss in the hippocampus by magnetic resonance spectroscopy and imaging. *Neurobiol. Aging* 20, 279–285. [https://doi.org/10.1016/s0197-4580\(99\)00022-6](https://doi.org/10.1016/s0197-4580(99)00022-6)
- Schwab, C., Akiyama, H., McGeer, E.G., McGeer, P.L., 1998. Extracellular neurofibrillary tangles are immunopositive for the 40 carboxy-terminal sequence of beta-amyloid protein. *J. Neuropathol. Exp. Neurol.* 57, 1131–1137. <https://doi.org/10.1097/00005072-199812000-00004>
- Schwab, C., McGeer, P.L., 2000. Abeta42-carboxy-terminal-like immunoreactivity is associated with intracellular neurofibrillary tangles and pick bodies. *Exp. Neurol.* 161, 527–534. <https://doi.org/10.1006/exnr.1999.7307>
- Selden, N.R., Gitelman, D.R., Salamon-Murayama, N., Parrish, T.B., Mesulam, M.M., 1998. Trajectories of cholinergic pathways within the cerebral hemispheres of the human brain. *Brain J. Neurol.* 121 (Pt 12), 2249–2257.
- Selemon, L.D., Goldman-Rakic, P.S., 1985. Longitudinal topography and interdigitation of corticostriatal projections in the rhesus monkey. *J. Neurosci. Off. J. Soc. Neurosci.* 5, 776–794.
- Sellami, L., Bocchetta, M., Masellis, M., Cash, D.M., Dick, K.M., van Swieten, J., Borroni, B., Galimberti, D., Tartaglia, M.C., Rowe, J.B., Graff, C., Tagliavini, F., Frisoni, G., Finger, E., de Mendonça, A., Sorbi, S., Warren, J.D., Rohrer, J.D., Laforce, R., Genetic FTD Initiative, GENFI, 2018. Distinct Neuroanatomical Correlates of Neuropsychiatric Symptoms in the Three Main Forms of Genetic Frontotemporal Dementia in the GENFI Cohort. *J. Alzheimers Dis. JAD* 65, 147–163. <https://doi.org/10.3233/JAD-180053>

- Sevigny, J., Chiao, P., Bussière, T., Weinreb, P.H., Williams, L., Maier, M., Dunstan, R., Salloway, S., Chen, T., Ling, Y., O’Gorman, J., Qian, F., Arastu, M., Li, M., Chollate, S., Brennan, M.S., Quintero-Monzon, O., Scannevin, R.H., Arnold, H.M., Engber, T., Rhodes, K., Ferrero, J., Hang, Y., Mikulskis, A., Grimm, J., Hock, C., Nitsch, R.M., Sandrock, A., 2016. The antibody aducanumab reduces A β plaques in Alzheimer’s disease. *Nature* 537, 50–56.
<https://doi.org/10.1038/nature19323>
- Shi, M., Sui, Y.-T., Peskind, E.R., Li, G., Hwang, H., Devic, I., Gingham, C., Edgar, J.S., Pan, C., Goodlett, D.R., Furay, A.R., Gonzalez-Cuyar, L.F., Zhang, J., 2011. Salivary tau species are potential biomarkers of Alzheimer disease. *J. Alzheimers Dis.* 27, 299–305. <https://doi.org/10.3233/JAD-2011-110731>
- ShIPLEY, M., REYES, P., 1991. Anatomy of the Human Olfactory Bulb and Central Olfactory Pathways, in: Laing, D.G., Doty, R.L., Breipohl, W. (Eds.), *The Human Sense of Smell*. Springer, Berlin, Heidelberg, pp. 29–60.
https://doi.org/10.1007/978-3-642-76223-9_2
- SILMAN, I., 2021. The multiple biological roles of the cholinesterases. *Prog. Biophys. Mol. Biol., On the Physics of Excitable Media. Waves in Soft and Living Matter, their Transmission at the Synapse and their Cooperation in the Brain* 162, 41–56.
<https://doi.org/10.1016/j.pbiomolbio.2020.12.001>
- SILVER, A., 1974. *The biology of cholinesterases*. North-Holland Pub. Co. ; American Elsevier Pub. Co., Amsterdam; New York.
- SIMA, A.A., DEFENDINI, R., KEOHANE, C., D’AMATO, C., FOSTER, N.L., PARCHI, P., GAMBETTI, P., LYNCH, T., WILHELMSSEN, K.C., 1996. The neuropathology of chromosome 17-linked dementia. *Ann. Neurol.* 39, 734–743.
<https://doi.org/10.1002/ana.410390609>
- SONTAG, E., NUNBHAKDI-CRAIG, V., LEE, G., BRANDT, R., KAMIBAYASHI, C., KURET, J., WHITE, C.L., MUMBY, M.C., BLOOM, G.S., 1999. Molecular Interactions among Protein Phosphatase 2A, Tau, and Microtubules IMPLICATIONS FOR THE REGULATION OF TAU PHOSPHORYLATION AND THE DEVELOPMENT OF TAUOPATHIES. *J. Biol. Chem.* 274, 25490–25498.
<https://doi.org/10.1074/jbc.274.36.25490>
- SOUTER, S., LEE, G., 2009. Microtubule-associated protein tau in human prostate cancer cells: Isoforms, phosphorylation, and interactions. *J. Cell. Biochem.* 108, 555–564. <https://doi.org/10.1002/jcb.22287>
- SPIRES-JONES, T.L., HYMAN, B.T., 2014. The intersection of amyloid beta and tau at synapses in Alzheimer’s disease. *Neuron* 82, 756–771.
<https://doi.org/10.1016/j.neuron.2014.05.004>

- Spittaels, K., Van den Haute, C., Van Dorpe, J., Bruynseels, K., Vandezande, K., Laenen, I., Geerts, H., Mercken, M., Sciot, R., Van Lommel, A., Loos, R., Van Leuven, F., 1999. Prominent Axonopathy in the Brain and Spinal Cord of Transgenic Mice Overexpressing Four-Repeat Human tau Protein. *Am. J. Pathol.* 155, 2153–2165. [https://doi.org/10.1016/S0002-9440\(10\)65533-2](https://doi.org/10.1016/S0002-9440(10)65533-2)
- Squire, L.R., 1992. Memory and the hippocampus: A synthesis from findings with rats, monkeys, and humans. *Psychol. Rev.* 99, 195–231. <https://doi.org/10.1037/0033-295X.99.2.195>
- Starkstein, S.E., Kremer, J., 2001. The Disinhibition Syndrome and Frontal-Subcortical Circuits, in: Lichter, D.G., Cummings, J.L. (Eds.), *Frontal-Subcortical Circuits in Psychiatric and Neurological Disorders*. Guilford Press, pp. 163–176.
- Steele, J.C., Richardson, J.C., Olszewski, J., 1964. Progressive Supranuclear Palsy: A Heterogeneous Degeneration Involving the Brain Stem, Basal Ganglia and Cerebellum With Vertical Gaze and Pseudobulbar Palsy, Nuchal Dystonia and Dementia. *Arch. Neurol.* 10, 333–359. <https://doi.org/10.1001/archneur.1964.00460160003001>
- Stern, Y., 2002. What is cognitive reserve? Theory and research application of the reserve concept. *J. Int. Neuropsychol. Soc.* 8, 448–460. <https://doi.org/10.1017/S1355617702813248>
- Sternfeld, M., Ming, G., Song, H., Sela, K., Timberg, R., Poo, M., Soreq, H., 1998. Acetylcholinesterase enhances neurite growth and synapse development through alternative contributions of its hydrolytic capacity, core protein, and variable C termini. *J. Neurosci. Off. J. Soc. Neurosci.* 18, 1240–1249.
- Stewart, D.J., Inaba, T., Tang, B.K., Kalow, W., 1977. Hydrolysis of cocaine in human plasma by cholinesterase. *Life Sci.* 20, 1557–1563. [https://doi.org/10.1016/0024-3205\(77\)90448-9](https://doi.org/10.1016/0024-3205(77)90448-9)
- Stieler, J.T., Bullmann, T., Kohl, F., Tøien, Ø., Brückner, M.K., Härtig, W., Barnes, B.M., Arendt, T., 2011. The Physiological Link between Metabolic Rate Depression and Tau Phosphorylation in Mammalian Hibernation. *PLoS ONE* 6. <https://doi.org/10.1371/journal.pone.0014530>
- Stinton, N., Atif, M.A., Barkat, N., Doty, R.L., 2010. Influence of smell loss on taste function. *Behav. Neurosci.* 124, 256–264. <https://doi.org/10.1037/a0018766>
- Sultan, A., Nessler, F., Violet, M., Bégard, S., Loyens, A., Talahari, S., Mansuroglu, Z., Marzin, D., Sergeant, N., Humez, S., Colin, M., Bonnefoy, E., Buée, L., Galas, M.-C., 2011. Nuclear tau, a key player in neuronal DNA protection. *J. Biol. Chem.* 286, 4566–4575. <https://doi.org/10.1074/jbc.M110.199976>

- Sussman, J.L., Harel, M., Frolow, F., Oefner, C., Goldman, A., Toker, L., Silman, I., 1991. Atomic structure of acetylcholinesterase from *Torpedo californica*: a prototypic acetylcholine-binding protein. *Science* 253, 872–879. <https://doi.org/10.1126/science.1678899>
- Swerdlow, R.H., 2007. Pathogenesis of Alzheimer's disease. *Clin. Interv. Aging* 2, 347–359.
- Szegletes, T., Mallender, W.D., Thomas, P.J., Rosenberry, T.L., 1999. Substrate binding to the peripheral site of acetylcholinesterase initiates enzymatic catalysis. Substrate inhibition arises as a secondary effect. *Biochemistry* 38, 122–133. <https://doi.org/10.1021/bi9813577>
- Tagliavini, F., Pilleri, G., Gemignani, F., Lechi, A., 1983. Neuronal loss in the basal nucleus of Meynert in progressive supranuclear palsy. *Acta Neuropathol. (Berl.)* 61, 157–160. <https://doi.org/10.1007/BF00697397>
- Takashima, A., Murayama, M., Murayama, O., Kohno, T., Honda, T., Yasutake, K., Nihonmatsu, N., Mercken, M., Yamaguchi, H., Sugihara, S., Wolozin, B., 1998. Presenilin 1 associates with glycogen synthase kinase-3 β and its substrate tau. *Proc. Natl. Acad. Sci.* 95, 9637–9641. <https://doi.org/10.1073/pnas.95.16.9637>
- Taylor, P., Brown, J.H., 1999. Synthesis, Storage and Release of Acetylcholine. *Basic Neurochem. Mol. Cell. Med. Asp.* 6th Ed.
- Telles, S.C.L., Alves, R.C., Chadi, G., 2011. Periodic limb movements during sleep and restless legs syndrome in patients with ASIA A spinal cord injury. *J. Neurol. Sci.* 303, 119–123. <https://doi.org/10.1016/j.jns.2010.12.019>
- Terada, S., Ishizu, H., Haraguchi, T., Takehisa, Y., Tanabe, Y., Kawai, K., Kuroda, S., 2000. Tau-negative astrocytic star-like inclusions and coiled bodies in dementia with Lewy bodies. *Acta Neuropathol. (Berl.)* 100, 464–468. <https://doi.org/10.1007/s004010000213>
- Thal, D.R., Rüb, U., Orantes, M., Braak, H., 2002. Phases of A beta-deposition in the human brain and its relevance for the development of AD. *Neurology* 58, 1791–1800. <https://doi.org/10.1212/wnl.58.12.1791>
- Townsend, M., Mehta, T., Selkoe, D.J., 2007. Soluble A β Inhibits Specific Signal Transduction Cascades Common to the Insulin Receptor Pathway*. *J. Biol. Chem.* 282, 33305–33312. <https://doi.org/10.1074/jbc.M610390200>
- Tsang, S.W.Y., Lai, M.K.P., Kirvell, S., Francis, P.T., Esiri, M.M., Hope, T., Chen, C.P.L.-H., Wong, P.T.-H., 2006. Impaired coupling of muscarinic M1 receptors to G-proteins in the neocortex is associated with severity of dementia in Alzheimer's disease. *Neurobiol. Aging* 27, 1216–1223. <https://doi.org/10.1016/j.neurobiolaging.2005.07.010>

- Uchino, A., Takao, M., Hatsuta, H., Sumikura, H., Nakano, Y., Nogami, A., Saito, Y., Arai, T., Nishiyama, K., Murayama, S., 2015. Incidence and extent of TDP-43 accumulation in aging human brain. *Acta Neuropathol. Commun.* 3, 35. <https://doi.org/10.1186/s40478-015-0215-1>
- Umahara, T., Tsuchiya, K., Ikeda, K., Kanaya, K., Iwamoto, T., Takasaki, M., Mukai, K., Shibata, N., Kato, S., 2002. Demonstration and distribution of tau-positive glial coiled body-like structures in white matter and white matter threads in early onset Alzheimer's disease. *Neuropathol. Off. J. Jpn. Soc. Neuropathol.* 22, 9–12. <https://doi.org/10.1046/j.0919-6544.2002.00422.x>
- Uversky, V.N., 2002. What does it mean to be natively unfolded? *Eur. J. Biochem.* 269, 2–12. <https://doi.org/10.1046/j.0014-2956.2001.02649.x>
- Valotassiou, V., Papatriantafyllou, J., Sifakis, N., Tzavara, C., Tsougos, I., Psimadas, D., Fezoulidis, I., Kapsalaki, E., Hadjigeorgiou, G., Georgoulas, P., 2015. Clinical Evaluation of Brain Perfusion SPECT with Brodmann Areas Mapping in Early Diagnosis of Alzheimer's Disease. *J. Alzheimers Dis.* 47, 773–785. <https://doi.org/10.3233/JAD-150068>
- Valotassiou, V., Sifakis, N., Papatriantafyllou, J., Angelidis, G., Georgoulas, P., 2011. The Clinical Use of SPECT and PET Molecular Imaging in Alzheimer's Disease, The Clinical Spectrum of Alzheimer's Disease -The Charge Toward Comprehensive Diagnostic and Therapeutic Strategies. IntechOpen. <https://doi.org/10.5772/18825>
- van Koppen, C.J., Kaiser, B., 2003. Regulation of muscarinic acetylcholine receptor signaling. *Pharmacol. Ther.* 98, 197–220. [https://doi.org/10.1016/S0163-7258\(03\)00032-9](https://doi.org/10.1016/S0163-7258(03)00032-9)
- Varani, L., Hasegawa, M., Spillantini, M.G., Smith, M.J., Murrell, J.R., Ghetti, B., Klug, A., Goedert, M., Varani, G., 1999. Structure of tau exon 10 splicing regulatory element RNA and destabilization by mutations of frontotemporal dementia and parkinsonism linked to chromosome 17. *Proc. Natl. Acad. Sci.* 96, 8229–8234. <https://doi.org/10.1073/pnas.96.14.8229>
- Violet, M., Chauderlier, A., Delattre, L., Tardivel, M., Chouala, M.S., Sultan, A., Marciniak, E., Humez, S., Binder, L., Kaye, R., Lefebvre, B., Bonnefoy, E., Buée, L., Galas, M.-C., 2015. Prefibrillar Tau oligomers alter the nucleic acid protective function of Tau in hippocampal neurons in vivo. *Neurobiol. Dis.* 82, 540–551. <https://doi.org/10.1016/j.nbd.2015.09.003>
- Violet, M., Delattre, L., Tardivel, M., Sultan, A., Chauderlier, A., Caillierez, R., Talahari, S., Nesslany, F., Lefebvre, B., Bonnefoy, E., Buée, L., Galas, M.-C., 2014. A major role for Tau in neuronal DNA and RNA protection in vivo under physiological and hyperthermic conditions. *Front. Cell. Neurosci.* 8, 84. <https://doi.org/10.3389/fncel.2014.00084>

- Viscidi, E., Litvan, I., Dam, T., Juneja, M., Li, L., Krzywy, H., Eaton, S., Hall, S., Kupferman, J., Höglinger, G.U., 2021. Clinical Features of Patients With Progressive Supranuclear Palsy in an US Insurance Claims Database. *Front. Neurol.* 12.
- Von Economo, C., 1968. Encephalitis lethargica. *Wien Kin Wschr* 18, 324–28.
- Von Economo, C., 1930. Sleep as a problem of localization. *J. Nerv. Ment. Dis.* 71, 249–259. <https://doi.org/10.1097/00005053-193003000-00007>
- Walker, L.C., 2020. A β Plaques. *Free Neuropathol.* 1, 31. <https://doi.org/10.17879/freeneuropathology-2020-3025>
- Wallace, L.M.K., Theou, O., Darvesh, S., Bennett, D.A., Buchman, A.S., Andrew, M.K., Kirkland, S.A., Fisk, J.D., Rockwood, K., 2020. Neuropathologic burden and the degree of frailty in relation to global cognition and dementia. *Neurology* 95, e3269–e3279. <https://doi.org/10.1212/WNL.0000000000010944>
- Wang, Y., Loomis, P.A., Zinkowski, R.P., Binder, L.I., 1993. A novel tau transcript in cultured human neuroblastoma cells expressing nuclear tau. *J. Cell Biol.* 121, 257–267. <https://doi.org/10.1083/jcb.121.2.257>
- Warren, N.M., Piggott, M.A., Perry, E.K., Burn, D.J., 2005. Cholinergic systems in progressive supranuclear palsy. *Brain* 128, 239–249. <https://doi.org/10.1093/brain/awh391>
- Wegiel, Jerzy, Kuchna, I., Nowicki, K., Frackowiak, J., Mazur-Kolecka, B., Imaki, H., Wegiel, Jarek, Mehta, P.D., Silverman, W.P., Reisberg, B., deLeon, M., Wisniewski, T., Pirttilla, T., Frey, H., Lehtimäki, T., Kivimäki, T., Visser, F.E., Kamphorst, W., Potempska, A., Bolton, D., Currie, J.R., Miller, D.L., 2007. Intraneuronal A β immunoreactivity is not a predictor of brain amyloidosis- β or neurofibrillary degeneration. *Acta Neuropathol. (Berl.)* 113, 389–402. <https://doi.org/10.1007/s00401-006-0191-4>
- Weingarten, M.D., Lockwood, A.H., Hwo, S.Y., Kirschner, M.W., 1975. A protein factor essential for microtubule assembly. *Proc. Natl. Acad. Sci. U. S. A.* 72, 1858–1862. <https://doi.org/10.1073/pnas.72.5.1858>
- West, T., Kirmess, K.M., Meyer, M.R., Holubasch, M.S., Knapik, S.S., Hu, Y., Contois, J.H., Jackson, E.N., Harpstrite, S.E., Bateman, R.J., Holtzman, D.M., Verghese, P.B., Fogelman, I., Braunstein, J.B., Yarasheski, K.E., 2021. A blood-based diagnostic test incorporating plasma A β 42/40 ratio, ApoE proteotype, and age accurately identifies brain amyloid status: findings from a multi cohort validity analysis. *Mol. Neurodegener.* 16, 30. <https://doi.org/10.1186/s13024-021-00451-6>
- Whitehouse, P.J., Price, D.L., Clark, A.W., Coyle, J.T., DeLong, M.R., 1981. Alzheimer disease: evidence for selective loss of cholinergic neurons in the nucleus basalis. *Ann. Neurol.* 10, 122–126. <https://doi.org/10.1002/ana.410100203>

- Whitwell, J.L., Höglinger, G.U., Antonini, A., Bordelon, Y., Boxer, A.L., Colosimo, C., van Eimeren, T., Golbe, L.I., Kassubek, J., Kurz, C., Litvan, I., Pantelyat, A., Rabinovici, G., Respondek, G., Rominger, A., Rowe, J.B., Stamelou, M., Josephs, K.A., 2017. Radiological biomarkers for diagnosis in PSP: Where are we and where do we need to be? *Mov. Disord. Off. J. Mov. Disord. Soc.* 32, 955–971. <https://doi.org/10.1002/mds.27038>
- Wilcock, D.M., DiCarlo, G., Henderson, D., Jackson, J., Clarke, K., Ugen, K.E., Gordon, M.N., Morgan, D., 2003. Intracranially Administered Anti-A β Antibodies Reduce β -Amyloid Deposition by Mechanisms Both Independent of and Associated with Microglial Activation. *J. Neurosci.* 23, 3745–3751. <https://doi.org/10.1523/JNEUROSCI.23-09-03745.2003>
- Wilcock, G.K., Esiri, M.M., Bowen, D.M., Smith, C.C., 1982. Alzheimer's disease. Correlation of cortical choline acetyltransferase activity with the severity of dementia and histological abnormalities. *J. Neurol. Sci.* 57, 407–417. [https://doi.org/10.1016/0022-510x\(82\)90045-4](https://doi.org/10.1016/0022-510x(82)90045-4)
- Wilhelmsen, K.C., Lynch, T., Pavlou, E., Higgins, M., Nygaard, T.G., 1994. Localization of disinhibition-dementia-parkinsonism-amyotrophy complex to 17q21-22. *Am. J. Hum. Genet.* 55, 1159–1165.
- Will, C.L., Lührmann, R., 2011. Spliceosome structure and function. *Cold Spring Harb. Perspect. Biol.* 3. <https://doi.org/10.1101/cshperspect.a003707>
- Williams, A., Zhou, S., Zhan, C.-G., 2019. Discovery of potent and selective butyrylcholinesterase inhibitors through the use of pharmacophore-based screening. *Bioorg. Med. Chem. Lett.* 29, 126754. <https://doi.org/10.1016/j.bmcl.2019.126754>
- Wilson, R.S., Yu, L., Trojanowski, J.Q., Chen, E.-Y., Boyle, P.A., Bennett, D.A., Schneider, J.A., 2013. TDP-43 Pathology, Cognitive Decline, and Dementia in Old Age. *JAMA Neurol.* 70, 1418–1424. <https://doi.org/10.1001/jamaneurol.2013.3961>
- Wisniewski, H.M., Sadowski, M., Jakubowska-Sadowska, K., Tarnawski, M., Wegiel, J., 1998. Diffuse, Lake-like Amyloid- β Deposits in the Parvopyramidal Layer of the Presubiculum in Alzheimer Disease. *J. Neuropathol. Exp. Neurol.* 57, 674–683. <https://doi.org/10.1097/00005072-199807000-00004>
- Witter, M.P., Doan, T.P., Jacobsen, B., Nilssen, E.S., Ohara, S., 2017. Architecture of the Entorhinal Cortex A Review of Entorhinal Anatomy in Rodents with Some Comparative Notes. *Front. Syst. Neurosci.* 11. <https://doi.org/10.3389/fnsys.2017.00046>

- Witter, M.P., Naber, P.A., van Haefen, T., Machielsen, W.C.M., Rombouts, S.A.R.B., Barkhof, F., Scheltens, P., Lopes da Silva, F.H., 2000. Cortico-hippocampal communication by way of parallel parahippocampal-subicular pathways. *Hippocampus* 10, 398–410. [https://doi.org/10.1002/1098-1063\(2000\)10:4<398::AID-HIPO6>3.0.CO;2-K](https://doi.org/10.1002/1098-1063(2000)10:4<398::AID-HIPO6>3.0.CO;2-K)
- Yokota, T., Hirose, K., Tanabe, H., Tsukagoshi, H., 1991. Sleep-related periodic leg movements (nocturnal myoclonus) due to spinal cord lesion. *J. Neurol. Sci.* 104, 13–18. [https://doi.org/10.1016/0022-510x\(91\)90210-x](https://doi.org/10.1016/0022-510x(91)90210-x)
- Yoshida, H., Ihara, Y., 1993. Tau in paired helical filaments is functionally distinct from fetal tau: assembly incompetence of paired helical filament-tau. *J. Neurochem.* 61, 1183–1186. <https://doi.org/10.1111/j.1471-4159.1993.tb03642.x>
- Yu, J.-Z., Rasenick, M.M., 2006. Tau associates with actin in differentiating PC12 cells. *FASEB J. Off. Publ. Fed. Am. Soc. Exp. Biol.* 20, 1452–1461. <https://doi.org/10.1096/fj.05-5206com>
- Yu, Y., Run, X., Liang, Z., Li, Y., Liu, F., Liu, Y., Iqbal, K., Grundke-Iqbal, I., Gong, C.-X., 2009. Developmental regulation of tau phosphorylation, tau kinases, and tau phosphatases. *J. Neurochem.* 108, 1480–1494. <https://doi.org/10.1111/j.1471-4159.2009.05882.x>
- Zhukareva, V., Mann, D., Pickering-Brown, S., Uryu, K., Shuck, T., Shah, K., Grossman, M., Miller, B.L., Hulette, C.M., Feinstein, S.C., Trojanowski, J.Q., Lee, V.M.-Y., 2002. Sporadic Pick's disease: a tauopathy characterized by a spectrum of pathological tau isoforms in gray and white matter. *Ann. Neurol.* 51, 730–739. <https://doi.org/10.1002/ana.10222>

APPENDIX A

SUPPLEMENTARY DATA

Table A.1 Statistical analysis of the mean neuropathological aggregate scores in regions of interest related to cognitive function in cognitively normal octogenarians and older (CNOO) male compared to female brains

	A β Plaques			Tau Neurofibrillary Tangles			pTDP-43 Neuronal Cytoplasmic Inclusions			AChE Plaques			BChE Plaques		
	Male Mean Score (SD)	Female Mean Score (SD)	<i>p</i> value	Male Mean Score (SD)	Female Mean Score (SD)	<i>p</i> value	Male Mean Score (SD)	Female Mean Score (SD)	<i>p</i> value	Male Mean Score (SD)	Female Mean Score (SD)	<i>p</i> value	Male Mean Score (SD)	Female Mean Score (SD)	<i>p</i> value
rPFC^a	3.00 (0)	3.00 (0)	1	0.20 (0.45)	1.20 (0.45)	0.008**	0 (0)	0 (0)	1	1.80 (1.64)	2.60 (0.89)	0.375	1.80 (1.64)	2.80 (0.45)	0.251
DG	1.50 (1.73)	2.00 (1.41)	0.647	1.75 (0.96)	1.60 (0.89)	0.815	0.50 (1.00)	1.20 (1.64)	0.458	1.33 (1.53)	1.00 (1.41)	0.764	0.50 (0.58)	1.20 (1.64)	0.415
CA1	1.25 (1.50)	1.60 (1.34)	0.723	3.00 (0)	2.60 (0.89)	0.407	0.75 (1.50)	1.00 (1.23)	0.79	0.75 (1.50)	1.20 (1.30)	0.644	0.75 (0.96)	1.00 (1.41)	0.772
CA2	0.50 (1.00)	0.40 (0.55)	0.853	1.50 (1.00)	2.00 (1.23)	0.532	0 (0)	0 (0)	1	0 (0)	0.20 (0.45)	0.576	0.25 (0.50)	0.20 (0.45)	0.879
CA3	1.50 (1.73)	0.80 (1.30)	0.51	1.00 (0)	1.20 (1.10)	0.729	0 (0)	0.60 (0.55)	0.07	0 (0)	0.40 (0.55)	0.178	0.50 (0.58)	1.00 (1.23)	0.48
S	1.25 (1.50)	2.20 (1.30)	0.343	2.75 (0.50)	1.80 (1.10)	0.156	0.75 (1.50)	0.80 (0.84)	0.951	0.75 (1.50)	1.40 (1.52)	0.541	0.50 (0.58)	1.00 (1.23)	0.48
PrS	1.50 (1.73)	3.00 (0)	0.182	2.25 (0.50)	1.60 (0.89)	0.238	0.25 (0.50)	0.60 (0.55)	0.356	0.75 (1.50)	1.60 (1.34)	0.399	0.50 (0.58)	2.40 (0.89)	0.008**
PaS	1.50 (1.73)	2.00 (1)	0.632	2.00 (0.82)	1.80 (1.10)	0.771	0 (0)	0.40 (0.55)	0.178	0.75 (1.50)	0.80 (0.84)	0.951	0.50 (0.58)	1.40 (0.89)	0.127
EC	1.50 (1.73)	3.00 (0)	0.182	3.00 (0)	2.60 (0.89)	0.407	0.25 (0.50)	0.40 (0.55)	0.685	0.75 (1.50)	1.40 (1.14)	0.482	1.00 (1.16)	1.80 (1.10)	0.323

192

^aRegions: CA, cornu Ammonis; DG, dentate gyrus; EC, entorhinal cortex; PaS, parasubiculum; PrS, presubiculum; rPFC, rostral prefrontal cortex; S, subiculum

Table A.2 Statistical analysis of the mean neuropathological aggregate scores in regions of interest related to cognitive function in Alzheimer’s disease males compared to female brains

	A β Plaques			Tau Neurofibrillary Tangles			pTDP-43 Neuronal Cytoplasmic Inclusions			AChE Plaques			BChE Plaques		
	Male Mean Score (SD)	Female Mean Score (SD)	<i>p</i> value	Male Mean Score (SD)	Female Mean Score (SD)	<i>p</i> value	Male Mean Score (SD)	Female Mean Score (SD)	<i>p</i> value	Male Mean Score (SD)	Female Mean Score (SD)	<i>p</i> value	Male Mean Score (SD)	Female Mean Score (SD)	<i>p</i> value
rPFC^a	3.00 (0)	3.00 (0)	1	2.00 (0.71)	2.20 (1.10)	0.74	0.60 (1.34)	0.20 (0.45)	0.545	3.00 (0)	3.00 (0)	1	3.00 (0)	3.00 (0)	1
DG	2.40 (0.89)	2.60 (0.89)	0.733	2.20 (1.10)	2.60 (0.55)	0.493	1.20 (1.64)	1.00 (1.23)	0.833	1.75 (0.96)	2.60 (0.89)	0.212	3.00 (0)	3.00 (0)	1
CA1	2.20 (1.10)	2.80 (0.45)	0.306	3.00 (0)	3.00 (0)	1	1.00 (1.41)	1.20 (1.30)	0.822	1.60 (0.89)	2.40 (0.89)	0.195	3.00 (0)	3.00 (0)	1
CA2	1.20 (1.30)	0.60 (0.55)	0.371	2.40 (0.89)	2.60 (0.55)	0.681	0.60 (0.89)	0.40 (0.55)	0.681	1.33 (0.58)	1.00 (0)	0.423	1.20 (1.10)	1.60 (1.14)	0.587
CA3	0.80 (0.84)	1.40 (1.14)	0.371	2.20 (1.10)	2.80 (0.45)	0.306	0.60 (0.89)	0.40 (0.55)	0.681	1.00 (0)	1.40 (0.89)	0.482	1.20 (1.10)	2.00 (1.00)	0.262
S	2.80 (0.45)	2.60 (0.89)	0.667	3.00 (0)	3.00 (0)	1	1.20 (1.64)	1.20 (1.10)	1	2.00 (0.71)	2.20 (0.84)	0.694	2.60 (0.55)	2.80 (0.45)	0.545
PrS	3.00 (0)	3.00 (0)	1	2.80 (0.45)	2.80 (0.45)	1	0.80 (1.30)	0.20 (0.45)	0.359	3.00 (0)	2.20 (1.10)	0.178	3.00 (0)	3.00 (0)	1
PaS	3.00 (0)	3.00 (0)	1	2.25 (0.96)	3.00 (0)	0.215	0.50 (1.00)	0.50 (1.00)	1	3.00 (0)	2.00 (1.16)	0.182	2.75 (0.50)	2.80 (0.45)	0.879
EC	3.00 (0)	3.00 (0)	1	3.00 (0)	3.00 (0)	1	1.20 (1.64)	1.20 (1.30)	1	2.40 (0.89)	2.40 (0.89)	1	3.00 (0)	3.00 (0)	1

^aRegions: CA, cornu Ammonis; DG, dentate gyrus; EC, entorhinal cortex; PaS parasubiculum; PrS, presubiculum; rPFC, rostral prefrontal cortex; S, subiculum

Table A.3 Statistical analysis of the mean neuropathological aggregate scores in regions of interest related to cognitive function in male cognitively normal octogenarian and older (CNOO) compared to Alzheimer's disease (AD) brains

	A β Plaques			Tau Neurofibrillary Tangles			pTDP-43 Neuronal Cytoplasmic Inclusions			AChE Plaques			BChE Plaques		
	CNOO Mean Score (SD)	AD Mean Score (SD)	p value	CNOO Mean Score (SD)	AD Mean Score (SD)	p value	CNOO Mean Score (SD)	AD Mean Score (SD)	p value	CNOO Mean Score (SD)	AD Mean Score (SD)	p value	CNOO Mean Score (SD)	AD Mean Score (SD)	p value
rPFC^a	3.00 (0)	3.00 (0)	1	0.20 (0.45)	2.00 (0.71)	0.001**	0 (0)	0.60 (1.34)	0.374	1.80 (1.64)	3.00 (0)	0.178	1.80 (1.64)	3.00 (0)	0.178
DG	1.50 (1.73)	2.40 (0.89)	0.396	1.75 (0.96)	2.20 (1.10)	0.539	0.50 (1.00)	1.20 (1.64)	0.458	1.33 (1.53)	1.75 (0.96)	0.673	0.50 (0.58)	3.00 (0)	0.003**
CA1	1.25 (1.50)	2.20 (1.10)	0.307	3.00 (0)	3.00 (0)	1	0.75 (1.50)	1.00 (1.41)	0.805	0.75 (1.50)	1.60 (0.89)	0.323	0.75 (0.96)	3.00 (0)	0.018**
CA2	0.50 (1.00)	1.20 (1.30)	0.407	1.50 (1.00)	2.40 (0.89)	0.197	0 (0)	0.60 (0.89)	0.208	0 (0)	1.33 (0.58)	0.053	0.25 (0.50)	1.20 (1.10)	0.156
CA3	1.50 (1.73)	0.80 (0.84)	0.498	1.00 (0)	2.20 (1.10)	0.07	0 (0)	0.60 (0.89)	0.208	0 (0)	1.00 (0)	N/A	0.50 (0.58)	1.20 (1.10)	0.289
S	1.25 (1.50)	2.80 (0.45)	0.128	2.75 (0.50)	3.00 (0)	0.391	0.75 (1.50)	1.20 (1.64)	0.685	0.75 (1.50)	2.00 (0.71)	0.14	0.50 (0.58)	2.60 (0.55)	<0.001***
PrS	1.50 (1.73)	3.00 (0)	0.182	2.25 (0.50)	2.80 (0.45)	0.125	0.25 (0.50)	0.80 (1.30)	0.456	0.75 (1.50)	3.00 (0)	0.058	0.50 (0.58)	3.00 (0)	0.003**
PaS	1.50 (1.73)	3.00 (0)	0.182	2.00 (0.82)	2.25 (0.96)	0.705	0 (0)	0.50 (1.00)	0.391	0.75 (1.50)	3.00 (0)	0.058	0.50 (0.58)	2.75 (0.50)	0.001**
EC	1.50 (1.73)	3.00 (0)	0.182	3.00 (0)	3.00 (0)	1	0.25 (0.50)	1.20 (1.64)	0.277	0.75 (1.50)	2.40 (0.89)	0.078	1.00 (1.16)	3.00 (0)	0.041*

^aRegions: CA, cornu Ammonis; DG, dentate gyrus; EC, entorhinal cortex; PaS parasubiculum; PrS, presubiculum; rPFC, rostral prefrontal cortex; S, subiculum

Table A.4 Statistical analysis of the mean neuropathological aggregate scores in regions of interest related to cognitive function in female cognitively normal octogenarian and older (CNOO) compared to Alzheimer's disease (AD) brains

	A β Plaques			Tau Neurofibrillary Tangles			pTDP-43 Neuronal Cytoplasmic Inclusions			AChE Plaques			BChE Plaques		
	CNOO Mean Score (SD)	AD Mean Score (SD)	p value	CNOO Mean Score (SD)	AD Mean Score (SD)	p value	CNOO Mean Score (SD)	AD Mean Score (SD)	p value	CNOO Mean Score (SD)	AD Mean Score (SD)	p value	CNOO Mean Score (SD)	AD Mean Score (SD)	p value
rPFC^a	3.00 (0)	3.00 (0)	1	1.20 (0.45)	2.20 (1.10)	0.114	0 (0)	0.20 (0.45)	0.374	2.60 (0.89)	3.00 (0)	0.374	2.80 (0.45)	3.00 (0)	0.374
DG	2.00 (1.41)	2.60 (0.89)	0.446	1.60 (0.89)	2.60 (0.55)	0.066	1.20 (1.64)	1.00 (1.23)	0.833	1.00 (1.41)	2.60 (0.89)	0.065	1.20 (1.64)	3.00 (0)	0.07
CA1	1.60 (1.34)	2.80 (0.45)	0.118	2.60 (0.89)	3.00 (0)	0.374	1.00 (1.23)	1.20 (1.30)	0.809	1.20 (1.30)	2.40 (0.89)	0.128	1.00 (1.41)	3.00 (0)	0.034*
CA2	0.40 (0.55)	0.60 (0.55)	0.58	2.00 (1.23)	2.60 (0.55)	0.347	0 (0)	0.40 (0.55)	0.178	0.20 (0.45)	1.00 (0)	0.016*	0.20 (0.45)	1.60 (1.14)	0.034*
CA3	0.80 (1.30)	1.40 (1.14)	0.461	1.20 (1.10)	2.80 (0.45)	0.016*	0.60 (0.55)	0.40 (0.55)	0.58	0.40 (0.55)	1.40 (0.89)	0.066	1.00 (1.23)	2.00 (1.00)	0.195
S	2.20 (1.30)	2.60 (0.89)	0.587	1.80 (1.10)	3.00 (0)	0.04*	0.80 (0.84)	1.20 (1.10)	0.535	1.40 (1.52)	2.20 (0.84)	0.332	1.00 (1.23)	2.80 (0.45)	0.015*
PrS	3.00 (0)	3.00 (0)	1	1.60 (0.89)	2.80 (0.45)	0.028*	0.60 (0.55)	0.20 (0.45)	0.242	1.60 (1.34)	2.20 (1.10)	0.461	2.40 (0.89)	3.00 (0)	0.208
PaS	2.00 (1)	3.00 (0)	0.089	1.80 (1.10)	3.00 (0)	0.07	0.40 (0.55)	0.50 (1.00)	0.853	0.80 (0.84)	2.00 (1.16)	0.112	1.40 (0.89)	2.80 (0.45)	0.014*
EC	3.00 (0)	3.00 (0)	1	2.60 (0.89)	3.00 (0)	0.374	0.40 (0.55)	1.20 (1.30)	0.242	1.40 (1.14)	2.40 (0.89)	0.161	1.80 (1.10)	3.00 (0)	0.07

^aRegions: CA, cornu Ammonis; DG, dentate gyrus; EC, entorhinal cortex; PaS, parasubiculum; PrS, presubiculum; rPFC, rostral prefrontal cortex; S, subiculum

APPENDIX B

COPYWRITE PERMISSION LETTERS

Journal List > IOS Press Open Library > PMC5438481



[J Alzheimers Dis.](#) 2017; 58(2): 491–505.

PMCID: PMC5438481

Published online 2017 May 11. Prepublished online 2017 Apr 28.

PMID: [28453492](#)

doi: [10.3233/JAD-170164](#)

Quantification of Butyrylcholinesterase Activity as a Sensitive and Specific Biomarker of Alzheimer's Disease

[Ian R. Macdonald](#)^a, [Selena P. Maxwell](#)^a, [George A. Reid](#)^a, [Meghan K. Cash](#)^a, [Drew R. DeBay](#)^a and [Sultan Darvesh](#)^{a,b,c,*}

Debomoy Lahiri, Handling Associate Editor

▾ [Author information](#) ▾ [Article notes](#) ▾ [Copyright and License information](#) [Disclaimer](#)

^aDepartment of Medical Neuroscience, Dalhousie University, Halifax, NS, Canada

^bDepartment of Medicine (Neurology and Geriatric Medicine), Dalhousie University, Halifax, NS, Canada

^cDepartment of Chemistry and Physics, Mount Saint Vincent University, Halifax, NS, Canada

*Correspondence to: Sultan Darvesh, Room 1308, Camp Hill Veterans' Memorial, 5955 Veterans' Memorial Lane, Halifax, NS, B3H 2E1, Canada. Tel.: +1 902 473 2490; Fax: +1 902 473 7133; E-mail: sultan.darvesh@dal.ca.

Accepted 2017 Mar 12.

[Copyright](#) IOS Press and the authors. All rights reserved

This is an open access article distributed under the terms of the [Creative Commons Attribution Non-Commercial \(CC BY-NC 4.0\) License](#), which permits unrestricted non-commercial use, distribution, and reproduction in any medium, provided the original work is properly cited.

Do I need to request permission to re-use work from another STM publisher? +

Do I need to request permission to text mine Elsevier content? +

Can I include/use my article in my thesis/dissertation? -

Yes. Authors can include their articles in full or in part in a thesis or dissertation for non-commercial purposes.

Which uses of a work does Elsevier view as a form of 'prior publication'? +

How do I obtain permission to use Elsevier Journal material such as figures, tables, or text excerpts, if the request falls within the STM permissions guidelines? +

How do I obtain permission to use Elsevier Journal material such as figures, tables, or text excerpts, if the amount of material I wish to use does not fall within the free limits set out in the STM permissions guidelines? +

How do I obtain permission to use Elsevier Book material such as figures, tables, or text excerpts? +

